ISSN 0021-9673

VOL. 477 NO. 1 AUGUST 23, 1989

Gerhard Schomburg Honour Issue

JOURNAL OF CHROMATOGRAPHY

INTERNATIONAL JOURNAL ON CHROMATOGRAPHY, ELECTROPHORESIS AND RELATED METHODS

ELSEVIER

JOURNAL OF CHROMATOGRAPHY

Scope. The *Journal of Chromatography* publishes papers on all aspects of chromatography, electrophoresis and related methods. Contributions consist mainly of research papers dealing with chromatographic theory, instrumental development and their applications. The section *Biomedical Applications*, which is under separate editorship, deals with the following aspects: developments in and applications of chromatographic and electrophoretic techniques related to clinical diagnosis or alterations during medical treatment; screening and profiling of body fluids or tissues with special reference to metabolic disorders; results from basic medical research with direct consequences in clinical practice; drug level monitoring and pharmacokinetic studies; clinical toxicology; analytical studies in occupational medicine.

Submission of Papers. Papers in English, French and German may be submitted, in three copies. Manuscripts should be submitted to: The Editor of *Journal of Chromatography*, P.O. Box 681, 1000 AR Amsterdam, The Netherlands, or to: The Editor of *Journal of Chromatography, Biomedical Applications*, P.O. Box 681, 1000 AR Amsterdam, The Netherlands. Review articles are invited or proposed by letter to the Editors. An outline of the proposed review should first be forwarded to the Editors for preliminary discussion prior to preparation. Submission of an article is understood to imply that the article is original and unpublished and is not being considered for publication elsewhere. For copyright regulations, see below.

Subscription Orders. Subscription orders should be sent to: Elsevier Science Publishers B.V., P.O. Box 211, 1000 AE Amsterdam, The Netherlands, Tel. 5803 911, Telex 18582 ESPA NL. The *Journal of Chromatography* and the *Biomedical Applications* section can be subscribed to separately.

Publication. The *Journal of Chromatography* (incl. *Biomedical Applications*) has 37 volumes in 1989. The subscription prices for 1989 are:

J. Chromatogr. + *Biomed. Appl.* (Vols. 461–497):
Dfl. 6475.00 plus Dfl. 999.00 (p.p.h.) (total *ca.* US$ 3737.00)

J. Chromatogr. only (Vols. 461–486):
Dfl. 5200.00 plus Dfl. 702.00 (p.p.h.) (total *ca.* US$ 2951.00)

Biomed. Appl. only (Vols. 487–497):
Dfl. 2200.00 plus Dfl. 297.00 (p.p.h.) (total *ca.* US$ 1248.50).

Our p.p.h. (postage, package and handling) charge includes surface delivery of all issues, except to subscribers in Argentina, Australia, Brasil, Canada, China, Hong Kong, India, Israel, Malaysia, Mexico, New Zealand, Pakistan, Singapore, South Africa, South Korea, Taiwan, Thailand and the U.S.A. who receive all issues by air delivery (S.A.L. — Surface Air Lifted) at no extra cost. For Japan, air delivery requires 50% additional charge; for all other countries airmail and S.A.L. charges are available upon request. Back volumes of the *Journal of Chromatography* (Vols. 1–460) are available at Dfl. 195.00 (plus postage). Claims for missing issues will be honoured, free of charge, within three months after publication of the issue. Customers in the U.S.A. and Canada wishing information on this and other Elsevier journals, please contact Journal Information Center, Elsevier Science Publishing Co. Inc., 655 Avenue of the Americas, New York, NY 10010. Tel. (212) 633-3750.

Abstracts/Contents Lists published in Analytical Abstracts, ASCA, Biochemical Abstracts, Biological Abstracts, Chemical Abstracts, Chemical Titles, Chromatography Abstracts, Current Contents/Physical, Chemical & Earth Sciences, Current Contents/Life Sciences, Deep-Sea Research/Part B: Oceanographic Literature Review, Excerpta Medica, Index Medicus, Mass Spectrometry Bulletin, PASCAL-CNRS, Referativnyi Zhurnal and Science Citation Index.

See inside back cover for Publication Schedule, Information for Authors and information on Advertisements.

0378-4347/89/$03.50

This issue is printed on acid-free paper.

Printed in The Netherlands

For contents see p. VII

JOURNAL OF CHROMATOGRAPHY

VOL. 477 (1989)

JOURNAL *of* CHROMATOGRAPHY

INTERNATIONAL JOURNAL ON CHROMATOGRAPHY,
ELECTROPHORESIS AND RELATED METHODS

ELSEVIER
AMSTERDAM — OXFORD — NEW YORK — TOKYO

0021-9673/89/$03.50

Printed in The Netherlands

SPECIAL ISSUE

HONOUR ISSUE

on the occasion of the 60th birthday of

GERHARD SCHOMBURG

Guest Editor

K.-P. HUPE

(Waldbronn, F.R.G.)

VOL. 477, NO 1 JOURNAL OF CHROMATOGRAPHY AUGUST 23, 1989

CONTENTS

HONOUR ISSUE ON THE OCCASION OF THE 60TH BIRTHDAY OF GERHARD SCHOMBURG

In articles with more than one author, the name of the author to whom correspondence should be addressed is indicated in the article heading by a 6-pointed asterisk (*)

Journal of Chromatography, 477 (1989) 1
Elsevier Science Publishers B.V., Amsterdam — Printed in The Netherlands

60TH BIRTHDAY OF GERHARD SCHOMBURG

On August 22nd this year, Gerhard Schomburg, one of the protagonists of chromatography, has celebrated his 60th birthday.

The chromatographic community has known Gerhard Schomburg for many years, from scientific meetings throughout the world, as a presenter of fascinating new results and a lively and impulsive participant in discussions, as an organizer of symposia and for the last several years as the chairman of the Arbeitskreis Chromatographie of the Gesellschaft Deutscher Chemiker.

Gerhard Schomburg studied chemistry at the University of Bonn. His doctoral thesis, prepared under Nobel Laureate Karl Ziegler and submitted to the Technische Hochschule Aachen, was on infrared spectroscopy. In 1956 he became head of the chromatography department of the Max-Planck-Institut für Kohlenforschung and in 1965 also of the chromatography laboratories of the Max-Planck-Institut für Strahlenchemie, both in Mühlheim/Ruhr. Through his work and presence over the years, this city has become one of the places of pilgrimage for both experts and novices in chromatography.

Gerhard Schomburg's research interests encompass all kinds of chromatography including gas, liquid and supercritical fluid chromatography. His special focus for many years has been on capillary gas chromatography with both basic research on, and development of, highly efficient and selective methods as well as automated systems. It is this part of his work which has very substantially contributed to the practical acceptance and proliferation of this method. In recent years he has also made remarkable contributions to the development of novel phases for the liquid chromatographic separation of ions and enantiomers.

He teaches chromatography at the Universities of Wuppertal and Bochum and gives courses and seminars on various aspects of chromatography. He is author of a textbook on gas chromatography and has published his scientific work in more than 180 papers. He is an editor of the journal *Chromatographia.*

Gerhard Schomburg's contributions to the advancement of chromatography have been recognized by many awards. He received the Tswett Memorial Medal from the Scientific Council on Chromatography of the Academy of Sciences of the U.S.S.R. (1978), the M.S. Tswett Medal of the International Symposia on Advances in Chromatography (1983), the A. J. P. Martin Award of the Chromatography Society of Great Britain (1984) and the Stephen Dal Nogare Award of the Chromatography Forum of the Delaware Valley, U.S.A. (1986). In 1987 he was awarded an honorary doctorate from the University of Duisburg, F.R.G.

With warm congratulations let us join in wishing Gerhard Schomburg many more productive years in good health and with much success.

Waldbronn (F.R.G.) KLAUS-PETER HUPE

Journal of Chromatography, 477 (1989) 3–24
Elsevier Science Publishers B.V., Amsterdam — Printed in The Netherlands

CHROM. 21 169

DEACTIVATION WITH POLYMETHYLHYDROSILOXANE

A COMPARATIVE STUDY WITH CAPILLARY GAS CHROMATOGRAPHY AND SOLID-STATE ^{29}Si NUCLEAR MAGNETIC RESONANCE SPECTROSCOPY

M. HETEM*, G. RUTTEN, B. VERMEER, J. RIJKS, L. VAN DE VEN, J. DE HAAN and C. CRAMERS

Eindhoven University of Technology, Laboratory of Instrumental Analysis, P.O. Box 513, 5600 MB Eindhoven (The Netherlands)

SUMMARY

Deactivation of fused-silica capillary columns and vitreous silica surfaces with polymethylhydrosiloxanes (PMHS) at temperatures between 240 and 360°C was investigated by gas chromatography (GC) and solid-state ^{29}Si NMR spectroscopy. The influence of temperature, amount of water at the surface and film thickness on the stability and nature of the polymer deactivation layer was studied by solid-state ^{29}Si NMR of the model substrate Cab-O-Sil, a fumed silica. These NMR measurements match the GC results and offer additional information relating to the nature of the deactivating layer at surfaces silylated under various reaction conditions. Differences in the nature and structure of the deactivating film occur when the silica surface is coated with a different thickness. Optimum deactivation is achieved when a few monolayers of densely cross-linked polymers anchored to the silica surface are formed. On top of this thin, rigid layer, longer mobile polymer chains containing unreacted silicon hydride groups are present. After optimum deactivation, the fused-silica capillary column wall shows no interaction with various critical test components as used in GC practice. The deactivating films exhibit good thermal stability and solvent resistance.

INTRODUCTION

Substantial improvements in non-polar surface deactivation and modification of the inner wall of fused-silica capillary columns at lower temperatures have been made in recent years by the use of several kinds of methylhydrosiloxanes[1,2]. Mostly, mixtures of linear and cyclic polymers are used. The advantages of the use of polymethylhydrosiloxanes (PMHS) for the modification of fused-silica capillary column walls are the lower silylation temperatures, the relatively short reaction times and the high degree of effective deactivation. Narrow-bore fused-silica columns modified with PMHS coated with non-polar stationary phases have shown excellent deactivation also in capillary liquid and supercritical fluid chromatography[3,4].

0021-9673/89/$03.50

Although very effective deactivation of fused-silica capillary columns with PMHS was achieved with an optimum silylation time and temperature, the exact nature of the deactivating film inside fused-silica capillaries is not yet known. Some workers have explained the effective deactivation of methylhydrosiloxanes by the formation of a very thin film[2] (film thickness of a few monolayers), where all hydrogen groups have reacted with silanol groups into a dense network of cross-linked polymer bonded to the surface via siloxane linkages and with methyl groups protruding upwards from the surface. Although this explanation accounts for the character of the deactivated capillaries observed in gas chromatographic (GC) tests, in view of the high original hydrogen content it is bold to assume that the silylated film is devoid of hydrogen groups.

Here we describe deactivation with PMHS inside fused-silica capillaries and on Cab-O-Sil, a vitreous silica, as a model substrate for fused-silica material that allows spectrometric surface characterization. Fused-silica capillary columns deactivated with PMHS were tested for inertness, acidity and thermal and chemical stability after silylation between 260 and 320°C for various reaction times. Further, the influence of traces of water present on the inner wall before silylation was studied.

PMHS-modified fused-silica capillaries were subjected to a test for remaining silanol activity and acid or basic adsorption[5–7]. The deactivated uncoated fused-silica capillaries were tested by a double column method[8], using a thick-film apolar precolumn as reference.

The use of fumed vitreous silica for model experiments in combination with solid-state NMR spectroscopy has proved to be a powerful tool for the study of surface moieties after silylation[5,9]. Solid-state ^{29}Si NMR provides information on the nature, amount and chemical properties of the groups formed at the surface of the silica. PMHS coated with different film thicknesses on both dried and wetted Cab-O-Sil was silylated between 240 and 360°C for various reaction times. In this study the relative amounts of organo-siliceous surface moieties not directly connected to the surface were determined by ^{29}Si magic-angle spinning (MAS) NMR. ^{29}Si cross-polarization magic-angle spinning (CP-MAS) NMR provided information about the mobility of the anchored and auto cross-linked PMHS chains by contact-time variation experiments. Also, the relative amounts of the siliceous moieties directly attached to the silica surface were determined by ^{29}Si CP-MAS NMR.

The results of the measurements on silylated Cab-O-Sil match the retention behaviour and peak shape of the test compounds on the likewise deactivated fused-silica capillaries very well.

THEORY

In contrast to polydimethylsiloxanes, in which siloxane bonds are broken at high temperatures to react with surface silanols[10], the bonding of PMHS with surface silanols proceeds through condensation[11]:

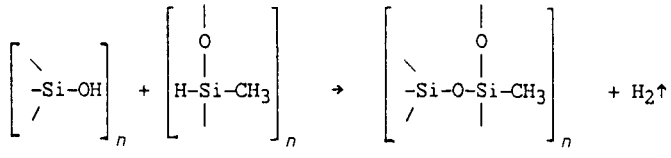

(1)

This reaction proceeds rapidly at moderate temperatures (around 290°C). If some physisorbed water is present on the surface, it interferes by hydrolysis of the silicon–hydrogen bond and intra- or intermolecular cross-linking of PMHS can occur according to the following successive reactions:

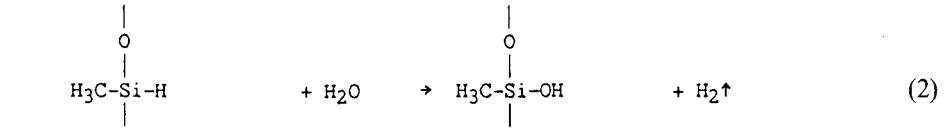

(2)

methylhydrosiloxane — methylhydroxysiloxane

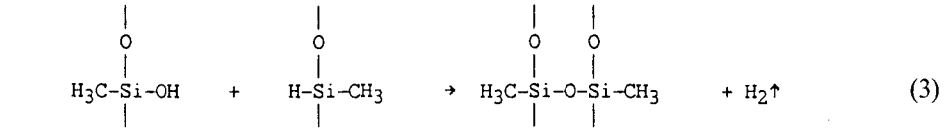

(3)

methylhydroxy-siloxane + methylhydro-siloxane → cross-linked PMHS

The presence of water also causes extra silanol activity, which should be reduced by the deactivation of the siliceous surface. Another problem can be the hydrogen content of the deactivating film. Unreacted hydrosiloxanes could exhibit hydrogen bonding with eluting compounds and interfere with the chromatographic process.

In this study, the effects of the reaction temperature, the film thickness and the water content of the surface are parameters which were considered.

EXPERIMENTAL

Materials

The PMHS material PS 122 (50% Si–H, η = 85 cS, liquid) was obtained from Petrarch Systems (Bristol, PA, U.S.A.). The amount of methylhydrodisiloxysilane groups, as determined by high-resolution (HR) ^{29}Si liquid NMR was 96 ± 1%. The only other significant signal in the ^{29}Si NMR spectrum was assigned to trimethylsiloxysilane (see below). The fused-silica capillary column material used was a gift from Chrompack (Middelburg, The Netherlands). Cab-O-Sil M5 (Cabot, Tuscola, IL, U.S.A.) was a gift from Heybroek & Co. Handelmij (Amsterdam, The Netherlands). The specific surface area of grade M5, according to the manufacturer's specification, is 200 ± 25 m^2/g; a value of 200 m^2/g was used in this study. The solvents were all of analytical-reagent grade from Merck (Darmstadt, F.R.G.), except the demineralized, deionized water, which was obtained with a Milli-Q system (Millipore, Bedford, MA, U.S.A.).

Deactivation and evaluation of fused-silica capillaries

A piece of 85 m × 0.25 mm I.D. fused-silica capillary column material was conditioned by flushing with helium at 290°C for 2 h. After drying, 90% of the fused-silica capillary was filled with 10% (w/w) hydrochloric acid and flame-sealed at

both ends. Hydrothermal treatment was performed by heating at 120°C for 90 min. After this treatment, the column was rinsed with deionized water until neutral and with methanol for 30 min. It was then dried again by flushing with helium at 140°C for 1 h and cut into five sections: four sections had lengths of *ca.* 18 m and the fifth section (*ca.* 12.5 m) was rinsed with deionized water and dried at room temperature by flushing with helium for 1 h.

These five capillaries were coated dynamically with a 1% (v/v) solution of PS 122 in *n*-pentane. A coating speed of approximately 25 cm min^{-1} was applied. According to Bartle[12], this results in a film thickness of approximately 10 nm (assumed viscosity, $1.8 \cdot 10^{-3}$ kg m^{-1} s^{-1}, and surface tension, $2.5 \cdot 10^{-2}$ N m^{-1}).

After coating with PMHS, the columns were flushed with helium for 15 min and flame-sealed. Silylation was carried out at different temperatures and reaction times (see Table I). Subsequently, the capillaries were carefully rinsed with 10 column volumes of dichloromethane to avoid plugging and conditioned by purging with helium at 290°C for 30 min.

For evaluation, the deactivated fused-silica capillary columns were connected via a zero-dead-volume connector (Valco Instruments, Houston, TX, U.S.A.), to a thick-film reference column (24 m × 0.32 mm I.D.) of CP-Sil 5 CB (Chrompack), a chemically bonded polydimethylsiloxane (film thickness, d_f = 1.1 μm; phase ratio = 72), showing as little adsorption as possible. In this way column evaluation can be performed with mixtures. It allows the observation of peak shapes, measurements of column polarity by means of retention indices and quantitative comparison of column activities for differently deactivated capillaries.

The connected columns were placed in a Carlo Erba (Milan, Italy) Model 5300 gas chromatograph equipped for split injection and flame ionization detection (FID). Helium was used as the carrier gas. The test runs were performed isothermally at 110°C and chromatograms were recorded with an SP 4290 integrator with a 256K data memory (Spectra-Physics, San Jose, CA, U.S.A.). The injector and detector temperature were each 250°C.

A test mixture consisting of activity markers for various active sites on the column wall before or after deactivation or coating is specified in Table II. It was used for the determination of column wall activity with respect to adsorption.

The solute test mixture contained ten components, five C_{10}–C_{14} *n*-alkanes and

TABLE I
DEACTIVATED FUSED-SILICA CAPILLARIES

Column No.	*Length (m) (I.D. 0.25 mm)*	*Silylation*		*Special treatment*
		Temperature(°C)	*Time (h)*	
1	17.90	260	2	–
2	17.90	290	2	–
3	17.70	310	2	–
4	17.90	290	8	–
5	12.65	290	2	Rinsed with water before coating
6[a]	17.90	–		Reconditioned at 290°C for 65 h

[a] Column 2.

TABLE II
TEST MIXTURE FOR EVALUATION OF DEACTIVATED CAPILLARIES

Elution order on CP-Sil 5 CB	*Compound*	*Symbol*	*Concentration ($\mu g\ ml^{-1}$ cyclohexane)*	*Activity marker for*
1	Decane	10	119.0	–
2	1-Octanol	C_8-OH	112.4	Exposed siloxane bonds, weak
3	2,6-Dimethylphenol	DMP	118.3	Exposed basic sites, strong
4	Undecane	11	116.6	–
5	2,6-Dimethylaniline	DMA	114.7	Exposed acid silanol, strong
6	Dodecane	12	114.4	–
7	1-Aminodecane	Am	116.4	Shielded acid silanol, weak
8	Tridecane	13	107.8	–
9	Nicotine	Nic	121.0	Acid silanol, weak
10	Tetradecane	14	128.4	–

five compounds susceptible to various column wall activities. The mean linear velocity of the carrier gas in the deactivated capillaries was kept between 30 and 35 cm s^{-1}; the velocity in the reference column was typically about 25 cm s^{-1}. The splitting ratio varied between 1:50 and 1:100. The injection volume was 1 μl, corresponding to an amount on the column of typically 1–3 ng for each component.

After the first evaluation, column 2 was reconditioned for 65 h at 290°C under helium and tested again as column 6. The original fused-silica capillary column material was also tested and for comparison the test mixture was also injected on to the reference column.

Kováts retention indices were calculated taking the elution time of methane as the dead time. Peak areas were normalized to *n*-decane = 100% and corrected for relative weight, but were not corrected for FID response factors.

Silylation of Cab-O-Sil and ^{29}Si solid-state NMR measurements

Cab-O-Sil M5 was pretreated by ignition at 720°C and rehydrated as described previously[9]. Part of the Cab-O-Sil was dried further over phosphorus pentoxide in a vacuum desiccator for several weeks and will be referred to as "dry Cab-O-Sil". Another part of the Cab-O-Sil was conditioned in air over a saturated solution of potassium bromide (84% relative humidity). This batch of Cab-O-Sil contained 5.5% (w/w) of water, which corresponds to 15.3 μmol m^{-2} siliceous surface. This batch will be referred to as "wet Cab-O-Sil".

The dry Cab-O-Sil was coated with the equivalent of 0.98 and 0.20 g of PMHS per gram, resulting in a "thick-film" coating of 5 nm and a "thin-film" coating of 1 nm thickness, respectively. For this purpose 10% (v/v) PMHS was dissolved in *n*-pentane and added to the required amount of Cab-O-Sil. The *n*-pentane was evaporated slowly under reduced pressure in a rotary evaporator at room temperature. The coated Cab-O-Sil was dried further in an oven at 100°C under atmospheric pressure.

The wet Cab-O-Sil was coated with 0.93 and 0.19 g of PMHS per gram, resulting in films of the same thickness as described above. After evaporation of the *n*-pentane,

the coated Cab-O-Sil was conditioned in a GC oven with temperature programming from 40 to 80°C at 5°C/min followed by 15 min at 80°C to prevent evaporation of adsorbed water.

About 0.4 g of coated Cab-O-Sil was placed in a quartz glass reaction ampoule (20 cm × 1 cm I.D., wall thickness 1 mm). A constriction was drawn in the middle of the tube.The tube was evacuated twice while cooled in dry-ice because of the volatility of some short linear and cyclic methylhydrosiloxane polymers and of the remaining water. It was filled with helium to atmospheric pressure both times. Finally, the ampoule was sealed to give a volume of about 8 ml.

After sealing, the ampoule was wrapped in aluminium foil, placed in a well ventilated oven and heated at the required temperature for several hours. After silylation the ampoule was opened and the contents were washed twice with dichloromethane and dried overnight in a vacuum oven at 110°C. Table III lists the silylated Cab-O-Sil samples. The carbon contents of a few silylated Cab-O-Sil samples were obtained with a Perkin-Elmer (Norwalk, CT, U.S.A.) Model 240 Analyzer.

With these samples, various solid-state ^{29}Si NMR measurements were carried out in order to gain information about the chemical properties, the nature and the mobility of the deactivating film at the silicious surface. Solid-state ^{29}Si NMR spectra were obtained on a Bruker CXP 300 spectrometer at 59.63 MHz. The samples were spun at *ca.* 3.5 kHz using aluminium oxide rotors of the standard Bruker double-bearing type.

From the 5-nm PMHS-coated Cab-O-Sil samples, ^{29}Si MAS NMR spectra were obtained with a pulse interval of 10 s, an acquisition time of 100 ms and an accumulation of typically 256 free induced decays (FIDs) in 4K data points. Prior to

TABLE III
PMHS MODIFIED CAB-O-SIL SAMPLES AND ^{29}Si SOLID-STATE NMR MEASUREMENTS

Sample	*Film thickness (nm)*	*Silylation*		*Water content [% (w/w) with respect to PMHS]*	*^{29}Si NMR[a] measurements*
		Temperature (°C)	*Time (h)*		
1	5	240	12	–	MAS
2	5	280	12	–	MAS, CT
3	5	320	12	–	MAS
4	5	360	12	–	MAS, CT
5	5	290	4	5.9[b]	MAS, CT
6	5	290	4	–	MAS, CT
7	1	280	8	–	CP-MAS, CT
8	1	300	8	–	CP-MAS
9	1	320	8	–	CP-MAS
10	1	360	8	–	CP-MAS
11	1	280	8	29.6[b]	CP-MAS
12	1	320	8	29.6	CP-MAS
13	1	360	8	29.6	CP-MAS

[a] MAS = magic-angle spinning; CT = contact-time variation experiments; CP-MAS = cross-polarization magic-angle spinning.

[b] 5.5% (w/w) water with respect to Cab-O-Sil.

Fourier transformation the data files were zero-filled to 16K data points. The spectral width was 20 kHz and no line broadening was applied.

From the 1-nm PMHS-coated Cab-O-Sil samples ^{29}Si CP-MAS NMR spectra were obtained using a contact time of 15 ms, a pulse interval of 5 s and an acquisition time of 25.6 ms. Typically 500 FIDs were accumulated in 1K data points, zero-filled to 8K prior to Fourier transformation. The spectral width was 20 kHz. A line broadening of 15 Hz was used prior to zero-filling and Fourier transformation.

For cross-polarization experiments with variable contact times, a series of nineteen contacts ranging from 0.1 to 40 ms were applied. Typically 6 × 50 FIDs were accumulated for each contact. The other spectral parameters were the same as above, except for a line broadening of 10 and 30 Hz prior to zero-filling and Fourier transformation for the 5- and 1-nm PMHS-coated Cab-O-Sil, respectively.

RESULTS AND DISCUSSION

Characterization of the PMHS used

An HR ^{29}Si NMR spectrum of the PMHS reagent used (PS 122) is given in Fig. 1. One sharp signal is detected at −34.7 ppm upfield from tetramethylsilane (TMS). This signal is assigned to the methylhydrodisiloxysilane groups (D_2H or methylhydrosiloxanes) of the various polymers present in this reagent[13]. The relative amount of trimethylsiloxysilane end groups (M_1) (signal at +9 ppm) is less than 5% in this sample. This indicates that only a small amount of short linear polymers is present in PS 122. A gas chromatographic–mass spectrometric (GC–MS) analysis of PS 122 on

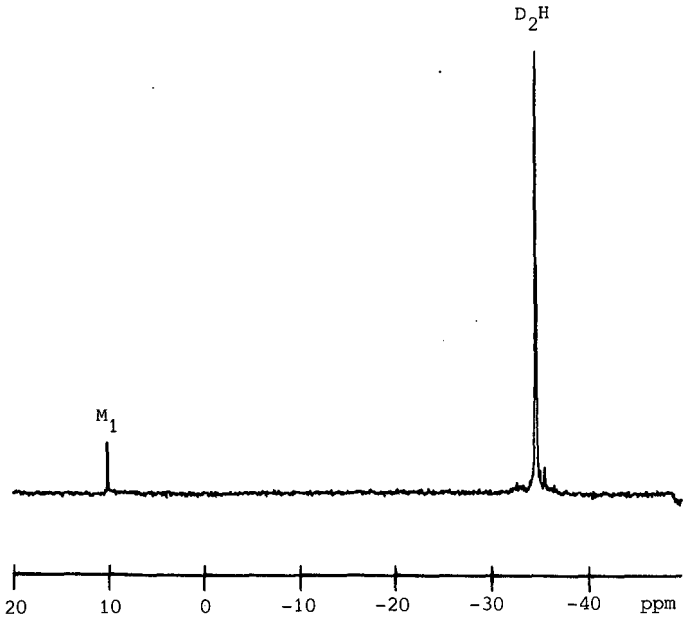

Fig. 1. HR ^{29}Si NMR spectrum of the PMHS reagent, PS 122, used for deactivation. N_s = 23 000; pulse interval time, 10 s; acquisition time, 100 ms.

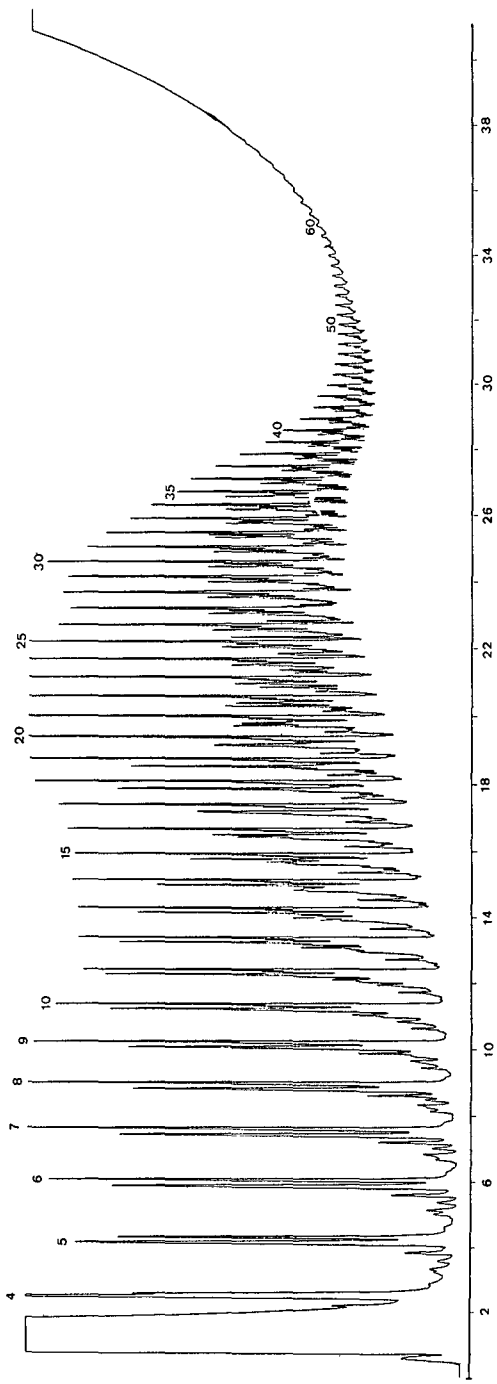

Fig. 2. Chromatogram of the PMHS reagent PS 122. Chromatographic conditions: OV-1 column (25 m × 0.32 mm I.D.), $d_f = 0.1$ μm; carrier gas, helium; temperature programme, initial temperature 80°C for 2 min, increased at 10°C min^{-1} to 380°C, then at 5°C min^{-1} to 410°C. The peak numbers represent the methylhydrosiloxysilane units in the various polymers.

a thin-film apolar column showed an extremely large dispersion of both cyclic and linear polymethylhydrosiloxanes. The chromatogram of PS 122 recorded with FID (Fig. 2) starts with cyclic and linear tetramers and continues up to 66 methylhydrosiloxysilane units. Probably polymers containing over 70 units are present in this sample.

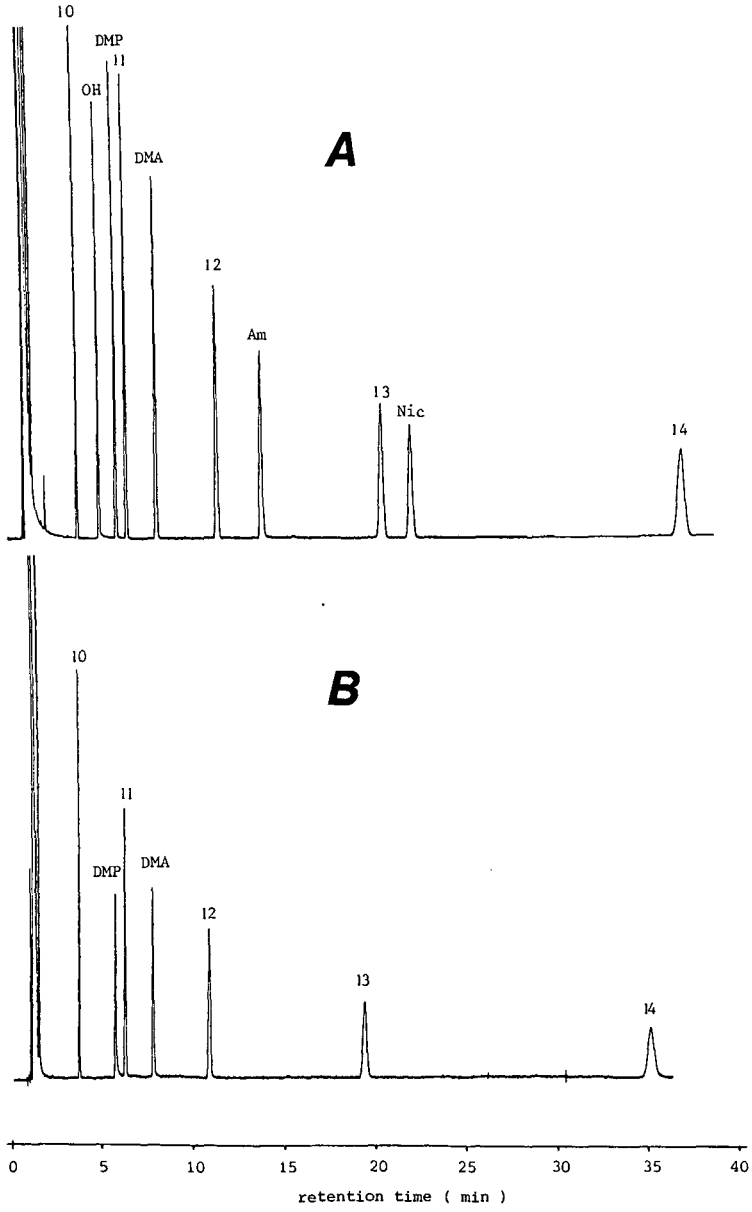

Fig. 3. Representative chromatograms of the thick-film reference column (A) and an untreated capillary (B) characterized with the double column system. Test conditions: helium carrier gas, isothermal operation at 110°C. For peak identifications of the test mixture, see Table II.

Evaluation of the PMHS-deactivated fused-silica capillaries

The recorded chromatograms of the reference column and the reference column connected to a piece of untreated fused-silica capillary column are shown in Fig. 3. Corresponding Kováts retention indices and normalized peak areas for all evaluated fused-silica capillaries and the reference column are given in Table IV.

The untreated piece of fused-silica capillary showed strong adsorption for all selective compounds in the test mixture. 1-Octanol (C_8-OH), 1-aminodecane (Am) and nicotine (Nic) did not elute at all, and 2,6-dimethylphenol (DMP) and 2,6-dimethylaniline (DMA) showed tailing and a decrease in the normalized peak areas, indicating strong acid silanol activity and the presence of basic sites.

Optimum deactivation was observed after silylation at 290°C for 2 h (column 2, Fig. 4), which is in agreement with results reported by Woolley *et al.*[2,11]. The peak shapes of all components as eluted from the dual column system were similar to those on elution from the reference column alone. Deactivation at a lower temperature (260°C, column 1) resulted in a substantial increase in the wall activity, especially towards Am and Nic, which did not elute, and DMA, which partly eluted. This indicates that acid activity remained on the inner wall. Deactivation took place but was not yet completed, which is also evident from adsorption of C_8-OH; interaction with exposed siloxane bridges[5,7] is responsible for this adsorption.

Deactivation at a higher temperature (310°C, column 3) or with a longer silylation time (8 h, column 4) demonstrated remaining, probably shielded, weak acid silanol activity. DMP and DMA showed no interactions with the column wall, but C_8-OH was adsorbed mildly, again indicating little activity of exposed siloxane bridges. A small amount of water on the inner surface prior to coating (column 5) is detrimental for the deactivating film formed during silylation (see Fig. 4). The selective compounds were all partly adsorbed and showed increased retention indices. This deactivated capillary demonstrated the largest adsorption of C_8-OH and DMP.

Reconditioning column 2 at 290°C for 65 h gave no increase in the activity of the column wall (column 6, Table IV). All components eluted in the same way as before

TABLE IV

NORMALIZED PEAK AREAS (*NA*) AND RETENTION INDICES (*I*) FOR MARKER COMPOUNDS IN THE TEST MIXTURE DETERMINED WITH A DUAL-COLUMN METHOD

Column No.	*Marker compound*									
	1-Octanol		*DMP*		*DMA*		*Aminodecane*		*Nicotine*	
	NA	*I*	*NA*	*I*	*NA*	*I*	*NA*	*I*	*NA*	*I*
Reference column	80	1050.2	94	1082.5	100	1139.2	96	1233.3	81	1312.6
1	66	1064.1	91	1076.3	74	1132.7	0	–	0	–
2	80	1050.3	94	1082.9	99	1139.8	95	1233.4	81	1313.0
3	65	1050.0	92	1080.4	96	1136.8	86	1235.5	75	1312.6
4	64	1049.2	93	1078.4	97	1134.8	88	1233.0	70	1309.2
5	43	1051.3	80	1083.3	84	1140.8	20	1239.4	26	1314.6
6 (*ex.* 2)	79	1049.7	93	1076.6	98	1137.1	93	1234.5	80	1313.0
7[a]	0	–	76	1082.5	85	1139.6	0	–	0	–

[a] Untreated fused-silica capillary (length 18.1 m).

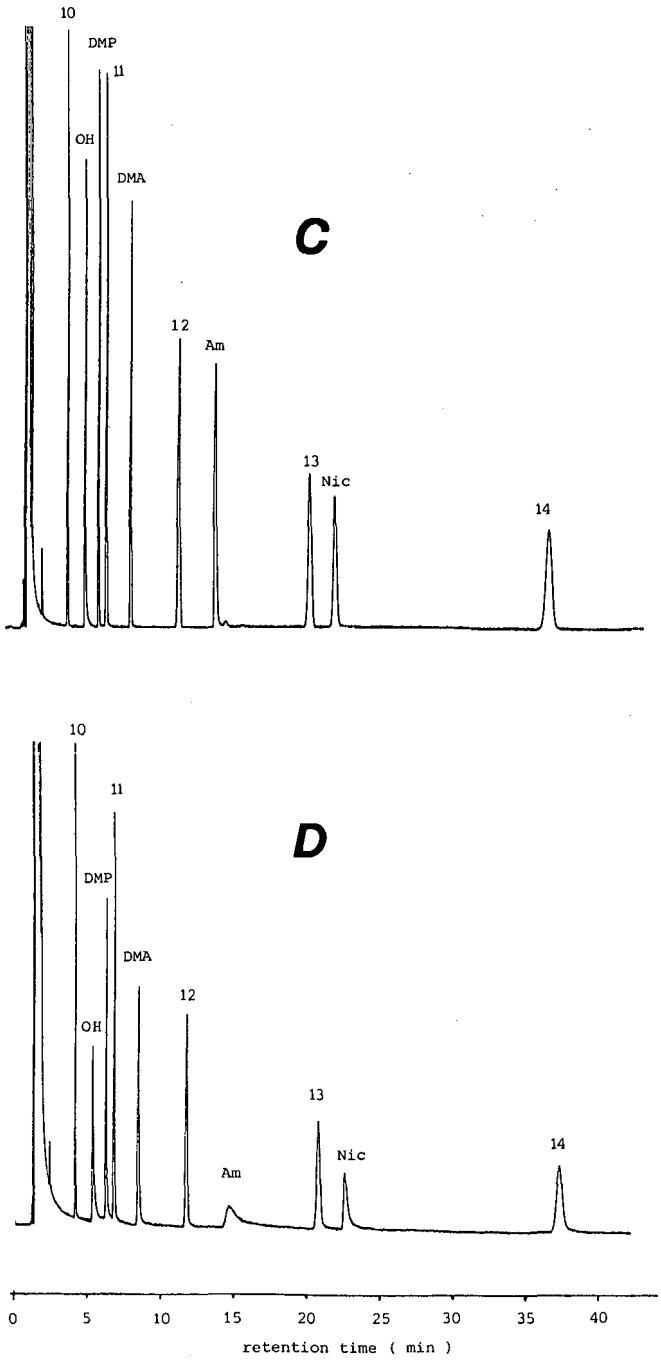

Fig. 4. Representative chromatograms of the optimum deactivated capillary (C) and the prewetted capillary, deactivated under optimum conditions (D). Test conditions: helium carrier gas, isothermal operation at 110°C. For peak identifications of the test mixture, see Table II.

conditioning. The column showed very good thermal stability, even after this long period of conditioning. The resistance towards solvents was evaluated by rinsing with *n*-pentane, dichloromethane and liquid carbon dioxide. No change in normalized peak areas or retention indices was noticed.

^{29}Si NMR measurements of PMHS-silylated Cab-O-Sils

The average carbon content determined after washing and drying of thick-film deactivated Cab-O-Sil was about 9.5% (w/w). Two exceptions were observed: the sample silylated at 240°C showed a lower content, *viz.*, 8.0% (w/w) carbon, probably caused by washing of unreacted PMHS from the surface, and the silylated wet Cab-O-Sil showed a 9.8% (w/w) carbon content, owing to slightly more cross-linking.

The formation of various siloxysilane surface moieties on Cab-O-Sil coated with a thick-film PMHS, silylated at temperatures ranging from 240 to 360°C for 12 h (Cab-O-Sil samples 1–6), was investigated by ^{29}Si MAS NMR. The spectra are presented in Fig. 5 and Table V lists chemical shifts most relevant to this paper. The relative ratios of the ^{29}Si MAS NMR signals, representing siliceous surface moieties, of Cab-O-Sil samples 1–6 are listed in Table VI.

From these spectra it can be concluded that the silylation products have chemical shifts mainly in the −35 ppm region, indicating that only methylhydrosiloxanes are anchored to the surface. The shape of the narrow signals at −35.3 and −36.1 ppm indicates that the methylhydroxysiloxane units are still part of mobile polymer chains now anchored to the silica surface. This was confirmed by contact-time variation experiments (see below). The methylhydrodisiloxysilane group with a chemical shift at −35.3 ppm has two identical unreacted neighbouring groups, whereas the group with a chemical shift at −36.1 ppm has one methyltrisiloxysilane (T_3) on the α-position[13] (see Fig. 6). This T_3 group is responsible for intra- and intermolecular cross-linking of the polymer chains (see reaction 3) or surface attachment at the silica (see reaction 1). Most of the T_3 groups on these silylated Cab-O-Sil samples were formed with the silica surface (see the appearance of a broad signal at −66.2 ppm). With increasing temperature the polymer chains degrade and react with the surface.

TABLE V

SILOXANE/SILANE FUNCTIONALITY NOTATION, TYPICAL ^{29}Si CHEMICAL AND SUBSTITUENT-INDUCED SHIFTS

Compound	*Chemical (spectral) functionality*	*Topological (network) functionality*	*Code*	*Chemical shift (ppm downfield from TMS)*
Trimethylsiloxysilane	M	1	M_1	+9
Methylhydrodisiloxysilane[a]	D	2	D_2H	−36
Methylhydroxydisiloxysilane	T	2	T_2	−55
Methyltrisiloxysilane	T	3	T_3	−66
Hydroxysiloxane	Q	3	Q_3	−101
Tetrasiloxysiloxane	Q	4	Q_4	−110

[a] Substituent-induced shift (ppm downfield from TMS) for methylhydrodisiloxysilane: $D_2H \cdot D_2H \cdot D_2H$ −35.3 ppm = D_2H; $D_2H \cdot D_2H \cdot T_3$ −36.1 ppm = D_2H', one methyltrisiloxysilane on the α-position (see Fig. 6).

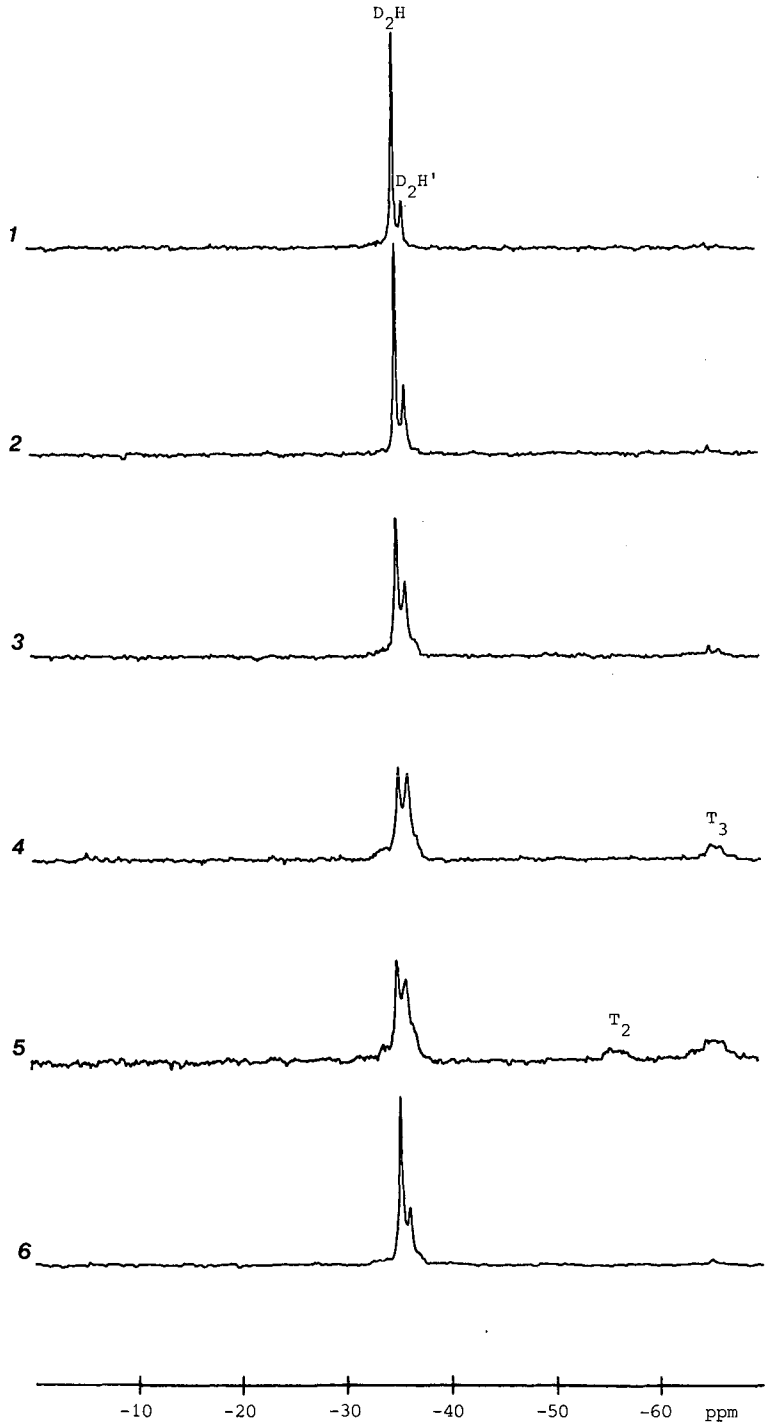

Fig. 5. ^{29}Si MAS NMR spectra of thick-film PMHS-silylated Cab-O-Sil samples 1–6. N_s = 256; pulse interval time, 10 s; acquisition time, 100 ms.

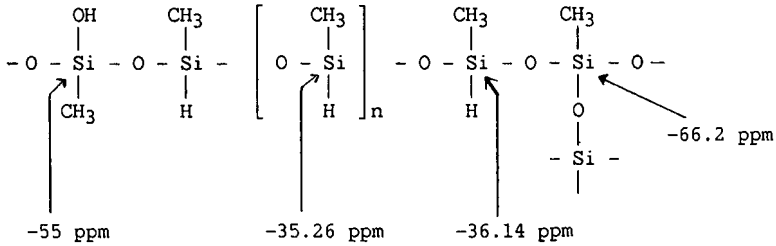

Fig. 6. Chemical shifts of possible surface siloxane moieties after silylation with PMHS.

Using contact-time variation experiments in ^{29}Si CP-MAS NMR, the mobilities of the methylhydrodisiloxysilane groups (D_2H and D_2H') and, if present, of the methyltrisiloxysilane (T_3) groups were determined. Contact-time (CT) curves of Cab-O-Sil samples 2 (280°C/12 h) and 4 (360°C/12 h) are presented in Fig. 7.

Solid-state ^{13}C NMR contact-time variation experiments showed similar curves for the Cab-O-Sil samples to those obtained with octyl-modified reversed-phase high-performance liquid chromatographic (HPLC) silica in our laboratory[14], as shown in Fig. 8. For the two methyl groups and C_1 the maxima in the CT curves were between 5 and 10 ms, caused by the close connection to the rigid silica surface of these groups, resulting in only slight mobility. For C_4 and C_5 the maxima were about 25 ms, indicating greater mobility than for methyl and C_1 groups. The maximum for C_8 was above 30 ms, indicating a high mobility owing to the large distance to the surface bond.

The CT curves for sample 2 indicate that mobile methylhydrosiloxane chains are still present after silylation at 280°C. The maximum intensity for the signals in the −35 ppm region was observed for a contact time of *ca.* 27 ms. This equals the mobility of a C_6 group in the octyl chain in Fig. 8. The deactivating film can be conceived as two

TABLE VI

RELATIVE AMOUNTS OF ^{29}Si SOLID-STATE NMR SIGNALS OF SURFACE MOIETIES ON SILYLATED CAB-O-SIL SAMPLES

Cab-O-Sil sample No.	*^{29}Si NMR measurement*	*Relative ratio of ^{29}Si NMR signals*			
		D_2H	D_2H'	T_2	T_3
1	MAS	0.82	0.18	–	–
2	MAS	0.71	0.29	–	–
3	MAS	0.54	0.43	–	0.03
4	MAS	0.39	0.49	–	0.12
5	MAS	0.40	0.44	0.05	0.11
6	MAS	0.71	0.29	–	–
7	CP-MAS	–	0.55	–	0.45
8	CP-MAS	–	0.44	–	0.56
9	CP-MAS	–	0.37	–	0.63
10	CP-MAS	–	0.18	–	0.83
11	CP-MAS	–	0.31	0.05	0.64
12	CP-MAS	–	0.24	0.06	0.70
13	CP-MAS	–	0	0.10	0.90

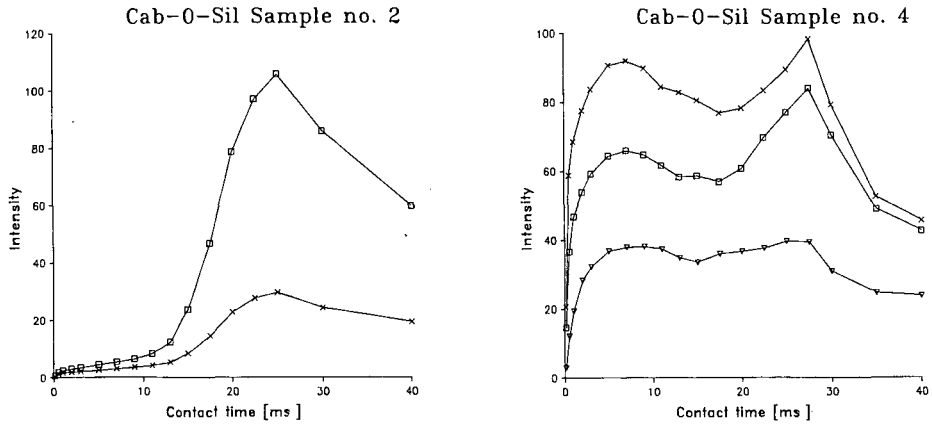

Fig. 7. Contact-time variation curves with observed chemical shifts for surface siloxane moieties of PMHS-silylated Cab-O-Sil samples 2 and 4. N_s = 300; pulse interval time, 10 s; acquisition time, 100 ms. Sample 2: □, −35.25; ×, −36.07 ppm. Sample 4: □, −35.45; ×, −36.27; ▽, −66.3 ppm.

layers: a dense cross-linked network near the surface anchored through methyltrisiloxysilane, only a few monolayers thick and with longer mobile methylhydrosiloxane polymers attached to this rigid layer (see Fig. 9). The total number of methyltrisiloxysilane cross-linking groups is very small. After silylation of 360°C the CT curves demonstrated at least two distinct maxima at contact times of *ca.* 7 and 27 ms, indicating that two coherent methylhydrosiloxysilane systems are present in the deactivating film: a small amount of mobile, slightly cross-linked methylhydrosiloxane polymer, similar to silylation at 280°C, on top of a rigid layer with many immobile small-chain segments anchored to the surface and intensely cross-linked polymers.
Cab-O-Sil sample 5 was originally a wet Cab-O-Sil coated with 5 nm of PMHS, silylated at 290°C for only 4 h. As a reference also a dry Cab-O-Sil was coated and silylated in the same way (Cab-O-Sil 6). Their ^{29}Si MAS spectra are shown in Fig. 5. The ratio between the signals at −35.3 and −36.1 ppm was influenced by the presence of water; more short-chain segments were present in the silylated film of sample 5. The amount of methyltrisiloxysilane (T_3) was increased by enhanced cross-linking and surface attachments and an extra signal at −55 ppm, corresponding to not yet cross-linked methylhydroxydisiloxysilanes (T_2), was detected (see reaction 2). These T_2 groups add extra silanol activity to the modified silica surface. CT curves were also recorded for Cab-O-Sil sample 5 and are presented in Fig. 10. The CT curves for Cab-O-Sil sample 6 were similar to those of sample 2 shown in Fig. 7. From the ^{29}Si MAS NMR spectrum one would expect that a more rigid extensively cross-linked layer

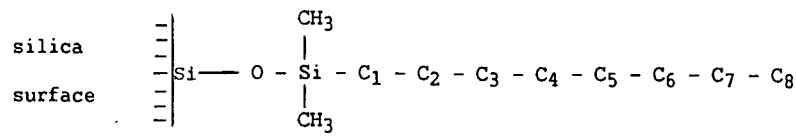

Fig. 8. Octyl-modified reversed-phase HPLC silica.

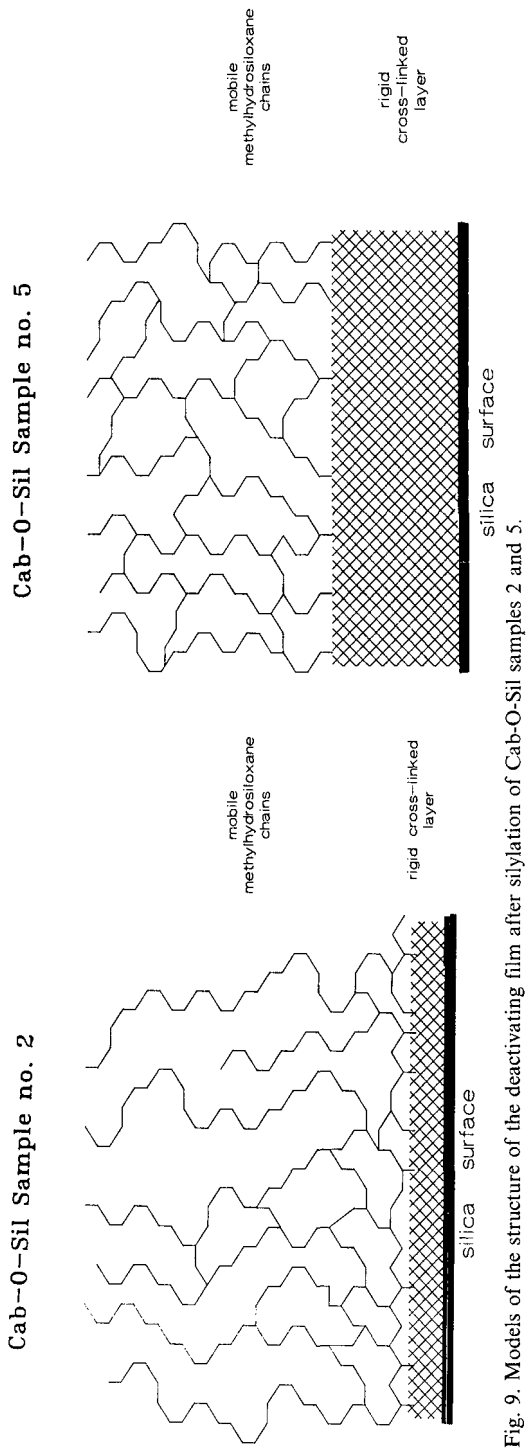

Fig. 9. Models of the structure of the deactivating film after silylation of Cab-O-Sil samples 2 and 5.

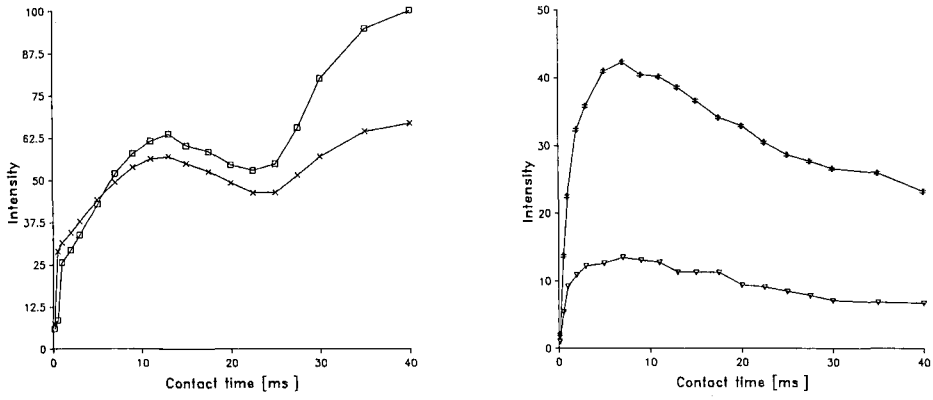

Fig. 10. Contact-time variation curves with observed chemical shifts for surface siloxane moieties of PMHS-silylated Cab-O-Sil sample 5. N_s = 300; pulse interval time, 10 s; acquisition time, 100 ms; line broadening, 10 Hz. □, −35.3; ×, −36.1; ▽, −56.8; +, −66.1 ppm.

was formed. This is shown by the CT curves for the T_2 and T_3 groups, but the CT curves for D_2H and D_2H' show a second maximum with an optimum contact time longer than 40 ms, again indicating long, flexible methylhydrosiloxane chains, probably on top of the rigid layer (see Fig. 9). In all thick-film deactivated Cab-O-Sil samples mobile methylhydrosiloxane chains were observed. This indicated the presence of exposed hydrogen groups as part of the deactivating film.

The carbon content of thin-film deactivated Cab-O-Sil silylated at 280°C was about 4.4% (w/w). This suggested that a deactivating film more than a few monolayers thick was formed. However, from the 1-nm coated Cab-O-Sil samples it was not possible to obtain ^{29}Si MAS NMR spectra within a reasonable time, because of the long relaxation times. This also confirms the more rigid structure of the deactivating film.

The ^{29}Si CP-MAS NMR spectra of silylated Cab-O-Sil samples 7–10 coated with a thin PMHS coating are shown in Fig. 11. These samples demonstrate a structure of the siloxane moieties different from the thick film; the methylhydrosiloxane chains were degraded. The remaining methylhydrodisiloxysilanes (mainly D_4H') were anchored to the surface via methyltrisiloxysilanes and formed a rigid, fairly thin film, as is demonstrated by the CT curves in Fig. 12. Pronounced maxima for D_2H' and T_3 groups are observed between 10 and 20 ms. These groups exhibit approximately the same mobility as C_3 (Fig. 8) in the octyl chain of a reversed-phase C_8 silica. The silylated films consisted of a densely cross-linked network of D_2H' and T_3 groups anchored to the surface via T_3 groups.

As the temperature increased from 280 to 300°C, the amount of D_2H and D_2H' groups decreased and the amount of T_3 groups increased. Above 300°C no significant changes in the amount of T_3 groups were observed. Deactivation of wet Cab-O-Sil with 1 nm of PMHS even caused a total loss of methylhydrodisiloxysilane moieties at a silylation temperature of 360°C owing to conversion into methyltrisiloxysilanes (T_3) and to a smaller extent into methylhydroxydisiloxysilanes (T_2) (see also Fig. 11). The total amount of T_2 groups did not change with increasing temperature. These

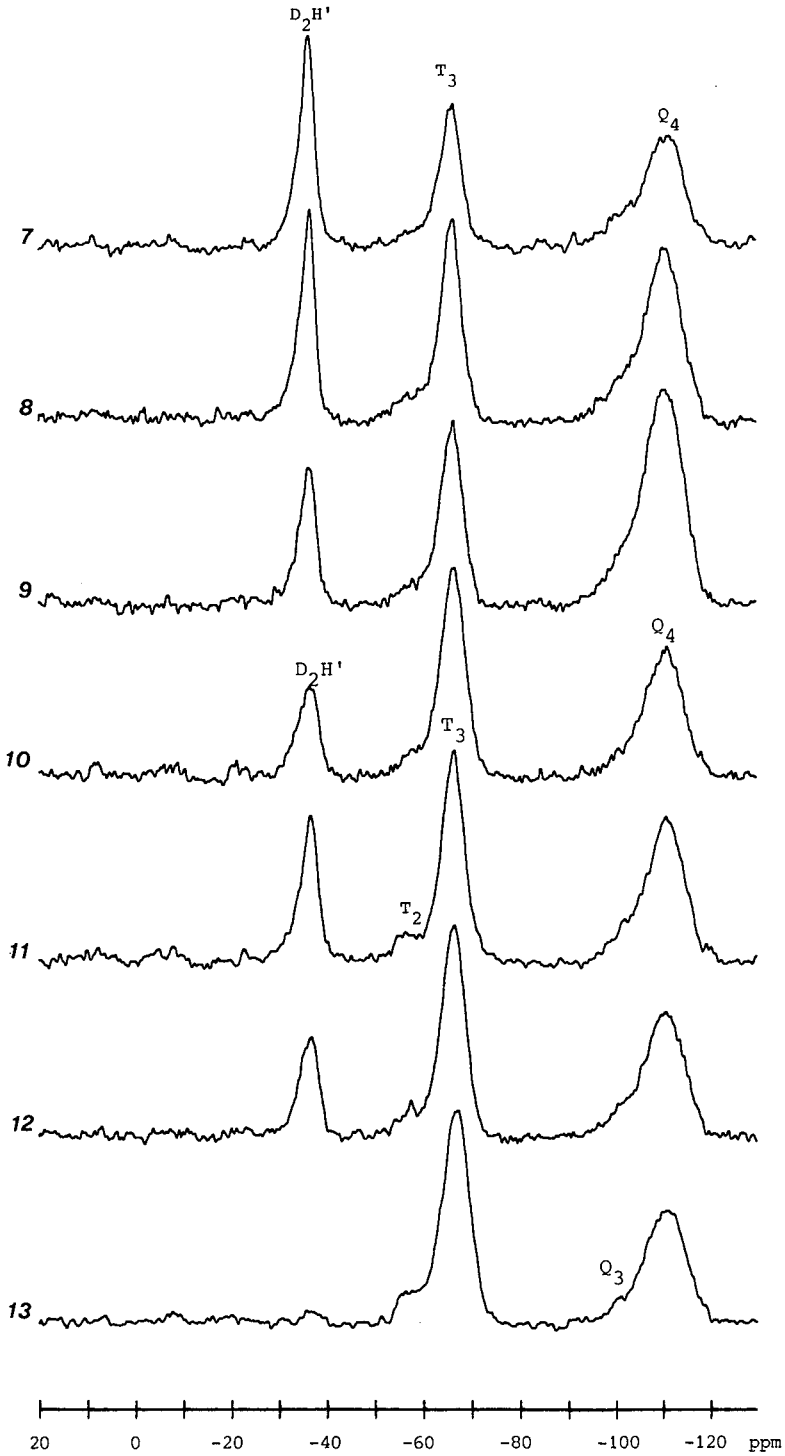

Fig. 11. ^{29}Si CP-MAS NMR spectra of thin-film PMHS-silylated Cab-O-Sil samples 7–13. N_s = 500; pulse interval time, 5 s; contact time, 15 ms; acquisition time, 25.6 ms; line broadening, 15 Hz.

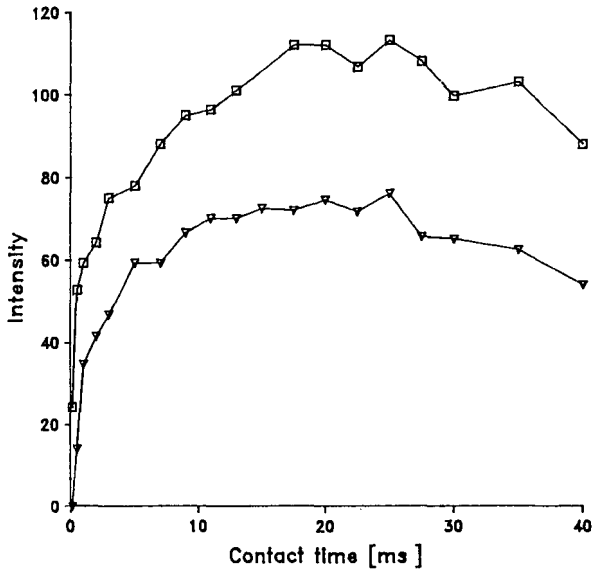

Fig. 12. Contact-time variation curves with observed chemical shifts for surface siloxane moieties of PMHS-silylated Cab-O-Sil sample 7. N_s = 300; pulse interval time, 5 s; acquisition time, 25.6 ms; line broadening, 30 Hz. □, −36.2; ▽, −66.1 ppm.

unconverted T_2 groups add extra silanol activity to the silylated surface, as mentioned above. At silylation temperatures around 290°C a remaining substantial amount of methylhydrodisiloxysilanes was still detected (see Table VI), although the broad signal at −36.5 ppm implied that most of these groups had converted neighbours and were part of a rigid and thus shielding film.

The 1-nm PMHS films showed different physical and chemical properties to deactivating films silylated after coating with 5 nm of PMHS. Relatively more T_3 groups were observed, causing a rigid and dense network. No long, flexible methylhydrosiloxane polymer chains were detected. The amounts of silicon hydride groups in the network were relatively low in comparison with thick films, but not negligible. At silylation temperatures below 300°C over 50% of the surface siloxane groups contained hydrogen when dry Cab-O-Sil was deactivated. Only part of these hydrogen groups will be shielded by the rigid structure.

Silylation of Cab-O-Sil as a model for deactivation of fused silica

In any comparison between results obtained with model chemistry, as introduced in this and earlier papers[5,9,10], on the one hand, and actual deactivation of fused-silica columns as judged by GC, on the other, the thickness of the deactivating film plays a crucial role. It was shown above with solid-state ^{29}Si NMR that the natures of the films obtained on Cab-O-Sil on deactivation with PMHS layers of 1 and 5 nm differ considerably.

With fused-silica columns, according to equations for dynamic coating as applied by Bartle[12], the thickness was *ca.* 10 nm. Consequently, one should compare these fused-silica capillaries with thick-film silylated Cab-O-Sil samples as prepared in

this study. After silylation of Cab-O-Sil with PMHS for several hours at 280–290°C, with a stoichiometry corresponding to a film thickness of 5 nm, an anchored network was obtained close to the surface of Cab-O-Sil with only slight cross-linking (see above). Of the total methylhydrosiloxane units that were attached to the surface, only *ca.* 20% occupied α-positions with respect to surface attachment or cross-linking after silylation. It proved difficult to detect the methyltrisiloxanes (directly attached to the Cab-O-Sil surface) by ^{29}Si MAS NMR, mainly because of their relatively low concentration of *ca.* 5–10%. In spite of this apparent low conversion of methylhydrosiloxanes to methyltrisiloxysilanes which attached the polymer chain tightly to the silica surface, the surface was adequately covered and deactivated, as shown by the GC experiments (see Fig. 4).

In earlier reports, the high deactivation efficiency of various PMHS forms and other organosilicon hydride deactivating agents was attributed to the almost complete conversion of hydrogen–silicon bonds into siloxane bonds (reactions 1–3). In this study we observed that methylhydrosiloxanes show a high reactivity towards silanol groups, in particular to those which are Brønstedt acids. In order to achieve a more or less complete conversion of the silicon hydride groups, a temperature of *ca.* 360°C is required. In our opinion it seems that one of the main advantages of silylating agents containing silicon hydride moieties is connected with the small (Van der Waals) dimensions of these groups rather than with their allegedly high intrinsic reactivities[1,11,15]. The lack of reaction propensity of the chains towards the surface silanol groups, however, does not prevent a tight attachment of the chain to the surface (the surface silanol groups have disappeared). Further, cross-linking of the chains near the surface, although of low overall concentration, provides additional surface screening. Remaining silicon hydride groups on the chains apparently do not interfere with the elution of the appropriate test components in GC experiments.

Deactivation under more severe conditions (higher temperatures and/or longer reaction periods) mainly caused an increase in the extent of cross-polymerization near the surface. However, the mobilities of the chains protruding upwards from this layer were not affected significantly, as was shown by variable-contact time ^{29}Si CP-MAS NMR (see above). An increase in the adsorption of 1-octanol by cross-linking products became noticeable in the GC experiments. Cross-linking serves to increase the total amount of siloxane bonds in the deactivating film. Intuitively, one would expect these siloxane moieties to be rather shielded (inaccessible), but this seems only partially true when coating a column wall with a thick film (*ca.* 10 nm) of PMHS. Woolley *et al.*[2] reported optimum silylation after 4 h at 300°C with PMHS, after which a very thin deactivating film was formed. In the determination of the capacity of these films, a film thickness of 1–4 monolayers was assumed. An exact experimental determination from the chromatographic retention of such a film thickness is hardly feasible. Therefore, we assume here that a cross-linked layer near the surface is formed with a thickness similar to that postulated by Woolley *et al.* Moreover, on top of these initial layers we observed long, mobile methylhydrosiloxane chains. These chains could play a role in the anchoring of phenyl-containing stationary phases during radical-induced cross-linking[16]. A complete rigid, densely cross-linked film exists only after silylation at optimum temperature of a thin-film coated silica.

The influence of water, present at the silica surface, on the silylation is evident; advanced cross-linking occurs and a relatively thick rigid layer is formed near the

surface containing methyltrisiloxysilanes, methylhydrodisiloxysilanes and a small amount of active, unreacted methylhydroxydisiloxysilanes. These hydroxyl groups caused strong adsorption of all critical components present in the test mixture in GC. When coated with a thick film again a top layer of mobile methylhydrosiloxane chains appears after silylation at 280°C. Very small amounts of water are necessary for cross-linking of a thin rigid layer near the surface and increase the surface anchoring of the methylhydrosiloxane network. The appropriate amount of water is present after severe leaching, extensive flushing with water and drying at a moderate temperature of 140°C. Remaining, probably physisorbed, water influences the structure and attachment of the deactivating film near the surface. Too high a content of water yields unreacted hydroxyl groups and increased activity of the surface. Further, the thickness of the densely cross-linked layer is increased proportionally with the amount of water present at the surface before silylation.

CONCLUSIONS

In conclusion, PS 122 is an efficient PMHS-deactivating reagent for fused-silica capillary column walls for the preparation of non-polar columns. The advantage of organosilicon hydride agents for deactivation of fused-silica capillary columns is the small (van der Waals) dimension of the silicon hydride and their selective reactivity towards the Brønstedt acid silanol groups. The intrinsic reactivity of silicon hydride to form siloxane bonds is not sufficient to provide total conversion of the silicon hydride groups. Important differences in the nature and structure of the deactivating films on the silica surface have been established between coatings with a thickness of 5 or 1 nm. When coated with a 5-nm film, the remaining methylhydrosiloxane groups are part of anchored mobile longer polymer chains protruding upwards on top of a densely cross-linked network of polymers near the surface. Physisorbed water present at the surface before silylation provides a good deactivating film on the fused-silica capillary column wall under optimum silylation conditions of 290°C for 2 h. Too high a content of water present before silylation leads to increasing activity caused by exposed siloxane bonds and methylhydroxydisiloxy silanes in the polymer network.

The optimum deactivating film exhibits excellent thermal stability and solvent resistance. No decrease in either film thickness or deactivation was observed on the silylated Cab-O-Sil samples or inside the deactivated capillaries after the completed deactivation of these surfaces.

ACKNOWLEDGEMENTS

The investigations were supported by The Netherlands Foundation for Chemical Research (SON) with financial aid from The Netherlands Organization for Scientific Research (NWO). The authors thank Chrompack for supplying the capillary column material. Grateful acknowledgement is due to Mrs. Denise Tjallema for preparing the manuscript.

REFERENCES

1 C. L. Woolley, R. C. Kong, B. E. Richter and M. L. Lee, *J. High Resolut. Chromatogr. Chromatogr. Commun.*, 7 (1984) 329–332.
2 C. L. Woolley, K. E. Markides and M. L. Lee, *J. Chromatogr.*, 367 (1986) 23–34.
3 O. v. Berkel, H. Poppe and J. G. Kraak, *Chromatographia*, 24 (1987) 739–744.
4 B. W. Wright and R. D. Smith, *J. High Resolut. Chromatogr. Chromatogr. Commun.*, 9 (1096) 73–77.
5 G. Rutten, J. de Haan, L. van de Ven, A. van de Ven, H. van Cruchten and J. Rijks, *J. High Resolut. Chromatogr. Chromatogr. Commun.*, 8 (1985) 664–672.
6 M. L. Lee, R. C. Kong, C. L. Woolley and J. S. Bradshaw, *J. Chromatogr. Sci.*, 22 (1984) 135–142.
7 K. Grob, Jr., G. Grob and K. Grob, *J. High Resolut. Chromatogr. Chromatogr. Commun.*, 156 (1978) 1–20.
8 G. Schomburg, H. Husmann and F. Weeke, *Chromatographia*, 10 (1977) 580–587.
9 G. Rutten, A. van de Ven, J. de Haan, L. van de Ven and J. Rijks, *J. High Resolut. Chromatogr. Chromatogr. Commun.*, 7 (1984) 607–672.
10 M. Hetem, G. Rutten, L. van de Ven, J. de Haan and C. Cramers, *J. High Resolut. Chromatogr. Chromatogr. Commun.*, 11 (1988) 510–516.
11 C. L. Woolley, K. E. Markides and M. L. Lee, *J. Chromatogr.*, 367 (1986) 9–22.
12 K. D. Bartle, *Anal. Chem.*, 45 (1973) 1831–1836.
13 E. A. Williams and J. D. Cargiolli, *Annu. Rep. NMR Spectrosc.*, 9 (1979) 247–249.
14 L. van de Ven and J. de Haan, personal communication.
15 C. L. Woolley, K. E. Markides, M. L. Lee and K. D. Bartle, *J. High Resolut. Chromatogr. Chromatogr. Commun.*, 9 (1986) 506–514.
16 W. Noll, *Chemie und Technologie der Silicone*, Verlag Chemie, Weinheim, 2. Auflage, 1968, Section 2.4.1.

Journal of Chromatography, 477 (1989) 25–38
Elsevier Science Publishers B.V., Amsterdam — Printed in The Netherlands

CHROM. 21 453

DOSIER- UND TRENNSÄULENSCHALTSYSTEME FÜR DIE HOCHAUFLÖSENDE GASANALYTIK

FRIEDHELM MÜLLER*, HEINZ MÜLLER und HORST STRAUB
Siemens AG, Analysentechnik, Östliche Rheinbrückenstrasse 50, 7500 Karlsruhe 21 (F.R.G.)

SUMMARY

Gas sampling- and column-switching systems in high-resolution gas analysis

The introduction of capillary separation columns with solid porous layers, so-called PLOT columns for the gas chromatographic analysis of gases causes the substitution of conventional techniques which were developed for packed separation columns by systems compatible to capillary columns. This particularly applies to automatic gas sampling- and column-switching systems. It is described that new pressure- and flow-controlled switching techniques are remarkably qualified for high-resolution gas chromatography. A representative example of application is given to demonstrate the development and relevancy to the practice of such systems.

EINLEITUNG

Die Gaschromatographie (GC) ist die Methode der Wahl zur vollständigen Analyse von mehr oder weniger komplex zusammengesetzten Gasmischungen. Gasanalytik ist ein wesentlicher Bestandteil der Gesamtanalytik in verschiedenen Industriezweigen wie z.B. chemische und petrochemische Industrie, Verfahrenstechnik, Energieversorgung, Umweltschutz und andere. Sie ist ein äusserst leistungsfähiges Instrument in den Bereichen Forschung und Entwicklung, Qualitätsüberwachung, Prozesskontrolle usw. und findet dementsprechend im Labor oder unmittelbar beim Prozess statt (off-line oder on-line). Bei den Gasen, die mittels GC bestimmt werden, handelt es sich oft um Edelgase, die sog. Inertgase H_2, O_2, N_2, ferner um die Verbrennungsgase CO und CO_2 sowie die leichten Kohlenwasserstoffe (KW) C_1–C_4 mit unterschiedlicher Struktur und unterschiedlichem Sättigungsgrad.

Die klassischen Methoden der Gasanalytik basieren auf dem Einsatz von gepackten Trennsäulen[1–5]. Entsprechend der enormen Vielfalt von Gasanalysen wurden Trennphasen unterschiedlicher Polarität und Trenncharakteristik entwickelt[6], d.h. dass die stationäre Phase auf das Trennproblem zumindest teilweise abgestimmt werden kann. Die Trennleistung gepackter Säulen ist jedoch in vielen Fällen nicht ausreichend, so dass komplex zusammengesetzte Gasproben bzw. Gasproben mit Komponenten aus unterschiedlichen Stoffgruppen nicht mit einer einzelnen Säule getrennt werden können. Eine Leistungssteigerung ist möglich durch

0021-9673/89/$03.50

Kombination von Trennsäulen mit unterschiedlichem Trennverhalten, d.h. letztendlich durch multidimensionale GC. Im Normalfall sind die Trennsäulen über mechanische Umschaltventile (Drehschieber- oder Membranventile) untereinander verbunden. Diese können sich unter Umständen nachteilig auf die chromatographische Trennung auswirken bzw. die chromatographischen Möglichkeiten der Trennsäulen einschränken. Konstruktionsbedingte Totvolumina und adsorptiv wirksame Werkstoffe (Metallkörper, Membranen, Dichtungen) können Memory und Peakverbreiterung verursachen, Fremdgase (Umgebungsluft) gelangen per Diffusion in Spuren in das GC System, die Temperaturbelastbarkeit der Ventile ist in der Regel niedriger als die der Säulen, und die hohe thermische Masse lässt kein schnelles Temperaturprogramm zu. Für die automatische Gasdosierung werden normalerweise baugleiche Ventile eingesetzt, so dass die negativen Einflüsse auch dort auftreten können.

Mit Einführung der Kapillarsäulen mit festen porösen Trennphasen, den sog. porous layer open tubular (PLOT) Säulen wird auch im Bereich der Gasanalytik hochauflösende GC möglich[7–9]. PLOT Säulen unterscheiden sich von den konventionellen Flüssigfilm-Kapillarsäulen durch ihre wesentlich höhere Retentionskraft. Diese hat ihre Ursache darin, dass PLOT Säulen nicht nach dem gas–flüssig Prinzip (Löslichkeit), sondern nach dem gas–fest Prinzip (Adsorption) trennen. Mit den PLOT Säulen können die bekannten Vorteile der Kapillartrennsäulen gegenüber gepackten Säulen wie kurze Analysenzeit, hohe Auflösung, niedrige Nachweisgrenzen, niedrigeres Temperaturniveau für Gase mit langer Retentionszeit, höhere Temperatur für niedrigsiedende Gase (zum Teil kann auf Ofenkühlung verzichtet werden), Vielseitigkeit, komfortables Handling usw. auch in der Gasanalytik genutzt werden. Dies hat jedoch zur Folge, dass die für gepackte Trennsäulen entwickelten Ventiltechniken für Probendosierung und Trennsäulenschaltung nicht mehr oder nur noch bedingt einsetzbar sind. Kapillarsäulen-kompatible Schaltsysteme müssen, soweit vorhanden, an PLOT Säulen adaptiert bzw. neu entwickelt werden.

Als Funktionsprinzip bietet sich diesbezüglich die "ventillose", pneumatisch gesteuerte Schalttechnik an. Dieses Prinzip wurde erstmals von Deans[10] zum Umschalten gepackter Trennsäulen beschrieben. Die Vorteile dieser Technik, insbesondere für Kapillarsäulen, wurden von Schomburg sehr früh erkannt und angewendet. Aufgrund von Anregungen durch Schomburg entwickelte Müller[11] die Trennsäulenschaltung nach dem "Live"-Prinzip, deren Leistungsfähigkeit und Vielseitigkeit Schomburg und andere in zahlreichen eindrucksvollen Applikationsbeispielen aus den verschiedensten Bereichen mit flüssigen Proben und Flüssigfilm-Kapillarsäulen beweisen konnten[12–23].

In der vorliegenden Arbeit werden am Beispiel einer für die Gasanalytik repräsentativen Applikation, nämlich der Bestimmung gelöster Gase in Transformatorenölen, gerätetechnische und applikative Entwicklungen in der Gasanalytik aufgezeigt. Dieses Applikationsbeispiel ist insofern repräsentativ für die Gasanalytik als mit diesem GC System die typischen Stoffgruppen Edelgase, Inertgase, Verbrennungsgase und leichte Kohlenwasserstoffe erfasst werden können.

Die Säulenschaltung für die Kapillartrennsäulen basiert auf dem Live-Prinzip. Die Auswahl des jeweiligen Dosiersystems orientiert sich in erster Linie am Druckniveau der zu analysierenden Probe (Unterdruck, Atmosphärendruck oder Überdruck). Die Dosiersysteme arbeiten zum Teil rein pneumatisch, teilweise wird Ventiltechnik mit pneumatischer Technik kombiniert.

EXPERIMENTELLES

Sämtliche in dieser Arbeit vorgestellten Dosier- und Säulenschaltsysteme wurden auf Siemens Gaschromatographen SiChromat (Einfach- oder Doppelofengerät) installiert und getestet. Die beschriebenen Applikationsbeispiele wurden ebenfalls auf SiChromat Gaschromatographen realisiert.

ENTWICKLUNGEN IN DER GASANALYTIK AM BEISPIEL DER ANALYSE GELÖSTER GASE IN TRANSFORMATORENÖLEN

Gepackte Trennsäulen mit Ventiltechnik

Zur Beurteilung des Betriebszustandes von Grosstransformatoren werden aus deren Isolierölen Proben entnommen und in einer speziell dafür entwickelten Apparatur entgast und die Ausgasungsprodukte gaschromatographisch quantifiziert[24]. Ein GC System für die Aufgabenstellung, bestehend aus einem Gasdosierventil (Membranventil), vier gepackten Trennsäulen, vier Säulenumschaltventilen (Membranventile), einem Wärmeleitsfähigkeitsdetektor (TCD = thermal conductivity detector) und einem FID (flame ionization detector) mit Methanizer, ist in Fig. 1 dargestellt. Das System ist so konzipiert, dass die Inertgase, CO und CH_4 auf dem TCD, das CO_2 (über den Methanizer) und die Kohlenwasserstoffe auf dem FID bestimmt werden. Die entsprechenden Chromatogramme sind in Fig. 2 dargestellt. Im TCD Chromatogram (Fig. 2a) fällt ein Basislinienversatz beim H_2 Peak auf. Dieser Einbruch verfälscht die H_2 Messung. Er wird dadurch verursacht, dass beim Dosieren der Probe, die in einem Druckbereich von *ca.* 20 mbar bis Atmosphärendruck vorliegen kann, der Trägergasdruck kurzzeitig abfällt; dieser Druckstoss wandert mit Totzeit durch das GC System. Zusätzliche Schwierigkeiten bereitet bei dieser Applikation das Abstimmen von Säulenlängen und Strömungen in den jeweils erforderlichen Ventilstellungen, weil drei Säulen am FID enden und die gleichzeitige

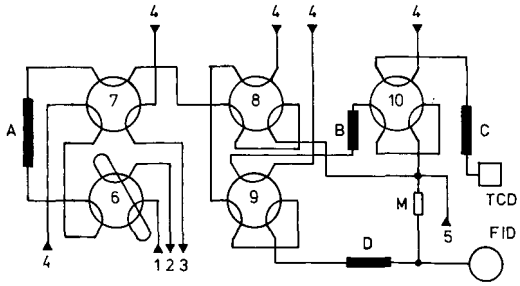

Fig. 1. Trennsäulenschaltung mit mechanischen Ventilen. (1) Probeneingang; (2) Probenausgang; (3) Backflush-Ausgang; (4) Trägergaseingänge mit unterschiedlichen Trägergasdrücken; (5) Eingang für Hydrierwasserstoff; (6) Dosierventil; (7) Backflush-Ventil; (8) Umschaltventil: schaltet den Trägergasstrom von der Säule A kommend zum Methanizer M oder über Ventil 9 auf die Säule D; (9) Umschaltventil: schaltet den Trägergasstrom vom Ventil 8 kommend auf die Säulen B oder D; (10) Umschaltventil: schaltet den Trägergasstrom vom Ventil 9 über die Säule B kommend zum Methanizer M oder zur Säule C; (M) Methanizer; (A) Trennsäule: Porapak S 80/100, 0,3 m × 2 mm I.D.; (B) Trennsäule: Porapak N 80/100, 1 m × 2 mm I.D.; (C) Trennsäule: Molekularsieb 5A 80/100, 1 m × 2 mm I.D.; (D) Trennsäule: Spherosil X0B 075, 2 m × 2 mm I.D.

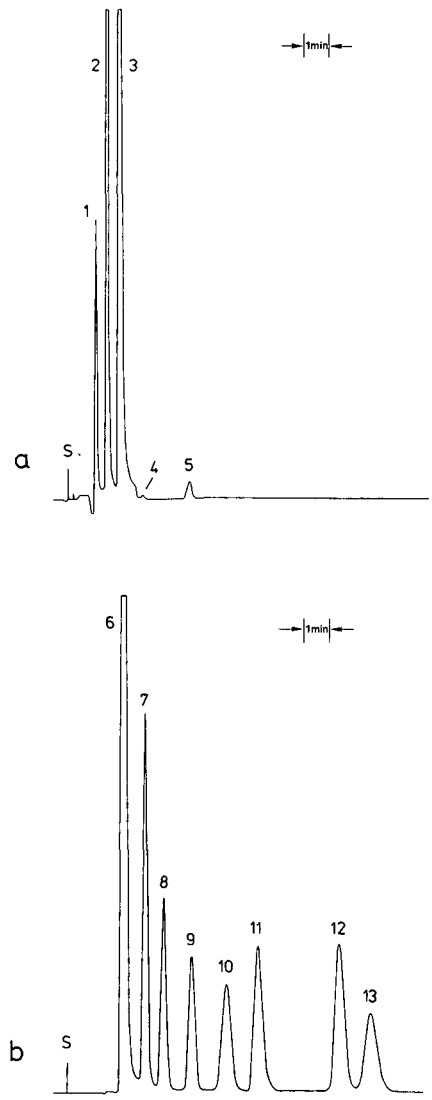

Fig. 2. Chromatogramm eines Gasgemisches erhalten mit der Trennsäulenschaltung nach Fig. 1. (S) Start; (1) Wasserstoff; (2) Sauerstoff; (3) Stickstoff; (4) Methan; (5) Kohlenmonoxid; (6) Kohlendioxid; (7) Ethen; (8) Ethan; (9) Ethin; (10) Propan; (11) Propen; (12) Iso-butan; (13) *n*-Butan. Trennsäulen siehe Fig. 1. Trägergas: Argon; Analysentemperatur; 75°C. (a) Chromatogramm TCD; (b) Chromatogramm FID.

Elution von Komponenten aus verschiedenen Säulen verhindert werden muss. Ein derart komplexes GC System ist äusserst empfindlich gegenüber Retentionszeitverschiebungen einer oder mehrerer Säulen, was z.B. durch unterschiedlichen Feuchtegehalt im Trägergas sehr leicht passieren kann. Schliesslich kann ein solches System nur über längere Zeit ausreichend konditioniert werden, weil die Maximaltemperatur der Umschaltventile auf 160°C limitiert ist.

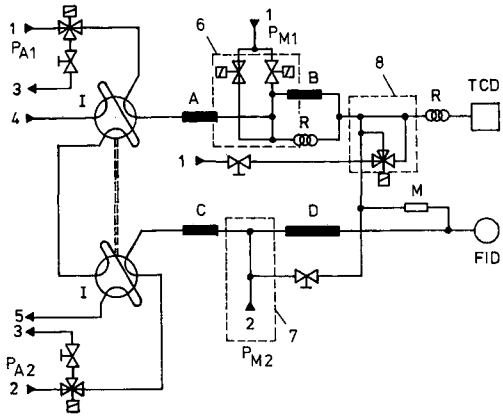

Fig. 3. Pneumatische Trennsäulenschaltung nach Deans[10]. (1) Trägergaseingänge für Argon; (2) Trägergaseingänge für Wasserstoff; (3) Backflush-Ausgänge; (4) Probeneingang; (5) Probenausgang; (6) Trennsäulenverteilerschaltung nach Deans; (7) Backflush-Schaltung nach Deans; (8) Ventillose Kopplung beider Trennsystem nach Deans; (M) Methanizer; (p_{A1}) Trägergasdruck vor den Säulen A und B; (p_{M1}) Trägergasdruck zwischen den Säulen A und B; (p_{A2}) Trägergasdruck vor den Säulen C und D; (p_{M2}) Trägergasdruck zwischen den Säulen C und D; (I) Dosierventile; (A) Trennsäule: Porapak S 80/100, 0,75 m × 3 mm I.D.; (B) Trennsäule: Molekularsieb 5A 0,2–0,3, 2 m × 3 mm I.D.; (C) Trennsäule: 5% Ucon NB 5100, Chromosorb P 0,15–0,20, 1 m × 3 mm I.D.; (D) Trennsäule: Spherosil XOB 075 100/120, 6 m × 3 mm I.D.

Gepackte Trennsäulen mit pneumatischer Säulenschaltung

Gestiegene Ansprüche an die Nachweisgrenzen von CH_4 und CO sowie der hohe Zeitbedarf für den Abgleich der Gasflüsse, z.B. bei Veränderung der Retentionszeiten oder beim Austausch einer Säule, hatten eine Modifizierung der Applikation zur Folge, wie aus Fig. 3 ersichtlich. Prinzipielle Unterschiede zu der vorher beschriebenen Methode sind die Doppeldosierung über zwei Dosierventile, die Auftrennung auf zwei unterschiedlichen GC Systemen, die erst unmittelbar vor den Detektoren miteinander verbunden sind, und das Wegfallen von Säulenumschaltventilen. Das Umschalten von Gasflüssen auf unterschiedliche Säulen wird hier pneumatisch, d.h. ohne Ventile im Probenweg nach der von Deans[10] beschriebenen Methode realisiert. Die dazugehörigen Chromatogramme sind in Fig. 4 dargestellt. Auch diese Applikation beinhaltet vier Trennsäulen.

Eine ähnliche Lösung mit pneumatischer Säulenschaltung wurde von Harke *et al.*[25] vorgeschlagen. Hier werden nur drei Trennsäulen eingesetzt, allerdings unter Verzicht auf Trennleistung zwischen Ethen und Ethin.

Kapillarsäulen und Live-Schaltung

Die hohe Trennleistung der PLOT Säulen erlaubt die Reduzierung der Säulenzahl von vier gepackten auf zwei Kapillarsäulen, mit denen die gleichen Komponenten bestimmt werden können. Das GC System ist in Fig. 5 dargestellt. Wesentliche Elemente sind die Unterdruckdosierung (die später ausführlich beschrieben wird), zwei Kapillartrennsäulen (länge 30 m und 20 m, I.D. 0,53 mm) die Live-Schaltung sowie ein TCD und ein FID mit integriertem Methanizer, die hintereinander geschaltet sind. Der FID dient gleichzeitig als Monitordetektor. Diese

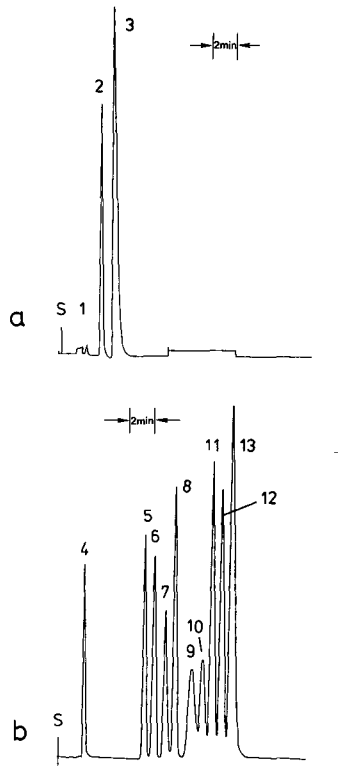

Fig. 4. Chromatogramm eines Gasgemisches erhalten mit der Trennsäulenschaltung nach Fig. 3. (S) Start; (1) Wasserstoff; (2) Sauerstoff; (3) Stickstoff; (4) Kohlendioxid; (5) Methan; (6) Ethan; (7) Ethen; (8) Propan; (9) Kohlenmonoxid; (10) Ethin; (11) Iso-butan; (12) *n*-Butan; (13) Propen. Trennsäulen siehe Fig. 3. Trägergas: Argon und Wasserstoff (siehe Fig. 3); Analysentemperatur: 75°C; (a) Chromatogramm TCD; (b) Chromatogramm FID.

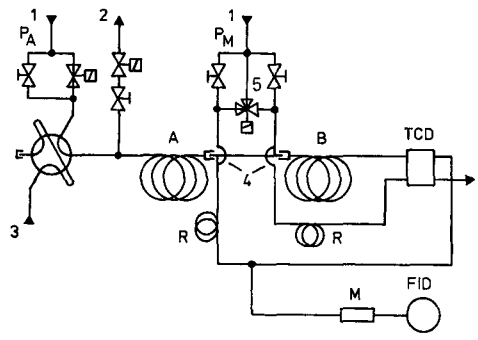

Fig. 5. Live-Trennsäulenschaltung mit Kapillarsäulen. (1) Trägergaseingänge; (2) Backflush-Ausgang; (3) Anschluss zur Unterdruckdosiervorrichtung; (4) Live-T-Stück; (5) Live-Schaltung; (p_A) Trägergasdruck vor beiden Trennsäulen; (p_M) Trägergasdruck zwischen beiden Trennsäulen; (R) Restriktion; (M) Methanizer; (A) Trennsäule: GSQ, 30 m × 0,53 mm I.D.; (B) Trennsäule: Molekularsieb 5A, 20 m × 0,53 mm I.D.

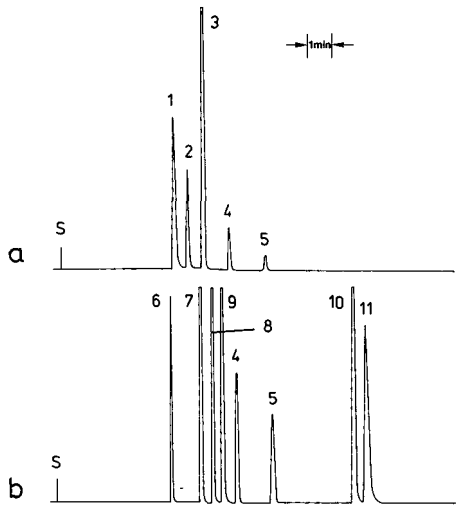

Fig. 6. Chromatogramm eines Gasgemisches erhalten mit der Trennsäulenschaltung nach Fig. 5. (S) Start; (1) Wasserstoff; (2) Sauerstoff; (3) Stickstoff; (4) Methan; (5) Kohlenmonoxid; (6) Kohlendioxid; (7) Ethen; (8) Ethin; (9) Ethan; (10) Propen; (11) Propan. Trennsäulen siehe Fig. 5. Trägergas: Argon; Analysentemperaturen: Säule A: 50°C, 5,5 min → 15°C/min → 110°C, 9 min; Säule B: 106°C isotherm. Trägergas: Argon, (a) Chromatogramm TCD; (b) Chromatogramm FID.

Anordnung erlaubt die Bestimmung der Inertgase auf dem TCD, der Kohlenwasserstoffe, des CO_2 und des CO auf dem FID (mit Methanizer) mit einer einzigen Dosierung. Fig. 6 zeigt die mit diesem System erhaltenen Chromatogramme.

Gasdosiersysteme für Kapillarsäulen

Unterdruckdosierung. Um die im Transformatorenöl gelösten Gase messen zu können, werden die Öle per Unterdruck entgast und nach Zwischenspeicherung in einem Probenvorratsbehälter beim Unterdruck dosiert. Die Unterdruckdosierung ist in Fig. 7 schematisch wiedergegeben. Sie besteht im wesentlichen aus einem 6-Wege Drehschieberventil mit Aussenbespülung, einer Füllschleife, einer Hilfsgasversorgung, einer Vakuumpumpe, zwei Absperrventilen und dem Probengefäss. Sie kann sowohl für Kapillarsäulen (mit Split) also auch für gepackte Säulen eingesetzt werden.

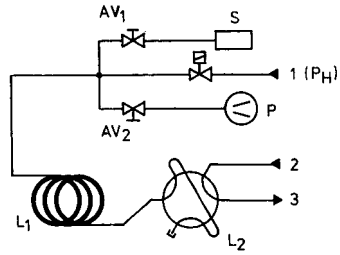

Fig. 7. Unterdruckdosiervorrichtung. (1) Hilfsgasdruck (p_H) = Trägergasdruck; (2) Trägergaseingang; (3) zur Trennsäule; (P) Vakuumpumpe; (S) Probenvorratsbehälter; (L_1) Füllschleife; (L_2) Dosierschleife; (AV) Absperrventile.

Die Dosierung läuft folgendermassen ab:

(1) Das gesamte Dosiersystem wird von der Dosierschleife bis zum geschlossenen Absperrventil AV1 und geschlossenen Magnetventil mit Hilfe der Vakuumpumpe evakuiert.

(2) Das Absperrventil AV2 wird geschlossen und AV1 geöffnet; somit kann die Probe in das evakuierte Dosiersystem expandieren.

(3) AV1 wird wieder geschlossen und das Magnetventil geöffnet; das dabei einströmende Hilfsgas drückt die Probe in die Dosierschleife und erhöht den Probendruck auf Trägergasdruck (einstelbar mit Druckregler DR).

(4) Die Dosierschleife wird über das 6-Wege Ventil druckstossfrei in das GC System geschaltet; die GC Analyse beginnt.

Entscheidend bei dieser Technik ist die Anpassung der Volumina der Füll- und Dosierschleife unter Berücksichtigung des minimalen Probendruckes. Bei vorgegebenem Dosiervolumen ist das Volumen der Füllschleife nach den kombinierten Gasgesetzen von Boyle-Mariotte und Gay-Lussac gegeben wie folgt:

$$\frac{p_1 V_1}{T_1} = \frac{p_2 V_2}{T_2}$$

p ist der Druck, V das Volumen und T die Temperatur eines idealen Gases.

Für konstante T gibt es

$$p_m V_{L1} = p_H V_{L2}$$

$$V_{L1} = \frac{p_H}{p_m} V_{L2}$$

p_m ist der minimale Probendruck, p_H der Hilfsgasdruck, V_{L1} das Mindestvolumen der Füllschleife und V_{L2} das Volumen der Dosierschleife.

Die Gleichung gilt nur für ideale Gase und unter der Voraussetzung, dass an der Grenze zwischen Probe und Hilfsgas keine Durchmischung stattfindet. In der Praxis sollte das Volumen der Füllschleife *ca.* 20% grösser sein als theoretisch errechnet. Damit ist sichergestellt, dass die Grenze zwischen Probe und Hilfsgas bzw. die dort auftretende Mischzone sich ausserhalb der Dosierschleife befindet; dies verhindert Einbussen in der Reproduzierbarkeit. Bei höherem Probendruck gelangt mehr Probe in das evakuierte System, d.h. nach dem Aufdrücken mit Hilfsgas auf gleichen Druck liegt ein grösseres Probenvolumen vor; die Mischzone zwischen Probe und Hilfsgas befindet sich irgendwo in der Füllschleife. Es ist sichergestellt, dass nur Probe über die Dosierschleife in das GC System gelangt.

Diese Technik bietet entscheidende Vorteile:

(1) Eliminierung des Druckstosses beim H_2 Peak, der durch das Schalten des Dosierventils verursacht wird, wie ein Vergleich der Chromatogramme von konventioneller Technik (Fig. 2a) mit Unterdruckdosierung (Fig. 6a) zeigt.

(2) Druckschwankungen der Probe bleiben ohne Einfluss auf das Analysenergebnis solange der Minimaldruck nicht unterschritten wird, weil jeweils das gleiche Probenvolumen (Volumen der Dosierschleife) unter gleichem Druck dosiert wird. Dies wird anschaulich durch Fig. 8 dokumentiert. Dieses Schaubild zeigt die

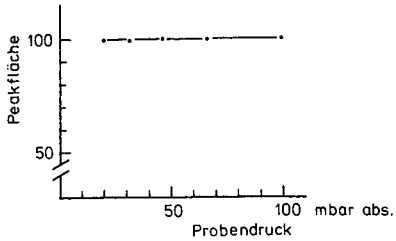

Fig. 8. Peakfläche *versus* Probendruck.

Peakfläche einer Messkomponente als Funktion des Probendruckes. Man erkennt, dass ab 20 mbar aufwärts das Analysenergebnis konstant und druckunabhängig ist.

Deans-Dosierung. Die Deans-Dosierung[26] ist ein pneumatisches Dosiersystem, das keine bewegten Teile und keine adsorptiv wirksame Dichtungsmaterialien im Probenweg hat. Es kann problemlos diffusionsdicht gegen Umgebungsluft aufgebaut werden. Sie ist, ebenso wie die Unterdruckdosierung, kompatibel mit Kapillar- und gepackten Säulen. Fig. 9 zeigt schematisch den Aufbau der Deans-Dosierung. Voraussetzung für diese Dosiertechnik ist, dass der Probendruck konstant und höher ist als der Trägergasdruck. Es handelt sich hier um eine Strömungsschaltung, bei der durch Umschalten des Trägergases indirekt Probe in das Trennsystem geschaltet wird. Durch Variation der Dosierdauer kann die Dosiermenge verändert werden. Es muss genügend Probe zur Verfügung stehen, so dass ein Probenfluss eingestellt werden kann, der grösser ist als der Trägergasfluss durch Säule und Split.

Das Dosiersystem kennt zwei Zustände:

(1) Das Magnetventil ist so geschaltet, dass Trägergas geradeaus (Richtung a–b) durch das Dosierrohr (inneres Rohr) auf die Trennsäule strömt. Aus der kleinen Öffnung (X) im Dosierrohr strömt zusätzlich Trägergas in die Ringkammer aus, in die auch Probe mit dem Durchfluss Q_S einströmt. Trägergas und Probe strömen als Q_t aus dem System aus. Wenn die Durchflüsse entsprechend der Bedingung

$$Q_t > Q_S > Q_C$$

mit Q_t der ausströmende Volumenstrom, Q_S der Volumenstrom der Probe und Q_C der Volumenstrom über die Säule, eingestellt sind, verhindert eine Sperrströmung des

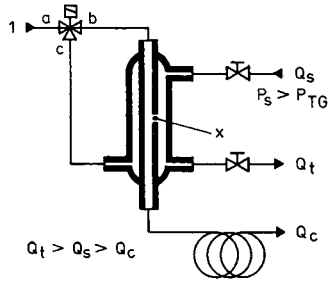

Fig. 9. Deans-Dosiervorrichtung. (1) Trägergaseingang; (p_S) Probendruck; (p_{TG}) Trägergasdruck; (Q_S) Probendurchfluss; (Q_t) Gesamtdurchfluss; (Q_C) Trennsäulendurchfluss.

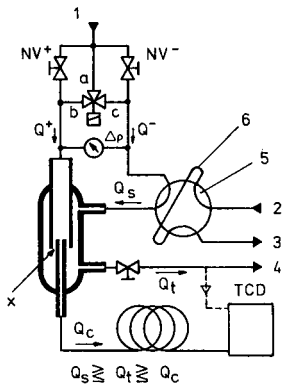

Fig. 10. Live-Dosiervorrichtung. (1) Trägergaseingang; (2) Probeneingang (Probendruck $\gtrless$ Trägergasdruck); (3) Probenausgang; (4) Gesamtdurchfluss-Ausgang; (5) Vordosierventil; (6) Vordosierschleife mit grossen Volumen; (NV) Nadelventile; (Q_S) Trägergasdurchfluss über das Dosierventil; (Q_t) Gesamtdurchfluss; (Q_C) Trennsäulendurchfluss.

Trägergases durch die Öffnung X, dass Probe in das Dosierrohr eintritt. Entsprechend der Austrittsöffnung muss die Sperrströmung so gewählt werden, dass die Austrittsgeschwindigkeit grösser ist als die Diffusionsgeschwindigkeit des kleinsten Moleküls.

(2) Dosierstellung. Das Magnetventil ist so geschaltet, dass das Trägergas zum unteren Anschluss der Ringkammer strömt (Richtung a–c). Der geradeaus-Weg (Richtung a–b) ist jetzt abgesperrt, die Sperrströmung durch die Öffnung X im Dosierrohr wird abgebaut und Probe kann von der Ringkammer durch X über das Dosierrohr auf die Säule strömen. Da entsprechend der o.g. Bedingung ($Q_S > Q_C$) der Probenstrom grösser ist als die Strömung über die Säule, fliesst die überschüssige Probe zum Ausgang und sperrt somit den Trägergasfluss zur Öffnung X. Der Trägergasdruckregler sorgt für konstante Druckverhältnisse an der Dosierstelle. Zum Beenden des Dosiervorgangs wird das Magnetventil wieder in den Zustand (1) geschaltet.

Der kleinvolumige Aufbau der Schalteinrichtung erlaubt kurze Schaltzeiten ($t < 0{,}5$ s) und somit Dosiermengen von *ca.* 0,1 ml. Diese Dosiertechnik arbeitet ebenso wie die Unterdruckdosierung: druckstossfrei. Allerdings ist die Strömungseinstellung kritisch, da Q_S nicht direkt messbar ist und sich bei Probendruckschwankungen ändert.

Live-Dosierung. Die Live-Dosierung[27] kann als Synthese aus Elementen der Ventildosierung, der Deans-Dosierung und der Live-Schaltung betrachtet werden. Sie besitzt die wesentlichen Vorteile der Deans-Schaltung wie Abwesenheit bewegter Teile im eigentlichen Dosiersystem, keine adsorptive Dichtungsmaterialien, keine Druckschwankungen beim Dosieren und variables Dosiervolumen; sie ist aber gleichzeitig unabhängig vom Probendruck. Ausserdem müssen die drei Strömungen nicht aufeinander abgestimmt sein. Der Aufbau der Live-Dosierung ist in Fig. 10 dargestellt. Sie besteht aus einem 6-Wege Ventil mit ausreichend grosser Dosierschleife, der eigentlichen Dosiereinheit, die der Deans-Dosierung ähnelt und einem Trägergasversorgungssystem wie bei der Live-Schaltung.

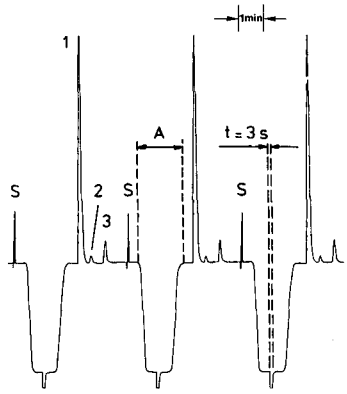

Fig. 11. Chromatogramm erhalten mit Live-Dosiervorrichtung. (Q_t wird über den TCD-Vergleichszweig geleitet.) (S) Start; (A) Probenpfropflänge (gemessen mit TCD-Vergleichszweig); t (Dosierzeit) = 3 S. (1) Wasserstoff; (2) Sauerstoff; (3) Stickstoff. Trennsäule: Molekularsieb 5A 25 m × 0,53 mm I.D.; Trägergas: Stickstoff 0,7 bar; Detektor: TCD, Messbereich 2^8; Analysentemperatur: 80°C.

Der Funktionsablauf ist folgender:

(1) Trägergas strömt über den Zweig Q^+ und Q^- in die Dosiereinheit, wobei der Fluss über Q^- niedriger ist also über Q^+. In der Dosiereinheit strömt am Ringspalt X aufgrund des eingestellten Differenzdruckes $-\Delta p$ Trägergas aus.

(2) Die Dosierschleife des 6-Wege Ventils wird mit Probe gefüllt (Füllstellung).

(3) Das 6-Wege Ventil wird umgeschaltet (Dosierstellung). Das Trägergas über Q^- spült den Probenpfropf aus der Dosierschleife heraus und am Ringspalt X in der Dosiereinheit vorbei.

(4) Durch Umschalten des Magnetventils (von Richtung a–b in Richtung a–c) zum richtigen Zeitpunkt wird der Differenzdruck umgedreht ($+\Delta p$) und der

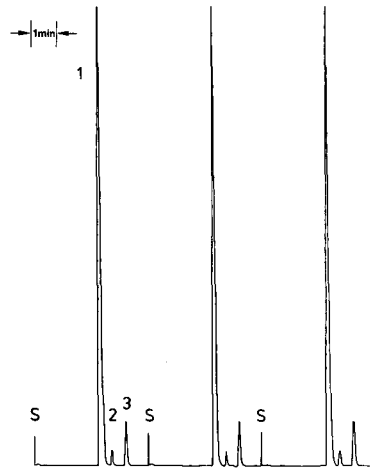

Fig. 12. Chromatogramm erhalten mit Live-Dosiervorrichtung. (Q_t wird ins Freie geleitet.) (S) Start; (1) Wasserstoff; (2) Sauerstoff; (3) Stickstoff. Trennsäule: Molekularsieb 5A 25 m × 0,53 mm I.D.; Trägergas: Stickstoff 0,7 bar; Detektor: TCD, Messbereich 2^7; Analysentemperatur: 80°C.

Trägergasfluss durch das Dosierrohr drastisch reduziert. Die Strömung durch den Ringspalt X wird umgedreht und Probe fliesst durch den Spalt X ins Dosierrohr. Durch Umschalten des Magnetventils in den ursprünglichen Zustand wird der eigentliche Dosiervorgang beendet. Der Rest der Probe strömt mit Q_t aus dem Dosiersystem. Wenn am Ausgang Q_t ein Detektor angeschlossen ist, kann damit der Konzentrationsverlauf des Probenpfropfes bzw. die per Dosierung aus dem Pfropf herausgeschnitte Proben-"Scheibe" beobachtet werden, wie in Fig. 11 dargestellt. Durch Variation der Schaltzeit des Magnetventils kann die Dicke der herausgeschnittenen "Scheibe" und damit das Dosiervolumen optimal angepasst werden. Für eine gute Reproduzierbarkeit ist es wichtig, dass die dosierte Probe aus dem Plateau des am Ringspalt vorbeiströmenden Probenpfropfes herausgeschnitten wird. Durch Einsatz dieser Technik speziell in der Spurenanalytik ist es möglich, die an den Verschraubungen der Dosierschleife eventuell eindiffundierende Luft am Ringspalt vorbeizuführen (ansteigende und abfallende Flanke des Probenpfropfes) und somit für die GC Analyse auszublenden. Das bedeutet höhere Genauigkeit der Analyse, bessere Nachweisgrenzen und höhere Reproduzierbarkeit. Fig. 12 zeigt die Reproduzierbarkeit, die mit dem Live-Dosiersystem erreicht wird. Q_t ist dabei nicht an den Detektor angeschlossen. In Fig. 13 sind Chromatogramme dargestellt, die bei der

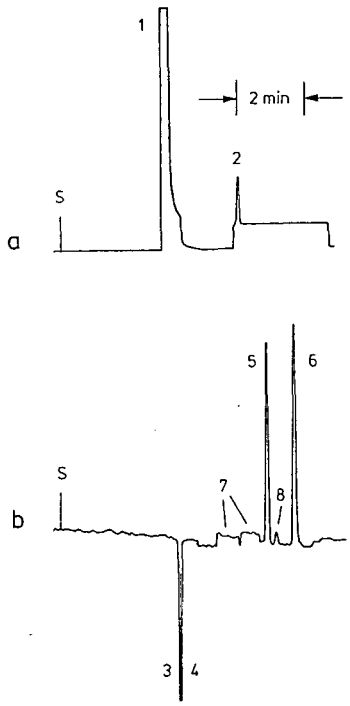

Fig. 13. Chromatogramm erhalten mit Live-Dosierung. Probe: Umgebungsluft, 0,25 ml. Live-Trennsäulenschaltung mit Trennsäulen: (A) Poraplot Q, 25 m × 0,53 mm I.D., 30°C; (B) Molekularsieb 5A, 25 m × 0,53 mm I.D., 30°C. Trägergas: Helium 5 ml/min. (1) Argon–Sauerstoff–Stickstoff; (2) Kohlendioxid; (3) Neon; (4) Wasserstoff; (5) Krypton; (6) Methan; (7) Schnittreste von 1; (8) Schaltpeak. (a) Chromatogramm TCD (Säule A); (b) Chromatogramm HeD (Säule B).

Analyse von Umgebungsluft erhalten wurden. Die Probe wurde mit der Live-Dosierung injiziert, mittels Live-Trennsäulenschaltung[11–16] mit zwei unterschiedlichen Trennsäulen aufgetrennt und die Einzelkomponenten mit einem TCD und einem Heliumionisationsdetektor (HeD) nachgewiesen.

SCHLUSSFOLGERUNGEN

Die Verwendung von Kapillartrennsäulen in der Gasanalytik hat zur Folge, dass konventionelle Schalttechniken, die für gepackte Säulen entwickelt wurden, nicht mehr oder nur noch mit Einschränkungen genutzt werden können. Dies gilt insbesondere für automatische Dosier- und Trennsäulenschaltsysteme auf der Basis mechanisch bewegter Ventile. In der vorliegenden Arbeit wurde gezeigt, dass pneumatisch gesteuerte Systeme, d.h. Systeme, deren Schaltzustand durch Änderung von Druck oder Volumenstrom des Trägergases beeinflusst werden kann, hervorragend für die hochauflösende Gasanalytik geeignet sind. Für die Trennsäulenschaltung in der multidimensionalen Gasanalytik hat sich die Live-Schaltung, installiert in einem Doppelofen-GC, sehr gut bewährt. Die Auswahl des optimalen Dosiersystems muss sich in erster Linie am Druckniveau der zu analysierenden Probe orientieren. Es wurde eine Unterdruckdosierung entwickelt für Gasproben, deren Druck unter dem Atmosphärendruck liegt. Proben, die in ausreichender Menge und mit konstantem und ausreichend hohem Druck verfügbar sind (z.B. aus Gasflaschen), können über die Deans-Dosierung dosiert werden. Die Live-Dosierung ist druckunabhängig und kann problemlos auch bei ständig wechselnden Druckverhältnissen verwendet werden. Sie eignet sich auch für Proben, die im Unterdruckbereich vorliegen. Der Einsatz der Live-Dosierung ist über die Gasanalytik hinaus auch für die Flüssigdosierung nach Vorverdampfung der flüssigen Probe möglich.

Sämtliche hier vorgestellten Schaltsysteme für die (multidimensionale) Hochleistungs-Gasanalyse können automatisch betrieben werden und demzufolge sowohl unter Labor- als auch unter Prozessbedingungen eingesetzt werden.

DANK

Wir danken Herrn Priv.-Doz. Dr. Dr. h.c. Gerhard Schomburg für die zahlreichen Anregungen, Hinweise und Unterstützungen auf dem Gebiet der Gaschromatographie, die er uns während der mehr als sechzehnjährigen engen Zusammenarbeit zukommen liess.

ZUSAMMENFASSUNG

Die Einführung von Kapillartrennsäulen mit festen porösen Trennphasen, sog. PLOT Säulen, für die GC Analytik von Gasen hat zur Folge, dass konventionelle Techniken, die für gepackte Trennsäulen entwickelt wurden, durch kapillarsäulenkompatible Systeme ersetzt werden müssen. Das gilt insbesondere für automatische Dosier- und Trennsäulenschaltsysteme. Es wird gezeigt, das neue druck- und strömungsgesteuerte Schalttechniken für die hochauflösende Gasanalytik hervorragend geeignet sind. An einem repräsentativen Applikationsbeispiel wird die Entwicklung und Praxisrelevanz derartiger Systeme aufgezeigt.

LITERATUR

1 E. Leibnitz und H. G. Struppe, *Handbuch der Gas-Chromatographie*, 2. Aufl., Verlag Chemie, Weinheim, 1970.
2 *ASTM Standards*, D 1945-64.
3 G. E. Pollok, D. O'Hara und O. L. Hollis, *J. Chromatogr. Sci.*, 22 (1984) 343.
4 *International Organization for Standardization, ISO*, 6569 (1981).
5 *International Organization for Standardization, ISO*, 6974 (1984).
6 R. Mindrup, *J. Chromatogr. Sci.*, 16 (1978) 380.
7 J. De Zeeuw, R. C. De Nijs und L. T. Henrich, *J. Chromatogr. Sci.*, 25 (1987) 71.
8 R. C. De Nijs und J. De Zeeuw, *J. Chromatogr.*, 279 (1983) 41.
9 H. Schaller, *Laborpraxis* (1988), zur Veröffentlichung vorgelegt.
10 D. R. Deans, *U.K. Pat.*, 1,236,937.
11 F. Müller, *Pat. DE* 2,80,123 C2.
12 G. Schomburg, *Laborpraxis*, 6 (4) (1982) 356.
13 G. Schomburg, H. Husmann und E. Hübinger, *J. High Resolut. Chromatogr. Chromatogr. Commun.*, 7 (1984) 404.
14 G. Schomburg, H. Husmann und E. Hübinger, *J. High Resolut. Chromatogr. Chromatogr. Commun.*, 8 (1987) 395.
15 G. Schomburg, F. Weeke, F. Müller und M. Oréans, *Chromatographia*, 16 (1982) 87.
16 G. Schomburg, F. Weeke und R. G. Schaefer, *J. High Resolut. Chromatogr. Chromatogr. Commun.*, 8 (1985) 388.
17 F. P. Di Sanzo, J. L. Lane und R. E. Yoder, *J. Chromatogr. Sci.*, 26 (1988) 206.
18 N. G. Johansen, *J. High Resolut. Chromatogr. Chromatogr. Commun.*, 7 (1984) 487.
19 J. C. Duinker, D. E. Schulz und G. Petrick, *Anal. Chem.*, 60 (1988) 478.
20 H. J. Stan, *Lebensmittelchem. Gerichtl. Chem.*, 42 (1988) 31.
21 P. A. Rodriguez und C. L. Eddy, *J. Chromatogr. Sci.*, 24 (1986) 18.
22 H. Neumann und H.-P. Meyer, *J. Chromatogr.*, 391 (1987) 442.
23 H. Müller, *Laborpraxis*, 23 (1988) 654.
24 H. Schliesing und K. Soldner, *Elektrizitätswirtschaft*, 8 (1976) 195.
25 L. Harke und W. Strubert, *Siemens Analysentechnische Mitteilungen*, Nr. 209, 1977.
26 Patent "Deans-Dosierung", *U.K. Pat. GB* 2,055,608 A.
27 Live-Dosierung, *Int. Patentanmeldung*, PCT/DE 88/00640.

Journal of Chromatography, 477 (1989) 39–47
Elsevier Science Publishers B.V., Amsterdam — Printed in The Netherlands

CHROM. 21 463

TURBULENT FLOW IN CAPILLARY GAS CHROMATOGRAPHY

A. VAN ES*, J. RIJKS and C. CRAMERS
Eindhoven University of Technology, Department of Chemical Technology, Laboratory of Instrumental Analysis, P.O. Box 513, 5600 MB Eindhoven (The Netherlands)

SUMMARY

The possibilities of turbulent flow capillary gas chromatography for increasing the speed of analysis were examined by use of previously developed sample introduction, detection and registration systems, which are compatible with peak widths in the millisecond range. Existing theoretical models for axial turbulent dispersion in capillary columns were evaluated experimentally. Substantially decreases in reduced plate heights were obtained ($h < 1$) for unretained components at an average linear velocity of 15 m/s for column diameters of 320 μm. Unfortunately, the plate height increased greatly with increasing solute capacity factor (by a factor 15 from $k = 0$ to $k = 1$). Comparison with theoretical models shows that this effect is mainly due to mobile phase mass transfer. Therefore, the gain in analysis speed is limited to low capacity factors. In addition the pressure drop required is considerably higher than for a comparable improvement in speed obtained by decreasing the column inside diameter.

INTRODUCTION

An efficient way to increase the speed of analysis in capillary gas chromatography (GC) is a reduction of the column diameter[1]. However, the lack of compatible instrumentation has been a serious obstruction so far for the successful application of narrow-bore columns (I.D. < 100 μm). Recently, we have developed and evaluated sample introduction, detection and registration systems compatible with peak widths in the millisecond range[2,3]. Very rapid separations are possible, *e.g.*, nine components separated in 0.5 s), with column diameters down to 10 μm I.D. However, the minimum useful column diameter is strongly limited by the detector sensitivity. Moving towards smaller column diameters, the sample capacity decreases more rapidly than the minimum detectable amount, thus reducing the dynamic range of the column detector system. At the column diameter where the minimum detectable amount is equal to the sample capacity, a further reduction of the column diameter is useless, unless more sensitive detectors become available. With currently available detectors this point is reached at a column diameter of about 5–10 μm. In practice the column diameter must be well above these values dependent upon the required dynamic range. It is clear that this limits the gain in analysis speed.

0021-9673/89/$03.50

A reduction in the column diameter lowers the contribution of the velocity profile (C_m term) to the chromatographic dispersion. The chromatographic dispersion can also be lowered by changing the velocity profile.

A possible way to change the velocity profile is coiling the column into a helix, which induces a secondary flow. This effect is extensively described by Tijssen *et al.*[4,5] for GC and liquid chromatography (LC). Another way is to create turbulent flow. With turbulent flow the velocity profile is largely flattened, thus decreasing flow inequalities; further, the effective diffusion coefficient of the component is considerably increased by convective contributions. As a consequence, peak broadening in the mobile phase due to the velocity profile is expected to be largely reduced. This has in fact been observed in chemical engineering studies of gas as well as liquid flow in pipes[6]. Reduced plate heights down to 0.5 are obtained at Reynolds numbers, Re, of $2 \cdot 10^4$ for unretained components. The Reynolds number is defined here as

$$\mathrm{Re} = ud_c/v$$

where u = linear velocity, d_c = column diameter and v = kinematic viscosity.

In this paper the possibility of using turbulent flow in capillary GC to increase the speed of analysis is studied. Normal bore columns are used (320 μm I.D.) because of their advantages of a good dynamic range (being the ratio of the sample capacity and the minimum detectable amount) and relatively easy column technology. Only a few experimental results on turbulent flow in GC have been reported, dating back to some 20 years ago[7,8]. The results were not as promising as expected, possibly due to instrumental contributions or a significant influence of the stationary phase. Furthermore, the theoretical models on turbulent dispersion reported give rather different results which do not agree well with experimental results.

In this work recently developed instrumentation for narrow-bore columns was used, which is suitable for peak widths of a few milliseconds. Stationary phase effects were minimized by selecting a suitable thin film column. The experimental data were compared with those obtained by the different theoretical models. The potential of turbulent flow to increase the analysis speed was evaluated and compared with that of a reduction in column diameter.

THEORETICAL

Turbulent flow is a well known phenomenon in chemical engineering. In a study of gas flow in pipes Flint and Eisenklam[6] have reported experimental and theoretical results for turbulent dispersion of unretained components as a function of the Reynolds number, Re. Curves of the reduced plate height, $h = H/d_c$, *versus* Re are characterized by a maximum at the transition from laminar to turbulent flow (Re approximately 2300) and thereafter a pronounced lowering of h down to 0.5 at $\mathrm{Re} = 2 \cdot 10^4$.

Flint's theory was in good agreement with the experimental results, but it is emphasized that different velocity profiles have to be used, especially for the regime $\mathrm{Re} < 6000$, where the most radical changes in the form of the velocity profile occur. Although the foregoing applies only for unretained components, it suggests that an high gain in analysis speed is possible with turbulent flow in GC. The theory of GC in

open tubular columns with laminar flow leads to the generally accepted Golay–Giddings plate height equation. Under turbulent conditions, this expression is no longer valid since the radial velocity profile is no longer parabolic and becomes velocity dependent. In addition radial mass transfer is enhanced by convection.

In 1966 Pretorius and Smuts[9] reported a theoretical model for turbulent dispersion, based on the Aris general dispersion theory, which allows for a non-parabolic velocity profile and a variable diffusion coefficient. In their calculation, different empirical velocity profiles from literature data were used together with radial diffusion profiles (convection superimposed on molecular diffusion), derived from the velocity profiles.

For a capacity factor $k = 0$, the calculated plate height for different Re numbers agreed well with the foregoing results of Flint and Eisenklam. The calculation was also performed for the chromatographically more interesting case of $k=1$. Here h also decreases with Re down to a value of about 2 at $\mathrm{Re}=2 \cdot 10^4$. The ratio between h for $k=0$ and for $k=1$ was about the same for turbulent as for laminar flow. From this theoretical study Pretorius and Smuts[9] concluded that turbulent flow in GC may improve the analysis speed by a factor of 10, compared with laminar flow. In 1982 Martin and Guiochon[10] calculated the peak broadening under turbulent flow conditions according to the Aris general dispersion theory. They used a fixed (theoretical) velocity profile throughout the whole turbulent region. Furthermore a radial diffusion profile derived from literature data was assumed. The results of their calculation differ substantially from those of Pretorius and Smuts. First, a plot of h *versus* Re shows an increase in h with increasing Re for all capacity factors. This is conflict with prior experimental data[6,8]. Presumably this arises from the use of a fixed velocity profile throughout the whole turbulent region.

A second remarkable difference is the large influence of the capacity factor on h. Although for $k=0$ the calculated h is very low ($h=0.25$, $\mathrm{Re}=2 \cdot 10^4$), it increases by a factor of 100 on going from $k=0$ to $k=1$. The few experiments made with turbulent flow in capillary GC also showed a significant increase in h with increasing k (refs. 7 and 8). Contrary to Pretorius and Smuts, Martin and Guiochon concluded that the potential of turbulent flow in GC is limited. In 1979, Tijssen[11] also derived an equation for turbulent dispersion in a systematic study of axial dispersion in helically coiled columns. It starts with a mass balance and assumes a turbulent velocity profile (see Fig. 1)

$$\frac{u}{\bar{u}} = \frac{6}{5}\left[1 - \left(\frac{r}{R}\right)\right]^{10} \tag{1}$$

where u = local velocity, $\bar{u}$ = average velocity, r = radial coordinate and R = column radius.

Neglecting axial diffusion and resistance to mass transfer in the stationary phase, this finally leads to

$$C_m = \frac{R^2}{D_R} \frac{1 + 14k + 55k^2}{168(1 + k)^2} \tag{2}$$

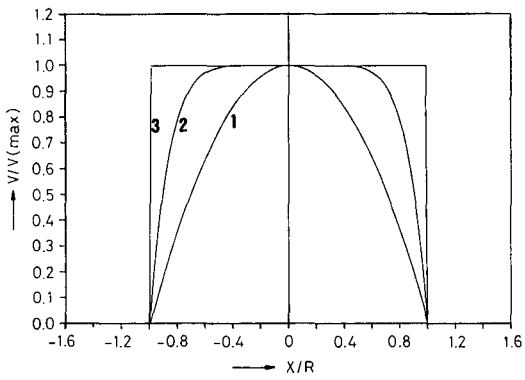

Fig. 1. Laminar turbulent velocity profiles: 1, parabolic; 2, 10th power (eqn. 1); 3, perfectly flat.

C_m = term describing the resistance to mass transfer in the mobile phase and D_R = average turbulent diffusion coefficient.

In the derivation no radial diffusion profile is used, but an average overall turbulent diffusion coefficient, D_R, is assumed. Although there exists a finite laminar sublayer in which interphase mass transfer is governed by molecular diffusion, it is assumed that this contribution is negligible for turbulent flow at sufficiently high Re numbers.

A remarkable property of eqn. 2 is the large influence of k on C_m. The latter increases by a factor of 17.5 on going from $k=0$ to $k=1$, which is much less than Martin and Guiochon have calculated (factor of 100), but is still significantly more than for optimum laminar fow (factor of 2). For the theoretical case of a perfectly flat velocity profile, Giddings[12] and Tijssen[11] have found the following:

$$C_m = \frac{R^2}{4D_R}\left(\frac{k}{1+k}\right)^2 \tag{3}$$

Contrary to expectation, the C_m term is only zero for $k=0$; it has a finite value for all other k values.

The discrepancies between the existing theories for turbulent dispersion are summarized in Table I. For comparison, the values under optimum laminar flow

TABLE I
DISCREPANCIES BETWEEN EXISTING THEORIES FOR TURBULENT DISPERSION
Re = 10^4.

	$h = H/d_c$	
	$k=0$	$k=1$
Pretorius	0.6	3
Guiochon	0.2	65
Tijssen	0.8	12
Golay (optimum laminar)	0.3	0.6

conditions are also presented. It seems that the high capacity factor dependence of turbulent dispersion is an intrinsic property of turbulent flow, which arises from the shape of the velocity profile.

EXPERIMENTAL

Experiments under turbulent flow conditions were performed with fused-silica columns having an internal diameter of 320 μm, lengths ranging from 25 to 5 m and a stationary phase film thickness of 0.12 μm CP-Sil 5 CB (Chrompack, Middelburg, The Netherlands). The sample introduction system consisted of a pneumatically actuated Valco four-port valve (VICI AG; Valco, Schenkon, Switzerland) with an internal rotor (6 nl) which allows input band widths as low as 1 ms (ref. 3). The valve was mounted on top of a Carlo Erba 4160 gas chromatograph (Carlo Erba, Milan, Italy).

The carrier gas (nitrogen) pressure was controlled with a Tescom 44-1100 high pressure regulator (up to 100 bar) (Tescom, Minneapolis, MN, U.S.A.). Flame ionization detection could not be used due to extinguishing of the flame. Therefore, a low cell volume (40 μl) photoionization detector (HNU Systems, Newton, MA, U.S.A.) was used throughout all experiments. The amplifier was modified to lower the time constant to about 2 ms. Considering the high column flow-rates involved (>1 l/min), peak broadening due to the cell volume will be negligible. Since ordinary chartspeed recorders are far too slow, chromatograms were recorded on a digital storage oscilloscope (Nicolet, Madison, WI, U.S.A.), capable of sampling at a maximum rate of 1 MHz.

RESULTS AND DISCUSSION

Plots of log h *versus* log Re both for $k=0$ and $k=1$ are shown in Fig. 2. The transition from laminar to turbulent flow occurs at a Re of about 2300. Before this critical Re is reached, some incipient turbulent phenomena reduce the plate height, as reported in the literature[5]. Beyond the critical Re a pronounced decrease in the plate height is observed. For $k=0$, h reaches a value of about 0.8 at Re $= 1.5 \cdot 10^4$. This curve is in good agreement with earlier theoretical and experimental results for unretained components[6]. The gap between the two curves in Fig. 2 is a measure of the ratio between h for $k=0$ and $k=1$.

It is clear that for laminar flow beyond the optimum this gap becomes constant, on the other hand with turbulence this gap increases considerably with increasing degree of turbulence. This behaviour is also shown in Fig. 3, where the reduced plate height is plotted *versus* the capacity factor at Re $=$ 6200. By comparing the experimental curve with the Tijssen theory (eqn. 2) and with laminar flow, both normalized at $k=0$, it is seen that the experimental results are fitted reasonably well with the function of k in eqn. 2. From $k=0$ to $k=1$ the experimental value of h changes by a factor of 19, whereas a factor of 17.5 was calculated. Under optimum laminar conditions these h values differ by only a factor of 2.1. These results are in contradiction with the theory of Martin and Guiochon[10]. They calculated this difference to be 100-fold under turbulent conditions.

Using eqn. 2, an absolute value for h can be calculated, provided that the

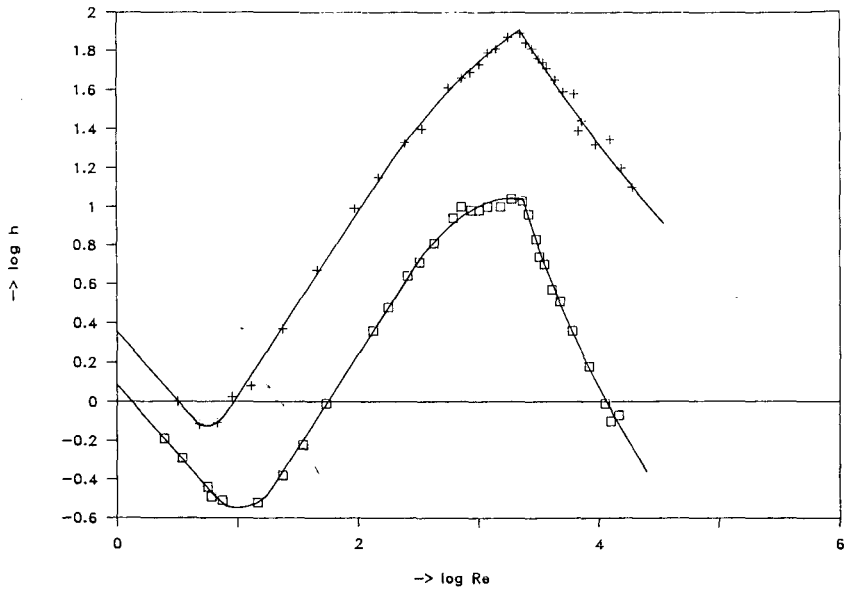

Fig. 2. Turbulent dispersion *versus* Reynolds number, for $k = 0$ (□) and $k = 1$ (+).

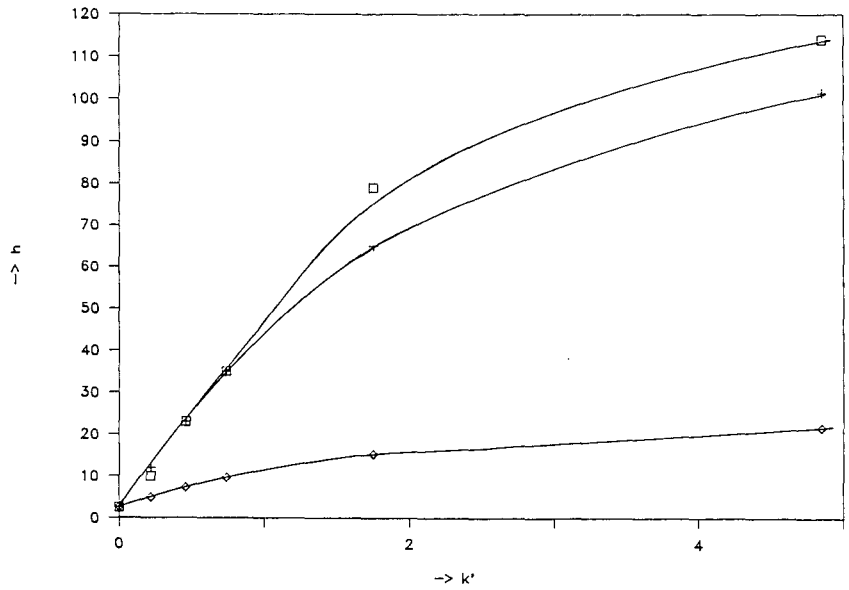

Fig. 3. Turbulent dispersion *versus* capacity factor (Re=6200): □, experimental; +, with turbulence; ◇, with laminar flow.

turbulent diffusion coefficient is known. According to empirical relationships[10] the turbulent diffusion coefficient is

$$D_R/D_m^\circ = 1 + 0.009\mathrm{Re}^{0.84} \cdot \mathrm{Sc} \tag{4}$$

where D_R = average cross-sectional turbulent diffusion coefficient, D_m° = molecular diffusion coefficient, Sc = ν/D_m°, and ν = kinematic viscosity.

Calculation with eqns. 2 and 3 at Re = $1.5 \cdot 10^4$ gives for $k=0$ and $k=1$, respectively, $h=0.8$ (experimental $h=0.8$) and $h=12$ (experimental $h=13$). It must be noted that the fit is less close at lower Re numbers. Obviously, the results depend upon the accuracy of the velocity profile, which changes with Re, particularly for lower Re numbers. In the theory of Tijssen a 10th power profile was used (eqn. 1). In the literature, however, a 7th power profile is often proposed as an approximation for the velocity profile in the range $6 \cdot 10^3 < \mathrm{Re} < 10^5$ (ref. 13). Using this profile, we calculated according to the theory of Tijssen:

$$C_m = \frac{R^2}{D_R} \frac{0.85 + 10.3k + 34.5k^2}{100(1+k)^2} \tag{5}$$

This gives $h=1$ and $h=15$ for $k=0$ and 1 respectively. Comparing this with the former profile, the results differ only slightly.

Although at lower Re values appropriate velocity profiles can be found, the Tijssen concept will probably no longer be valid. It assumes an overall turbulent diffusion coefficient, whereas at lower Re the influence of a laminar sublayer with molecular diffusion can probably no longer be neglected.

So far the resistance to mass transfer in the stationary phase has been neglected. Considering the high carrier gas velocities involved (up to 15 m/s), the reliability of this assumption must be verified. The resistance to mass transfer in the stationary phase is not affected by the flow profile in the mobile phase[10,11]. Assuming a liquid diffusion coefficient, $D_L = 5 \cdot 10^{-6}$ cm^2/s (ref. 14), $k=1$ and $\bar{u}=15$ m/s, the reduced plate height of the resistance to mass transfer in the stationary phase is calculated to be $h_s=0.22$. This may be considered negligible in the foregoing results.

In order to answer the question of whether turbulent flow can increase the analysis speed, the ratio $H/\bar{u}$ has to be considered. For a fixed (required) plate number and capacity factor, the analysis time is proportional to the ratio $H/\bar{u}$. Under turbulent conditions this ratio was determined according to the experimental results at the highest Re in Fig. 1 (Re = $1.5 \cdot 10^4$, $\bar{u}=15$ m/s) by incorporating the experimental dependence of h on k in Fig. 2. For laminar flow the theoretical $H/\bar{u}$ at the optimum was taken, using a molecular diffusion coefficient, $D_m = 0.1 \cdot 10^{-4}$ m^2/s (carrier gas nitrogen)[15].

The resulting gain, G, in analysis speed with turbulent flow relative to laminar flow is given in the first column of Table II for different capacity factors. The second column gives an estimate of the gain in analysis speed in the (theoretical) case of a very narrow bore column requiring the same pressure drop as under turbulent conditions. In Fig. 4 a typical separation under turbulent conditions is presented. This clearly demonstrates again the high dependence of h on k. Another aspect which has to be

TABLE II

GAIN, G, IN ANALYSIS SPEED

First column: between turbulent ($Re = 10^4$) and optimum laminar flow for different capacity factors, k, carrier gas, nitrogen; $D_m = 1 \cdot 10^{-5}$ m^2/s; column, $L = 5$ m, I.D. $= 0.32$ mm; $d_f = 0.12$ μm. Second column: when using a narrow bore column requiring the same pressure drop as under turbulent conditions ($\Delta p = 50$ bar, I.D. 3 μm).

k	G (turbulent)	G (laminar)
0	13	100
0.5	4	100
1	3	100
2	3	100
4.5	3	100

considered is the pressure drop associated with turbulent flow. The inlet pressure required for a given Re can be calculated[10] from

$$p_i^2 - p_o^2 = \frac{316.4\eta^2 \cdot Re^{7/4} \, LRT}{Md_c^3} \tag{6}$$

where p_i,p_o = inlet and outlet pressures, η = dynamic viscosity, L = column length, R = gas constant, T = column temperature and M = molecular weight of the carrier gas. For example, a 5 m × 0.32 mm column requires an inlet pressure of 36 bar (nitrogen) to obtain $Re = 10^4$. For He or H_2 as the carrier gas the pressure drop would even be larger. The gain in analysis speed is insufficient to compensate for the larger pressure drop. The same gain can be obtained more easily under laminar flow conditions by using hydrogen as the carrier gas, and/or applying a vacuum at the column outlet[16] and/or a reduction of the column diameter[15].

CONCLUSIONS

Low reduced plate heights can be obtained under turbulent conditions especially for unretained components ($h = 0.8$ at $Re = 1.5 \cdot 10^4$). Unfortunately, the dependence of the plate height on the capacity factor is significantly higher than under laminar

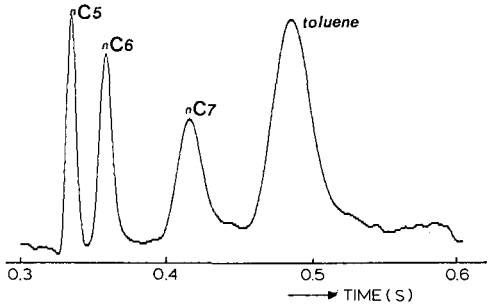

Fig. 4. Representative chromatogram of an hydrocarbon headspace sample under turbulent flow conditions. Column: $L = 5$ m, I.D. $= 0.32$ mm; $d_f = 0.12$ μm; $p_i = 50$ bar.

conditions. Consequently, the gain in analysis speed is limited in practice. Taking into account that an high pressure drop is required for turbulent flow, a reduction of the column diameter is a better approach to increase the analysis speed. From the theoretical models on turbulent dispersion reported in the literature, only the Tijssen theory gave acceptable agreement with the experimental plate heights at various capacity factors. In this theory the resistance to mass transfer in the mobile phase is calculated with a turbulent velocity together with an overall turbulent diffusion coefficient. Therefore, the large influence of the capacity factor on the plate height is an intrinsic property of turbulent flow, which can be explained from the shape of the velocity profile.

REFERENCES

1 C. A. Cramers and P. A. Leclercq, *CRC Crit. Rev. Anal. Chem.*, 20 (1988) 117.
2 A. van Es, J. Janssen, C. Cramers and J. Rijks, *J. High Resolut. Chromatogr. Chromatogr. Commun.*, 11 (1988) 852.
3 A. van Es, J. Janssen, R. Bally, C. Cramers and J. Rijks, *J. High Resolut. Chromatogr. Chromatogr. Commun.*, 10 (1987) 273.
4 R. Tijssen, *Sep. Sci.*, 13 (1978) 681.
5 R. Tijssen, N. van den Hoed and M. Kreveld, *Anal. Chem.*, 59 (1987) 1007.
6 L. Flint and P. Eisenklam, *Can. J. Chem. Eng.*, 47 (1969) 101.
7 J. Giddings, W. Man Waring and M. Myers, *Science (Washington, D.C.)*, 154 (1966) 146.
8 F. Doue and G. Guiochon, *Sep. Sci.*, 5 (1970) 197.
9 V. Pretorius and T. Smuts, *Anal. Chem.*, 38 (1966) 274.
10 M. Martin and G. Guiochon, *Anal. Chem.*, 54 (1982) 159.
11 R. Tijssen, *Ph. D. Thesis*, University of Technology, Delft, 1979.
12 J. Giddings, *Dynamics of Chromatography*, Marcel Dekker, New York, 1965.
13 R. B. Bird, W. E. Stewart and E. N. Lightfoot, *Transport Phenomena*, Wiley, New York, 1960.
14 C. A. Cramers, C. van Tilburg, C. Schutjes, J. Rijks, G. Rutten and R. de Nijs, *Proc. 5th Int. Symp. on Capillary Chromatography, Riva del Garda, 1983*, p. 76.
15 C. P. M. Schutjes, E. A. Vermeer, J. A. Rijks and C. A. Cramers, *J. Chromatogr.*, 253 (1982) 1.
16 C. A. Cramers, G. J. Scherpenzeel and P. A. Leclercq, *J. Chromatogr.*, 203 (1981) 207.

Journal of Chromatography, 477 (1989) 49–52
Elsevier Science Publishers B.V., Amsterdam — Printed in The Netherlands

CHROM. 21 479

Note

High boiling organic traces in drinking water

Quantitative analysis by liquid–liquid enrichment within the analytical glass capillary

R. E. KAISER* and R. RIEDER
Institute for Chromatography, P.O. Box 1141, D-6702 Bad Dürkheim-1 (F.R.G.)

The latest European regulations about drinking water analysis make it necessary to check for a wide variety of organic key compounds in drinking water in the sub-ppb[a] range. Without primary enrichment, more or less all regulated analytical methods available today are unsuitable for this purpose. There are in addition serious problems of taking, storing and manipulating the sample which may lead to incorrect determinations, and simple technical and human problems when the enrichment step commences with sample volumes of $\geqslant 1$ l water.

It is known that any surface adsorbs/desorbs any trace until an equilibrium is reacted between the phases and the matrix. This process is controlled by displacement chromatography at quite slow rates of material transport. Therefore large volumes of water in a completely full bottle may stay stable for weeks providing there are no biochemical changes or no mechanical movement by means of temperature gradients or mechanical forces. From such a large volume (litres) a small subsample (few ml) can be taken and placed into a freshly flamed glass container without further contact with surfaces, etc. The final container can be made absolutely clean outside as well as inside. We use flame stable coloured glass (ws in Fig. 1) heated in clean air to above 450°C and then cooled in clean air.

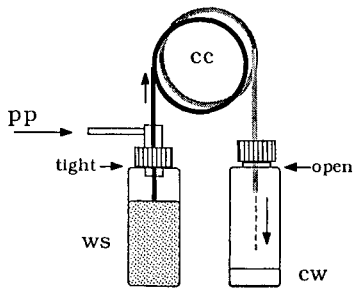

Fig. 1. Passage of sample through the glass capillary: pp = programmed gas pressure; ws = water sample; cw = clean water after passage through the glass capillary (cc).

[a] Throughout this article the American billion (10^9) is meant.

0021-9673/89/$03.50

Let us consider PNA analysis in water at the level of 20 ng/l = 0.02 ppb (w/w). By avoiding any further manipulation step, the possibility of getting true accurate quantitative PNA data is increased. We enrich the PNA onto an immobilized 0.25 μm thick film of PS-089 (94–96% dimethyl- / 4–6% diphenylsiloxane) terminated on the inner glass wall of a 0.3 mm I.D. glass capillary. Through such a 20-m analytical glass capillary (no fused-silica columns for many and obvious reasons) the water sample is forced by pressure programmed nitrogen. The enriching analytical glass capillary also serves as the analytical separation capillary.

An analytical process with enrichment into a "zero volume" of a specific solvent and quantitative specific analysis directly within this enrichment system will avoid many trace analysis problems like contamination from added solvents, other chemicals like sorption repellers, transfer of concentrates, changing containers, etc.

We modified a very similar concept developed by Zlatkis and Wang[1] as described below (see Figs. 1–4).

A 5-ml volume of a drinking water sample was transferred to the flame cleaned flask (ws). A 20 m × 0.3 mm I.D. glass capillary (cc) was then inserted into the room temperature sample so as to make a gas tight seal. Nitrogen gas pressure was applied, starting with 0.3 bar, then increased to 3 bar within 6 min. After 30 min the water sample had been forced through the glass capillary (cc) at room temperature and the excess of gas had pushed the water out of the capillary. The inside of the capillary (cc) is coated with an immobilized 0.25 μm thick film of PS-089 (see above). Many organic traces at the sub-ppb level remain sorbed under these conditions. A second experiment with the same water sample showed 100% transfer from water into the capillary film of all six key PNAs.

The inlet of the glass capillary was placed into the cold sample inlet of a gas chromatograph and the outlet of the glass capillary was placed into the detector. A very thin extra resistance capillary connects the glass capillary outlet with the detector inlet in a T-piece configuration. About 10 to 30 mm of the glass capillary inlet remained in a cool portion of the chromatograph sample inlet or just outside in the laboratory atmosphere.

A low carrier gas pressure was applied at the detector–capillary outlet T-piece connection. The gas chromatographic (GC) oven was heated at 30°C/min to 320°C. All traces volatile enough at 320°C were back flushed into the cold inlet zone.

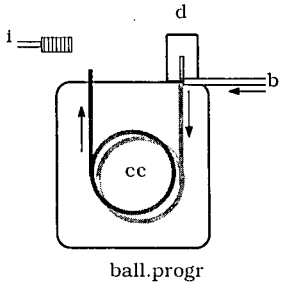

Fig. 2. Back flush and focusing of the wall-enriched sample traces: d = flame ionization detector; b = back flush gas, clean N_2; i = closure (septum) of the GC inlet, here open; ball.progr = temperature programme (30°C/min up to 320°C).

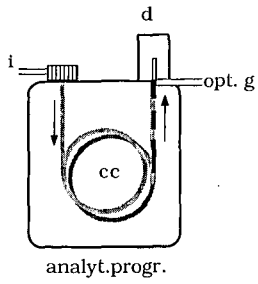

Fig. 3. Analysis of the enriched traces: opt.g = optimizing add-on gas for greater detector specificity and absolute quantitation, *i.e.*, to enable work at the response plateau; analyt.progr., for PNA analysis is shown in Fig. 4, initial temperature 50°C, then raised at 20°C/min to 160°C, followed by 7°C/min to 330°C.

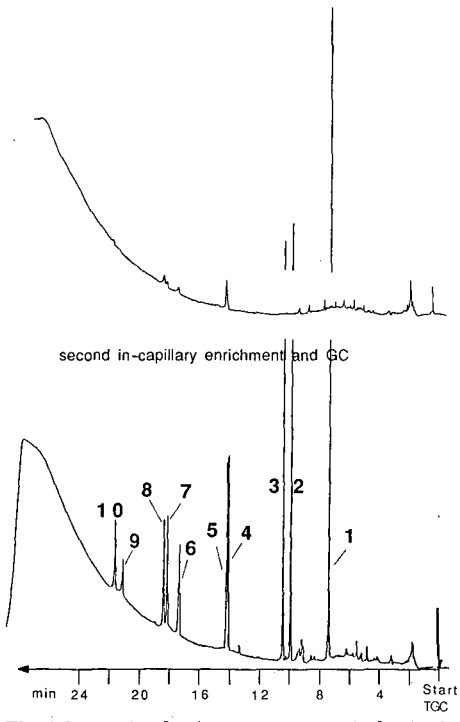

Fig. 4. Example of a chromatogram and of a check chromatogram of the "extracted" sample. Sample: 0.02 ppb each of anthracene (1), fluoranthene (2), pyrene (3), triphenylene (4), chrysene (5), benzo-[*k* + *b*]fluoranthene (6), benzo[*a*]pyrene (7), perylene (8), indopyrene (9), and benzo[*ghi*]perylene (10) in 5 ml water. Instrument: DANI 6500 gas chromatograph with flame ionization detection. Carrier gas pressures: inlet, p_i, 1.4 bar hydrogen; outlet, p_o, 0.5 bar nitrogen. In the upper chromatogram traces of PNAs 4–10 may be seen but no PNA 1 and 2! As no PNA traces are detectable in super clean "zero water" enrichments this may indicate a "memory" effect of the sample glass container prior to the "second extraction". We did not "flame clean" this container prior to the second experiment.

The GC oven was allowed to cool. The inlet was tightened, carrier gas applied and the inlet region heated. The enriched substances start to travel from a local position within the capillary as if they are being sampled on-line. However there is no diluting solvent! If sharp peaks are seen in the chromatogram there is no solvent effect nor retention gap effect, etc., *i.e.*, we have plain capillary GC of the substances. A 20-ng/l sample will contain 20 pg/ml = 5 × 20 = 0.1 ng total PNAs. There is no split nor any specific loss besides that which occurs during the storage of the sample in the 10-ml container (ws).

Temperature programmed GC of the in-capillary enriched substances extracted from the sample into the capillary phase film was then commenced.

The chromatogram was quantitated. We prefer the absolute quantitation using eqn. 1 but one can in addition work with artificial samples or add-on samples using many of the well known standard procedures for relative quantitation

$$\text{Concn. PNA}_x = it/q = hbE_1E_2A_S/q \cdot \text{FSD} \cdot P_SV_S \text{ (g/l)} \quad (1)$$

where i = peak signal in ampere, t = peak width at half height in s, or it = integral in coulomb, q = specific response in C/g for the PNA named x, h = peak height (mm), b = peak width (mm) or hb = integral of the PNA_x peak in mm^2, E_1, E_2 = sensitivity factors of the signal electronics, A_S = ion current in ampere producing a recorder signal of FSD (full scale deflection) in mm, P_S = paper speed (mm/s) and V_S = water sample volume in litre. The parameters h, b, E_1, E_2, A_S, FSD, P_S and q can be summarized as the integral value produced specifically by 1 g of PNA_x, *i.e.*, I_x.

REFERENCE

1 A. Zlatkis and F. Wang, *Anal. Chem.*, 55 (1983) 1848.

Journal of Chromatography, 477 (1989) 53–57
Elsevier Science Publishers B.V., Amsterdam — Printed in The Netherlands

CHROM. 21 514

Note

Gas chromatographic analysis of thermoplastic aromatic polyamides after alkali fusion

N. HARAHAP, R. P. BURFORD and J. K. HAKEN*
Department of Polymer Science, The University of New South Wales, P.O. Box 1, Kensington, 2033 N.S.W. (Australia)

Aromatic polyamides have been developed with superior thermal properties and include poly(*p*-phenyleneterephthalamide) (*e.g.*, Du Pont "Kevlar" and Enka "Arenka") and poly(*m*-phenyleneisophthalamide) (*e.g.*, Du Pont "Nomex"). These polymers have been analysed by fusion gas chromatography (GC) by Haken and Obita[1]. More complex aromatic poly(amide-imides) have also appeared. The Amoco product "A-1", the condensation product of trimellitic anhydride, 4,4′-methylenediamine and *m*-phenylenediamine, has also been successfully analysed[2]. A wide range of mixed aromatic polyamides and amide-imides now exists, and numerous examples of these have been described (see for example ref. 3). Commercial examples of high-modulus fibres are Teiujin "HM-50" prepared from a equimolar mixture of *p*-phenylenediamine and 3,4′-diamino-diphenylether with terephthaloyl chloride, while mixed aromatic fibres are also produced in the U.S.S.R. (*e.g.*, "SVM"[3] and "Twerlon"[4].

Recently, amorphous aromatic copolyamides have been reported by Sikkema[5,6]. An example is that prepared from equimolar amounts of *p*-aminobenzoic acid, *m*-aminobenzoic acid, isophthalic acid and 4,4′-methylenedianiline, although alternatives in which the 4,4′-methylenedianiline is replaced by 4,4′-sulfonyldianiline exist. This form of analogue is expected to improve back-bone flexibility, in a similar way to that claimed for "Sulfon I" and "Sulfon T", the condensation products of 4,4′-diaminodiphenylsulfone with isophthalic or terephthalic acid, respectively[4]. The mixed aromatic copolyamides are claimed to have much better solvent resistance than other amorphous, high-temperature polymers such as polysulfones, polyetherimide and polyether sultone. These materials are stated by Akzo[7] to be difficult to analyse and the analysis described below is believed to be previously unreported.

In this paper is described the application of alkali fusion for the analysis of an amorphous aromatic copolyamide. The fusion reaction is carried out at 300°C for 2 h by using the previously described flux-containing reagent[8]. The fragments after cleavage are converted into derivatives to allow examination by using GC.

EXPERIMENTAL

Sample

A sample of powdered HTP-1 thermoplastic aromatic polyamide provided by The Akzo Research Laboratories, Arnhem, The Netherlands, was used for analysis.

0021-9673/89/$03.50

the sample contains *p*-aminobenzoic acid, *m*-aminobenzoic, isophthalic acid and 4,4′-methylenedianiline in equimolar ratios.

Alkali fusion

The alkali fusion was carried out with 200 mg of polymer samples and 13 g of potassium hydroxide–sodium acetate (95:5) according to the procedure previously reported[8]. The reaction was achieved by heating the polymer reagent mixture in a stainless-steel tube at 300°C for 2 h.

After cooling, the contents were transferred to a beaker. This was followed by the addition of sufficient concentrated hydrochloric acid to bring the pH to about 7, where the isophthalic acid was liberated as a precipitate and the 4,4′-methylenedianiline dissolved. The aminobenzoic acids remain in solution during these procedures, either as the amine hydrochloride at low pH or as the potassium salt at high pH.

The isophthalic acid fragment was filtered by using a büchner funnel and washed with hydrochloric acid and dried at 100°C. This was converted into dimethyl isophthalate by refluxing with boron trifluoride–methanol reagent according to the previously reported procedure[8].

The filtrate containing amine fragments was rendered slightly basic by the addition of potassium hydroxide pellets to liberate the 4,4′-methylenedianiline which was recovered by extraction with 3 × 15 ml portions of chloroform. The chloroform solution was then concentrated and 3 ml of trimethysilylimidazole (TMSI) (TRI-SIL® Z, Pierce) were added. The mixture was continuously shaken for about 15 min at 50°C and then used for the GC analysis of the 4,4′-methylenedianiline fragment as its trimethylsilyl derivative.

The remaining aqueous layer containing *p*-aminobenzoic acid and *m*-aminobenzoic acid derivatives was adjusted to a pH of 6 with a 1 *M* hydrochloric acid solution. The pH needs to be closely controlled to enable separation of these aminobenzoic acids, as pH < 5 or > 7 will result in reformation of soluble salts. The liberated acids were recovered by extraction with 3 × 15 ml portions of chloroform. Both fragments were converted into their trimethylsilyl derivatives using the TMSI reagent. The concentrated chloroform solutions obtained after derivatisation of the acids was then used for the analysis of *p*-aminobenzoic acid and *m*-aminobenzoic acid fragments. The analytical scheme is shown in Fig. 1.

Gas chromatography

Gas chromatography was carried out on a Hewlett Packard 5750 Research Model gas chromatograph with a flame detector and helium as carrier gas (flow-rate was 60 ml min^{-1}). The separations were performed on a 12 ft. × ¼ in. O.D., aluminium column packed with 5% SE-30 on Celatom A.W. DCMS (72–85 mesh).

The trimethylsilyl derivative of 4,4′-methylenedianiline was eluted isothermally at 252°C, while derivatives of *m*-aminobenzoic acid and *p*-aminobenzoic acid were separated at 228°C.

Dimethyl isophthalate was eluted isothermally at 220°C using the same column.

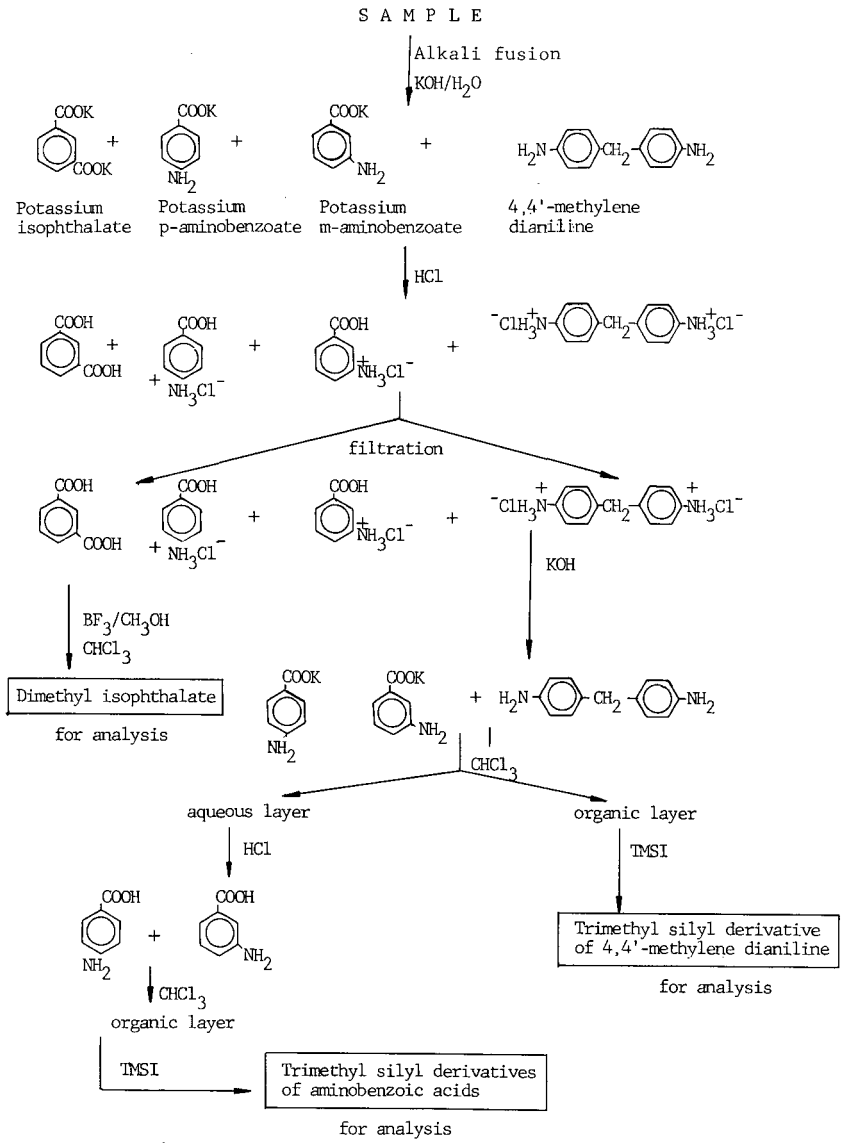

Fig. 1. Analytical scheme.

RESULTS AND DISCUSSION

The thermoplastic aromatic polyamide sample was successfully cleaved into *p*-aminobenzoic acid, *m*-aminobenzoic acid, isophthalic acid and 4,4′-methylenedianiline fragments by using alkali fusion. The cleavage was achieved after 2 h at 300°C. The fragments were readily separated by solvent extraction after adjusting the pH of the mixture as previously described.

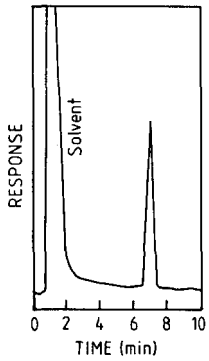

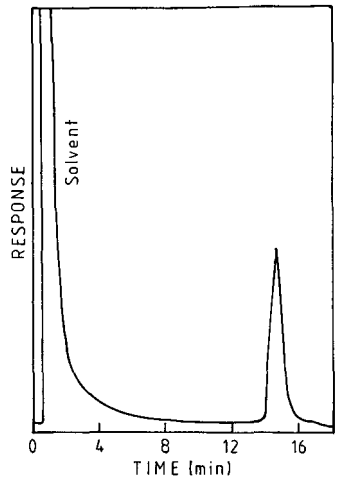

Fig. 2. Gas chromatogram showing the separation of dimethyl isophthalate.

Fig. 3. Gas chromatogram showing the separation of trimethylsilyl derivative of 4,4′-methylenedianiline.

Isophthalic acid was converted into dimethyl isophthalate by using boron trifluoride–methanol reagent. The derivative obtained was separated on a SE-30 column as shown in Fig. 2.

Aminobenzoic acids and 4,4′-methylenedianiline fragments were successfully separated as their trimethylsilyl derivatives on the same column. Fig. 3 shows a chromatogram of the trimethylsilyl derivative of 4,4′-methylenedianiline obtained by using GC. Schlueter and Siggia[9] determined the 4,4′-methylenedianiline as free amine on a free fatty acid phase column, while collaborators[2] have also reported the sep-

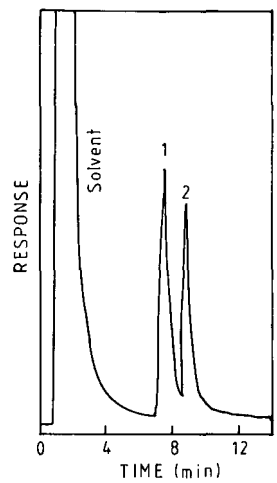

Fig. 4. Gas chromatogram showing the separation of trimethylsilyl derivatives of: (1) *m*-aminobenzoic acid and (2) *p*-aminobenzoic acid.

aration of a trifluoroacetic acid derivative of 4,4'-methylenedianiline. However, their work was performed by using liquid chromatography.

Fig. 4 shows the separation of the trimethylsilyl derivatives of the aminobenzoic acid isomers. The peaks corresponding to the trimethylsilyl derivatives of *m*-aminobenzoic and *p*-aminobenzoic acid show minor but acceptable overlap. Evaluation of various columns such as neopentyl glycol succinate, diethylene glycol succinate and Silar 10 CP was carried out before this successful result was obtained on a non-polar column.

Alkali hydrolytic fusion prior to GC has been described as a valuable method for the estimation of aminobenzoic acids, isophthalic acid and 4,4'-methylenedianiline from the thermoplastic aromatic polyamide sample.

The analyses have been carried out on a qualitative basis although it has been demonstrated that the degradative reactions[10] are complete or essentially so. Errors may be introduced in the extraction steps and may be of the order of 2.0%. This, however, may be minimised or eliminated either by carrying out the reactions as indicated, where separation of various functional classes is partially conducted for convenience, or by developing an analytical scheme without such extractions. Such a procedure has been reported for the quantitative analysis of dicarboxylic acids and polyols in silicone–polyester resins[11]. The quantitative analyses of diamines after alkali fusion has previously been reported by Schleuter and Siggia[9] and by Glading and Haken[12].

REFERENCES

1 J. K. Haken and J. A. Obita, *J. Chromatogr.*, 244 (1982) 265.
2 J. K. Haken and J. A. Obita, *J. Chromatogr.*, 244 (1982) 259.
3 H. G. Elias and F. Vohwinkel, *New Commercial Polymers 2*, Gordon and Breach, New York, 1986.
4 R. Swarski, *Lenzinger Ber.*, 45 (May) (1978) 28.
5 *U.S. Pat.*, 4,750,651, July 19 (1988).
6 D. J. Sikkema, in P. J. Lemstra and L. A. Kleintjens (Editors), *Proceedings 3rd Rolduc Polymer Meeting, Integration of Fundamental Polymer Science and Technology 3*, New York, 1988.
7 D. J. Sikkema, personal communication, 1988.
8 J. K. Haken, N. Harahap and R. P. Burford, *J. Chromatogr.*, 387 (1987) 223.
9 D. D. Schlueter and S. Siggia, *Anal. Chem.*, 49 (1977) 2349.
10 J. K. Haken, *J. Chromatogr.*, 406 (1987) 167.
11 J. K. Haken, N. Harahap and R. P. Burford, *J. Chromatogr.*, 452 (1988) 37.
12 G. J. Glading and J. K. Haken, *J. Chromatogr.*, 157 (1978) 404.

Journal of Chromatography, 477 (1989) 59–62
Elsevier Science Publishers B.V., Amsterdam — Printed in The Netherlands

CHROM. 21 547

Note

Practical aspects of recycle gas chromatography with capillary columns

D. ROBERTS and W. BERTSCH*
Department of Chemistry, Lloyd Hall, The University of Alabama, P.O. Box 870336, Tuscaloosa, AL 35487-0336 (U.S.A.)

Extracolumn dispersion and active surfaces are the most serious limitations to capillary column recycle gas chromatography (GC) with mechanical valves[1,2]. As the solute is switched from column to column, it must pass through a valve. The valve may act as an element of dispersion as well as a source of sites that offer specific interactions to the solutes to be chromatographed. Since the same column segments are to be used over and over, these factors must be rigorously controlled. The quality of column connections to the valve must be very high to prevent peak distortion due to unswept volumes. The exponentially modified Gaussian function can be used to evaluate peak distortion[1,3]. Methods of column activity testing[4] can be set up to determine the contribution of the valve materials toward adsorption, and perhaps catalysis of selected test compounds[5]. In this note, we address the cutting of fused-silica capillary columnns and assess the critical steps in making high-quality connections.

EXPERIMENTAL

A capillary column recycle gas chromatograph, based on an HP 5890A gas chromatograph and a microvalve (No. 4N6WT, VICI, Houston, TX, U.S.A.) was used as previously described[1]. A 30 m × 0.25 mm I.D. fused-silica column, coated with a 0.25-μm film of dimethylpolysiloxane (DB-1, J & W, Folsom, CA, U.S.A.) was cut in half so that two segments of equal length could be connected. Columns were cut with scribes by scratching the fused-silica surface perpendicular to the direction of the fiber axis, followed by pulling while the column is slightly bent[6]. Column ends were polished to a fine finish by using 6000-grit sand paper (Scientific Instrument Services, Ringoes, NJ, U.S.A.). The test method described by Grob[4] was used to evaluate column and valve activity under a variety of conditions. A commercially available standard (Fluka, Ronkonkona, NY, U.S.A.) was diluted 1:10 and 1:100 with hexane. The gas chromatograph was programmed from 40 to 65°C at 10°C/min, followed by a 1-min delay, and then from 65 to 140°C at 2°C/min.

RESULTS AND DISCUSSION

The importance of proper column cutting techniques has been stressed[7], and an

0021-9673/89/$03.50

entire paper by Roeraade[6] was devoted to the cutting of fused silica. It was pointed out that fused-silica tubing with thin walls is difficult to cut cleanly, and careful inspection of the surface may reveal a jagged or chipped surface. Difficulties may arise from two sources: unswept volumes and adsorptive surfaces. Bulk column material that finds its way into the column end during the cutting process should be removed. If a chipped surface results in the cut, the column flow is subjected to the fused-silica surface and in some cases the polyimide coating. In recycle GC, the effect of valve surfaces must also be considered. Materials used in valve construction are metals and synthetic/composite polymers. The effluent passes through a channel in the rotor and is therefore exposed to both types of surfaces. Some choice in the nature of the metal and rotor material is possible, *i.e.* the user can specify rotor and valve body materials.

Fig. 1 shows the effect of column connection techniques on chromatographic performance. Chromatogram A was obtained by connecting the 0.25-mm I.D. columns with a tapered glass union constructed in our laboratory. The union allowed the column ends to be butted together, and formed a tight seal with the fused-silica column by pressure against the polyimide layer. The column ends were inspected prior to connection to insure that reasonably good cuts were obtained. Chromatogram B was obtained after sanding the column ends and reconnection. Small particles of fused silica and polyimide were collected in the colum ends. Tailing is observed on the acid and free-base peaks. However, the effect is relatively minor. These particles can be removed by filling the column with a non-wetting solvent before grinding (*i.e.* hexane), followed by forceful expulsion. Fig. 2a–c shows scanning electron microscope photographs of the column material after (a) cutting, (b) sanding, and (c) particle removal. The jagged surface has been smoothed, and it is possible to obtain a perpendicular surface at the column end. The fused silica should be held at a 90° angle

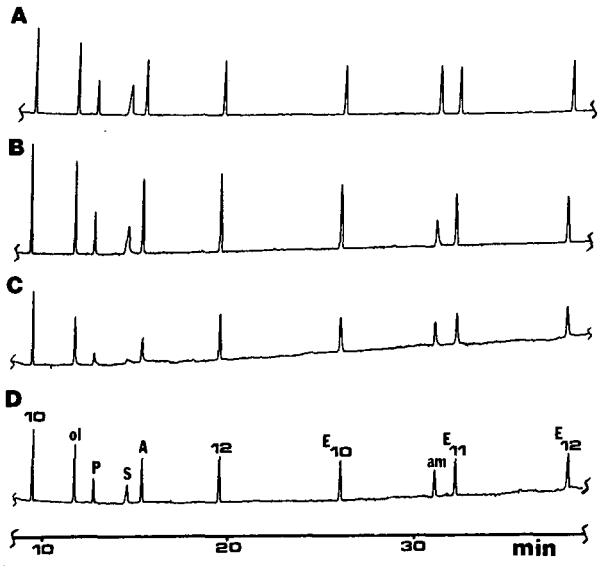

Fig. 1. Chromatograms of the test mix. (A) No extraneous material in the columns; (B) columns connected after sanding; (C) poor column-to-valve connections; (D) valve connections with polished ends.

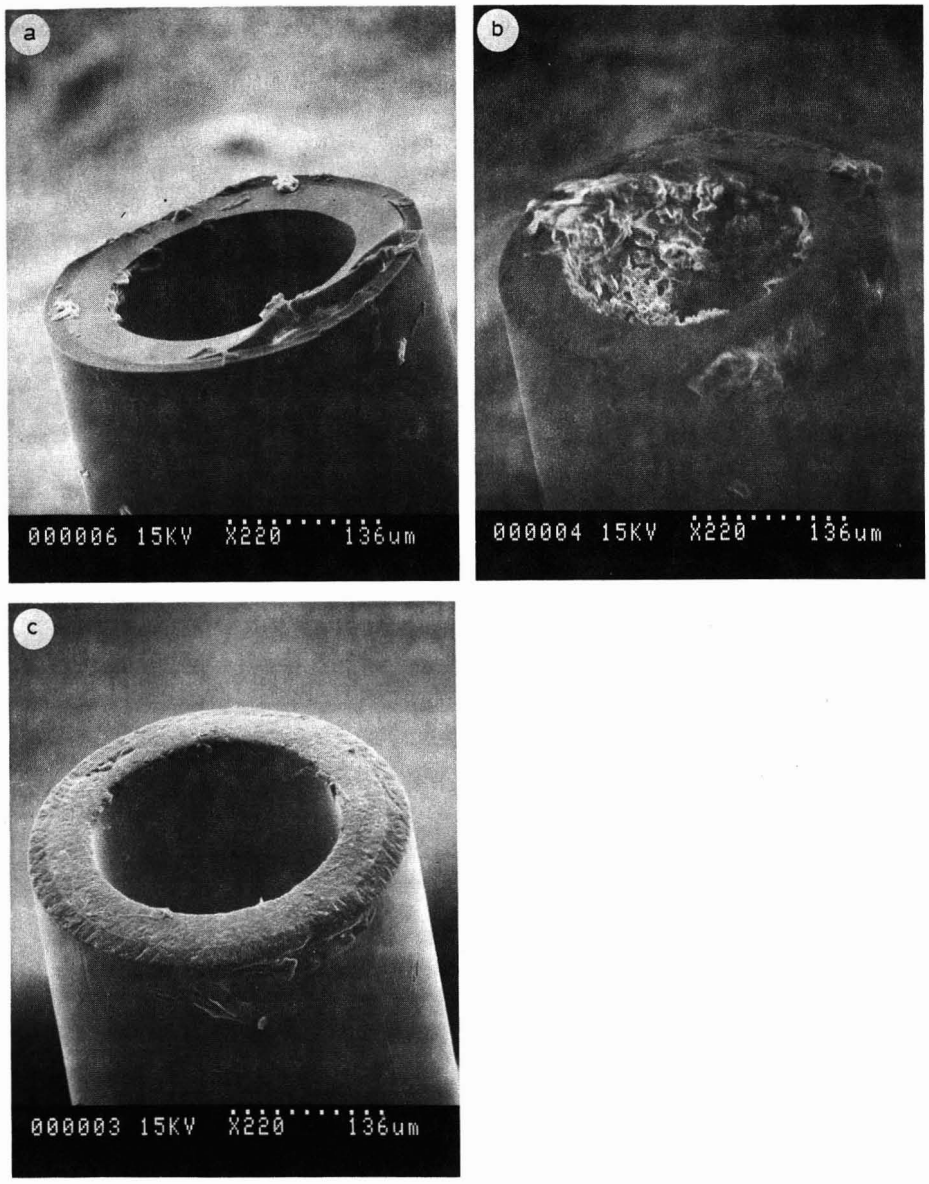

Fig. 2. SEM photographs of column end (a) after cutting, (b) after sanding, and (c) after washing.

in reference to the sanding material, and kept from bending when pressure is applied. This can be accomplished by insertion of the fused-silica end into a rigid structure that maintains a straight posture during sanding.

Exposure of the test sample to the materials of the valve during a single passage produces a slight reduction in the peak height of the amine, as shown in the chromatogram in Fig. 1D. No noticeable tailing from unswept volume was noticed. This is

expected since previous studies have shown that relative peak asymmetry is decreased at high capacity ratios[1]. To ascertain the concentration dependance of the valve activity, a more dilute solution of the standard was prepared. By chromatographing the minimum detectable quantities of the standard components, the relative effect of the adsorptive sites is magnified. Injection of the 1:100 diluted standard produced detectable peaks for all the components, with the exception of the acid and amine. Connections made with less than ideal column ends produce a small increase in the tailing of some of the components, as shown in the chromatogram in Fig. 1C. The alcohol, phenol, acid, aniline, and amine peaks show pronounced tailing. This indicates that the quality of the column connection to the valve is critical, and a smooth surface on the end of the column is essential to prevent unnecessary valve–solute contact. Although small changes are noticed, several valve passages are required for meaningful evaluations. Practical application of capillary recycle GC wil be presented in the near future[8].

REFERENCES

1 D. Roberts and W. Bertsch, *J. High Resolut. Chromatogr. Chromatogr. Commun.*, 11 (1988) 783.
2 W. Bertsch, *J. High Resolut. Chromatogr. Chromatogr. Commun.*, 1 (1978) 187.
3 D. Roberts, *Dissertation*, University of Alabama, 1989.
4 K. Grob, Jr., G. Grob and K. Grob, *J. Chromatogr.*, 156 (1978) 1.
5 S. T. Adam, *J. High Resolut. Chromatogr. Chromatogr. Commun.*, 11 (1988) 85.
6 J. Roeraade, *J. High Resolut. Chromatogr. Chromatogr. Commun.*, 6 (1983) 140.
7 W. G. Jennings, *Gas Chromatography with Glass Capillary Columns*, Academic Press, New York, 2nd. ed., 1980, p. 90.
8 D. Roberts and W. Bertsch, in preparation.

Journal of Chromatography, 477 (1989) 63–71
Elsevier Science Publishers B.V., Amsterdam — Printed in The Netherlands

CHROM. 21 606

OBSERVATIONS WITH HIGH-MOLECULAR-WEIGHT POLYETHYLENE GLYCOL STATIONARY PHASES IN CAPILLARY GAS CHROMATOGRAPHY

I. ADSORPTION *VERSUS* PARTITIONING CHROMATOGRAPHY

P. SANDRA*
Laboratory of Organic Chemistry, University of Gent, Krijgslaan 281 (S4), B-9000 Ghent (Belgium)
F. DAVID
Research Institute for Chromatography, P.O. Box 91, B-8610 Wevelgem (Belgium)
K. A. TURNER and H. M. McNAIR
Department of Chemistry, Virginia Polytechnic Institute and State University, Blacksburg, VA 24061 (U.S.A.)
and
A. D. BROWNSTEIN
Innophase Corporation, Portland, CT 06480 (U.S.A.)

SUMMARY

Fused-silica open-tubular capillary columns coated with high-molecular-weight polyethylene glycols of different origins have been evaluated. The chromatographic behaviour below and above the solid–liquid transition temperature was studied through measurements of the column efficiency, resolution and capacity factors as a function of the column temperature and the nature of the solutes.

INTRODUCTION

One of the five basic phases employed in capillary gas chromatography (CGC) is polyethylene glycol (PEG) with a high molecular weight[1,2]. PEGs have an unique selectivity and polarity and are particularly useful for the analysis of medium polar and polar compounds with molecular weights ranging from 20 to 300. High-molecular-weight PEG can be modified into an acidic form by reaction with nitroterephthalic anhydride (FFAP, free fatty acid phase) for the analysis of fatty acids from C_1 to C_{24} (ref. 3), and into an alkaline form for example by reaction with isocyanates for the analysis of free amines[4]. They are, therefore, intensively used in everyday CGC.

Nevertheless, as polyglycols and derivatives, the polymers nowadays used to manufacture PEG-coated capillary columns leave much to be desired. In many cases, industrial products are used, not synthesized for chromatography. Depending on the origin and on the batch, the molecular weight distribution varies and traces of cata-

0021-9673/89/$03.50

lysts from the polymerization process are present in various amounts and moreover may differ in nature. Therefore in CGC, the reproducibility of the efficiency, inertness, useful temperature range, maximum allowable operating temperature and even the selectivity and polarity is poor.

On the occasion of The Fourth International Symposium on Capillary Chromatography, Hindelang, May 1981 a round robin test was organized[5] to evaluate the (qualitative and quantitative) performance of capillary columns coated with apolar phases of the methyl silicone type and polar phases of the high-molecular-weight PEG type. For the apolar columns, interlaboratory data were excellent, whereas for the polar columns, interlaboratory and even intralaboratory data were poor.

Since then, we at the University of Gent and Virginia Polytechnic have continuously investigated PEG phases in CGC[6–9] and also evaluated the properties of commercial PEG columns. Developments with PEGs include the purification of industrial polyoxiranes[3], stabilization of the PEG film by adding antioxidants[4] and the evaluation of different immobilization and/or cross-linking procedures[10–16]. PEG substitutes with a polysiloxane structure were introduced[2,17]. The overall polarity of PEG, as measured by the Rohrschneider–McReynolds standards, can be approached but never its specific selective interactions.

This is Part I of a series of papers[18,19] to summarize our observations. It focuses on the solid–liquid transition of PEGs and on the implications for the chromatographic properties of columns. The chromatographic behaviour below and above the transition temperature of the different PEGs was studied by measuring the number of theoretical plates per metre (N/m), the resolution (TZ) and the capacity factors, k, as functions of the column temperature and nature of the solutes.

EXPERIMENTAL

The following columns were used.

Column 1: PEG NXL. 25 m × 0.25 mm I.D. fused-silica open-tubular (FSOT), coated with 0.5 μm of Bondable PEG (Innophase, Portland, CT, U.S.A.). The fused-silica tubing was flushed with dichloromethane and dried under nitrogen before static coating. The column was conditioned to 100°C only, to avoid cross-linking of the phase.

Column 2: PEG XL-200. Similar to column 1, but cross-linking was achieved by heating the column rapidly to 200°C after coating for 8 h, which gives the highest chromatographic efficiency[18].

Column 3: FFAP XL-200. Similar to column 2, but coated with Bondable FFAP (Innophase).

Column 4: PEG HM-2500. 10 m × 0.25 mm I.D. FSOT, coated with 0.2 μm of laboratory made cross-linkable PEG-2500. The polymer was obtained by condensation of PEG-2500 with triethoxysilylpropyl isocyanate. The FS tubing was leached with 3% HCl and dehydrated at 220°C. Deactivation was performed by coating the column dynamically with a 1% solution of PEG-1500 in dichloromethane and heat treatment at 280°C for 15 h. After flushing the column with dichloromethane, it was statically coated with the polymer. The column was then installed in a GC instrument and connected to a split–splitless vaporizing inlet system. *In situ* cross-linking was carried out by injecting splitless 3 × 1 μl distilled water (steam) at intervals of 5 min at

a column temperature of 150°C. By this treatment the ethoxy groups are hydrolyzed and polycondensation takes place.

Column 5: PEG HM-10000. 15 m × 0.32 mm I.D. FSOT, coated with 0.25 μm laboratory made cross-linkable PEG-10000. PEG-10000 was modified with triethoxysilylpropyl isocyanate. Column deactivation, coating and immobilization was as for column 4.

Column 6: PEG Comm.-1. 15 m × 0.32 mm I.D. FSOT, coated with 0.5 μm of chemically bonded PEG. Commercial column of relatively low MW.

Column 7: PEG Comm.-2. 25 m × 0.32 mm I.D. FSOT, coated with 1.3 μm of chemically bonded PEG. Commercial column of higher MW than column 6.

The columns were tested in an Hewlett-Packard 5890 GC instrument equipped with split injection and flame ionization (FID) detection. The carrier gas was nitrogen. Differential scanning calorimetry (DSC) and thermogravimetric analysis (TGA) were carried out on a DuPont 900 thermal analyzer. Superox 20 M for TGA comparison was obtained from RSL (Eke, Belgium).

RESULTS AND DISCUSSION

The useful temperature range is an important characteristic of a stationary phase for capillary GC. The minimum allowable operating temperature is the temperature at which the phase is in the liquid state so that partitioning (liquid–gas) chromatography occurs. The phase transition (solid to liquid) temperature is thus of upmost importance. This transition temperature can be measured by DSC analysis. As an illustration, Fig. 1 depicts the scan of commercial bondable PEG. The first heating (H_1) has the highest transition temperature (60°C) and a "shoulder" at the base of the peak is observed, which is most likely due to the cross-linking agent. The cooling transition (C) to solid occurs at a much lower temperature (34°C). Finally, the transition for the second heating (H_2) is slightly lower and the band is narrower than for the first heating. The "shoulder" has disappeared through reaction of the cross-linking agent during the first heating. The explanation for the difference in transition temperatures should be a combination of two factors: crystallization and cross-linking. High-molecular-weight PEGs exist for 60–70% as small crystallites which form large crystalline areas called spherulites. The large difference between the heating transition temperatures and the cooling transition temperature can be explained by a time lag due to crystallization. Generally, PEG crystallizes from its melted form in two stages. First nucleation occurs followed by growth of the crystalline nuclei to form macroscopic spherulites. The half-life for crystallization of PEG 20000 at 58°C is 80 min. During the crystallization time the observed melting point varies until the polymer is in equilibrium. The rapid heating and cooling rates (10°C/min) do not allow the polymer to achieve its lowest energy state at each point. Consequently, there is a reduced transition temperature upon cooling and an increased transition temperature upon heating. The rapid cooling rate applied has resulted in a very low degree of crystallinity. Cooling rates in CGC however are rapid, so the same phenomena will be observed in practical CGC. The difference between H_1 and H_2 is mainly due to cross-linking of the phase, which has the effect of delaying (or in some cases destroying at room temperature) the crystallinity of the polymer and thus lowering the melting point. The chromatographic interpretation of the DSC data explains some anomalies observed in practical work with PEG phases.

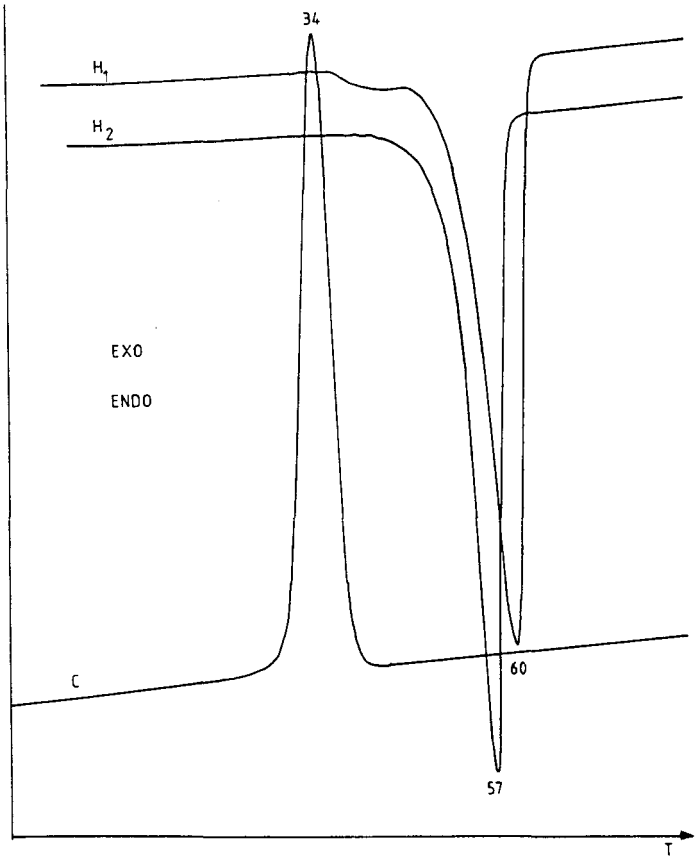

Fig. 1. DSC analysis of Bondable PEG. The analysis was performed in the following way: scan H_1, from −10 to 180°C, which is above the cross-linking temperature; scan C, cooling to −10°C; scan H_2, second heating to 180°C.

For a cross-linked column to work in the partitioning mode the minimum allowable operating temperature is 57°C. When an analysis is performed in a temperature programmed mode (for example from 60 to 180°C at 3°C/min) all compounds are eluted with narrow band widths (high efficiency). On cooling, however, the minimum allowable operating temperature shifts to a lower temperature dependent on the cooling rate, on the temperature reached and on the time interval before the next injection. It is thus possible for the second analysis to take place in the partitioning mode starting from 40°C! However, when the same analysis is then performed after a long delay (for example the next morning), complete PEG crystallization has occurred and compounds eluting between 40 and 60°C are only separated by an adsorption mechanism. It is obvious that the state of crystallization is all important and for the bondable PEG, to obtain reproducible k values, a minimum allowable operating temperature of 60°C is recommended. The phase becomes more homogeneous through cross-linking and displays a narrower transition range. The reaction of the cross-linking agent can also be deduced from a thermogravimetric analysis. The TGA

curve for Superox 20M (a linear polyoxirane) is flat to 320°C. This should correspond to the maximum allowable operating temperature of the phase. In CGC practice, however, such an high temperature stability can be reached only in a completely oxygen-free system. This is very difficult to achieve. Antioxidants can be added to the phase to delay decomposition but this then has an influence on the selectivity of the phase. The curve for a bondable high-molecular-weight PEG phase, on the other hand, shows a decrease from the movement the cross-linking agent starts to react at about 200°C. The cross-linked phase is then stable up to a temperature even higher (340°C) than the maximum allowable operating temperature of the Superox 20M phase. A very similar pattern is obtained when the TGA curve of Superox FA, the terephthalic acid derivative of Superox 20M, is recorded. Starting from 230–240°C, the terephthalic acid group is released and the phase loses its acidic properties. This is evidenced by tailing of free fatty acids after this heat treatment whereas other polar compounds are eluted with perfect peak shapes.

Fig. 2A shows plots of *N*/m *versus* temperature for *n*-undecane on the columns PEG NXL, XL-200 and FFAP XL-200. The curves are very similar in shape and there is a tremendous efficiency increase over a small different temperature range for each. This reflects the difference between a separation based on adsorption and one based on partitioning. The transition from adsorption to partitioning corresponds very well to the phase transition temperature deduced from the DSC analysis. The

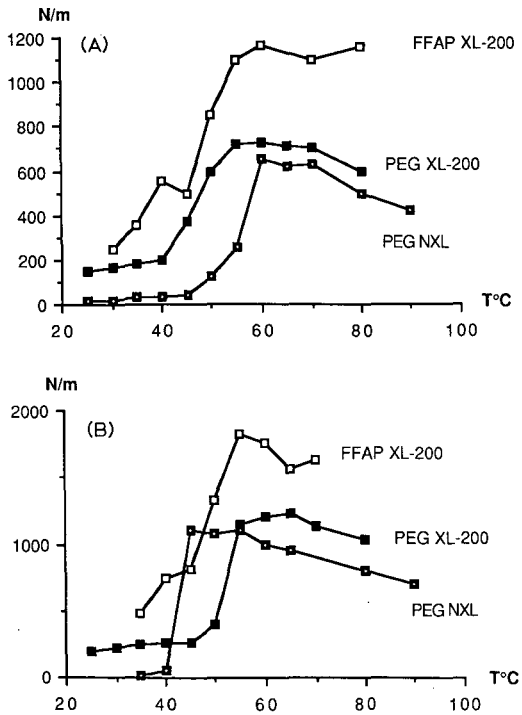

Fig. 2. Plots of *N*/m (plates per metre) *versus* temperature for *n*-undecane (A) and for *n*-butanol (B) on columns PEG NXL, XL-200 and FFAP XL-200.

temperatures are respectively 60°C for PEG NXL and FFAP XL-200, and 55°C for PEG XL-200. If the columns are operated in the adsorption mode, *i.e.*, below the minimum allowable operating temperature, the non-cross-linked column has the lowest efficiency. This is due to the high degree of crystallinity at low temperatures and, consequently, the slowest exchange of the solutes between the stationary phase and the mobile phase. In the partitioning mode, above 60°C PEG NXL and XL-200 have similar efficiencies. The FFAP XL-200 column, on the other hand, gives much higher plate numbers and much higher efficiencies than the corresponding PEG phases. The slope of the FFAP curve in the adsorption mode below 60°C is much steeper than the slope for the PEG phases. There is a "nod" in the curve around 45°C. The nitroterephthalic acid group most probably is responsible for this.

The efficiency and very surprisingly the transition temperature are strongly dependent on the nature of the solute. Fig. 2B depicts the N/m *versus* temperature curves for *n*-butanol as the solute on the same columns. The minimum allowable operating temperature values for PEG XL-200 and FFAP XL-200 are a few degrees lower than for the analysis of *n*-undecane (Fig. 2A) and surprisingly butanol seems to be separated in the partitioning mode at as low as 45°C on the PEG NXL column! On the three columns, much higher plate numbers are found for *n*-butanol than for *n*-undecane. On the PEG XL-200 column, 1200 plates per metre are calculated for butanol ($k = 5$) at 60°C but only 750 plates per metre for undecane ($k = 3$) at the same temperature. This is due to *n*-butanol having a lower diffusion coefficient than of *n*-undecane in PEG. Plots of N/m *versus* temperature were also constructed on the columns PEG Comm.-1 and Comm.-2. The curve for PEG Comm.-2 had the same shape as that for the columns in Fig. 2A but with a transition at 70°C. On the other hand, the curve for PEG Comm.-1 was nearly flat and decreased with temperature. This phase seems not to have any solid–liquid transition in the temperature range 20–100°C and the efficiency is nearly independent of the temperature! A possible explanation can be found in Fig. 3 where the N/m plot for PEG HM-10000 shows an increase in efficiency with temperature up to the maximum at 60°C corresponding to the maximum for the columns PEG NXL and FFAP XL-200. PEG HM-2500, on the other hand, has no visible transition temperature like PEG Comm.-1. The lower the molecular weight of the PEG, the lower is the solid–liquid transition temperature.

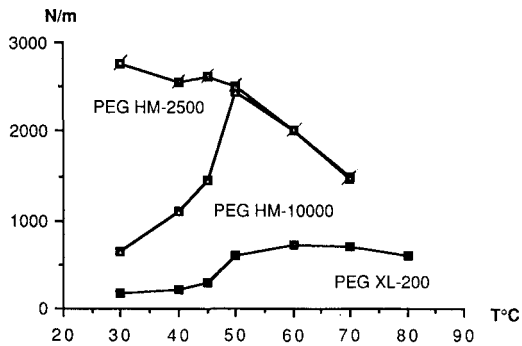

Fig. 3. Plots of N/m *versus* temperature for *n*-tridecane on PEG HM-2500 and HM-10000 and, for comparison, for *n*-undecane on PEG XL-200.

That this is valid for cross-linked phases is surprising. The starting phase in the PEG Comm.-1 column most likely also has a low molecular weight. PEG HM-2500 shows a dramatic decrease in efficiency as the temperature increases, but the PEG Comm. 1 column does not. An higher degree of cross-linking, resulting in a more homogeneous film at elevated temperatures in PEG Comm. 1 may be the reason.

The resolution (TZ value) between different solute pairs (*n*-decane–*n*-undecane, *n*-propanol–*n*-butanol, benzene–toluene) *versus* temperature was measured on several columns. For cross-linked columns, the plots are very similar in shape and the transition points differ only by a few degrees for the different solute pairs. A remarkable shift however was observed for the non-cross-linked film (Fig. 4). Obviously, there is a tremendous resolution increase over a small temperature range for all solute pairs, particularly alcohols. The use of these phases just above their melting temperature gives the best resolution. For the alkanes and aromatics, the maximum TZ value is obtained at 60°C, a temperature corresponding to the DSC value (Fig. 1). For the alcohols, however, a maximum TZ value is reached at 42–43°C. Are alcohols separated in the partitioning mode on a solid surface rich in hydroxyl groups through hydrogen bonding? The fact that this does not occur on cross-linked phases, where hydroxyl groups are no longer available, is support for this hypothesis.

Generally, the capacity factor, k, of a solute decreases with increasing solute volatility when the activity coefficients remain constant. The plots for *n*-undecane as a solute on the columns coated with the highest-molecular-weight PEGs (PEG NXL and XL-200 in Fig. 5A) show an obvious discontinuity at about 55°C. Around this transition temperature the adsorption plot changes to the one corresponding to partitioning. As the solid–liquid phase transition is approached from lower temperatures, the retention suddenly becomes longer due to the increasing liquid property of the PEG. The curves for PEG HM-2500 and Comm.-1 do not show this effect and only an exponential decrease can be noted (Fig. 5B). A very slight plateau may be seen for the PEG HM-10000 column between 50 and 60°C.

The crystallization delay time observed in the DSC analysis can also be demonstrated chromatographically. Column PEG NXL was heated to 70°C for 2 h, then cooled to 30°C with the oven closed and after 30 min dodecane was injected. The value of N was over 6000. 30 min later the number of plates had dropped to only 1500

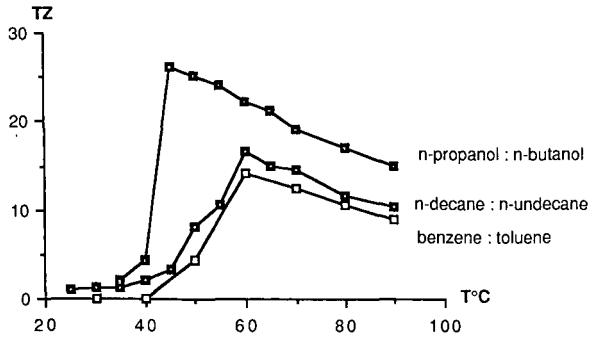

Fig. 4. Plots of TZ (resolution) *versus* temperature for *n*-decane–*n*-undecane, *n*-propanol–*n*-butanol and benzene–toluene on PEG NXL.

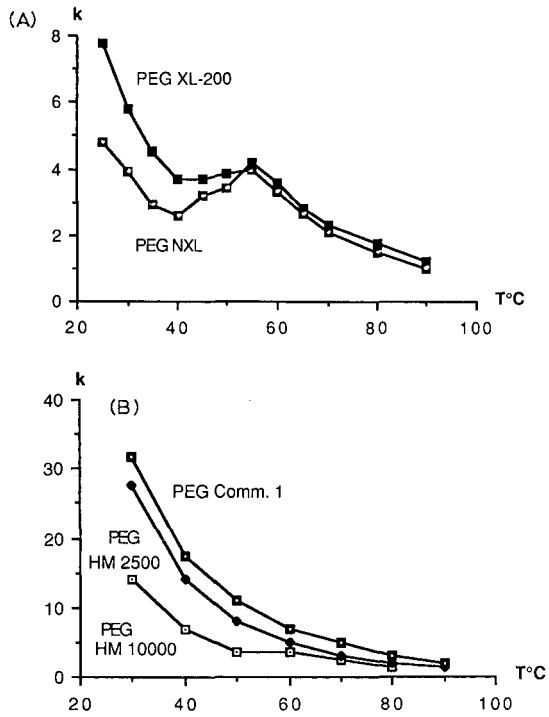

Fig. 5. Plots of the capacity factor, k, *versus* temperature (A) for *n*-undecane on PEG NXL and XL-200 and (B) for *n*-tridecane on PEG HM-2500 and HM-10000 and for *n*-dodecane on PEG Comm.-1.

and to about 1300 after 100 min. The capacity factor, k, decreased accordingly. The following day a slightly lower efficiency and capacity factor were recorded. The more crystallization that is achieved, the lower is the efficiency and the retention of dodecane. The crystallization delay time is important to obtain reproducible data where working below the phase transition temperature, although this must present a risk of poor results.

CONCLUSION

PEGs definitively have to be used above the solid–liquid transition temperature to obtain reproducible results. Above this minimum allowable operating temperature the highest efficiency is obtained. The transition temperature depends strongly on the chain length of the PEG: the shorter the chain length, the lower is the transition temperature. This behaviour remains valid for cross-linked PEGs.

REFERENCES

1 T. J. Stark, P. A. Larson and R. D. Dandeneau, *J. Chromatogr.*, 279 (1983) 31.
2 P. Sandra, F. David, M. Proot, G. Diricks, M. Verstappe and M. Verzele, *J. High Resolut. Chromatogr. Chromatogr. Commun.*, 8 (1985) 782.
3 P. Sandra, M. Verzele and J. Verzele, *Int. Lab.*, 1 (1983) 49.

4 P. Sandra, *Abstract Book Pittsburg Conference, New Orleans, February 22–26, 1988,* paper 018.
5 *Round Robin Test*, presented at the *4th International Symposium on Capillary Chromatography, Hindelang, May 1981.*
6 M. Van Roelenbosch, *Ph. D. Dissertation,* University of Gent, 1982.
7 I. Temmerman, *Ph. D. Dissertation*, University of Gent, 1984.
8 G. Diricks, *Ph. D. Dissertation,* University of Gent, 1986.
9 K. Turner, *Master of Science Thesis,* Virginia Polytechnic, Blacksburg, VA, 1988.
10 R. C. M. de Nijs and J. de Zeeuw, *J. High Resolut. Chromatogr. Chromatogr. Commun.*, 5 (1982) 501.
11 J. Buijten, L. Blomberg, K. Markides and T. Wannman, *J. Chromatogr.*, 268 (1983) 387.
12 H. Traitler, *J. High Resolut. Chromatogr. Chromatogr. Commun.*, 6 (1983) 60.
13 H. Traitler, *J. Chromatogr.*, 279 (1983) 49.
14 V. Martinez de la Gandara, J. Sanz and I. Martinez-Castro, *J. High Resolut. Chromatogr. Chromatogr. Commun.*, 7 (1984) 44.
15 M. V. Russo, G. C. Goretti and A. Liberti in P. Sandra (Editor), *Proc. Sixth Int. Symp. on Cap. Chrom.*, Hüthig, Heidelberg, 1985, p. 115.
16 M. Pryzbyciel, M. A. Santangello and M. D. Walla, in J. G. Nikelly (Editor), *Advances in Capillary Chromatography,* Hüthig, Heidelberg, 1986, 125.
17 C. A. Rouse, A. C. Finlinson, K. I. Jones, S. Sunpter, K. E. Markides, J. S. Bradshaw and M. L. Lee, *Abstract Book Pittsburg Conference, New Orleans, 1988,* paper 748.
18 P. Sandra, F. David, K. Turner and H. McNair, *J. High Resolut. Chromatogr. Chromatogr. Commun.*, in press.
19 P. Sandra, F. David, K. Turner and H. McNair, *J. High Resolut. Chromatogr. Chromatogr. Commun.*, in press.

Journal of Chromatography, 477 (1989) 73–86
Elsevier Science Publishers B.V., Amsterdam — Printed in The Netherlands

CHROM. 21 503

CONCURRENT ELUENT EVAPORATION WITH CO-SOLVENT TRAPPING FOR ON-LINE REVERSED-PHASE LIQUID CHROMATOGRAPHY–GAS CHROMATOGRAPHY

OPTIMIZATION OF CONDITIONS

KONRAD GROB
Kantonales Labor, P.O. Box, CH-8030 Zürich (Switzerland)

SUMMARY

The pressure drop over a restriction built into the carrier gas supply line allows monitoring of the carrier gas flow-rate during transfer of a liquid chromatographic eluent into a gas chromatograph. A high inlet pressure indicates blockage of the gas flow by the plug of sample liquid; a layer of evaporating solvent still reduces the flow-rate owing to its vapour pressure, causing the inlet pressure to remain above that prior to transfer. The decrease in the inlet pressure at the end of the transfer provides the signal for closing the vapour exit, but also gives information for the optimization of the co-solvent concentration in the sample and of the column temperature during transfer. The co-solvent peak within the highly attenuated solvent peak indicates the amount of co-solvent left in the precolumn after the main solvent has been fully evaporated, helping to find the optimum co-solvent concentration in the sample.

PERSONAL COMMENT

G. Schomburg and the analysis of aqueous samples

Efforts to analyse aqueous samples can be traced through a large part of the work of G. Schomburg and his group. Two approaches were examined. In the early days, two-dimensional gas chromatography (GC) was applied to remove water from the sample by a first column packed with Tenax, followed by analysis of the sample by capillary GC[1–3]. On the other hand, aqueous samples were directly injected (by split or on-column injection)[4,5] to try to overcome the various types of peak distortion and shifts in retention times observed as soon as the amount of water entering the capillary column exceeds a certain level. Experiments between these two approaches involved a capillary column inlet thermostated separately in a double oven instrument[6]. Results showed that direct injection may be a very useful method, but also that it is limited to sample volumes of a small fraction of up to a few microlitres, depending on the precautions taken. For coupling reversed-phase liquid chromatography (LC) with capillary GC, the approach involving preseparation with a packed precolumn is more promising, and it remains the hope that this work will be continued.

0021-9673/89/$03.50

There is a long tradition in that Schomburg's group and ours are working on similar subjects but in different directions. In addition to the fact that this stimulates a thorough investigation of the various aspects, it also results in two alternative approaches being developed to a level that allows a deep evaluation. The subject of this paper is certainly such a case. It is not obvious whether direct transfer of water-containing LC eluents by the described technique, or the less direct transfer, *e.g.*, via a Tenax column, will be the superior method. Seen from the angle of retention powers, Tenax offers important advantages. It strongly retains the solute material while the retention power for water is minimal. In this respect, butoxyethanol, the co-solvent used in the work described here, can certainly not compete.

INTRODUCTION

What is concurrent eluent evaporation with co-solvent trapping?

Concurrent eluent evaporation[7] means evaporation of the LC eluent during its introduction into the GC system. No liquid penetrates into the GC precolumn. This allows the transfer of very large volumes of eluent (the maximum being 20 ml[8]), but early peaks are lost and/or broadened owing to co-evaporation with the eluent[9]. As a consequence, analysis may only start *ca.* 50–120°C above the column temperature during transfer. This restriction is particularly important if relatively high-boiling solvents (such as water) are involved, calling for high oven temperatures during transfer[10]. Further, highly polar solvents do not produce phase soaking[11], causing the temperature difference between introduction and elution of the first well shaped peaks to be particularly large.

Co-solvent trapping

Loss and/or broadening of early peaks, as observed with concurrent eluent evaporation, is due to the absence of solvent trapping[12]. This solvent effect causes volatile solute material to be retained in the inlet of the GC precolumn up to the end of solvent evaporation. Solvent trapping is ineffective because solvent evaporation takes place at the front, instead of at the rear of the liquid.

Co-solvent trapping strongly reduces this deficiency of concurrent eluent evaporation. As described in previous papers[13,14], a small proportion of a high-boiling co-solvent is added to the main solvent. While the main solvent evaporates concurrently, part of the co-solvent is left at the evaporation site. It forms a layer of liquid on the capillary wall and spreads into the uncoated precolumn as the transfer proceeds. This co-solvent, located ahead of the evaporation site, retains volatile solute material providing solvent trapping.

Co-solvent trapping versus partially concurrent solvent evaporation

In its principles, concurrent solvent evaporation with co-solvent trapping approaches partially concurrent solvent evaporation[15,16]. Both leave a layer of condensed solvent ahead of the main evaporation site and at the end of the transfer, both cause this residual solvent to evaporate from the rear to the front of the layer, which is the prerequisite for obtaining solvent trapping.

In their realization, however, the techniques strongly differ. Partially concurrent solvent evaporation leaves behind part of the main solvent. Introduction must

occur below the solvent boiling point and presupposes an on-column interface. As a first step in practical work, the solvent evaporation rate must be determined in order to derive a suitable eluent flow-rate (which also determines the flow-rate through the LC column at least during transfer of the LC fraction of interest). The GC conditions must remain stable during transfer, as changes affect the evaporation rate. This practically rules out a pressure increase during transfer for accelerating the discharge of the vapours.

The alternative technique leaves behind an additional solvent, the co-solvent. The volume of non-evaporating solvent is simply determined by the concentration of the co-solvent in the main solvent and, to some extent, by the column temperature during transfer. The properties of the co-solvent can be selected according to the needs of solvent trapping, which is important with water, which has poor wettability characteristics and is a poor solvent for retaining typical GC components. Introduction of the LC fraction into the GC system occurs by the carrier gas (loop-type interface), and thus does not influence the choice of the LC flow-rate. Adjustment of conditions does not require the determination of the solvent evaporation rate. It does, however, presuppose some experimentation to find a suitable co-solvent concentration and column temperature during transfer (as the choice of optimally suited co-solvents is limited, such data are rapidly compiled). Finally, the carrier gas inlet pressure during transfer can vary to some extent, facilitating accurate closure of the solvent vapour exit and simple automation of this and some other events (see below).

Butoxyethanol as co-solvent

We proposed the use of butoxyethanol as a co-solvent[14]. It boils at 171°C, is water-miscible but is nevertheless well suited for retaining the components of relatively low polarity analysed by GC. Butoxyethanol forms an azeotropic mixture with water of 22:78 (v/v) at 98.7°C.

Purpose of this paper

After having described the background of concurrent eluent evaporation with co-solvent trapping[14], this paper deals with practical subjects such as the recognition of the moment for closing the vapour exit and the optimization of the two key parameters, the co-solvent concentration and the column temperature during transfer. Experimental results obtained under non-optimum conditions are discussed in detail in order to facilitate the optimization process.

The detailed study of butoxyethanol as a co-solvent may be surprising. However, this co-solvent showed promising preliminary results, also with methanol and acetonitrile and their mixtures with water, suggesting that this co-solvent could serve for virtually all reversed-phase eluents. Hence it might be sufficient to know a few sets of well optimized conditions.

INSTRUMENTAL: THE GAS SUPPLY SYSTEM

Experiments were carried out on a Carlo Erba 4160 gas chromatograph equipped with a loop-type interface as described previously[14]. Samples were introduced into the sample loop with a syringe. The interface differed from the conventional loop-type interface in three respects. First, the (glass press-fit) T-piece required for

back-flushing the sample valve was positioned inside the GC oven. Second, the solvent vapour exit was not completely closed but equipped with a strong restriction, allowing for a small purge flow-rate. Third, there was just an uncoated, but no retaining, precolumn upstream of the vapour exit.

A 5 m × 0.53 mm I.D. fused-silica capillary deactivated by phenyldimethylsilylation (MEGA, Legnano, Italy) served as a precolumn at the front end, connected to the press-fit T-piece of the solvent vapour exit. Separations were carried out on a 12 m × 0.32 mm I.D. glass capillary column coated with PS-255 (a methylsilicone) of 0.3-μm film thickness. The co-solvent, butoxyethanol, was specially purified by Fluka (Buchs, Switzerland) and is available as Nr. 20398.

Closure of the vapour exit

Concurrent eluent evaporation with co-solvent trapping relies on closure of the solvent vapour exit before the co-solvent is fully evaporated, otherwise the volatile solute material trapped by the co-solvent is lost through the vapour exit together with the last portion of the co-solvent. On the other hand, premature closure is undesirable, because passage of large volumes of vapours through the separation column would considerably prolong the evaporation time, correspondingly broadening the solvent peak.

Closure of the exit at the correct moment is particularly critical if the co-solvent concentration only slightly exceeds that co-evaporating with the main solvent, *i.e.*, if trapping occurs with a small amount of co-solvent. Further, the flow-rate through the vapour exit is usually high (around 100 ml/min in our case), causing the evaporation of the residual co-solvent to be rapid. Therefore, a system is required that allows accurate recognition of the moment when evaporation of the main solvent is completed. At a later stage, this function must be amenable to automation.

Flow-regulated gas supply

The standard loop-type interface for conventional concurrent eluent evaporation includes a flow-regulated carrier gas supply[17]. The flow regulator automatically increases the carrier gas inlet pressure during eluent transfers. As the plug of eluent blocks the gas flow, the flow regulator increases the inlet pressure up to the level determined by the pressure regulator situated behind the flow regulator. In addition to accelerating the discharge of the eluent vapours (increasing the rate of eluent evaporation), this provides an easy means of detecting the end of eluent transfer. The inlet pressure remains high up to the disappearance of the plug of liquid and the eluent vapours blocking the gas flow. This can be exploited for manual or automatic regulation of events timed after completion of the transfer. For instance, the solvent vapour exit and the GC run are started (with a delay) after this moment. The Carlo Erba automated LC–GC instrument works on this principle[18].

Pressure drop over restriction

In this work, closure of the vapour exit occurred by the same concept. However, a simple restriction (2 m × 0.25 mm I.D. stainless-steel capillary tubing) was used, serving the same purpose as a flow regulator. This restriction was placed after a pressure regulator and a first manometer (see Fig. 1). A second manometer, placed downstream of the restriction, indicated the same pressure as the first manometer

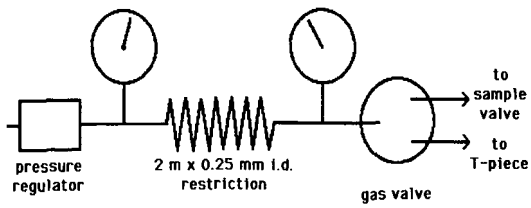

Fig. 1. Carrier gas supply system involving a restriction for accelerating eluent evaporation and for monitoring the carrier gas flow-rate during transfer.

when no gas flow passed the restriction (during transfer), while the pressure read on this second manometer was the lower the higher was the flow-rate through the restriction.

PATTERN OF THE PRESSURE DROP

The determination of the optimum co-solvent concentration in the LC eluent and of the most suitable column temperature during transfer is tedious when just based on the interpretation of chromatograms. Visual observation of the flooding liquid was not satisfactory because it was impossible to distinguish between the whole eluent and the co-solvent. However, two other techniques were used that are described below.

The pattern of the pressure drop towards the end of eluent evaporation, read from the second manometer, can be used as an interesting source of information about the evaporation process. Usually, pressure falls slowly and stepwise, indicating a gradual increase in the carrier gas flow-rate. The carrier gas flow-rate is still reduced owing to the vapours generated by the remaining solvent, this reduction depending on the vapour pressure of the liquid left in the column inlet (and the viscosities of the vapours and the carrier gas).

Fig. 2 illustrates this point by the course of the pressure observed on the second manometer during two transfers of 250-μl samples of water containing 22.5% of

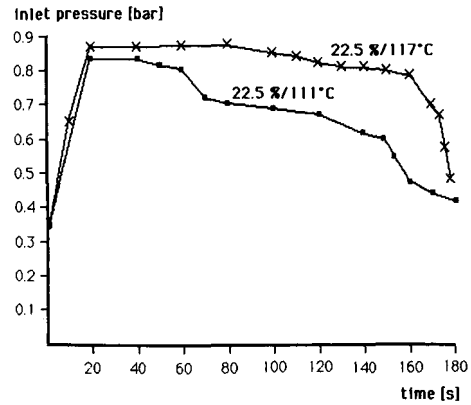

Fig. 2. Inlet pressure observed on the second manometer on transferring 250-μl volumes of water containing 22.5% of butoxyethanol at two different oven temperatures.

butoxyethanol. On starting the transfer, the pressure increased to the level of the first manometer, showing almost complete stoppage of the gas flow (there remains the small purge flow through the purge exit between the gas and the sample valve). The subsequent pressure changes depended on the eluent and the column temperature. At a moderately high temperature (the maximum is *ca.* 120°C, see below), the pressure remained at the maximum for about 90 s. Afterwards, the pressure fell slightly to a level maintained for another about 50 s, then decreased rapidly to *ca.* 0.45 bar. This level, about 0.1 bar above that before starting transfer (with an open vapour exit), would have been maintained for another 15 s, but closure of the vapour exit occurred as soon as the pressure dropped below 0.5 bar. As closure of this exit caused a reduction in the flow-rate, the pressure increased again to 0.65 bar (and further increased to 0.75 bar during temperature programming).

Blockage of the carrier gas flow obviously occurs through an eluent plug reaching into the entrance of the oven-thermostated precolumn (see Fig. 3A). The first decrease in inlet pressure was accompanied by a small gas flow leaving the vapour exit. The eluent plug must have disappeared at this time; the remaining eluent formed a thick layer on the wall of the precolumn (Fig. 3B). As the vapour pressure was still nearly as high as the carrier gas inlet pressure, the gas phase flowing through the precolumn consisted almost exclusively of eluent vapour, which explains the small carrier gas flow-rate. However, evaporation of the azeotropic butoxyethanol–water mixture caused the boiling point of the residual solvent mixture to increase and the vapour pressure to decrease. As a consequence, the carrier gas flow-rate slowly increased and the pressure read on the manometer decreased. At a late stage of the evaporation, the water was evaporated, leaving behind the excess of butoxyethanol (Fig. 3C). As the boiling point of butoxyethanol is high, the vapour pressure de-

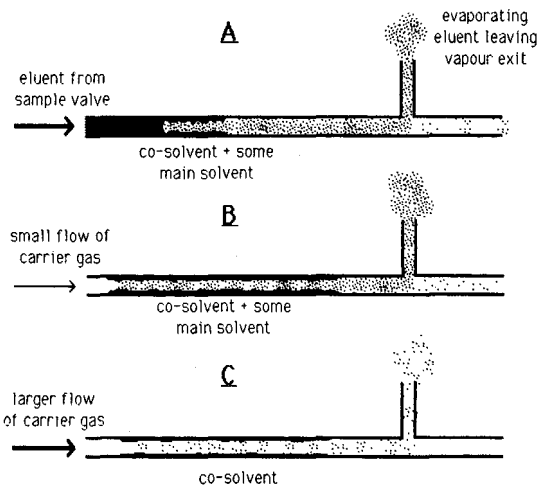

Fig. 3. Transfer by concurrent eluent evaporation with co-solvent trapping. (A) The eluent plug completely blocks the carrier gas; only eluent vapour flows through the uncoated precolumn, most of it leaving through the vapour exit. (B) The plug of liquid has disappeared; the thick layer of co-solvent and main solvent on the capillary wall exhibits a vapour pressure that allows a small flow-rate of carrier gas to pass. This flow-rate increases as water evaporates. (C) Only co-solvent is left in the uncoated precolumn, with a low vapour pressure that allows a large carrier gas flow-rate to pass. Now the vapour exit must be closed.

creased considerably, the carrier gas flow-rate increased and the inlet pressure fell to the 0.45 bar observed at the end. The evaporation of butoxyethanol at 117°C is relatively slow, but it was nevertheless advisable to close the vapour exit rapidly at this stage, because the volume of residual co-solvent only amounted to a few microlitres.

Transfers at higher temperatures

Transfer at temperatures exceeding 117°C caused the inlet pressure to remain at the maximum for longer times, *i.e.*, for 150 s at 119°C and for 185 s at 121°C. This extra time was mainly at the cost of the subsequent period with the slightly lower pressure (although the total evaporation time also slightly increased). Towards the end of solvent evaporation, the pressure decreased more rapidly. At 125°C, it fell straight back to 0.35 bar. This pressure corresponded to that prior to transfer and indicates that no co-solvent was left in the pre-column after disappearance of the eluent plug, *i.e.*, that no noticeable co-solvent layer was formed. Apparently, the oven temperature of 125°C was too high for obtaining co-solvent trapping under the conditions used.

Transfers at relatively low temperatures

On transferring the same sample at 111°C (Fig. 2), the pressure remained at the maximum only for *ca.* 40 s, then decreased to a level where it remained more or less stable for *ca.* 90 s. The rapid disappearance of the plug of liquid is explained by its deep penetration into the uncoated precolumn (to a point where the reduced pressure corresponded to its vapour pressure). As soon as no further liquid was supplied from the rear, the carrier gas opened a channel through the plug; the remaining fairly large volume of liquid was spread on the wall of the precolumn. During the subsequent 90 s, water and butoxyethanol evaporated azeotropically, leaving behind the excess of butoxyethanol. Butyloxyethanol has a low vapour pressure, causing the carrier gas flow to increase and the inlet pressure to decrease to about 0.45 bar.

At column temperatures below 110°C, the pressure hardly reached the maximum. The temperature must have been too low to produce a vapour pressure resisting the inlet pressure; more or less the whole volume of liquid rushed into the precolumn. Of course, the temperature was still above the boiling point of the solvent mixture at ambient pressure and, as the pressure at the vapour exit is not far above ambient, one would expect the liquid to be stopped within the precolumn. However, as evaporation is a violent process, some liquid left the precolumn (as observed in the resulting chromatograms; see below).

The lower temperature limit depends on the capacity of the uncoated precolumn and the sample volume introduced. If the capacity is small, only a small proportion of the liquid may spread into the precolumn. For the pressure diagram, this means that the pressure must remain at the maximum for a long period, which is achieved by a relatively high column temperature during transfer.

Speed of solvent evaporation

The pressure profile also provides some information about the speed of solvent evaporation. At 117°C, nearly all the solvent evaporated during about 170 s. As the total volume of vapour generated by the 250-μl sample volume was *ca.* 300 ml, the gas and vapour flow-rate within the precolumn was just above 100 ml/min.

CO-SOLVENT PEAK

The shape of the highly attenuated solvent peak is another useful source of information about co-solvent evaporation. Fig. 4 shows a chromatogram for a 250-μl sample of esters in water containing 22.5% of butoxyethanol. The solvent peak with a total width of 3.7 min is strongly attenuated (2^{21}). During the first part, the vapour exit was open; the flow-rate through the separation column was very small (low pressure at the T-piece), causing some delay on the first appearance of the solvent peak and a very low response due to small amounts of vapour carried through the separation column. After a first "hill", small "peaks" are observed. These "peaks" cannot represent individual substances, but show thrusts of violent evaporation (delayed evaporation), causing portions of vapour to be pushed into the separation column.

The vapour exit was closed 160 s after starting transfer (*i.e.*, in the centre of the solvent peak). With a delay corresponding to the gas hold-up time of the separation column, the pen started to rise. If closure of the exit occurred early (prematurely), the pen rose slowly or even produced a low shoulder (as is shown in the centre chromatogram of Fig. 7). This indicated that primarily water vapour passed through the column; the detector (flame ionization) shows only the butoxyethanol. Finally, the pen rose to a broad peak (shown in black in all chromatograms), representing butoxyethanol. The height of this peak depended on the column temperature (determining the vapour pressure of the co-solvent).

The size of the co-solvent peak indicates the amount of co-solvent left in the pre-column on closing the vapour exit and can be used for optimizing the co-solvent concentration, as will be shown by the following examples.

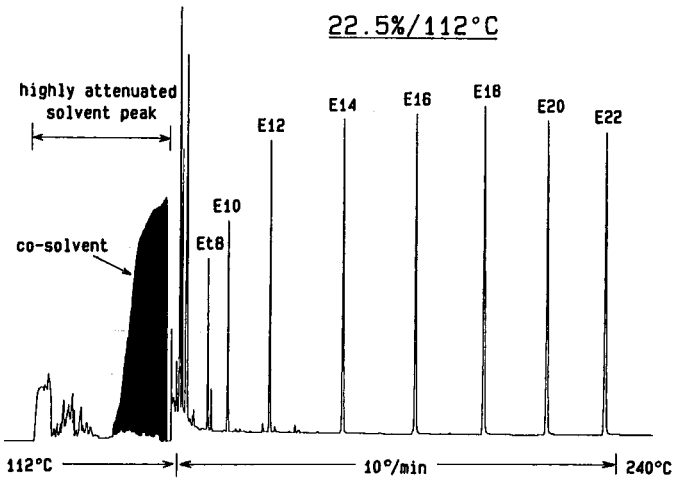

Fig. 4. Successful concurrent eluent evaporation with co-solvent trapping. Methyl esters of C_{10}–C_{22} acids (E10-E22) and ethyl octanoate (Et8), 0.1 ppm in water containing 22.5% of butoxyethanol (co-solvent). Transfer of a 250-μl volume at 112°C; inlet pressure behind the restriction, 0.9 bar (H_2). The solvent peak is highly attenuated to show its shape. The black peak indicates the amount of co-solvent left in the precolumn after complete evaporation of the main solvent.

Optimum conditions

The chromatogram in Fig. 4 shows successful co-solvent trapping. The loss of volatile solute materials is small. Methyl ester peaks down to methyl tetradecanoate (E14) are perfect in shape and size, indicating complete solvent trapping (without co-solvent trapping, even a large proportion of the E22 is lost). The methyl dodecanoate peak (E12) is *ca.* 10% too small; methyl decanoate (E10) is lost to the extent of *ca.* 50%, and 70% of the ethyl octanoate (Et8) is missing. The three first eluted peaks must be considered to be partially trapped[19]; part of this material co-evaporated with the solvent and was lost through the vapour exit. Losses do not depend on the elution temperatures from the separation column but on retention by the co-solvent layer.

From the fact that the pressure remained at the maximum only for *ca.* 60 s, we concluded that intense flooding of the pre-column had occurred (see above). The size of the co-solvent peak (black) is near the optimum (see below).

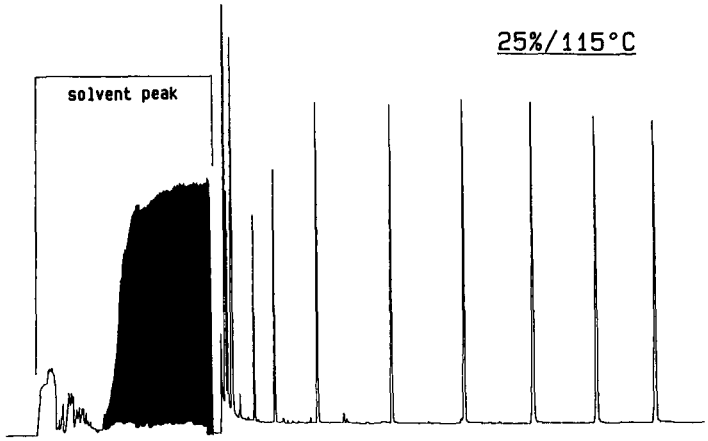

Fig. 5. Same as Fig. 4, but with a slightly increased concentration of butoxyethanol.

Fig. 5 shows a chromatogram resulting from a sample containing 25% of co-solvent. Losses of early ester peaks are reduced; the E12 peak is now of the correct size. On the other hand, the co-solvent peak is much broader (*ca.* 2.8 min compared with *ca.* 1.4 min in Fig. 4), indicating that the extra 2.5% of co-solvent resulted in more than double the amount of co-solvent being left behind on the precolumn wall at the end of solvent evaporation. Using a 30% co-solvent concentration, the co-solvent peak was more than doubled in width compared with Fig. 5, without noticeably improving the recovery of the two earliest peaks. The total solvent peak width was now just above 8 min. If this is of no concern for the 250-μl volume introduced, the unnecessary extra width of the solvent peak would hardly be tolerated any longer on increasing the sample volume, *e.g.*, to 1 ml. Considering the optimum trapping efficiency and minimal solvent peak width, we conclude that the optimum co-solvent concentration is 22.5–25%.

Insufficient co-solvent concentration

Fig. 6 shows two chromatograms of samples containing only 20% of co-solvent, a concentration clearly below that in the azeotropic mixture. The results depended on the transfer temperature, but were always unsatisfactory. At 117°C, there is a clearly visible co-solvent peak. However, even methyl tetradecanoate (E14) was partially lost. The co-solvent layer responsible for trapping the volatile solutes might have been built up only after a considerable part of the sample had evaporated, causing large losses during the first period of the transfer. At a transfer temperature of 114°C, the co-solvent peak was very small and the losses even affected the last peak (E22).

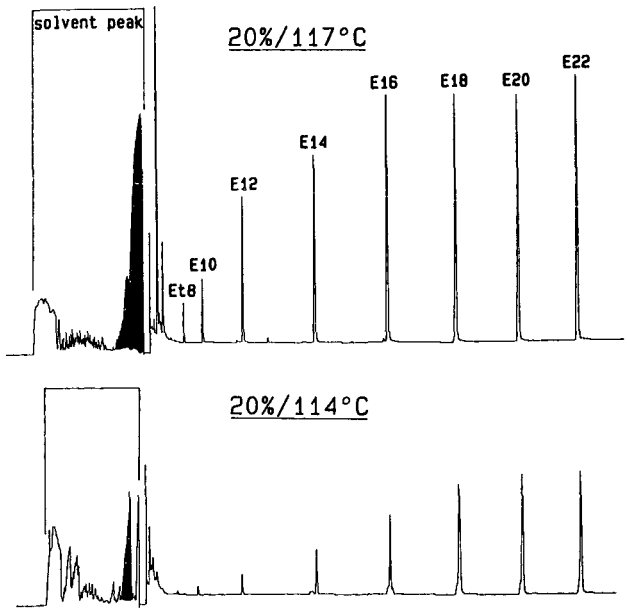

Fig. 6. Increased losses of solute material on reducing the co-solvent concentration to 20%.

It was surprising to observe co-solvent trapping effects when using co-solvent concentrations below that in the azeotropic mixture (*ca.* 22%). One would expect that a layer of water is left behind after complete azeotropic evaporation of the co-solvent. However, the presence of a co-solvent peak in the chromatograms contradicts this expectation. In this context it was interesting that clearly higher co-solvent concentrations (at least 25% butoxyethanol in water) were required when heating a short section of the precolumn inlet inside a vaporizing injector (280°C), as suggested by Noij *et al.*[20]. For this experiment, a 0.32 mm I.D. fused-silica capillary, inserted into the inlet of the 0.53 mm I.D. precolumn, passed from the oven to the top of the vaporizing injector and back into the oven again (indicated in Fig. 3 in ref. 14). The very narrow curve at the top of the injector was prepared by a correspondingly deformed press-fit connector. After complete evaporation of the sample in this vaporization loop, part of the solvent recondensed in the oven-thermostated precolumn.

Basically, the same equilibrium between the condensed phase and the gas phase should result as when starting out from evaporation in the oven-thermostated precolumn. However, this is obviously not completely true, showing that we have not yet fully explained solvent evaporation.

Excessive transfer temperature

The chromatograms in Fig. 7 show the consequences of an excessively high oven temperature during transfer for the sample containing 22.5% of butoxyethanol. At 121°C, the co-solvent peak was still fairly large. However, losses of component material reached up to E14. This temperature was right at the limit, because with transfer at 120°C the E14 peak was still of perfect size and the loss of E12 hardly exceeded that at 112°C (Fig. 4). An increase in the transfer temperature by another 1°C (to 122°C, centre chromatogram) caused the losses to extend up to the last peak. There is still a substantial co-solvent peak, but the co-solvent layer was probably formed only after a substantial proportion of the sample had been transferred. As mentioned above, the early eluted shoulder of the co-solvent peak indicates premature closure of the vapour exit. Finally, at 125°C, losses of solute material were severe. No co-solvent peak was observed and, after concurrent evaporation of the main solvent, the pressure dropped directly to 0.35 bar, confirming the absence of co-solvent in the precolumn at the end of the water evaporation.

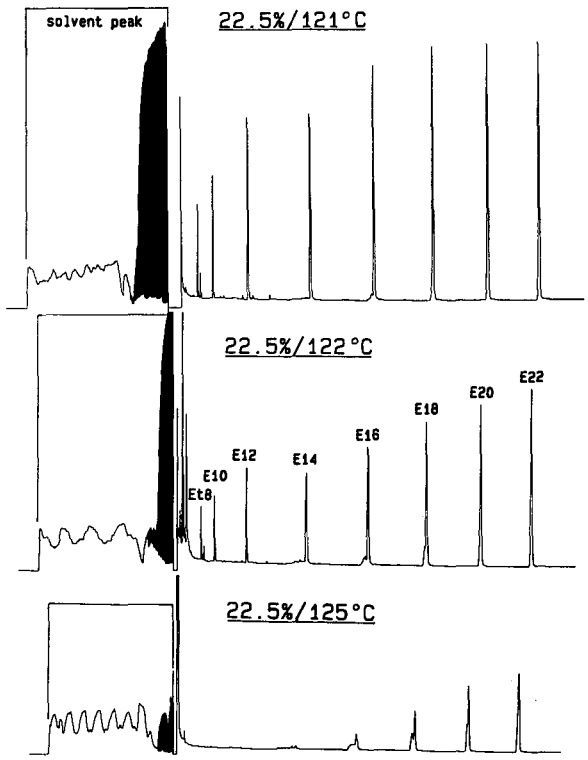

Fig. 7. Results observed with a column temperature during transfer slightly exceeding the optimum, using 22.5% of co-solvent.

Insufficient transfer temperature

Fig. 8 shows the result of a transfer carried out at an excessively low column temperature. The pressure hardly reached the maximum, indicating that the plug of liquid passed almost unhindered into the precolumn (although, as mentioned above, the pressure drop within the precolumn should have stopped the flow of liquid in the second half of the precolumn). As deduced from the peak sizes, *ca.* 20% of the sample must have penetrated into the T-piece of the vapour exit, presumably owing to "shooting" liquid, the result of irregular and violent evaporation. There, a major portion of the liquid left through the vapour exit, while a smaller part entered the separation column. In the separation column, the liquid was spread by the flow of gas and vapours, resulting in band broadening in space. As the corresponding solute material is ahead of the material chromatographed normally, it elutes prematurely (black peaks indicated by arrows in Fig. 8).

The lower temperature limit for the transfer was *ca.* 110°C, as also deduced from the rapid decrease in the time the pressure remained at the maximum. At 110°C, some chromatograms showed peak distortion such as that shown in Fig. 8, whereas the peaks in others were of perfect shape and height. As the evaporation is violent, the lower temperature limit is not very reproducible.

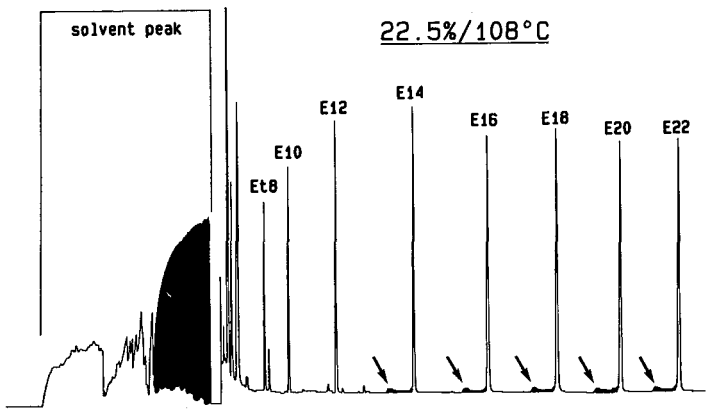

Fig. 8. Lower limit of the column temperature during transfer: the flow of liquid exceeds the T-piece of the solvent vapour exit; part of the sample flows into the separation column, producing the low pre-peaks shown in black and indicated by arrows.

Delayed closure of the vapour exit

Fig. 9 shows the result of closing the vapour exit with a delay of *ca.* 40 s. At closure, the pressure had decreased to 0.35 bar, the pressure observed before starting transfer, which signifies that no co-solvent was left in the precolumn. On the other hand, some co-solvent is still visible on the chromatogram. The esters were nearly completely lost up to E20; the small peaks of the earlier eluted esters indicate the splitting ratio at the vapour exit T-piece.

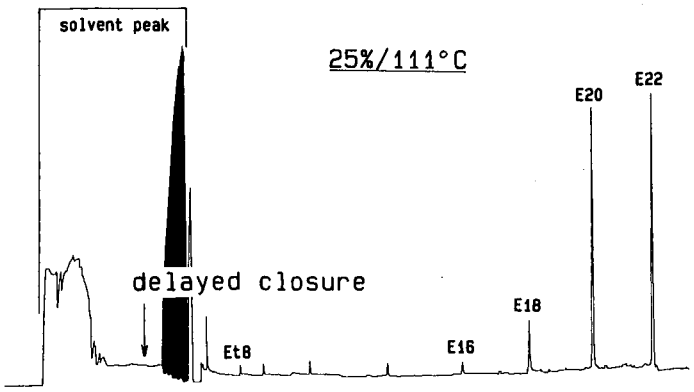

Fig. 9. Nearly complete loss of the volatile solutes on closing the vapour exit with a delay of *ca.* 40 s (conditions otherwise producing efficient co-solvent trapping).

SUMMARIZING GUIDELINES

Column temperatures during transfer are most rapidly optimized through the course of the pressure drop towards the end of the transfer, introducing the solvent mixture without any solute material. The pressure should remain at the maximum for a considerable part of the transfer time (limit towards lower temperature); on the other hand, it must not decrease rapidly at the end of the transfer (limit towards high temperature). During these transfers, the recorder runs at high attenuation, allowing the optimization of the co-solvent concentration by the size of the co-solvent peak.

Table I gives some preliminary guidelines on optimum butoxyethanol concentrations in different reversed-phase eluents and optimum column temperatures for transfer at an inlet pressure of 0.9 bar. Results were obtained from two similar experimental set-ups. Nevertheless, it was observed that the optimum temperatures differed by up to 7°C and the optimum butoxyethanol concentrations differed by up to 2% (absolute). The reason for these deviations is unknown. However, as the evaporation of water-containing liquids on hardly wetted surfaces is an irregular process, they are not really surprising.

TABLE I

APPROXIMATE OPTIMUM BUTOXYETHANOL CONCENTRATIONS AND COLUMN TEMPERATURES DURING TRANSFER (0.9 BAR INLET PRESSURE)

Main solvent	*% Butoxyethanol*	*Transfer temperature (°C)*
Water	23	110–120
50% Methanol	15	105–110
75% Methanol	8	96–103
Methanol	4.5	85– 93
50% Acetonitrile	15	107–115
75% Acetonitrile	10	102–110

REFERENCES

1 G. Schomburg, H. Husmann and F. Weeke, *J. Chromatogr.*, 112 (1975) 205.
2 G. Schomburg, *Separation*, 1 (1987) 3.
3 G. Schomburg, in P. Sandra (Editor), *Sample Introduction in Capillary GC, Vol. 1*, Hüthig, Heidelberg, 1985, p. 235.
4 E. Bastian, H. Behlau, H. Husmann, F. Weeke and G. Schomburg, in R. E. Kaiser (Editor), *Proceedings of the Fourth International Symposium on Capillary Chromatography, Hindelang, 1981*, Hüthig, Heidelberg, 1981, p. 465.
5 G. Schomburg, E. Bastian, H. Behlau, H. Husmann, F. Weeke, M. Oreans and F. Müller, *J. High Resolut. Chromatogr. Chromatogr. Commun.*, 7 (1984) 4.
6 G. Schomburg, in P. Sandra (Editor), *Proceedings of the Seventh International Symposium on Capillary Chromatography, Gifu, 1986*, Hüthig, Heidelberg, 1986, p. 27.
7 K. Grob, B. Schilling and Ch. Walder, *J. High Resolut. Chromatogr. Chromatogr. Commun.*, 9 (1986) 95.
8 K. Grob, H.-G. Schmarr and A. Mosandl, *J. High Resolut. Chromatogr. Chromatogr. Commun.*, in press.
9 K. Grob, *J. High Resolut. Chromatogr. Chromatogr. Commun.*, 10 (1987) 297.
10 K. Grob and Z. Li, *J. Chromatogr.*, 473 (1989) 423.
11 K. Grob and B. Schilling, *J. Chromatogr.*, 259 (1983) 37.
12 K. Grob, *J. Chromatogr.*, 279 (1983) 225.
13 K. Grob and E. Müller, *J. High Resolut. Chromatogr. Chromatogr. Commun.*, 11 (1988) 388 and 560.
14 K. Grob and Z. Li, *J. Chromatogr.*, 473 (1989) 411.
15 F. Munari, A. Trisciani, G. Mapelli, S. Trestianu, K. Grob and J. M. Colin, *J. High Resolut. Chromatogr. Chromatogr. Commun.*, 8 (1985) 601.
16 E. Noroozian, F. A. Maris, M. W. F. Nielen, R. W. Frei, G. J. de Jong and U. A. Th. Brinkman, *J. High Resolut. Chromatogr. Chromatogr. Commun.*, 10 (1987) 17.
17 K. Grob and J.-M. Stoll, *J. High Resolut. Chromatogr. Chromatogr. Commun.*, 9 (1986) 518.
18 F. Munari and K. Grob, *J. High Resolut. Chromatogr. Chromatogr. Commun.*, 11 (1988) 172.
19 K. Grob, *J. Chromatogr.*, 251 (1982) 235.
20 Th. Noy, E. Weiss, T. Herps, H. Van Cruchten and J. Rijks, *J. High Resolut. Chromatogr. Chromatogr. Commun.*, 11 (1988) 181.

Journal of Chromatography, 477 (1989) 87–93
Elsevier Science Publishers B.V., Amsterdam — Printed in The Netherlands

CHROM. 21 060

MICRO-LIQUID CHROMATOGRAPHY WITH DIODE ARRAY DETECTION

M. VERZELE*, G. STEENBEKE and J. VINDEVOGEL
Laboratory of Organic Chemistry, State University of Ghent, Krijgslaan 281 (S.4), B-9000 Ghent (Belgium)

SUMMARY

Commercial diode array detectors can be adapted to micro-liquid chromatography (LC) by replacing their detector cell with a miniaturized detector cell. In appropriate conditions, micro-LC can then generate an useful UV spectrum with 10 times less sample than needed with conventional LC. Some aspects of detector cell miniaturization are discussed. Results with two commercial diode array detectors, modified with a miniaturized detector cell, are presented.

INTRODUCTION

Micro-LC is liquid chromatography on packed fused-silica (or other) capillary columns with an internal diameter (I.D.) below 500 μm[1–3]. It has many advantages over "conventional" LC using mostly 4.6 mm I.D. columns[4]. One of these is better mass sensitivity. It is important to exploit this in conjunction with a diode array detector (DAD). With most commercial DAD instrumentation this is not possible because the detector cells are not adapted to micro-LC dimensions. In the present paper we report on cell modification for two commercial DAD instruments to allow micro-LC-DAD. Examples of chromatographic results are presented.

EXPERIMENTAL

The chromatographs with DAD used in the present study were an HP-1090 (Hewlett-Packard, Palo Alto, CA, U.S.A.) and an LKB-Diode Array Rapid Spectral Detector (LKB-Produkter, Bromma, Sweden). The columns were 4.6 mm I.D. Lichroma tubing for the "conventional" size LC, and polyimide-coated fused-silica capillaries of 320 μm I.D. (RSL, Eke, Belgium) for micro-LC. The packing material was in all cases 5-μm ROSiL-C_{18}-D (an octadecylated spherical silica gel from RSL). The miniaturized detector cells were developed at our laboratory and are now available from RSL.

0021-9673/89/$03.50

RESULTS AND DISCUSSION

Detector cell modification for micro-LC

Yang[5] has described how an empty extension of a fused-silica column, after the packed bed, can be used for UV detection in miniaturized LC. The protecting polyimide is removed over a small distance from the fused-silica capillary and detection is achieved by placing this part of the column in the light path of an UV detector. Yang calls this technique "on column" detection. The detector cell, which is part of the column, has a tubular shape. An easier way to achieve the same result is to build a separate detector block in which a piece of fused-silica capillary, free of polyimide over a few mm, is permanently mounted. In this case too the detector cell has a tubular shape. UV detectors with cassette-like detector flow-cells (like the Varian 2050, and similar Jasco, Wescan and Uvicon detectors, or the earlier fixed wavelength Varian Aerograph UV detector), can thus easily be modified for micro-LC. Exchange of the original cassette for a micro-LC cell cassette is readily achieved. Connection of the actual LC column via a 50 or 100 μm I.D. fused-silica capillary to this detector cassette is realized with a short piece of suitable PTFE tube or with "glass or fused silica column connectors".

Due to the tubular shape of these adapted detector flow-cells, they are very sensitive ro refractive index changes[6] (Fig. 1). The flow-cell acts as a dispersive medium. This increases the number of parameters that determine the eventual amount of light incident on the photosensitive device. Some of these parameters can be controlled in a suitable substitute detector cell block (internal and external diameter of the flow-cell; slit width; position and width of the entrance slit to the photo-sensitive device; alignment of the light beam, flow-cell and photo cell). Other parameters are much more difficult or cannot be controlled in/by an add-on substitute detector cell (convergence and divergence in the incident light beam; positioning of the refraction grid). Some of these points and the construction of a suitable add-on detector cell for micro-LC have been discussed by us[6].

Micro-LC on-column detection with a photo diode array detector was suggested by Yang in 1981[5]. Micro cells for multichannel UV detectors were discussed first (as happened so many times in micro-LC development) by Ishii *et al.*[7]. In that study, parallel (Z type) and cross flow-cells (on-column detection) are compared. The cells

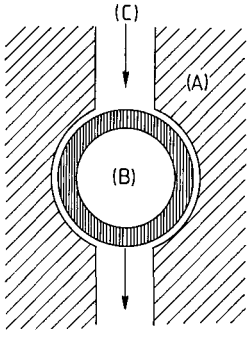

Fig. 1. Miniaturized cell design. Two piece block (A) with fused-silica capillary column (B) of 320 μm I.D. with spacers determining the slit width of 200 μm (C).

were developed specifically for the Micro Gate Photodiode Array Detector of Union Giken. Few technical details about the micro cell construction are available. Differences in the relative peak heights for a series of polycyclic aromatic hydrocarbons when changing from parallel to cross flow-cells are primarily ascribed to extra-column dead volume band broadening for earlier peaks with the parallel cell. A closer look at the chromatograms shows that this cannot be the explanation. If extra-column dead volume were mainly involved, the peak height change in question would follow a simple pattern, predictable for each compound and repeating itself in all the chromatograms shown. This is not the case. Some peaks (compounds) are more affected than others. The variations seem thus to be compound (spectrum) dependent. We have observed the same phenomenon with our cells. Furthermore, large hypsochromic or bathochromic shifts (10 nm or more) can sometimes be observed in the spectra by switching from one to another micro cell. This could result from imperfect alignment of the detector parts switching the light beam to higher or lower diodes in the array. This phenomenon may also account for variable peak height changes. The design of micro cells thus deserves closer and further attention.

Whatever the reasons for chromatigraphic peak intensity or wavelength changes in function of micro cell design, in order to obtain useful UV spectra strict adherence to the above mentioned principles has to be observed. Otherwise, wavelength-dependent refractive index effects lead to distorted UV spectra, and perhaps to different sensitivities when chromatograms are recorded at a single wavelength. Most essential is the slit width. Reducing the slit width however reduces the sensitivity. A compromise has to be adopted. Fig. 2a shows such a distorted UV spectrum for pyrene, obtained with a too wide 400-μm entrance slit of a modified flow-cell for the

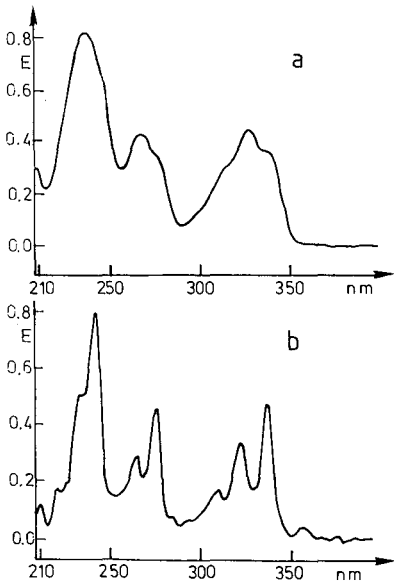

Fig. 2. UV spectra of pyrene solutions placed in micro cells: (a) with an unsatisfactory modified cell (HP-1090 diode array), (b) with an improved cell modification (HP-1090 diode array).

DAD of the HP-1090 liquid chromatograph. An improved cell design with a narrower 200-μm entrance slit (for a 320 μm I.D. detector tube as in Fig. 1), with very strict alignment of the light source, detector cell and photocell, produced an optimized flow-cell as described recently[6]. This leads to an UV spectrum for pyrene as shown in Fig. 2b, also obtained with the HP-1090 DAD. Such a spectrum is useful, but close comparison with a spectrum obtained with a larger cell shows minor differences, as discussed above.

A similar improved sub-microlitre detection cell can be placed in the LKB diode array detector in the same way as the conventional flow-cell. By simply changing the cassette, the detectors can either be used for conventional or for micro-LC. Fig. 3a shows the reversed-phase chromatogram of a mixture of five polyaromatic compounds on a conventional column. Fig. 4 shows the UV spectrum of the fourth peak (pyrene) obtained with the conventional 5-μl, 5-mm pathlength flow-cell (LKB-DAD). Fig. 3b shows the same separation on a micro-LC column with a micro detector cell in the LKB instrument, and Fig. 5 shows the spectrum for the fourth peak under these micro-LC conditions. A first conclusion is that micro-LC and the two DAD instruments mentioned, equipped with a micro cell, can give a useful UV spectrum via diode array detection.

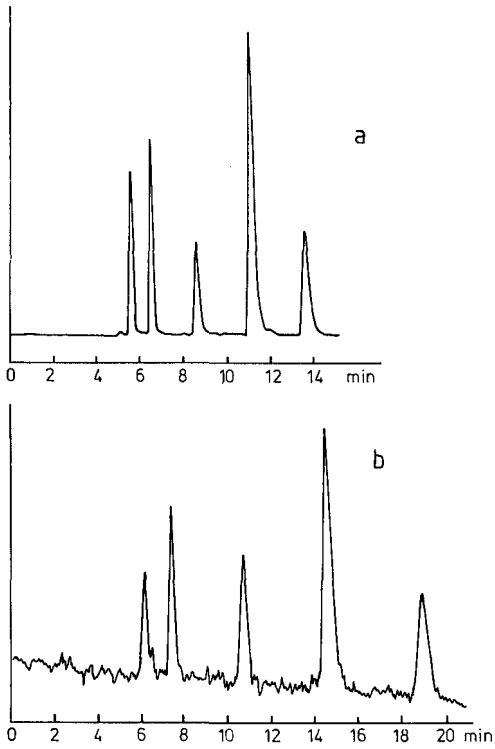

Fig. 3. Reversed-phase test chromatograms for (a) "conventional" and (b) micro-LC. (a) Column: 5 μm ROSiL-C_{18}-D (25 cm × 0.46 cm). Solvent: acetonitrile–water (75:25). Detection: 255 nm. Solvent flow-rate: 1 ml/min. Volume injected: 6.4 μl. (b) Column: 5 μm ROSiL-C_{18}-D (260 mm × 0.32 mm). Solvent: acetonitrile–water (72:25). Detection: 255 nm. Solvent flow-rate: 4.1 μl/min. Volume injected: 200 nl.

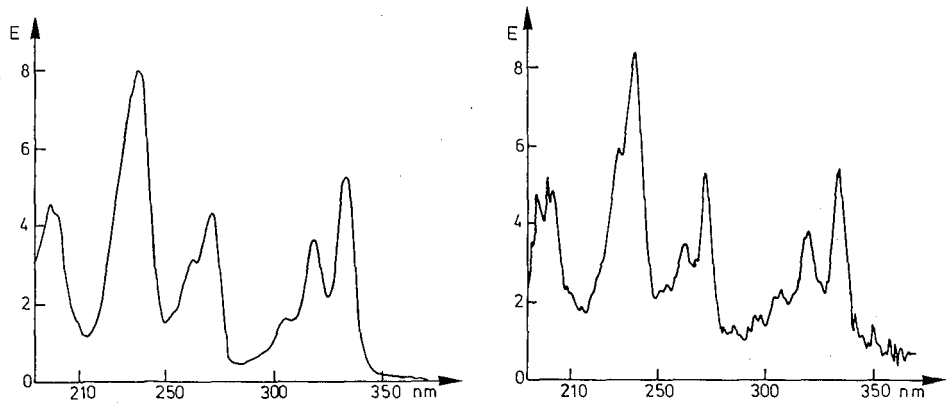

Fig. 4. UV spectrum of the fourth peak (pyrene) of Fig. 3a (conventional column, LKB diode array).

Fig. 5. UV spectrum of the fourth peak (pyrene) of Fig. 3b (micro-LC column with modified micro detector cell cassette LKB diode array).

Sensitivity of conventional versus micro-LC and DAD detection

Another important point is how large the smallest sample has to be that can just generate a useful spectrum. The dimensions of the columns under discussion are 250 mm × 4.6 mm and 260 mm × 0.32 mm. The volume ratio for the two columns is therefore 197, and the expected "elution dilution" or chromatographic dispersion is in favour of the micro-LC column by the same factor of 197. For the same concentration of the sample solutions and adapting the sample size to the column surface area ratio (in this case 206), the sensitivity of detection for the micro-LC system is reduced by the same factor. Under these conditions, the observed sensitivity will be determined mainly by the length of the detector cell. For the detector cells under discussion this favours conventional LC by a factor of about 15–30. Fortunately, the capacity of

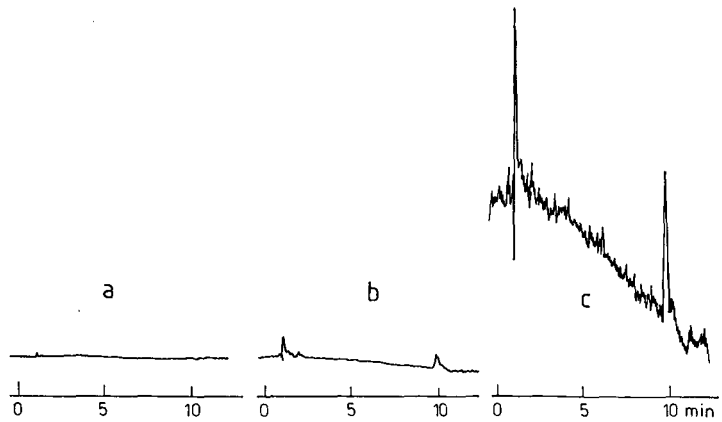

Fig. 6. Chromatograms of 10 ng pyrene under the conventional conditions of Fig. 3a, except that only 60 nl were injected. Unmodified HP-1090 diode array detector. (a) Normal attenuation setting; (b) 10 times more sensitive; (c) 100 times more sensitive.

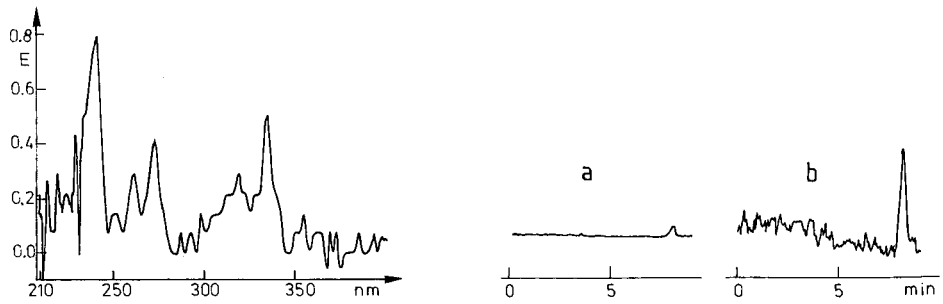

Fig. 7. UV spectrum for 10 ng pyrene obtained from the chromatogram in Fig. 6.

Fig. 8. Chromatograms of 1 ng pyrene under the micro-LC conditions of Fig. 3b, except that only 60 nl were injected. HP-1090 diode array detector with modified detector cell. (a) Normal attenuation setting; (b) 10 times more sensitive.

silica gel phases is larger than required by usual analytical samples. Therefore the samples injected on the micro-LC system can be larger than those that calculation would indicate. Still, under "normal" conditions, conventional LC is more sensitive than micro-LC because of the detection aspect just mentioned and because the amount of sample injected on the micro-LC column (if the same sample concentrations are used on both systems) is so much smaller. Therefore the chromatogram of Fig. 2b had to be recorded with a more sensitive attenuation setting as is seen by the noise ratio.

When the concentrations injected are different, but the injected mass of compound is the same, then the better mass sensitivity of the micro-LC system becomes apparent. This can be important when the sample size available is restricted. For our HP-1090 DAD system, the limit that can still generate an useful UV spectrum was estimated at about 10 ng[8]. Fig. 6 shows chromatograms produced on the HP-1090 for 10 ng pyrene with the column of Fig. 3a and with various attenuation settings. The signal-to-noise ratio is about 8. Fig. 7 shows the UV spectrum. The pyrene spectrum can just be recognized. The detection limit under these conditions is therefore indeed about 10 ng. Similar results for 1 ng on the micro-LC column are shown in Figs. 8 and 9. The signal-to-noise ratio is about 6. The UV spectrum is now even better than with the conventional system with 10 ng of sample.

The HP-1090 DAD, provided with a micro detector cell and with a micro-LC

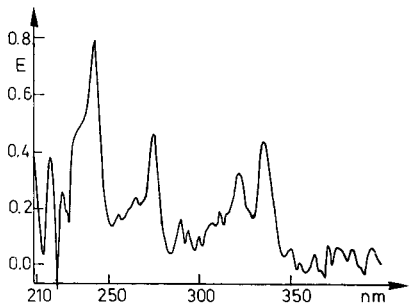

Fig. 9. UV spectrum for 1 ng pyrene obtained from the chromatogram in Fig. 8.

column, can thus generate a useful UV spectrum with about 1 ng of material. The newest instruments are about 10 times better[8]. Probably the micro cell construction can also be improved, so that still lower figures may be reached.

ACKNOWLEDGEMENTS

We thank the Instituut tot Aanmoediging van het Wetenschappelijk Onderzoek in Nijverheid en Landbouw (IWONL), the Nationaal Fonds voor Wetenschappelijk Onderzoek (NFWO) and the Ministerie voor Wetenschapsbeleid for financial support to the Laboratory. G.S. thanks Heineken Breweries, The Netherlands for a grant. We thank Hewlett-Packard for the gift of an HP-1090 DAD and LKB for lending their DAD instrument.

REFERENCES

1 M. Verzele and C. Dewaele, *J. High Resolut. Chromatogr. Chromatogr. Commun.*, 10 (1987) 280.
2 M. Verzele, M. De Weerdt, C. Dewaele, G. J. De Jong, N. Lammers and F. Spruit, *LC · GC, Mag. Liq. Gas Chromatogr.*, 4 (1986) 1162.
3 M. De Weerdt, C. Dewaele and M. Verzele, *J. High Resolut. Chromatogr. Chromatogr. Commun.*, 10 (1987) 553.
4 M. Verzele, C. Dewaele, M. De Weerdt, *LC · GC, Mag. Liq. Gas Chromatogr.*, 6 (1988) 966.
5 F. Yang, *J. High Resolut. Chromatogr. Chromatogr. Commun.*, 4 (1981) 83.
6 J. Vindevogel, G. Schuddinck, C. Dewaele and M. Verzele, *J. High Resolut. Chromatogr. Chromatogr. Commun.*, 11 (1988) 317.
7 D. Ishii, M. Goto and T. Takeuchi, *J. Chromatogr.*, 316 (1984) 441.
8 K.-P. Hupe, Hewlett-Packard, personal communication.

Journal of Chromatography, 477 (1989) 95–106
Elsevier Science Publishers B.V., Amsterdam — Printed in The Netherlands

CHROM. 21 365

PERFORMANCE OF POROUS SILICA LAYERS IN OPEN-TUBULAR COLUMNS FOR LIQUID CHROMATOGRAPHY[a]

P. P. H. TOCK, C. BOSHOVEN, H. POPPE* and J. C. KRAAK
Laboratory for Analytical Chemistry, University of Amsterdam, Nieuwe Achtergracht 166, 1018 WV Amsterdam (The Netherlands)
and
K. K. UNGER
Institut für Anorganische und Analytische Chemie, Johannes-Gutenberg Universität, 6500 Mainz (F.R.G.)

SUMMARY

Progress has been made in the preparation of porous silica layers in fused-silica capillaries for open-tubular liquid chromatography. The porous silica layer is prepared by (i) static coating of the silica precursor, polyethoxysiloxane (PES), followed by (ii) converting the PES film into a porous silica layer with ammonia solution. The porous silica layer can be easily modified by silane reagents commonly used in packed column high-performance liquid chromatography. The performance of the silica layer with the different phase systems was tested with polyaromatic hydrocarbons and derivatized amino acids as samples.

INTRODUCTION

The search for greater resolving power in liquid chromatography is one of the major fields of activity in contemporary chromatographic research. Capillary chromatography [open-tubular liquid chromatography (OTLC)] is one of the possibilities for improving the resolving power significantly. This is the main reason why capillary liquid chromatography has been extensively examined both theoretically[1,2] and experimentally[3–14] in recent years.

From theoretical considerations[1,2], it has been found that the optimum capillary diameter is about 1–5 μm and that the external band broadening must be kept below 1 nl. It has been shown that these stringent requirements can be met in practice when applying on-column detection and split injection devices.

Despite these experimental improvements, a most difficult problem remains, namely that of the preparation of a stable and sufficiently thick stationary layer in columns with an inner diameter smaller than 10 μm. For a suitable phase ratio, the

[a] Part of this paper was presented at the *12th International Symposium on Column Liquid Chromatography, Washington, DC, June 19–24, 1988*. The majority of papers presented at this symposium have been published in *J. Chromatogr.*, Vols. 458, 459 and 460.

0021-9673/89/$03.50

stationary phase film thickness should be 0.3–2 μm in a 10-μm column, depending on the diffusion coefficient of the solute in the stationary phase[10]. The phase ratio should be high, first in order to be able to manipulate the retention and second, and possibly more important, in order to allow a sufficient loadability.

In capillary gas chromatography (GC), different stationary phases, such as cross-linked silicones and porous adsorbent layers, can be successfully coated in thin and thick films. The application methods include static coating[15], dynamic coating without[16] or with[17] a mercury plug and methods for depositing porous adsorbent layers, as reviewed by Ettre and Purcell[18] and de Zeeuw *et al.*[19]. Some of these stationary phases or coating techniques cannot be applied in OTLC. Recently, cross-linked silicones have been applied in 5- and 10-μm fused-silica capillaries by static[9,10], free-release[13] and "precipitation" coating[12]. The performances of these OTLC columns are in good agreement with theory. A disadvantage of the cross-linked silicone phases is that because of the low diffusion coefficient in the cross-linked phase[10] ($D_s = 7 \cdot 10^{-12}$ m^2/s), the film thickness should be small, which limits the mass loadability. The eluting concentration of the solute is proportional to the mass loadability, which implies that owing to the thin film in these columns detection problems may occur. The diffusion coefficient in porous materials is much larger (*ca.* $0.5 \cdot 10^{-9}$ m^2/s) and therefore the preparation of porous adsorbents layers in capillaries in principle offers better prospects.

In a previous paper[14], we described the preparation of a porous layer in 10–25-μm fused-silica columns by precipitation of porous silica from a dynamically coated film of polyethoxysiloxane (PES) with gaseous ammonia. Silica was chosen as the porous material because (i) the chemistry of silica, (ii) its use as a support or adsorbent in LC and (iii) the possibilities of modifying the silica surface are well documented. However, the thickness of the layer obtained by dynamic coating was too small and had to be increased. The deposition of a thicker film of PES can be achieved by repeated application of the dynamic coating procedure or by using static coating. The use of static instead of dynamic coating is advantageous because of (i) the possibility of coating thicker films in one step, (ii) easy control of the film thickness by varying the PES concentration in the coating solution and (iii) the possibility of using aqueous ammonia rather than gaseous ammonia in the conversion of PES into silica.

In this paper, the preparation and chemical modification of the porous silica layer is described. A number of different phase systems have been tested for various solutes.

THEORY

The plate height in OTLC is described by the extended Golay equation[20]:

$$H = \frac{2D_m}{u} + \frac{d_c^2 u}{96D_m} f_1(k') + \frac{2d_f^2 u}{3D_s} f_2(k') \quad (1)$$

where

$$f_1(k') = \frac{(1 + 6k' + 11k'^2)}{(1 + k')^2} \quad (2)$$

$$f_2(k') = \frac{k'}{(1 + k')^2} \tag{3}$$

D_m is the diffusion coefficient in the mobile phase, D_s is the diffusion coefficient in the stationary phase, k' is the capacity factor {zone capacity factor[21] when adsorption [reversed phase (RP), straight phase (SP)] is used}, u is the linear velocity of the mobile phase, H is the plate height, d_c is the inner diameter of the capillary and d_f is the thickness of the stationary layer.

Maximum film thickness

The desired film thickness, $d_{f,max}$, is limited by the decrease in efficiency caused by the third term in eqn. 1. As a more or less arbitrary, but reasonable, upper limit to the magnitude of this term, one can take 20% of the second term (the first can usually be neglected). On doing so, the following relationship for $k' = 3$ results:

$$d_{f,max} < \sqrt{0.12 D_s/D_m} \cdot d_c \tag{4}$$

Eluting concentration

To avoid external band broadening in OTLC with column diameters of 1–10 μm, the detection and injection volumes must be in the range 1–100 pl. To mitigate detection problems, the eluting concentration should be as high as possible. The eluting concentration is proportional to the sample load and is given by

$$C_m = \frac{M_{inj}}{V_{mp}\sqrt{2\pi N}} \frac{1}{(1 + k')} \frac{1}{MW} \tag{5}$$

where C_m is the outlet concentration (mol/m^3), V_{mp} is the volume of mobile phase in one plate, N is the plate number, M_{inj} is the amount injected in grams and MW is the molecular weight of the solute.

Increasing M_{inj} will eventually lead to mass overload. Both theoretically[22] and experimentally[23] it has been found that the relative peak broadening is a function of a dimensionless quantity m, in which the amount injected is normalized on the amount M_{pl} that can be sorbed into the stationary phase present in one plate. This normalization has the exact form

$$m = \frac{M_{inj}}{M_{pl}} \frac{k_\infty^2}{(1 + k_\infty)^2} \tag{6}$$

where k_∞ is the capacity factor at infinite dilution.

For Langmuir-type adsorption systems, M_{pl} is equal to the amount that saturates the surface in one plate. For liquid–liquid systems it is more difficult to estimate M_{pl}; however, it will be proportional to and of the same order as the amount of stationary phase in one plate, equal to $V_{sp}\rho_{sp}$[24]. In the above-mentioned studies, it was found that with $m = 2$ a 30% increase in the observed plate height is found. Defining m_{30} as the exact value of m at that point (it may have a different value for different solute–phase system combinations) it follows that

$$C_m^{max} = \frac{m_{30} V_{sp} \rho_{sp}}{V_{mp}\sqrt{2\pi N}} \frac{(k_\infty + 1)}{k_\infty^2} \frac{1}{MW} \quad (7)$$

$$= \frac{m_{30} \rho_{sp} V_s}{\sqrt{2\pi N} \cdot V_m} \frac{(k_\infty + 1)}{k_\infty^2} \frac{1}{MW} \quad (8)$$

where V_{sp} is the volume of stationary phase in one plate, V_s is the volume of the stationary phase, V_m is the volume of the mobile phase and ρ_{sp} is the density of the stationary phase. Eqn. 8 clearly indicates the importance of having a high phase ratio, which is limited, however, by eqn. 4.

With eqns. 4–8, some theoretical values have been calculated for three different phase systems, which in our opinion can be applied in OTLC. The results are given in Table I. The phase systems are (i) polymers (cross-linked silicones), (ii) porous layers used as an adsorbent (possibly modified) and (iii) porous layers used as a support for a stationary liquid (preferably with complete pore filling). The phase ratio of the porous adsorbent phase system was calculated assuming that the specific surface area of the porous silica layer is 300 m^2/g. From Table I it can be seen that from the point of view of mass loadability, porous layer columns are preferable to the polymer columns.

TABLE I

CALCULATED VALUES FOR THREE DIFFERENT PHASE SYSTEMS

d_c = 10 μm; N = 100 000; k' = 3; $D_m = 1 \cdot 10^{-9}$ m^2/s; H = 10 μm; MW = 200; ρ_{sp} = 1 g/ml.

Parameter	*Phase system*		
	Polymers	*Porous adsorbent*	*Liquid with porous support*
$d_{f,max}$ (μm)	0.30	2.5	2.5
C_m^{max} (mmol/l)	0.7	1.7	7.0
D_s (m^2/s)	$7 \cdot 10^{-12}$	$0.5 \cdot 10^{-9}$	$0.5 \cdot 10^{-9}$
M_{pl} (pmol)	≈0.5	≈1.0	≈5.0
Phase ratio (max.)	0.12	$3.7 \cdot 10^8$ m^{-1}[a]	1.25

[a] Equivalent to $m^2/l \cdot 10^{-3}$.

EXPERIMENTAL

Chemicals and materials

The solvents used were analytical reagent grade cyclohexane, methanol and ethanol (Merck, Darmstadt, F.R.G.), acetonitrile (Rathburn, Walkerburn, U.K.), methylene chloride, pentane, hexane, γ-butyrolactone (Janssen, Beerse, Belgium) and monochloroethane (Aldrich, Brussels, Belgium). Distilled water was first deionized through a PSC filter assembly (Barnstead, Boston, MA, U.S.A.). Prior to use, all solvents were filtered by vacuum suction over 0.5-μm filters (Type FH; Millipore, Bedford, MA, U.S.A.).

The polycyclic aromatics used as test compounds were obtained from Janssen and Aldrich. Stock solutions of the test compounds were prepared in the mobile phase.

Polyethoxysiloxane (PES) was prepared by hydrolytic polycondensation of tetraethoxysiloxane (Janssen). Monochlorodimethyloctadecylsilane (ODS) was obtained from Aldrich. The derivatization reagents *o*-phthaldialdehyde (OPA) and 4-chloro-7-nitrobenzo-2-oxa-1,3-diazole (NBD-Cl) were obtained from Merck and Aldrich, respectively.

The 10-μm fused-silica capillaries were obtained from Polymicro Technology (Phoenix, AZ, U.S.A.).

Apparatus

Fig. 1 shows schematically the experimental set-up for the OTLC system. It consisted of a thermostated solvent reservoir (volume 400 ml), which could be pressurized with helium and served as a constant pressure pump, and a 0.5-μl injection valve (Model 7520; Rheodyne, Berkely, CA, U.S.A.) equipped with a splitting device. The columns were fitted in a laboratory-made thermostated jacket connected to a circulating liquid thermostat (Type F; Haake, Berlin, F.R.G.). A helium–cadmium laser, λ = 325 nm (Model 356 XM; Omnichrome, Chino, CA, U.S.A.) was used as a light source for on-column fluorescence detection. The laser beam passed a 325-nm bandpass filter (Oriel, Stratford, CT, U.S.A.) and was focused with a quartz lens (f = 50 mm) (Melles Griot, Zevenaar, The Netherlands). The emitted light was collected at a 90° angle by a Fresnel lens (f = 16 mm), then passed a 380-nm cut-off filter (Oriel). With NBD-Cl, a helium–cadmium laser, λ = 442 nm (Model 4207 NB; Liconix, Sunnyvale, CA, U.S.A.) was used, in combination with a 442-nm bandpass filter (Oriel) and a 500-nm cut-off filter (Oriel). The intensity was measured with a photomultiplier tube (Type 6225 S; EMI, Hayes, U.K.) and the resulting current was converted into a voltage by means of an amplifier (Diomod 72-W; Knick, Berlin, F.R.G.). The protective layer was burned off at the end of the capillary over a length of 1 cm. The signal was recorded with a potentiometric recorder (Kompensograph; Siemens, Karlsruhe, F.R.G.).

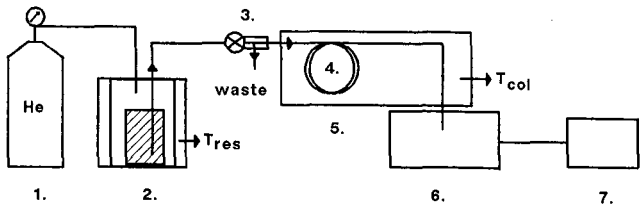

Fig. 1. Experimental set-up. 1, Helium bomb; 2, pressurized solvent reservoir; 3, injection valve with split injection; 4, capillary column; 5, thermostated jacket; 6, laser-induced fluorescence detector; 7, recorder.

Procedures

Preparation of a porous silica layer from PES. The deposition of a stable porous silica layer on the inner wall of fused-silica capillaries was performed by precipitation of silica from a solution of polyethoxysiloxane (PES). PES was prepared by hydrolytic polycondensation of tetraethoxysilane (TES) according to Unger and co-workers[25–27]. To 50 ml (0.22 mol) of TES dissolved in 30 ml of dry ethanol, 6.5 ml (0.36 mol) of water containing 70 μmol hydrochloric acid was added. This solution was

stirred vigorously for 1 h and refluxed for 6 h, then ethanol and hydrochloric acid were evaporated *in vacuo*.

The capillaries were treated with 1 *M* potassium hydroxide at room temperature for 2 h, then with 0.01 *M* hydrochloric acid at room temperature for 30 min, rinsed with water and finally dried for at least 2 h at 200–250°C whilst purging with dry helium (Fig. 2). Next the capillaries were filled with freshly prepared and degassed PES coating solution with pentane–monochloroethane or hexane–dichloromethane. The PES solution was prepared by dissolving PES in a polar solvent (dichloromethane or monochloroethane). Next, a non-polar solvent (hexane or pentane) was added until PES started to precipitate from the solution. Finally, PES was dissolved by adding a few drops more of the polar solvent. The solvent composition and the PES concentration were measured by weighing the amount of solvent added. The solvent was removed by evaporation under reduced pressure in a vacuum desiccator at one end of the capillary; the other end was closed with a septum. PES remained on the wall and was converted into silica by treatment with ammonia solution (pH 8–11) for 1 h, followed by rinsing with water for 2 h. The capillaries were dried by flushing with helium and could (i) be coated with PES again or (ii) be treated with a chemical modifier or (iii) be used as such in normal-phase chromatography.

Column diameters were determined as described previously[14].

Chemical modification. The dried capillary was flushed with a 5% (w/v) solution of ODS in toluene and heated at 140°C for 6 h. The capillary ends in a bottle of toluene to prevent blockage of the end of the capillary by precipitation of the silane reagent. Next the capillary was rinsed with toluene, acetonitrile or methanol before use. The liquid–liquid system was used as described previously[14].

Chemical derivatization of amino acids. The derivatization of amino acids with OPA was carried out according to Jones and Gilligan[28] and derivatization with NBD-Cl according to Ahnoff *et al.*[29].

RESULTS AND DISCUSSION

Static coating of polyethoxysiloxane (PES)

In a previous paper, the deposition of a porous silica layer was described[14]. The porous silica layer was prepared by dynamic coating of the silica precursor PES, which was converted into porous silica with gaseous ammonia. The main conclusion drawn was that this method is an elegant way to prepare a stationary layer, but resulted in a small phase ratio. The use of dynamic coating puts limits on the thickness of the silica layer and therefore static coating was suggested. In GC, static coating is used for preparing wall-coated open-tubular columns, with highly viscous non-polar polymers[30]. With static coating, the column is filled with a solution of the polymer in a volatile solvent. The solvent evaporates under reduced pressure and the polymer remains on the capillary wall. The polymers must be viscous, otherwise droplet formation and plugging, possibly caused by Rayleigh instability, will occur[30]. In our case we have to apply the same technique to coat PES, which is prepared by polycondensation from tetraethoxysilane (TES) and water. The kinematic viscosity can be adjusted in the range 10–20 000 cSt by varying the water-to-TES molar ratio from 1 to 1.5 (ref. 26). Adding more water to TES will result in the premature formation of silica gel, which cannot be used. Therefore, an even higher viscosity of the PES, which would be desirable, cannot be obtained.

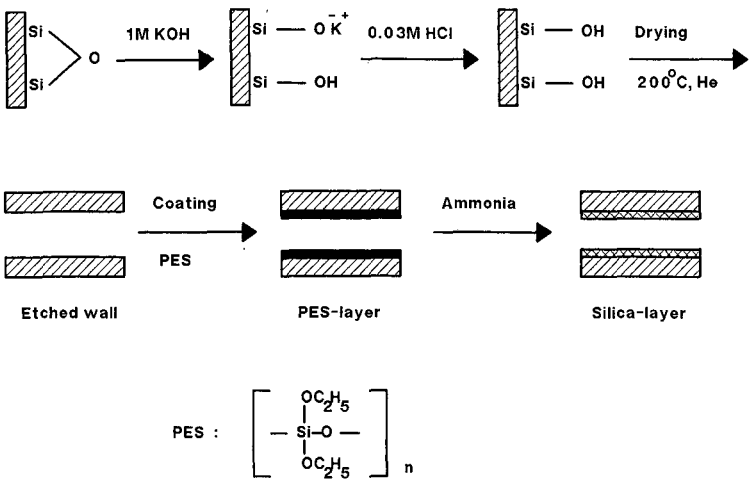

Fig. 2. Procedure for preparing porous silica layer.

The composition of the static coating solvent appeared to be critical. The solubility of PES in the solvent mixture should be carefully chosen. If the solubility of PES is good, then plugging of the solvent front during evaporation will occur. The concentration of PES in the solvent front will increase to such an extent that evaporation of the solvent will stop and the column becomes plugged. The solubility of PES should be lower, so that during evaporation PES precipitates on the wall and the coating process will proceed.

The choice of the solvent mixture was based on two factors: (i) the boiling temperature of the solvents should be around ambient, otherwise the coating process takes too long, and (ii) the polar solvent should preferably be more volatile than the non-polar solvent, in order to promote precipitation of PES at the outset of evaporation. The evaporation under reduced pressure was done from one end of the capillary, because static coating from both open ends of the capillary did not work. In this instance it appeared that the solvent plug moves to one end and out of the capillary. The static coating procedure, with dichloromethane–hexane as solvent mixture, takes about 2–3 days at room temperature, but often the capillary became plugged. With the monochloroethane–pentane mixture it was very laborious and difficult to make a good mixture, especially because the boiling temperature of monochloroethane is 12.3°C.

The PES concentration used was about 2% (v/v), which could give a layer thickness of 50 nm in a 10-μm tube. This choice was a compromise; higher concentrations were desirable because of the layer thicknesses that we were aiming for. However, the experimental problems in the coating process, which are negligible at concentrations below 1%, become insurmountable at concentrations above 2%. An alternative would be to obtain thick layers by repeating the coating. Although this has been applied successfully, it is a laborious approach.

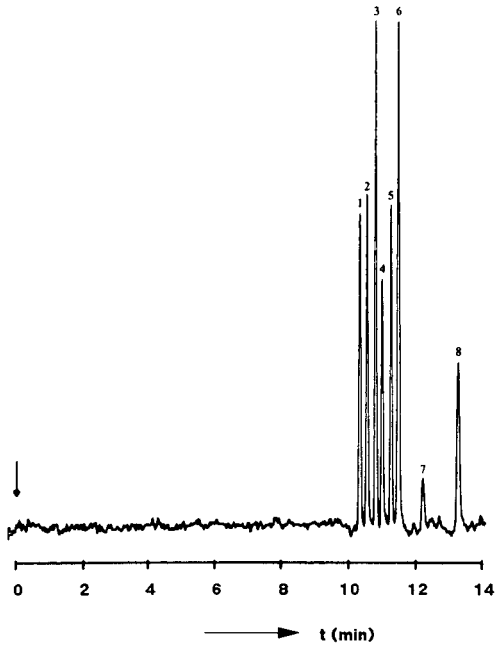

Fig. 3. LLC chromatogram of a capillary with a porous silica layer. Column, 1.55 m × 10.7 μm I.D.; mobile phase, cyclohexane saturated with γ-butyrolactone; stationary phase, γ-butyrolactone; linear velocity of mobile phase, 2.7 mm/s; inlet pressure, 0.9 MPa; T_{res} = 19.9°C; T_{col} = 20.0°C; V_{inj} = 23 pl; phase ratio, 0.019. Peaks: 1 = 9,10 diphenylanthracene; 2 = 9-phenylanthracene; 3 = 9-methylanthracene; 4 = anthracene; 5 = pyrene; 6 = fluoranthene; 7 = 1,2-benzanthracene; 8 = 9-anthracenecarbonitrile.

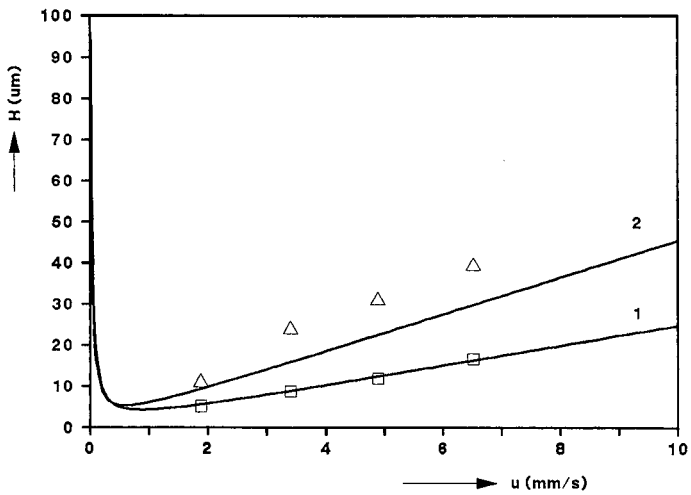

Fig. 4. *H versus u* curve for LLC capillary with porous silica layer. Column, 2 m × 10 μm I.D.; phase ratio, 0.038. 1, Theoretical curve for anthracene; 2, theoretical curve for benzo[*a*]pyrene; □, anthracene (k' = 0.26); △, benzo[*a*]pyrene (k' = 0.58).

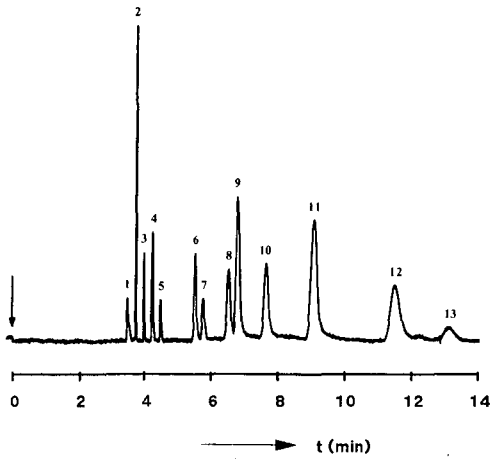

Fig. 5. Reversed-phase chromatogram for a capillary with an ODS-modified porous silica layer. Column, 1.34 m × 11.48 μm I.D.; mobile phase, acetonitrile–water (2:3); linear velocity of mobile phase, 6.4 mm/s; inlet pressure, 2 MPa; V_{inj} = 39 pl. Peaks: 1 = unretained; 2 = unknown; 3 = naphthoquinone; 4 = 9-anthracenemethanol; 5 = anthrone; 6 = 9-anthracenecarbonitrile; 7 = anthracene; 8 = fluoranthene; 9 = pyrene; 10 = 9-vinylanthracene; 11 = 1,2-benzanthracene; 12 = 9-phenylanthracene; 13 = benzo-[*a*]pyrene.

Chromatography

Solvent-generated liquid–liquid column (LLC) system. It was shown previously[14] that a non-viscous polar liquid, γ-butyrolactone, can be generated dynamically in the pores of a porous silica layer by pumping through cyclohexane saturated with γ-butyrolactone. It appeared possible to retain polycyclic aromatics on this phase system. Fig. 3 shows a chromatogram of eight polycyclic aromatics obtained on a 10.7-μm liquid–liquid column with a phase ratio of 0.019. For another capillary

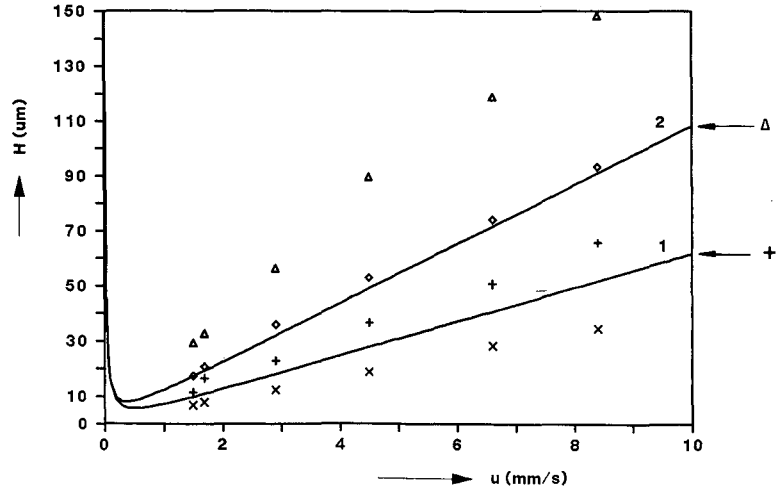

Fig. 6. *H versus u* curve for a capillary with an ODS-modified porous silica layer. 1, Theoretical curve for anthracene; 2, theoretical curve for 1,2-benzanthracene; ×, 9-anthracenecarbonitrile; +, anthracene; ◇, fluoranthene; △, 1,2-benzanthracene. Other details as in Fig. 5.

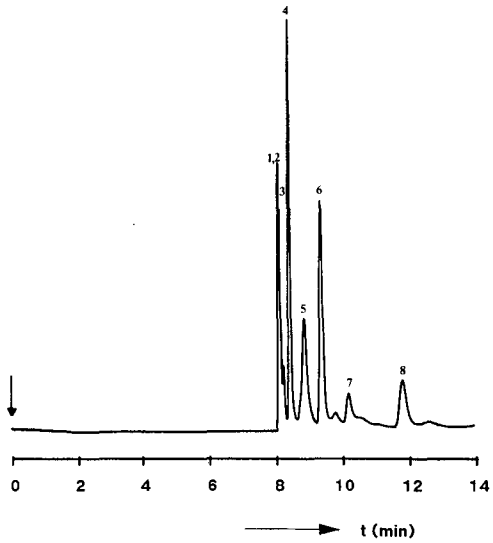

Fig. 7. Separation of some OPA-amino acids by reversed-phase OTLC. Column, 1.34 m × 11.48 μm I.D.; mobile phase, methanol–phosphate buffer (pH 7) (3:7); linear velocity of mobile phase, 2.7 mm/s. Peaks: 1 = glutamate; 2 = asparagine; 3 = threonine; 4 = alanine; 5 = histidine; 6 = valine; 7 = phenylalanine; 8 = leucine. Other details as in Fig. 5.

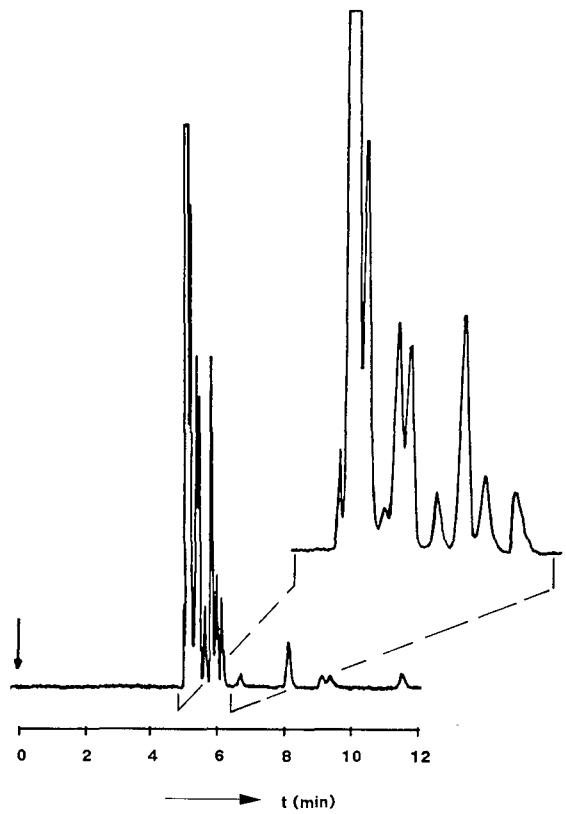

Fig. 8. Separation of some NBD-Cl amino acids by reversed-phase OTLC. Column, 2 m × 10 μm I.D.; mobile phase, acetonitrile–phosphate buffer (pH 7) (1:9); linear velocity of mobile phase, 7.0 mm/s. Other details as in Fig. 5.

a graph of *H versus u* was recorded (Fig. 4). Fig. 4 also shows theoretically calculated *H versus u* curves based on data obtained earlier for the diffusion coefficient[31]. The agreement is excellent for anthracene ($k' = 0.26$), whereas for benzo[*a*]pyrene ($k' = 0.58$) the agreement is within 30%. Although the phase ratio for these columns is still small, these results do illustrate the potential of liquid–liquid OTLC.

Reversed-phase chromatography. The applicability of phase systems with different kinds of chemistry in HPLC is well documented, and the reaction of silane reagents with silica can be simply carried out. For OTLC these silane reagents have hardly been used, but via the deposition of a porous silica layer in 10-μm capillaries this kind of chemistry can be applied in OTLC. Fig. 5 shows a chromatogram of polycyclic aromatics separated isocratically within 15 min on an 11.5-μm capillary with a chemically modified porous silica layer. The recorded *H versus u* curve (Fig. 6) shows fair agreement with the theory. The deviation at higher velocities can probably be explained by an incorrect value of the calculated diffusion coefficient by Wilke and Chang[32]. In Figs. 7 and 8 two chromatograms are shown with an isocratic separation of derivatized amino acids with OPA and NBD-Cl. From Figs. 5–8 it can be seen that reversed-phase OTLC in capillaries with a porous silica layer is possible. Other kinds of chemical modifications can probably also be used.

CONCLUSION

The preparation of porous silica layers in 10-μm open-tubular columns shows attractive features. The method described for depositing these layers is very elegant, because high-temperature treatments and other rigorous conditions are not necessary. However, in the static and dynamic coating steps serious experimental problems were encountered. The layer thickness, obtained by these coating procedures, is still too small.

The insufficient viscosity of PES is probably one of the drawbacks to static coating in 10-μm tubes. This problem was aggravated during our experiments because relatively high PES concentrations were used. This leads to even worse stability of the once formed PES layer, and also slows the evaporation. However, with the prepared porous silica layers excellent results in liquid–liquid and reversed-phase chromatography were obtained. It is expected that several other kinds of stationary phase modifications can be applied in these columns. Other routes for obtaining thick porous silica layers, using other silica precursors, are currently under consideration.

ACKNOWLEDGEMENTS

The authors thank Peter Schoenmakers, Philips Research Laboratories, for critical discussions and Dick Schoutsen for practical assistance. Support for this work was provided by the Netherlands Foundation for Chemical Research (SON), with financial aid from the Netherlands Organization for Scientific Research (NWO) under grant 700-344-003.

REFERENCES

1 J. H. Knox and M. Saleem, *J. Chromatogr. Sci.*, 7 (1969) 614.
2 J. H. Knox and M. T. Gilbert, *J. Chromatogr.*, 186 (1979) 405.
3 D. Ishii and T. Takeuchi, *J. Chromatogr. Sci.*, 18 (1980) 462.
4 J. W. Jorgenson and E. J. Guthrie, *J. Chromatogr.*, 255 (1983) 335.
5 M. J. Sepaniak, J. D. Vargo, C. N. Kettler and M. P. Maskarinec, *Anal. Chem.*, 56 (1984) 1252.
6 J. B. Phillips, D. Luu, J. B. Pawliszyn and G. C. Carle, *Anal. Chem.*, 57 (1985) 2779.
7 H. P. M. van Vliet and H. Poppe, *J. Chromatogr.*, 346 (1985) 149.
8 L. A. Knecht, E. J. Guthrie and J. Jorgenson, *Anal. Chem.*, 56 (1984) 479.
9 S. Folestad, B. Josefsson and M. Larsson, *J. Chromatogr.*, 391 (1987) 347.
10 O. van Berkel, J. C. Kraak and H. Poppe, *Chromatographia*, 24 (1987) 739.
11 H. Poppe, J. C. Kraak, O. van Berkel-Geldof and P. P. H. Tock, in P. Sandra (Editor), *Proceedings of the Ninth Congress on Capillary Chromatography, Monterey, CA, 1988*, Hüthig Verlag, Heidelberg, pp. 345–354.
12 P. R. Dluzneski and J. W. Jorgenson, *J. High Resolut. Chromatogr. Chromatogr. Commun.*, 11 (1988) 332.
13 O. van Berkel-Geldof, J. C. Kraak and H. Poppe, to be published.
14 P. P. H. Tock, G. Stegeman, R. Peerboom, H. Poppe, J. C. Kraak and K. K. Unger, *Chromatographia*, 24 (1987) 617.
15 J. Bouche and M. Verzele, *J. Gas Chromatogr.*, 6 (1968) 501.
16 G. Dijkstra and J. De Goey, *Gas Chromatography*, Academic Press, New York, 1958, p. 56.
17 G. Schomburg and H. Husmann, *Chromatographia*, 8 (1975) 517.
18 L. S. Ettre and J. E. Purcell, *Adv. Chromatogr.*, 10 (1974) 1.
19 J. de Zeeuw, R. C. M. de Nijs, J. C. Buyten, J. A. Peene and M. Mohnke, *J. High Resolut. Chromatogr. Chromatogr. Commun.*, 11 (1988) 162.
20 M. J. E. Golay, in H. Desty (Editor), *Gas Chromatography 1958*, Butterworths, London, 1958, pp. 36–55.
21 J. H. Knox and H. P. Scott, *J. Chromatogr.*, 282 (1983) 297.
22 H. Poppe and J. C. Kraak, *J. Chromatogr.*, 255 (1983) 395.
23 J. E. Eble, R. L. Grob, P. E. Antle and L. R. Snyder, *J. Chromatogr.*, 384 (1987) 25.
24 R. T. Ghijsen and H. Poppe, *J. High Resolut. Chromatogr. Chromatogr. Commun.*, 11 (1988) 271.
25 K. K. Unger, J. Schick-Kalb and K.-F. Krebs, *J. Chromatogr.*, 83 (1973) 5.
26 K. K. Unger, J. Schick-Kalb and B. Straube, *Colloid Polym. Sci.*, 253 (1975) 658.
27 K. K. Unger and B. Scharf, *J. Colloid Interface Sci.*, 55 (1976) 377.
28 B. N. Jones and J. P. Gilligan, *J. Chromatogr.*, 266 (1983) 471.
29 M. Ahnoff, I. Grundevik, A. Arfwidsson, J. Fonselius and B.-A. Persson, *Anal. Chem.*, 53 (1981) 485.
30 K. D. Bartle, C. L. Woolley, K. E. Markides, M. L. Lee and R. S. Hansen, *J. High Resolut. Chromatogr. Chromatogr. Commun.*, 10 (1987) 128.
31 J. P. Crombeen, H. Poppe and J. C. Kraak, *Chromatographia*, 22 (1986) 319.
32 C. P. Wilke and P. Chang, *AIChE J.*, 1 (1955) 264.

Journal of Chromatography, 477 (1989) 107–118
Elsevier Science Publishers B.V., Amsterdam — Printed in The Netherlands

CHROM. 21 410

OPTIMIZATION OF DETECTION SENSITIVITY FOR ENANTIOMERS OF METOPROLOL ON SILICA-BONDED α_1-ACID GLYCOPROTEIN

KARIN BALMÉR and BENGT-ARNE PERSSON
Bioanalytical Chemistry, AB Hässle, S-431 83 Mölndal (Sweden)
and
GÖRAN SCHILL*
Department of Analytical Pharmaceutical Chemistry, University of Uppsala, S-751 23 Uppsala (Sweden)

SUMMARY

On the chiral phases CHIRAL-AGP and EnantioPac, organic modifiers, pH and temperature have been varied with isocratic and gradient techniques to obtain minimum retention and maximum peak height by baseline resolution of *R*-and *S*-metoprolol. The decrease in retention obtained by gradient elution gives, by limiting baseline resolution, 20–60% greater peak heights than those obtained by the isocratic technique. A reduction of the retention by a change in the pH is more favourable than addition of modifiers such as acetonitrile or 2-propanol. It gives a smaller decrease in resolution by isocratic elution and a pH gradient can give considerably stronger peak compression than an acetonitrile gradient as indicated by an estimation of the detection limits. For metoprolol enantiomers, CHIRAL-AGP gives about three times lower reduced plate heights than does EnantioPac.

INTRODUCTION

Most drugs with chiral properties are used as racemic mixtures although in many cases the desired physiological effect is due mainly to one of the enantiomers. The pharmacokinetics can also be different for the antipodes and it is therefore important separately to investigate each form in order to estimate the therapeutic effect of administration of a racemic mixture[1].

Liquid chromatography is the technique employed most often for the resolution of enantiomers, and differences in retention are achieved by interaction of the solutes with another enantiomeric molecule, a chiral selector, which can be coupled to the solutes by covalent or coordinative bonds. The enantiomers of a 1,2-aminoalcohol like metoprolol can thus be separated as derivatives with 2,3,4,6-tetra-O-acetyl-β-D-glycopyranosyl isothiocyanate[2], with a complexing selector such as N-benzoxycarbonylglycyl-L-proline (ZGP) present in the mobile phase[3] and with a stationary phase containing a chiral selector such as α_1-acid glycoprotein (AGP)[4] or cellulose tris-3,5-dimethylphenyl carbamate[5].

The determination of metoprolol in biological samples requires an high mass

0021-9673/89/$03.50

sensitivity. Low concentrations can be measured by fluorimetry[6], but the enantiomer peaks must be eluted in small volumes and with sufficient resolution. The choice of the chromatographic separation conditions is of great importance since it has been observed that many liquid chromatographic systems for chiral separation give rather wide peaks.

The present study was performed with silica-bonded AGP as the chiral phase. Two commercial phases were used, EnantioPac and CHIRAL-AGP, the latter being a recent development with improved separating efficiency and stability. The aim of the investigation was to develop chromatographic conditions for high detection sensitivity by complete resolution of the antipodes of metoprolol.

EXPERIMENTAL

Apparatus

The chromatograph comprised a Model 2150 pump with a Model 2152 gradient controller (LKB, Bromma, Sweden), a WISP 710 B autosampler (Waters Assoc., Milford, MA, U.S.A.) and a fluorescence detector LS4 (Perkin-Elmer, Norwalk, CT, U.S.A.), which was set at 228 nm (excitation) and 306 (emission), with slit widths of 10 nm. Chromatograms were recorded using a Model 4270 integrator (Spectra-Physics, San José, CA, U.S.A.).

The separation columns were EnantioPac, 100 mm × 4.0 mm, 10 μm (LKB) and CHIRAL-AGP, 100 mm × 4.0 mm, 5 μm (ChromTech, Stockholm, Sweden). The CHIRAL-AGP column was protected by a Brownlee DIOL guard column in a module (Brownlee Labs., Santa Clara, CA, U.S.A.). The temperature of the columns was controlled by a thermostat bath RMS 6 (Lauda, Königshofen, F.R.G.). The pH of the eluent was measured in a flow cell, constructed at AB Hässle, using a glass electrode GK 743500 and a Model 84 pH-meter (Radiometer, Copenhagen, Denmark) with a Perkin-Elmer 56 recorder (Hitachi, Tokyo, Japan).

Chemicals and reagents

The racemate and the separate enantiomers of metoprolol and α-hydroxymetoprolol were synthesized at the Department of Organic Chemistry, Hässle. 2-Propanol was of high-performance liquid chromatography (HPLC) grade and acetonitrile of specially pure HPLC grade S (Rathburn Chemicals, Walkerburn, U.K.). All other reagents and buffer substances were of analytical grade (E. Merck, Darmstadt, F.R.G.). Water used in the mobile phase was from a Milli-Q system (Millipore, Molsheim, France).

Chromatographic system

The mobile phase comprised phosphate buffer (I = 0.02) modified with 2-propanol or acetonitrile in isocratic or gradient mode. In the pH gradient system the mobile phase contained 0.5% 2-propanol in phosphate buffer pH 7.5 (I = 0.02) (a) and 0.02 M sodium dihydrogenphosphate (b) in various proportions. The gradient pumping system had a volume of 2.0 ml from the mixing chamber to the column inlet, which was taken into account by making the sample injection coincide with the gradient reaching the column inlet. The solutes were injected dissolved in the mobile phase, if not stated otherwise. The volumes injected were 10 or 20 μl.

The flow-rate of the mobile phase was 0.3 ml/min for the EnantioPac and 0.5 ml/min for the CHIRAL-AGP column. The experiments were performed on a number of columns. The efficiency of the columns, expressed as the theoretical plate numbers, decreased after some time and many injections, but the separation factor, α, was almost constant. Reactivating the column by a low flow of 25% 2-propanol in water or 0.01 M H_3PO_4 was sometimes successful. The separate experimental series presented in a table or a figure were performed without change of the column.

Calculations

The parameters, used in the evaluation of the column and separation efficiency are the plate number, N, reduced plate height, h, α and resolution, R_s

$$N = 5.54(t_R/W_{\frac{1}{2}})^2$$

$$h = \text{column length}/(N \cdot \text{particle diameter})$$

$$\alpha = k'_S/k'_R$$

$$R_s = 2(t_{R_s} - t_{R_R})/(W_R + W_S)$$

where t_R = retention time in min, $W_{\frac{1}{2}}$ = width at the half peak height in min, W_R. W_S = widths of the peaks at the base in min and $k' = (t_R - t_0)/t_0$. The determination of t_0, *i.e.*, the retention time of a non-retained compound, was performed by injecting the hydrophilic α-hydroxymetoprolol. The content of 2-propanol in the mobile phase was increased gradually until no decrease of the retention time for α-hydroxy-metoprolol was noticed. The value of t_0 was 4.2 min (1.26 ml) for the EnantioPac column and 2.2 min (1.10 ml) for the CHIRAL-AGP column in this system.

RESULTS AND DISCUSSION

Properties of α_1-acid glycoprotein and the AGP columns

AGP is an human transport protein. Its molecular weight is about 41 000 and its isoelectric point is 2.7 in phosphate buffer. It contains a peptide chain with 181 amino acid units and five carbohydrate units, the latter constituting 45% of the molecular weight. There are numerous asymmetric centres in the peptide chain and the carbohydrate units but the chiral binding principle has so far not been elucidated[7].

The chiral stationary phase based on AGP was developed by Hermansson[8] and its properties and applications have been presented in a large number of publications (*cf.*, ref. 9). The commercial product EnantioPac contains the protein bound to diethylaminoethylsilica and immobilized by cross-linking. Eluents outside the range pH 4–7 should be avoided. CHIRAL-AGP is a newly developed product with improved chromatographic properties and stability. The useful range is up to pH 7.5 and temperatures between 3 and 40°C can be used.

The two AGP phases can be applied to chiral separations of moderately hydrophobic compounds having charged or hydrogen-bonding groups in the vicinity of the chiral centre. The retention and the chiral selectivity can be changed by uncharged modifiers in the aqueous mobile phase such as acetonitrile and lower

alcohols. Changes in the pH and temperature as well as the addition of charged modifiers are other means for regulation of retention and chiral selectivity[9].

Isocratic regulation of retention

The influence of two uncharged modifiers, acetonitrile and 2-propanol, on the retention of *R*-metoprolol and the chiral separation factor, α, on an EnantioPac column is demonstrated in Figs. 1 and 2. 2-Propanol has a strong effect even at concentrations below 1% while acetonitrile must be used in about five times higher concentrations to give the same decrease of k'_R. With both modifiers the decrease in the retention is accompanied by a rather limited decrease in the separation factor. The strong influence of the modifiers on the retention indicates an interaction with the AGP phase that is more specific than a simple competition for an hydrophobic binding site (*cf.*, ref. 9).

The effect of temperature changes is highly dependent on the structure of the solute[4,10]. An increase from 7 to 28°C decreases k' of *R*-metoprolol by about 20% on CHIRAL-AGP (Table I). On EnantioPac the temperature effect on k' seems to be somewhat larger, possibly due to a different binding of AGP to the silica matrix.

AGP has an isoelectric point of 2.7 and the negative charge and the binding ability for cationic solutes increase with pH, but the effect is dependent on the structure of the solute[4,10–12]. On CHIRAL-AGP the k' of *R*-metoprolol decreases to one third upon a decrease in pH of slightly more than one pH unit (Table II). This strong decrease in retention has, however, a very limited effect on the chiral selectivity. A comparison with other means for regulation of the retention indicates that a pH change that causes a similar change in k' has a considerably lower influence on the

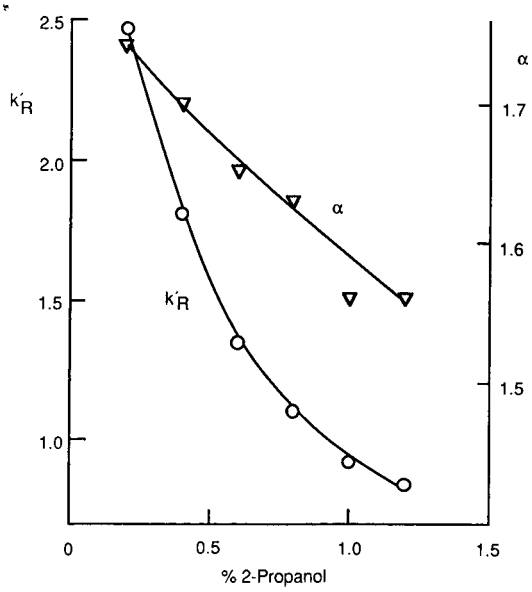

Fig. 1. Isocratic elution with 2-propanol as a modifier. Solid phase: EnantioPac. Temperature: 12°C. Mobile phase: phosphate buffer pH 7.0 with 2-propanol. Solutes: *R*- and *S*-metoprolol.

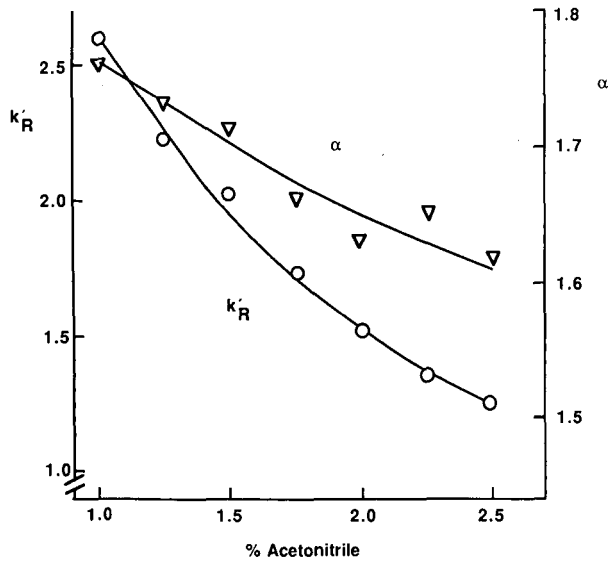

Fig. 2. Isocratic elution with acetonitrile as a modifier. Conditions as in Fig. 1, except: mobile phase, phosphate buffer pH 7.0 with acetonitrile.

chiral selectivity than changes in the modifier concentration or temperature, which might open possibilities to elucidate the nature of the chiral binding sites on AGP.

The phases with silica-bonded AGP give high chiral selectivity for compounds of widely different structures. In order to obtain chiral resolution this selectivity must be combined with good separating efficiency which is counteracted by many chiral solid phases giving rather wide solute peaks. The background to the low efficiency has not so far been explained but speculations on slow binding due to conformational changes have been presented[12]. Studies on EnantioPac have shown that the peak width is dependent on the structure of the solute, and that the temperature and the composition of the mobile phase can also have an influence[10,12].

CHIRAL-AGP gives better reduced plate heights than EnantioPac. Illustrations of the differences in separating efficiency are given in Tables I and III. Acetonitrile is

TABLE I

TEMPERATURE EFFECTS BY ISOCRATIC ELUTION

Solid phase: CHIRAL-AGP. Mobile phase: phosphate buffer pH 7.0 with 1.65% acetonitrile.

Temp. (°C)	k'_R	α	h_R	h_S	R_s
7	5.76	1.44	12	11	3.3
10	5.48	1.43	11	10	3.4
13	5.24	1.42	11	10	3.3
16	5.10	1.38	10	9	3.1
19	4.95	1.37	12	9	3.1
22	4.76	1.34	9	8	3.0
25	4.62	1.32	9	8	2.8
28	4.48	1.30	9	8	2.6

TABLE II

pH EFFECTS BY ISOCRATIC ELUTION

Solid phase: CHIRAL-AGP. Mobile phase: phosphate buffer with 0.5% 2-propanol. Temperature: 20°C.

pH	k'_R	α	R_s
7.50	7.67	1.53	3.6
7.29	6.69	1.54	3.2
7.08	4.82	1.52	2.9
6.91	4.25	1.51	2.8
6.69	3.30	1.49	2.4
6.40	2.53	1.45	2.0
6.02	1.42	1.38	–

the modifier in both experimental series. Table I shows the effect of temperature variation at constant modifier concentration on CHIRAL-AGP, whereas Table III gives the results obtained with EnantioPac when the modifier concentration is varied at constant temperature (12°C). CHIRAL-AGP gives about three times lower h values than does EnantioPac and the resolution, R_s is much higher despite the fact that the separation factor, α, on CHIRAL-AGP is lower under similar chromatographic conditions.

Improvement of detection sensitivity by chromatograhic means

The aim of the study was to develop chromatographic conditions that give complete resolution of the enantiomers and minimize the volumes in which the peaks are eluted.

The detection sensitivity can be improved by decreasing the retention until a limiting baseline resolution ($R_s = 1.5$ for symmetrical peaks) is obtained. On the AGP columns this can be performed in a systematic way by changing the modifier concentration, pH or temperature as indicated above. Application of the retention changing agent in a gradient mode is a convenient and rapid way of reaching the limiting conditions. Furthermore, if the principles for linear solvent strength gradients can be applied to this system, gradient elution should give better detection sensitivity than the corresponding isocratic elution when the resolution is the same[13,14].

TABLE III

ISOCRATIC ELUTION WITH ACETONITRILE AS THE MODIFIER

Solid phase: EnantioPac. Mobile phase: phosphate buffer pH 7.0 with acetonitrile. Temperature: 12°C.

Acetonitrile (%)	α	h_R	h_S	R_s
1.00	1.76	26	22	1.9
1.25	1.73	28	25	1.6
1.50	1.71	30	27	1.4
1.75	1.66	35	26	1.3
2.00	1.63	37	24	1.2
2.25	1.65	40	31	1.1
2.50	1.62	33	26	1.1

The evaluation of the sensitivity in gradient elution can be based on the peak width at the base, $W_b = 4\sigma_t$, or the signal per mol of solute at a given R_s. (Band widths in gradient elution can not be used for evaluation of the separating efficiency.) With a linear solvent strength gradient the sensitivity, s_g, is according to Snyder[13] given by

$$s_g = 1/G(1 + k_f) \quad (1)$$

where $k_f = 1/2.3b$ corresponds to k' of a solute band leaving the column in gradient elution, b expresses the steepness of the gradient and G is a band compression factor which is roughly equal to 0.8 at a moderate value of b.

The detection sensitivity, s_g, is improved by increasing the gradient steepness, *i.e.*, $1/b$ has an effect analogous to k' in isocratic liquid chromatography. Eqn. 1 shows furthermore that the sensitivity should be the same for all solutes independent of their retention. This means, *e.g.*, that the enantiomers in a racemate should give peaks of equal height.

Further means for improvement of detection sensitivity such as injection of large volumes of sample and use of microbore or capillary columns have not been included in this study.

Gradient elution with organic modifier

The resolution in gradient elution can be described by an expression analogous to that used for isocratic elution. Snyder[13] has shown that k' in the expression for R_s can be substituted for $\bar{k} = 1/1.3b$ when a linear solvent strength gradient is used. If other chromatographic conditions are unchanged, R_s will then be proportional to $[\bar{k}/(1 + \bar{k})]^2 = [1/(1 + 1.3b)]^2$. An increase in the gradient steepness, b, will obviously decrease R_s whereas the detection sensitivity is increased as shown above.

A comparison of the detection sensitivity by isocratic and gradient separation on CHIRAL-AGP with acetonitrile as the modifier is given in Fig. 3. Both elution modes have been adjusted to give the same resolution, $R_s = 2.0$. The amounts of *R*- and *S*-metoprolol injected are also the same, 36 pmol of each. The gradient elution gives two peaks of about equal height and the peak height quotients for the two enantiomers are $R_{grad}/R_{isocr} = 1.20$ and $S_{grad}/S_{isocr} = 1.62$, *i.e.*, 20 and 62% higher sensitivity for the gradient elution.

The expression for the influence of gradient steepness on detection sensitivity and resolution given above has been evaluated for a linear solvent strength gradient

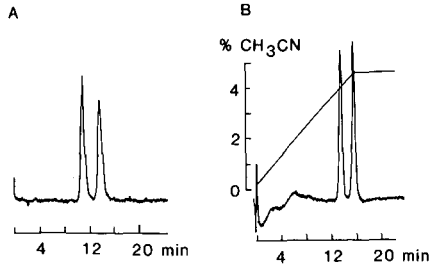

Fig. 3. Separation of metoprolol enantiomers. Solid phase: CHIRAL-AGP. Temperature: 20°C. Amount injected: 36 pmol of each. Mobile phase: phosphate buffer pH 7.0 with (A) isocratic elution and 2.25% acetonitrile; (B) gradient elution, starting with 0.1% acetonitrile, gradient 0.293%/min.

TABLE IV

ELUTION WITH 2-PROPANOL GRADIENT

Solid phase: EnantioPac. Mobile phase: phosphate buffer pH 7.0 with 2-propanol. Temperature: 3°C. Solutes: *R*- and *S*-metoprolol, 30 pmol of each.

2-Propanol		*Rel. peak height*		R_s
Start (%)	*Gradient (%/min)*	*R*	*S*	
0.24	–	1	0.70	1.5
0.2	0.010	1.08	0.86	1.5
0.2	0.015	1.16	0.97	1.5
0.1	0.020	1.19	1.14	1.5
0.1	0.027	1.19	1.14	1.4
0.04	0.048	1.35	1.35	1.1
0.04	0.064	1.54	1.54	1.1

and an adsorbing stationary phase. A qualitative test of its validity for the separation of metoprolol enantiomers on EnantioPac with 2-propanol as the modifier is presented in Table IV. EnantioPac gives an higher chiral selectivity than that of CHIRAL-AGP (see Tables I and III) but the separating efficiency with isocratic elution is much lower. Isocratic elution with 0.24% 2-propanol gives an almost complete resolution. Gradient elution with a steepness up to 0.02%/min gives no significant loss of resolution but the detection sensitivity is improved. The enantiomer peaks have about equal height and the increase of the detection sensitivity is 20% for the *R*-enantiomer and about 60% for the *S*-enantiomer. A steeper gradient gives a slight decrease in R_s but the sensitivity improvement is substantial: more than 50% for the *R*-enantiomer and more than 100% for the *S*-enantiomer.

The gradient studies show that the peak compression effects outbalance the decrease in retention difference between the enantiomers when the gradients are moderately steep. This indicates that the steepness of the modifier gradient on the AGP phase has a less strong influence on the resolution than indicated by the expression for R_s given by Snyder[13]. Gradient elution seems to be of special value as a tool for improvement of the detection sensitivity on the AGP phase.

Elution with pH gradients

The strong effect of pH on the retention of metoprolol on CHIRAL-AGP was shown in Table II. A further indication of the importance of pH is given by the chromatographic results shown in Fig. 4. The solutes are normally injected with mobile phase as the solvent and chromatogram A was obtained in that way. Chromatogram B was obtained with the same amount of solutes dissolved in 0.01 *M* H_3PO_4. The first peak (*R*-metoprolol) has the same width on both chromatograms, whereas the second peak (*S*-metoprolol) is significantly narrower in chromatogram B. Measurement of the pH in a flow cell inserted after the column showed that the phosphoric acid injected (10 μl) had caused a pH pulse that migrated with the same speed as that of *S*-metoprolol.

The pH effect on the retention can be used in gradient elution. The slow migration of the pH pulse shown in Fig. 4B indicates that the hydrophilic components

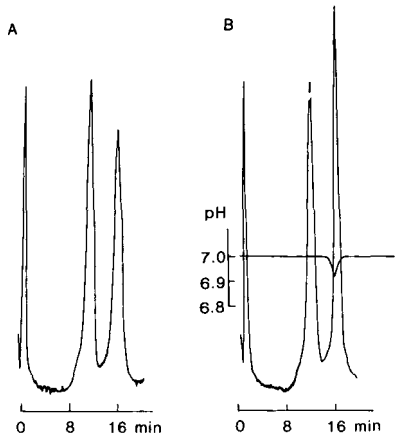

Fig. 4. Influence of sample solvent. Solid phase: EnantioPac. Temperature: 3°C. Mobile phase: phosphate buffer pH 7.0 with 1.5% acetonitrile. Solutes: *R*- and *S*-metoprolol. Sample solvents: (A) mobile phase; (B) 0.01 *M* H_3PO_4.

in the buffer will be retained. The effect of the pH gradient will depend on its migration relative to the solutes and the shape and the retention of the gradient must be determined experimentally. An example is given in Fig. 5. The gradient was obtained from phosphate buffer pH 7.5 and 0.02 *M* sodium dihydrogenphosphate and was applied to a CHIRAL-AGP column. The pH was measured in flow cells at the inlet and the end of the column. The gradient has the same shape before and after the column in the range pH 6.3–7.3 where the phosphate buffer has its highest capacity.

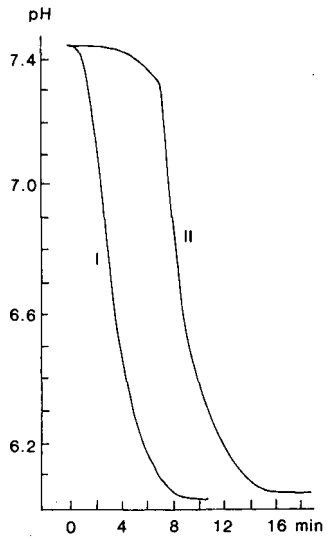

Fig. 5. Effect of the pH gradient. Solid phase: CHIRAL-AGP. Temperature: 20°C. Mobile phase: 0.5% 2-propanol in phosphate buffer pH 7.5 (I = 0.02) (a), 0.02 *M* sodium dihydrogenphosphate (b). Start: pH 7.4 (98% a + 2% b). Gradient: linear increase of b from 2 to 75% during 1 min. End: pH 6.05 (25% a + 75% b). pH measured in flow cells: I, before column; II, after column.

The deviations at lower buffer capacity might be due to the measuring technique. The retention and the shape of the gradient are highly dependent on the nature of the buffer components as has been found by studies of, *e.g.*, citrate buffers.

The application of pH gradients to the separation of *R*- and *S*-metoprolol on EnantioPac is shown in Fig. 6. The gradients covered the pH range 7.3–6.2 and the solutes were injected at such a time that the pH change mainly affected the last eluted *S*-enantiomer. The compression of the peak depends on the steepness of the gradient and the steepest gradient (Fig. 6C) increases the peak height of the *S*-enantiomer by a factor of about three compared to the isocratic elution (Fig. 6A). When the sample was injected so that both enantiomers were affected by the pH change incomplete separation was achieved.

CHIRAL-AGP has a considerably higher separating efficiency than EnantioPac and it is easy to apply a pH gradient in such a way that the detection sensitivity of both metoprolol enantiomers is improved with the maintenance of complete resolution. Some examples are given in Fig. 7. Isocratic separation at pH 7.5 with 0.5% 2-propanol as a modifier gives a separation with R_s = 3.3 (Fig. 7A). The high resolution gives excellent possibilities of application of pH gradients, and the effect of gradients with different steepness covering the range pH 7.5–6.0 are shown in Fig. 7C and D. The peak height improvements by gradient elution relative to the isocratic elution at pH 7.5 are summarized in Table V.

Fig. 7D shows a limiting baseline resolution obtained by the pH-gradient technique. The limiting resolution in isocratic elution obtained by pH adjustment is shown in Fig. 7B. The improvement of the detection sensitivity relative to isocratic elution at pH 7.5 is considerable as shown in Table V. However, gradient elution to the same limiting resolution gives a further improvement of 50–60%.

An estimation from Fig. 7D gives a detection limit, defined as three times the noise, of about 0.7 pmol of each enantiomer. The acetonitrile gradient in Fig. 3B gives an estimated detection limit of about 1.8 pmol. This indicates that the pH gradient

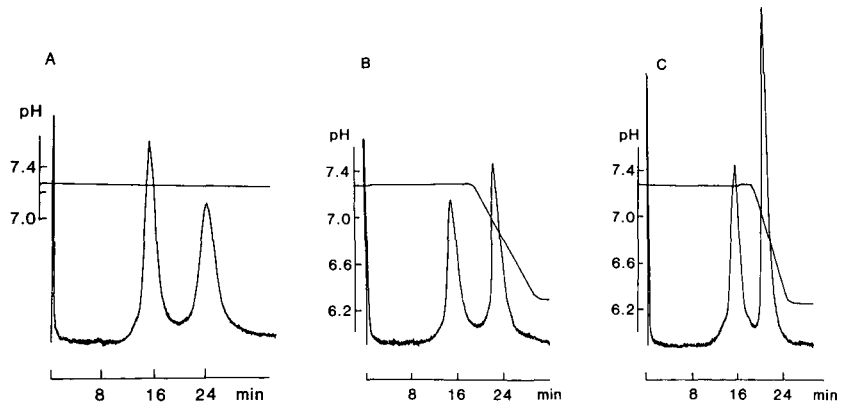

Fig. 6. Elution with a pH gradient. Solid phase: EnantioPac. Temperature: 5°C. Solutes: *R*- and *S*-metoprolol, 90 pmol of each. Mobile phase: see Fig. 5. (A) Isocratic, pH 7.3. (B) Start: pH 7.3 (96% a + 4% b). Gradient: linear increase of b from 4 to 75% during 25 min. End: pH 6.2 (25% a + 75% b). (C) pH as in (B), gradient time 1 min (preceded by isocratic elution for 4 min). The pH after the column is given.

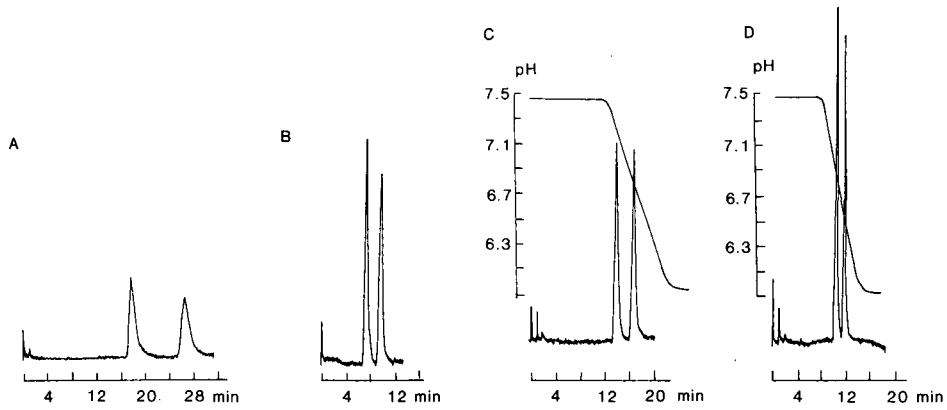

Fig. 7. Influence of pH by isocratic and gradient elution. Solid phase: CHIRAL-AGP. Temperature: 20°C. Solutes: *R*- and *S*-metoprolol, 18 pmol of each. Mobile phase: see Fig. 5. (A) Isocratic: pH 7.50. (B) Isocratic: pH 6.40. (C) Start: pH 7.5 (100% a). Gradient: linear increase of b from 0 to 75% during 15 min. End: pH 6.0 (25% a + 75% b). (D) pH as in (C), gradient time 1 min. The pH after the column is given.

gives a stronger peak compression than the acetonitrile gradient but quantitative conclusions can be made only if differences in the column properties, if any, are taken into consideration.

Improvement of detection sensitivity on AGP phases

The AGP phases can be used for separation of enantiomers of widely different structures but the influence on the chiral selectivity of modifiers, pH and temperature can be highly different even for structurally closely related substances[9,12]. It is important to remember that pH changes have different effects on the retention of cationic, anionic and uncharged substances. Certain enantiomers can be separated only in the presence of charged modifiers and addition of a modifier can sometimes even give rise to a reversal of the retention order between the solutes[4,9]. Preliminary studies of the effects of changes of the chromatographic conditions must be made before optimization of the sensitivity is attempted.

TABLE V

DETECTION SENSITIVITY BY ISOCRATIC AND GRADIENT ELUTION

Solid phase: CHIRAL-AGP. Mobile phase: phosphate buffer with 0.5% 2-propanol. Temperature: 20°C. Solutes: *R*- and *S*-metoprolol, 18 pmol of each.

pH		*Relative peak height*	
Start	*ΔpH/min*[a]	*R*	*S*
7.50	–	1	0.75
6.40	–	2.8	2.3
7.5	−0.1	2.5	2.4
7.5	−1.5	4.3	3.8

[a] Before the column.

The aim of the optimization should be the attainment of baseline resolution at the lowest possible retention by the gradient or isocratic technique. Modifier or pH gradients are tested with increasing steepness until limiting baseline resolution is obtained. Studies by the isocratic technique can be started at a low temperature with the initial aim of finding a pH modifier level that gives $R_s > 1.5$. The limiting baseline resolution can then be reached by increasing the temperature.

REFERENCES

1 E. J. Ariens, *Eur. J. Clin. Pharmacol.*, 26 (1984) 663.
2 A. J. Sedman and J. Gal, *J. Chromatogr.*, 278 (1983) 199.
3 C. Pettersson and M. Josefsson, *Chromatographia*, 21 (1986) 321.
4 G. Schill, I. Wainer and S. Barkan, *J. Liq. Chromatogr.*, 9 (1986) 641.
5 Y. Okamoto, M. Kawashima, R. Aburatani, K. Hatada, T. Nishiyama and M. Masuda, *Chem. Lett.*, 1237 (1986).
6 K. Balmér, Y. Zhang, P.-O. Lagerström and B.-A. Persson, *J. Chromatogr.*, 417 (1987) 357.
7 K. Schmid, in F. W. Putnam (Editor), *The Plasma Proteins,* Academic Press, New York, 1975, p. 184.
8 J. Hermansson, *J. Chromatogr.*, 269 (1983) 71.
9 J. Hermansson and G. Schill, in M. Zief and L. J. Crane (Editors), *Chromatographic Chiral Separation*, Marcel Dekker, New York, 1987, p. 245.
10 J. Hermansson and M. Eriksson, *J. Liq. Chromatogr.*, 9 (1986) 621.
11 J. Hermansson, K. Ström and R. Sandberg, *Chromatographia*, 24 (1987) 520.
12 G. Schill, I. W. Wainer and S. A. Barkan, *J. Chromatogr.*, 365 (1986) 73.
13 L. R. Snyder, in Cs. Horváth (Editor), *High-Performance Liquid Chromatography—Advances and Perspectives*, Vol. 1, Academic Press, New York, 1980, p. 207.
14 L. R. Snyder and M. A. Stadalius, in Cs. Horváth (Editor), *High-Performance Liquid Chromatography—Advances and Perspectives*, Vol. 4, Academic Press, New York, 1986, p. 195.

Journal of Chromatography, 477 (1989) 119–130
Elsevier Science Publishers B.V., Amsterdam — Printed in The Netherlands

CHROM. 21 411

QUANTITATIVE EXTRACTION OF THYMINE–THYMINE DIMER FROM A LARGE EXCESS OF THYMINE BY PREPARATIVE LIQUID CHROMATOGRAPHY

A. M. KATTI

University of Tennessee, Chemical Engineering Department, 575 Buehler Hall, Knoxville, TN 37996-1600 (U.S.A.); and Oak Ridge National Laboratory, Analytical Chemistry Division, Oak Ridge, TN 37831-6120 (U.S.A.)

R. RAMSEY

Oak Ridge National Laboratory, Analytical Chemistry Division, Oak Ridge, TN 37831-6120 (U.S.A.)

and

G. GUIOCHON*

University of Tennessee, Chemistry Department, Knoxville, TN 37996-1501 (U.S.A.); and Oak Ridge National Laboratory, Analytical Chemistry Division, Oak Ridge, TN 37831-6120 (U.S.A.)

SUMMARY

Extremely small amounts of thymine–thymine dimer can be extracted from thymine solutions using overloaded elution and shaving a narrow fraction at the front of the overloaded, later eluting thymine band. A two- or three-step procedure, involving the concentration and reinjection of the collected fraction, permits the preparation of solutions in which the ratio of the concentrations of the dimer and the monomer is close to unity compared with less than 1:25 000 in the original samples.

The theory of non-linear chromatography and the semi-ideal model permits the accurate prediction of the location of the trace component band and the determination of the appropriate time to start and stop collection of the enriched fraction.

INTRODUCTION

Exposure of deoxyribonucleic acids in living cells to ultraviolet radiation results in damaging structural alterations. The reported chemical lesions in the DNA material of some animal and plant systems include classes of pyrimidine cyclobutane dimers, pyrimidine hydrates, glycols, various addition products and some purine photoproducts[1]. The pyrimidine cyclobutane dimers (thymine–thymine, thymine–cytosine and cytosine–cytosine) are the most abundant, representing as much as 90% of the UV damage[1]. With physiologically significant exposures (*e.g.*, less than 10 J/m^2 at 254 nm), the concentration of these compounds is extremely low, of the order of 0.02% or less of the base concentration[2].

The accurate determination of these trace constituents requires adequate separation from the large amounts of the normal bases. A complete analytical procedure

0021-9673/89/$03.50

involves the quantitative extraction of the dimers from a mixture of regular bases, followed by derivatization of the dimers and their quantitative analysis by gas chromatography with electron-capture detection. This scheme makes possible the achievement of very low detection limits in spite of the small size of the samples available, which do not exceed 500 μg.

To aid in the selection of optimum conditions for the isolation and determination of trace amounts of thymine–thymine dimer, changes in the elution profile of this dimer on a high-performance liquid chromatographic (HPLC) column overloaded with thymine have been examined both experimentally and theoretically, using the semi-ideal model of non-linear chromatography described previously[3,4].

EXPERIMENTAL

Analyses were performed on a Waters liquid chromatographic system equipped with a Model 600E multi-solvent delivery system, a Model U6K injector and a Model 490 programmable multi-wavelength detector (Waters Chromatography Division, Millipore, Milford, MA, U.S.A.). Data were acquired at 210 and 300 nm by a Maxima 820 chromatography workstation (Dynamic Solutions, Millipore, Ventura, CA, U.S.A.).

The linear range of the UV detector used is not sufficient to permit detection of the monomer and the dimer simultaneously at the same wavelength, owing to the very low concentration of the latter in the samples. Accordingly, thymine–thymine dimer is monitored at 210 nm, because its response remains within the linear range of the detector, whereas thymine monomer is detected at 300 nm, where the absorbance is small enough to provide a linear response in the concentration range investigated. Two calibration graphs were determined.

An Alltech C_{18} HS (7 μm) column (250 mm $\times$ 4.6 mm I.D.) was used for the separations. High-purity water (Burdick & Jackson Labs., Muskegon, MI, U.S.A.), filtered through a 0.45-μm Nylon 66 membrane (Supelco, Bellefonte, PA, U.S.A.), was used for the mobile phase. Data were obtained at ambient temperature at a flow-rate of 1.0 ml/min.

Thymine was purchased from Sigma (St. Louis, MO, U.S.A.) and the *cis-syn*-5,6-thymine–thymine dimer was prepared by modifying the procedure of Wang[5], irradiating (at 254 nm) a frozen 0.1% aqueous solution of thymine. A white crystalline product was obtained and determined to be 99% pure dimer by HPLC. All standards were prepared in aqueous solution and calibration graphs were constructed from the peak heights at different concentrations.

The adsorption equilibrium isotherm of thymine in the chromatographic system used was measured by the method of elution by characteristic point (ECP)[6,7].

THEORETICAL

A semi-ideal model of chromatography was employed to model the separation of the thymine–thymine dimer from thymine. The mass balance equations for the ideal model were solved using numerical dispersion to account for the finite column efficiency[8].

The competitive Langmuir isotherm model was employed to relate the amount

adsorbed in the stationary phase at equilibrium to the concentration in the mobile phase. This isotherm provides a reasonable first approximation for most liquid–solid phase equilibria. The relationship giving the amount of component i sorbed at equilibrium with concentrations C_1 and C_2 of components 1 and 2, respectively, is

$$q_i = a_i C_i/(1 + b_1 C_1 + b_2 C_2) \quad (1)$$

Further simplifications to the competitive isotherm model were made in view of the nature of the problem. In this study, the concentration of the early eluting compound under the experimental conditions of interest, *i.e.*, the thymine–thymine dimer, is very low (between 1/1000 and 1/10 000). Hence the amount of sample injected is almost always insufficient for the dimer band to exhibit non-linear elution behavior. Therefore, it is not necessary to determine the coefficient b_1. As C_1 is very small, we can neglect the corresponding terms ($b_1 = 0$) and write as follows the competitive isotherm for the first component:

$$q_1 = a_1 C_1/(1 + b_2 C_2) \quad (2)$$

Similarly for the second component, the influence of such a small concentration of the dimer on the adsorption behavior of the monomer can be considered to be negligible, and therefore

$$q_2 = a_2 C_2/(1 + b_2 C_2) \quad (3)$$

Using these simplified isotherm models, the values of the coefficients a_i and b_i ($i = 1, 2$) are determined experimentally. From the retention time of a very small sample of thymine–thymine dimer, a_1 is determined, while a_2 and b_2 are derived from isotherm measurements made for thymine with the ECP method[4,6]. The isotherm data are then used to calculate the elution profiles of large samples of dilute solutions of thymine–thymine dimer in thymine.

RESULTS AND DISCUSSION

The elution chromatogram of a synthetic mixture of thymine monomer and thymine–thymine dimer is shown in Fig. 1. The retention time of the dimer is 1011 s and that of the monomer is 1101 s. The dead time, t_0, determined from the retention time of uracil is 195 s. The relative retention of the two components is 1.11, the resolution is 1.43 and the column efficiency is 5000 plates.

The adsorption equilibrium isotherm of thymine in the chromatographic system used was measured by the method of elution by characteristic point[6,7]. The data are reported in Fig. 2 by squares. The curvature of the isotherm is not very great within the range of concentrations in the mobile phase investigated, so the fit of the data on a Langmuir isotherm, as indicated by the solid line, is excellent.

The values of the coefficients obtained by a least-squares regression on eqn. 3 are $a_2 = 15.908$ ml/ml and $b_2 = 0.11774$ ml/mg. The coefficient a_1 is determined from the retention time of the pure dimer and is equal to 14.03 ml/ml.

Validity of the model

Knowing the adsorption isotherm, the porosity, the mobile phase velocity and

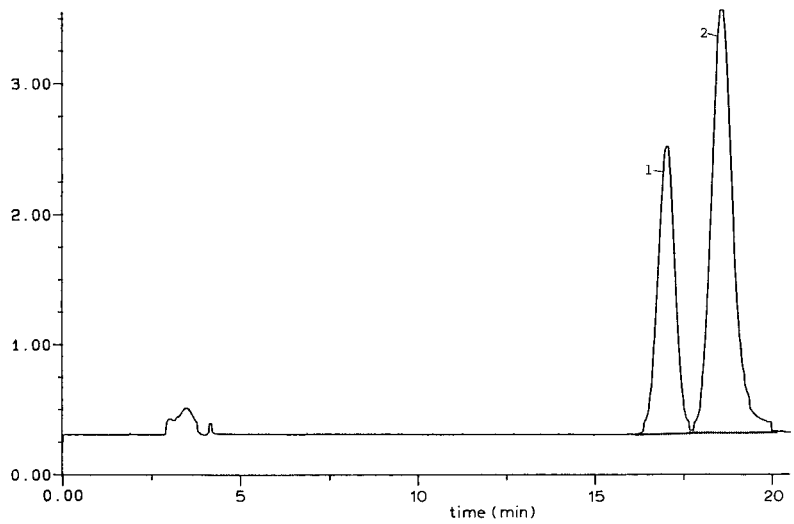

Fig. 1. Experimental chromatogram of a 1:1 mixture of thymine–thymine dimer (band 1) and thymine (band 2). Column, 250 mm × 4.6 mm I.D., packed with 7-μm C_{18} bonded-phase silica; mobile phase, distilled water; flow-rate, 1 ml/min; sample size, 1.1 μg of each component; UV detection at 210 nm. Ordinate, detector signal in arbitrary units.

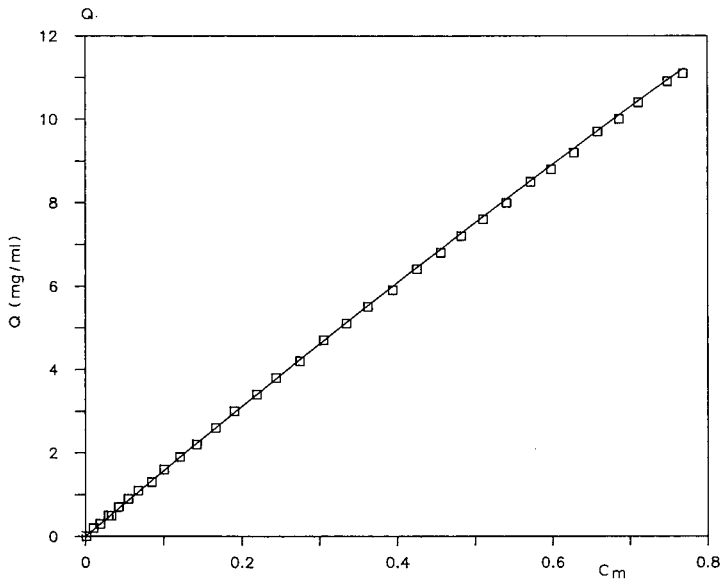

Fig. 2. Equilibrium isotherm of thymine obtained by the method of elution by characteristic point. Plot of the concentration of thymine adsorbed (Q) (mg/ml of column packing material) *versus* the concentration in the mobile phase at equilibrium (C_m) (mg/ml).

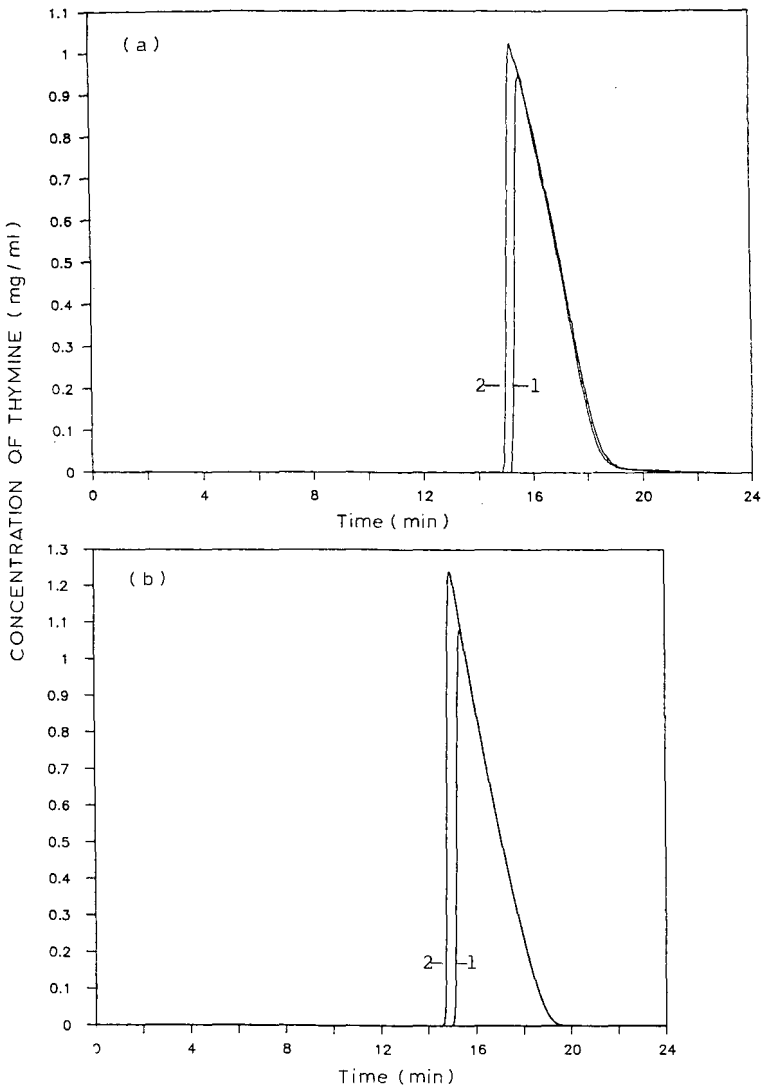

Fig. 3. Comparison between experimental and theoretical chromatograms. (a) Experimental chromatogram. Same conditions as in Fig. 1, except sample volume, (1) 1 ml and (2) 1.25 ml. Sample is a 2 mg/ml solution of thymine in water. (b) Predicted chromatograms based on the isotherm in Fig. 2, the measured efficiency and the sample size in (a).

the column dimensions, it is possible to make accurate predictions of the band profiles[3,4] of the thymine and the thymine–thymine dimer at different concentrations. Consider first the injection of a pure thymine solution at a concentration of 2 mg/ml. In Fig. 3a, curve 1 corresponds to a 1-ml injection and curve 2 to a 1.25-ml injection. The theoretically predicted profiles corresponding to the same experimental conditions are shown in Fig. 3b. They are in excellent agreement, except for a slight tail at the end of the elution band.

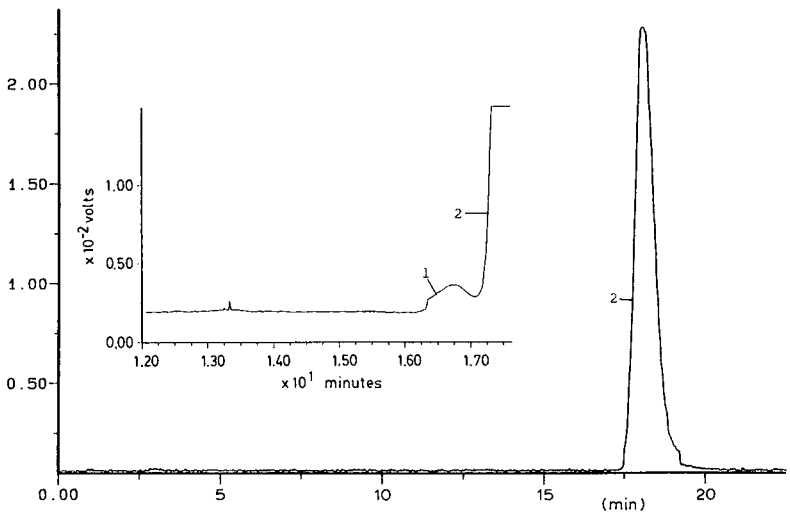

Fig. 4. Experimental chromatogram for a solution containing 82 ng of dimer (band 1) and 115 μg of thymine (band 2). The main figure shows the detector response at 300 nm (thymine) and the inset shows the detector response at 210 nm (dimer and thymine). Ordinates, detector response in volt.

This model also permits the prediction of the band profiles of binary mixtures. Fig. 4 shows an experimental uncalibrated band profile for a 1:1405 dimer–monomer mixture, recorded at 300 nm. The inset is an expansion of the dimer peak, recorded at 210 nm (see Experimental). Fig. 5 shows the predicted profile. The retention times of

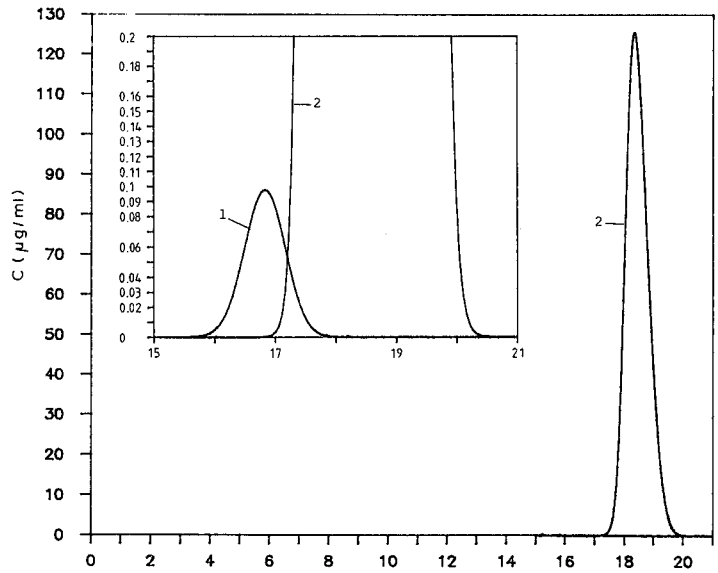

Fig. 5. Predicted chromatogram corresponding to the conditions in Fig. 4. The inset shows an expansion around the base of the thymine peak. 1, Elution profile of thymine; 2, elution profile of dimer. Ordinate: concentration (μg/ml); abscissa, time (min).

the peak maxima are the same for the theoretical and predicted profiles. Qualitatively, the peak shape of the experimental thymine band is very similar to the predicted band and the degree of resolution between the two bands is comparable. Similar results, not shown, were found for a 1:112 mixture.

Effect of sample size

The study of series of numerical solutions of the system of mass balance equations of the two compounds in the column (semi-ideal model[4]) allows the determination of the conditions of optimum operation. Fig. 6 shows the variation of the elution profile of 82 ng of dimer in samples containing increasing masses of thymine (0.082, 0.82, 2.0, 5.0 and 8.2 mg). This figure represents the calibrated detector response as if we were monitoring at a wavelength specific only to the dimer, totally excluding the thymine. Fig. 7 shows the elution profiles of thymine in the same samples, as if the calibrated detector response was now specific to thymine.

It can be seen from Figs. 6 and 7 that, on increasing the amount of thymine, the retention time of both compounds decreases and that the maximum concentration of the dimer band increases (Fig. 6). At the same time, the resolution between the two bands decreases. Eventually, at very large values of the sample size and/or at very low relative dimer concentrations, the small band of dimer is swallowed by the huge

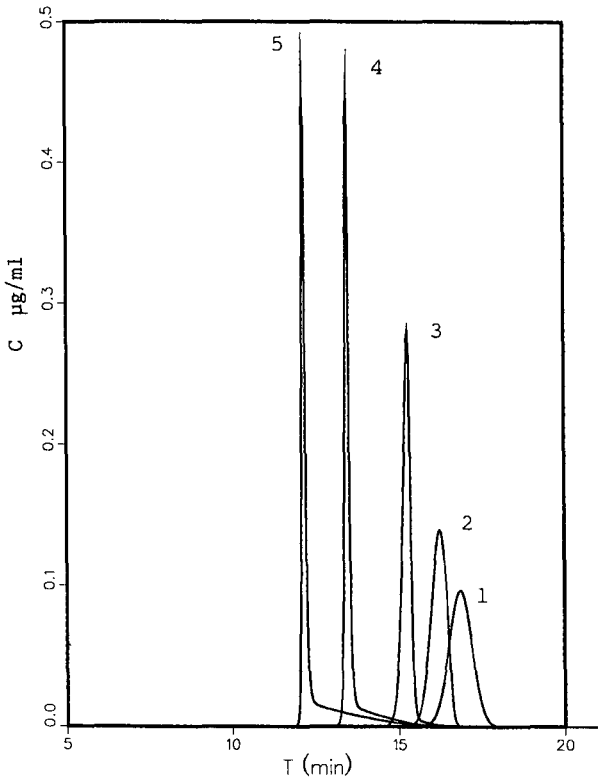

Fig. 6. Predicted dimer band profiles for samples containing 82 ng of the dimer in the presence of increasingly large amounts of thymine. Amount of thymine: 1, 0.082; 2, 0.82; 3, 2.5; 4, 5.0; 5, 8.2 mg.

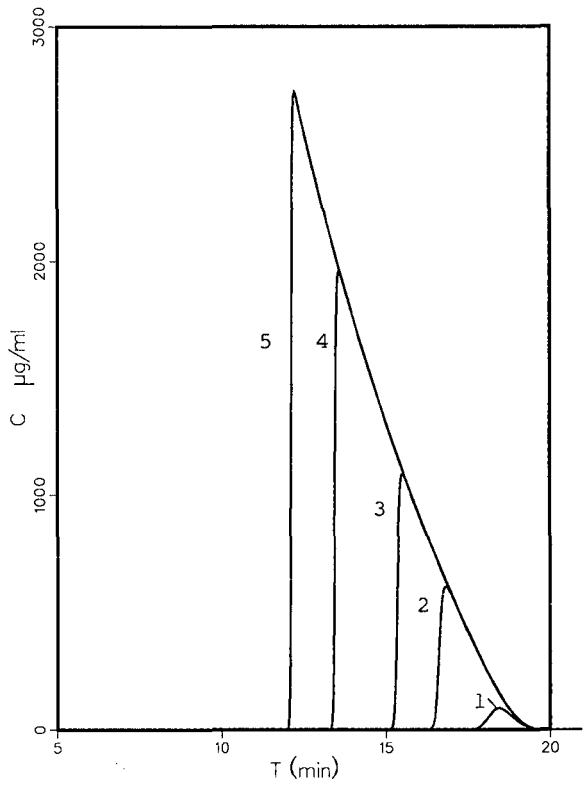

Fig. 7. Predicted thymine band profiles for samples containing increasingly large amounts of thymine in the presence of a constant amount (82 ng) of dimer. Amount of thymine: 1, 0.082; 2, 0.82; 3, 2.5; 4, 5.0; 5, 8.2 mg. Conditions as in Fig. 5.

monomer band (see Fig. 8). The same behavior is also seen when 8.2 or 0.82 ng of dimer is injected, only the maximum value of the ordinate is reduced to 0.05 and 0.005, respectively. The results in Fig. 6 are very important as they reveal a phenomenon often mentioned, but only casually, in the literature, regarding the displacement of the bands of minor or trace components by those of the main components when a column is overloaded.

The program also permits the determination of the optimum cutting time when the collection of the first band (the dimer) should be ended in order to achieve a recovery yield exceeding any given threshold. The lower the required value of the recovery yield, the larger is the proportion of the monomer that can be eliminated and the higher are the absolute and the relative concentrations of the dimer in the recovered fraction. Some typical results are given in Table I. A two-step collection scheme, with intermediate reinjection of the first collected fraction, has been attempted for very low values of the relative concentration of the dimer. The results are also given in Table I. All possible strategies of this sort could easily be simulated with the computer program, if needed, but our present needs were satisfied with the calculations just described.

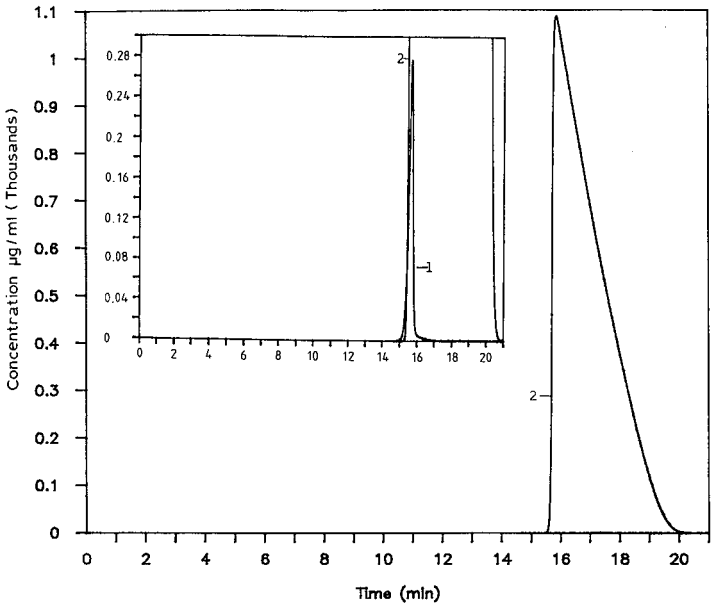

Fig. 8. Predicted band profiles for a sample of 82 ng of dimer (1) in the presence of 2 mg of thymine (2). The dimer band is shown in the inset. Conditions as in Fig. 5.

Enrichment simulation

The use of recycle techniques for the enrichment of traces of the dimer in the monomer was investigated numerically, which the program permits readily. The quantitative extraction of the dimer from 1:24 000 and 1:5000 (w/w) binary mixtures with the monomer was studied, using a sample containing 82 ng of dimer in the first instance and 400 ng of dimer in the second. This concentration range includes the estimate given above (0.02%) of the maximum concentration of structural alterations in DNA after physiologically significant radiation exposures[2].

TABLE I

ENRICHMENT BY RECYCLING

	Concentrations		
	Initial	*1st cycle*[a]	*2nd cycle*[a]
First case:			
Amount of dimer (ng)	82	78	74
Amount of thymine (mg)	2	0.13	$4.7 \cdot 10^{-5}$
Ratio (w/w)	1:24 300	1:1700	1:1.6
Second case:			
Amount of dimer (ng)	400	396	377.3
Amount of thymine (mg)	2	0.109	$3.45 \cdot 10^{-5}$
Ratio (w/w)	1:5000	1:290	10:1

[a] All yields are 95%.

Under these conditions the band is strongly overloaded, as can be observed in Fig. 8, showing the predicted elution bands for a 1:24 000 mixture containing 82 ng of dimer, and coelution of the two fronts takes place (see also Fig. 6, band 3). A fraction of the elution band was collected, so as to recover 95% of the early eluting component. This fraction contains a 1:1700 dimer–monomer mixture and its volume is between 1 and 2.5 ml, depending on the case. It was assumed that the volume of this fraction can be reduced to 100 μl and that it was reinjected, giving the chromatogram shown in Fig. 9. From this chromatogram, it was found that 95% of the dimer could be collected in a final fraction where it is considerably enriched to a ratio of 1:1.6.

A similar study was made with the 1:5000 mixture. After the first cycle, it was found that 95% of the early eluting compound could be recovered in a fraction containing a 1:287 (w/w) mixture. Note that substantial enrichment is obtained by accepting a slight decrease in yield. If a 99% yield was required, then only a 3-fold enrichment would occur, leaving a 1:1894 mixture. Subsequent reinjection of this first fraction led to a considerably enriched second fraction containing a 10:1 mixture.

Experimental study of enrichment

A comparison was made between the theoretical data in Figs. 8 and 9 and experimental results. Fig. 10 illustrates the elution chromatogram of 82 ng of dimer in the presence of 2 mg of thymine, monitored at 300 nm, with the experimental conditions as described above.

The retention times of the band front and of the rear boundary are in nearly quantitative agreement with Fig. 8. The slight difference in elution time is easily explained by the fact that the experiment was carried out several weeks after the

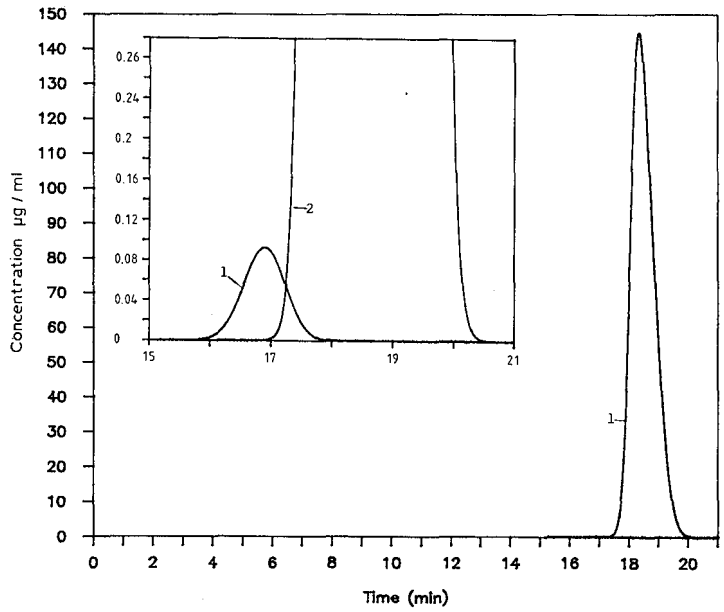

Fig. 9. Predicted band profiles for the first fraction collected (yield 95% for the dimer) for the chromatogram in Fig. 8. Conditions as in Fig. 5.

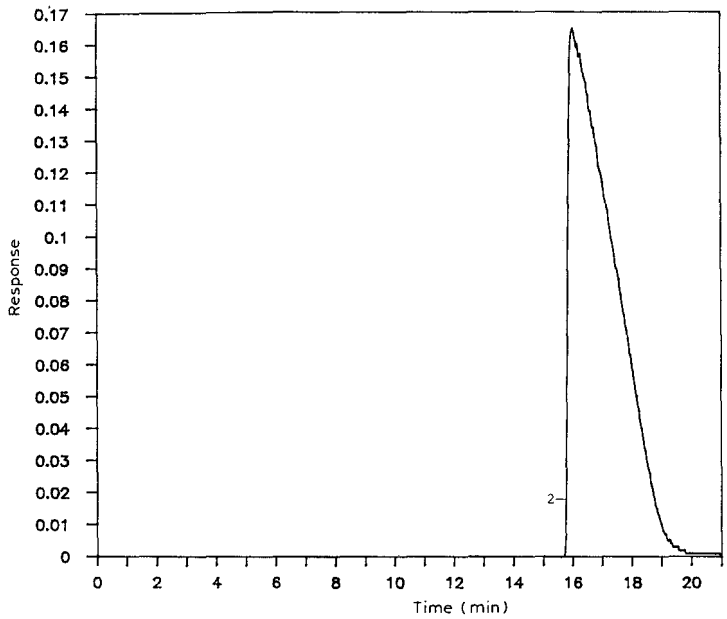

Fig. 10. Experimental band profile recorded with a UV detector at 300 nm for a sample of 82 ng of dimer in the presence of 2 mg of thymine. Only the thymine band (2) is visible. Experimental conditions as in Fig. 4.

determination of the isotherm. On collecting the eluate from 15.6 to 16.5 min, concentrating the fraction to 230 μl and reinjecting it under the same conditions, the chromatogram in Fig. 11 was recorded at 300 nm. The inset shows the chromatogram recorded with a detector setting at 210 nm.

The experimental chromatogram in Fig. 11 is in excellent agreement with the predicted result in Fig. 9. A good resolution is observed between the dimer and the thymine band, slightly better than predicted. The retention times of both bands are slightly shorter than predicted, which can be explained by the difficulty in reproducing the same flow-rate exactly. A more serious experimental problem prevents exact duplication of the conditions selected for the calculation runs, and also limits the reproducibility of these experimental results. The collection of fractions has to be made drop by drop, and the time when the last collected drop falls does not necessarily coincide with the optimum cutting time. As the amount of thymine recovered is very sensitive to the number of drops collected in the fraction, the composition of this fraction is different from that predicted. An experimental collection time slightly shorter than that used in the calculations explains the collection of smaller amounts of dimer and thymine, and hence a lower dimer yield and a better resolution between bands than predicted.

Hence overloaded elution permits the collection of highly enriched fractions of an impurity for their further quantitative analysis by other techniques that provide lower detection levels and better accuracy and precision, or possibly for investigation of their structure by sophisticated spectroscopic techniques, permitting the formal identification of molecules at extremely low sample sizes, but requiring pure samples.

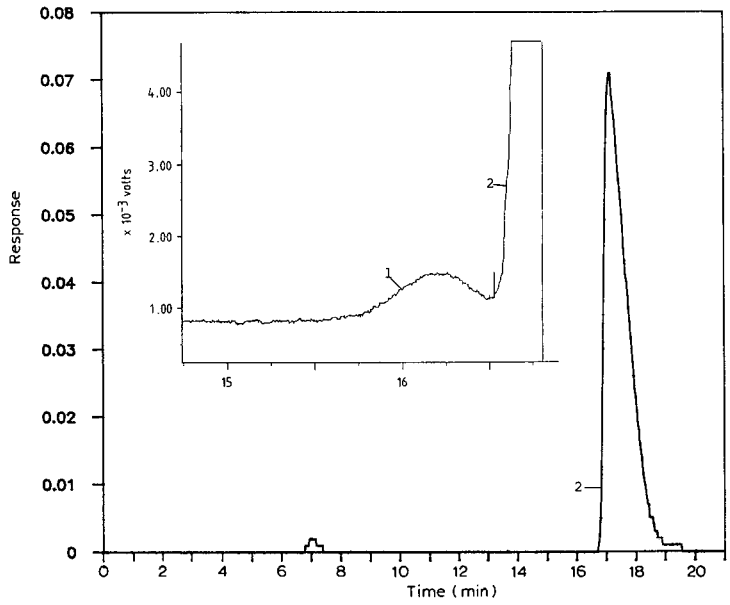

Fig. 11. Experimental band profiles for the first fraction collected during the analysis shown in Fig. 10. Main figure, UV detector signal set at 300 nm; inset, UV detector signal set at 210 nm. Experimental conditions as in Fig. 4.

The agreement between experimental results and the prediction of the semi-ideal model confirms the validity of the theory of non-linear chromatography previously developed[3,4].

ACKNOWLEDGEMENTS

This work was supported in part by Grant CHE-8519789 of the National Science Foundation and by the cooperative agreement between the University of Tennessee and the Oak Ridge National Laboratory, and was sponsored in part by the Office of Health and Environmental Research, U.S. Department of Energy, under contract DE-AC05-84OR21400 with Martin-Marietta Energy Systems, Inc.

We thank C.-H. Ho (Division of Analytical Chemistry, ORNL, Oak Ridge, TN) for synthesizing the pyrimidine dimer and Samir Ghodbane (Merck, Rahway, NJ) for fruitful discussions.

REFERENCES

1 M. H. Patrick and R. O. Rahn, in S. Y. Wang (Editor), *Photochemistry and Photobiology of Nucleic Acids, Vol. II, Biology*, Academic Press, New York, 1976, p. 184.
2 J. D. Love and E. C. Friedburg, *J. Chromatogr.*, 240 (1982) 475.
3 G. Guiochon, S. Golshan-Shirazi and A. Jaulmes, *Anal. Chem.*, 60 (1988) 1856.
4 G. Guiochon and S. Ghodbane, *J. Phys. Chem.*, 92 (1988) 3682.
5 S. Y. Wang, *Nature (London)*, 190 (1961) 690.
6 E. Cremer and J. F. K. Huber, *Angew. Chem.*, 73 (1961) 461.
7 S. Golshan-Shirazi, S. Ghodbane and G. Guiochon, *Anal. Chem.*, 60 (1988) 3630.
8 B. Lin and G. Guiochon, *Sep. Sci. Technol.*, 24 (1988) 31.

Journal of Chromatography, 477 (1989) 131–137
Elsevier Science Publishers B.V., Amsterdam — Printed in The Netherlands

CHROM. 21 589

LIMITATIONS OF HIGH-SPEED REVERSED-PHASE HIGH-PERFORMANCE LIQUID CHROMATOGRAPHY OBSERVED WITH INTEGRAL MEMBRANE PROTEINS

M. KEHL and F. LOTTSPEICH*
Max Planck Institut für Biochemie, Genzentrum, D-8033 Martinsried/Münich (F.R.G.)

SUMMARY

The use of high-speed reversed-phase high-performance liquid chromatography was evaluated for membrane proteins. Using the photosynthetic reaction centre of *Chromatium tepidum* as a model, parameters such as flow-rate, gradient steepness and contact time of the proteins with the stationary phase were investigated. The results demonstrate that for optimum recovery and resolution, the gradients applied should not be too steep and that very long gradient times may cause protein loss.

INTRODUCTION

In recent years, reversed-phase (RP) high-performance liquid chromatography (HPLC) has been established as an indispensible tool for separation of peptides and soluble proteins. However, today the RP-HPLC of very hydrophobic peptides and membrane proteins is still an extreme technical challenge. Because of solubility problems and the close hydrophobic interaction of these substances with reversed stationary phases, unacceptably low mass recoveries are often obtained. Membrane proteins are often insoluble in common solvents and require detergents with or without high salt concentrations to keep them in solution. Therefore, only a limited number of successful separations by RP-HPLC have been reported[1–18]. Mostly mobile phases containing strong acids of various concentrations were used with organic modifiers such as acetonitrile, ethanol, 2-propanol, butanol or mixtures of various organic compounds.

Recently, high-speed HPLC using high flow-rates, elevated temperatures and short columns was introduced[19]. The efficiency of the columns is based on specially designed micropellicular sorbents exhibiting favourable mass transfer characteristics and the fast diffusion rates and sorption kinetics at elevated temperatures. So far, these commercially available, specialized columns have proved well suited to the RP-HPLC of hydrophilic proteins and peptides but, in general, are too hydrophobic for application to integral membrane proteins. However, short columns packed with the stationary phases commonly used in protein chemistry can also be operated in a high-speed mode with ordinary modern HPLC equipment.

In this work, the influence of the contact time of the proteins with the stationary

0021-9673/89/$03.50

phase, the flow-rate and gradient steepness on the recovery and separation of integral membrane proteins using high-speed RP-HPLC was investigated. A partially purified reaction centre of the thermophilic photosynthetic purple bacterium *Chromatium tepidum* was used as a model system of integral membrane proteins[20]. This reaction centre is composed of four polypeptides, termed L (25 kDa), M (30 kDa), H (34 kDa) and cytochrome *c* subunit (44 kDa). It is structurally similar to the reaction centre of *Rhodopseudomonas viridis,* in which the subunits H, L and M are integral membrane proteins with several membrane spanning helices and the cytochrome subunit is a membrane-associated protein due to covalently bound fatty acids[21–23].

EXPERIMENTAL

The reaction centre of *C. tepidum* was kindly provided by Dr. R. Nozawa (Chemical Research Institute of Non-aqueous Solutions, Tohoku University, Sendai, Japan). The sample contained about 2.7 mg/ml of reaction centre in 20 m*M* Tris (pH 8.5), containing at least 0.05% (w/v) of lauryl-N,N-dimethylamine N-oxide (LDAO) and sodium chloride.

Chromatography was performed using an HP 1090 HPLC system (Hewlett-Packard, Waldbronn, F.R.G.) equipped with an HP 1040 diode-array detector and an autosampler.

An Aquapore RP-300 reversed-phase column (30 × 2.1 mm I.D.) (Applied Biosystems, Weiterstadt, F.R.G.), was used for the separations. The injection volume was 5 μl, which corresponded to approximately 12 μg of protein.

Gradient elution was performed using as solvent A 0.1% trifluoroacetic acid (HPLC/Spectro grade, Sequenal quality; Pierce, Rockford, IL, U.S.A.) in water and as buffer B 0.1% trifluoroacetic acid in acetonitrile (LiChrosolv, gradient grade; Merck, Darmstadt, F.R.G.). In all experiments a gradient from 5 to 95% of solvent B in solvent A was applied. The gradient time and flow-rate were changed in the different experiments. The oven temperature was kept at 50°C. Routinely after each separation two blank runs were done. The chromatograms were monitored at 206 nm, and the fractions were collected manually in Eppendorf vials. Fractions were further analysed by sodium dodecyl sulphate polyacrylamide gel electrophoresis (SDS-PAGE) (Minigel system; Biometra, Göttingen, F.R.G.) using standard conditions as described by Laemmli[24].

RESULTS AND DISCUSSION

The aim of this investigation was the evaluation of the use of high-speed RP-HPLC for the separation of integral membrane proteins. This separation is usually difficult because these proteins have many hydrophobic amino acid residues which interact with the hydrophobic stationary phase ligands, resulting in a requirement for high concentrations of organic solvent to elute the proteins. Usually membrane proteins can only be kept in solution in the presence of detergents. During chromatography when the detergents are separated from the protein, the proteins may precipitate on the column. An additional problem is that the detergents themselves may interact with the reversed-phase material and modify its surface, consequently changing the selectivities and causing irreproducible results.

For this work, the photosynthetic reaction centre of *C. tepidum* was chosen as a model protein system. The four subunits differ in size and hydrophobicity, allowing one to evaluate changes in the resolution and recovery of different integral membrane proteins. The reaction centre is structurally similar to that of *R. viridis*, and conclusions relating to hydrophobicity can be drawn from our previous experience with the structural studies on this complex molecule. In addition to this current work, the samples from this study will be further used for the structural analysis of the reaction centre of *C. tepidum*. Therefore, a volatile solvent system was chosen that allowed the samples to be applied directly to amino acid composition analysis and amino acid sequence analysis (data not shown). The amount of available starting material was approximately 3 mg. Owing to the limited amount of starting material and the further structural analyses, UV detection of the fractions was performed at 206 nm with high sensitivity using the trifluoroacetic acid–acetonitrile solvent system. This solvent system additionally leaves the samples better suited for analysis by SDS-PAGE than systems containing formic acid, where removal of the acid is difficult.

In preliminary experiments, several column materials, previously used for successful separations of hydrophilic proteins, were examined for the recovery of the L and M subunits of the reaction centre of *R. viridis* as tested by UV absorption and SDS-PAGE. Aquapore RP-300 (30 × 2.1 mm I.D.) (Molnar, Berlin, F.R.G.), TSK-C_{18}-NPR (35 × 4.6 mm I.D.) (Hewlett-Packard), Vydac C_4 and Vydac C_8 (25 × 4 mm I.D.) (Chrompack, Müllheim, F.R.G.) were all tested. Even though the separation and recovery of the more hydrophilic subunits (H and cytochrome subunits) of the reaction centre were the same with all the columns (data not shown), the recovery of the more hydrophobic subunits L and M was best with the Aquapore RP-300 column. This column was, therefore, chosen for the remainder of the investigations.

Fig. 1. shows different chromatographic conditions that were used for the evaluation of the influence of flow-rate, gradient steepness and contact time of the proteins with the stationary phase. Increasing gradient steepness is indicated by increasing shading of the circle. The chromatograms described by the horizontal lines represent a constant gradient time with different flow-rates which represent the different gradient steepness. The chromatograms with identically shaded circles represent

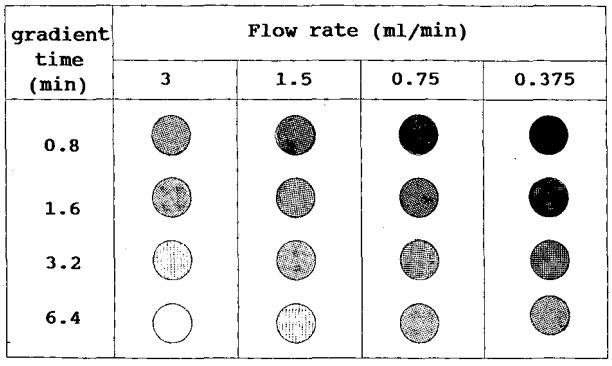

Fig. 1. Conditions used for high-speed RP-HPLC of the reaction centre of *C. tepidum*. Increasing shading of the circles corresponds to increasing gradient steepness.

separations using the same gradient. These were obtained by maintaining a constant gradient volume with changes in the gradient times and flow-rates. The vertical columns indicate chromatograms where the flow-rate was kept constant but the gradient time was changed, leading to different gradient shapes and different contact time of the proteins on the column.

In Fig. 2 a set of original experimental chromatograms are shown. In this instance a constant gradient time of 1.6 min was used, which corresponds to the conditions and results indicated in the second horizontal line of Fig. 1. The HPLC fractions were further analysed by SDS-PAGE. As an example, the results for the SDS gel corresponding to the uppermost chromatogram are shown in the lower right corner of Fig. 2. In the first fraction small amounts of hydrophilic proteins unrelated to the reaction centre were seen. The H subunit (34 kDa) was mostly found in fraction 2, but in fraction 3 a small amount of both H and cytochrome subunit were detected. The cytochrome subunit (44 kDa) was mostly found in fraction 4. Fraction 5 contained a mixture of subunits L and M (25 and 31 kDa, respectively). Both hydrophobic subunits (L and M) could be seen only as faint bands. Both of these subunits are difficult to analyse by SDS-PAGE owing to aggregation or precipitation of the proteins on top of the gel. This behaviour is generally observed in electrophoresis of membrane proteins (*e.g.*, reaction centre starting material, Fig. 2, lane RC). In the chromatograms using the steepest gradient conditions in the SDS gels only the two less hydrophobic subunits could be detected. The resolution using different chromatographic conditions resulting in high recovery was not significantly altered as evaluated by SDS-PAGE. However, it is obvious that both the resolution and the mass recovery are drastically diminished with the steepest gradient at the lowest flow-rate.

A comprehensive graphical presentation of the data obtained is shown in Fig. 3. At short gradient times a decrease in the recoveries of the proteins was observed. This may be caused either by the influence of the flow-rate or by the low gradient volume which corresponds to a very steep gradient.

The lowest flow-rate tended to give slightly lower recoveries when the chromatograms exhibiting the same gradient steepness were compared (similar shaded circles seen in the diagonals in Fig. 1). The conditions for these chromatograms are, for example, a gradient time of 1.6 min at a flow-rate of 0.375 ml/min and a gradient time of 0.8 min at a flow-rate 0.75 ml/min. However, the effect of flow-rate was not pronounced and may actually be caused by the longer contact time of the protein with the stationary phase.

The change in the gradient steepness had a drastic effect on the recoveries. Very clearly, a gradient volume that was too small (*i.e.*, a gradient which was too steep) caused severe protein loss, as seen in Fig. 3. However, if the gradient volume exceeded 1.2 ml this loss became negligible. With very small gradient volumes the change in the organic modifier content in the mobile phase was probably too rapid to allow the protein to migrate through the whole column. For proteins the graph of log k' *versus* percentage of organic modifier follows a steep parabolic curve[25]. Increasing the organic solvent concentration will cause only a slow migration of the protein along the column, or it will stick to the top of the column. As the organic solvent concentration is increased there is a small concentration window in which the protein will migrate efficiently. If the organic solvent concentration is increased further, the proteins will again be strongly retarded.

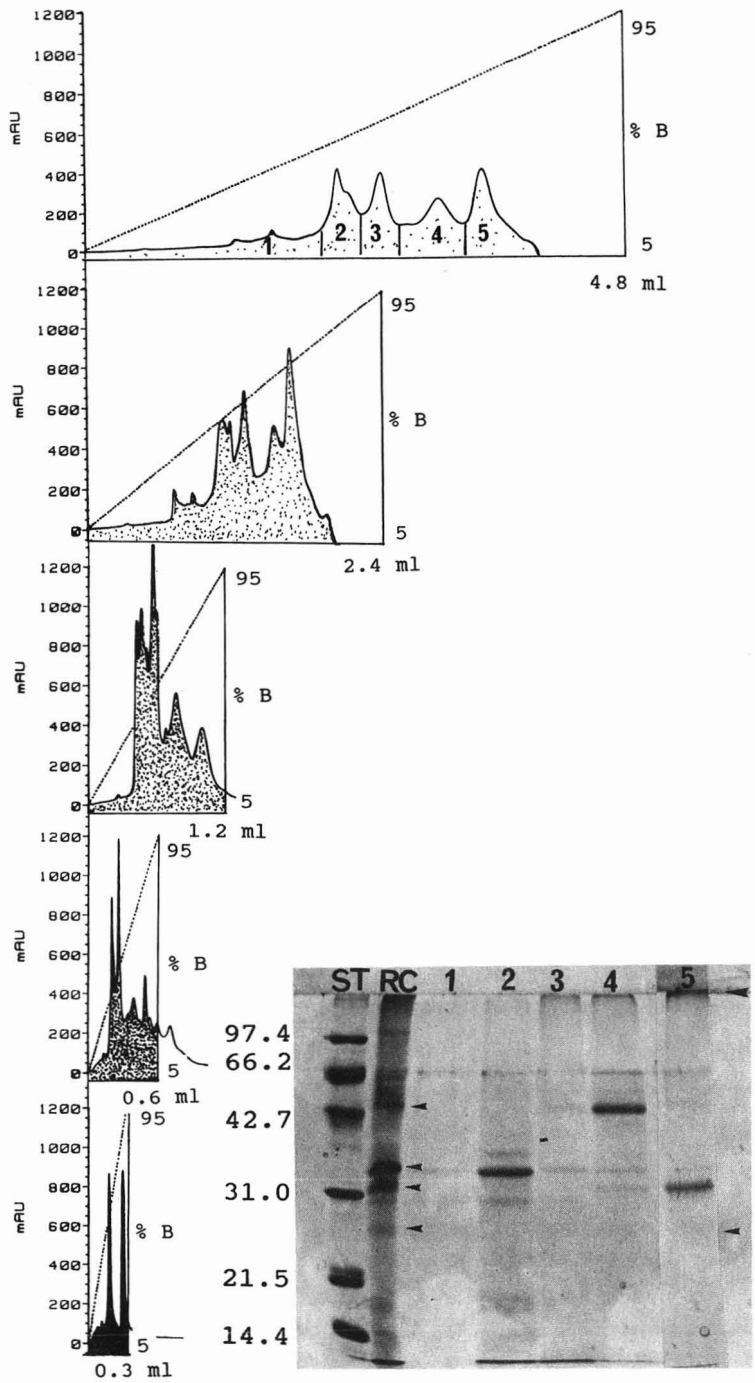

Fig. 2. Set of chromatograms using a constant gradient time of 1.6 min and flow-rates of 3, 1.5, 0.75, 0.375 and 0.187 ml/min (from top to bottom). For other conditions, see Experimental. In the right lower corner the Commassie Brilliant Blue-stained, SDS polyacrylamide gel of the fractions obtained from the top chromatogram is shown. RC, reaction centre; ST, reference proteins; molecular masses are given in kDa. The arrows indicate the main components of the RC, cytochrome *c* (44 kDa), H (34 kDa), M (30 kDa), L (25 kDa), and the protein precipitation on the top of the gel.

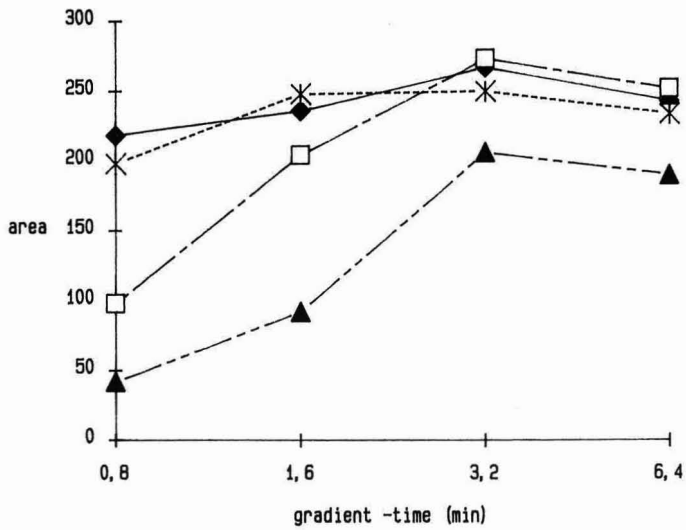

Fig. 3. Graphical presentation of the protein recovery obtained with various flow-rates (◆, 3; ∗, 1.5; □, 0.75; ▲, 0.375 ml/min) at different gradient times. Chromatographic conditions as given in Fig. 1 and Experimental.

There is a tendency for proteins with longer contact time with the stationary phase to elute with lower recoveries. This can been seen in Fig. 3, where there is a slight decrease in the recoveries at the longest gradient times. This observation was also previously made for other proteins[26]. However, all the chromatograms shown here were obtained in a high-speed mode and used a short gradient time to see a more marked effect of analysis time on recovery. Hence the influence of the contact time of membrane proteins with the stationary phase should be analysed in more detail using longer gradient times.

Exact quantification of the proteins recovered was difficult. The starting material was not pure, and some UV-absorbing byproducts interfered with quantification. The reaction centre complex is difficult to solubilize for application on to a SDS polyacrylamide gel, and the fractions collected after chromatography are more difficult to solubilize because they had to be dried for removal of the acid. Additionally, the hydrophobic subunits, L and M, precipitated, to a large extent, on top of the gel. Nevertheless, an approximate recovery of 50–80% of the total protein could be obtained under optimum conditions (see Fig. 3).

In conclusion, we feel that there is a clear optimum for resolution and recovery in the high-speed RP-HPLC of integral membrane proteins. The gradients should not be too steep and the gradient volume should exceed 1 ml. This is also advantageous for the resolution and circumvents the problems connected with the collection of small fractions. Very low flow-rates should be avoided and long gradient times may cause protein loss owing to irreversible binding of these hydrophobic proteins on to the column.

REFERENCES

1 G. W. Welling, R. van der Zee and S. Welling-Wester, *J. Chromatogr.*, 418 (1987) 223.
2 F. E. Regnier, *J. Chromatogr.*, 418 (1987) 115.
3 H. G. Khorana, G. E. Gerber, W. C. Herlihy, R. J. Anderegg, C. P. Gray, K. Nihei and K. Biemann, *Proc. Natl. Acad. Sci. U.S.A.*, 76 (1979) 5046.
4 Y. Takagaki, G. E. Gerber, K. Nihei and H. G. Khorana, *J. Biol. Chem.*, 255 (1980) 1536.
5 J. Heukeshoven and R. Dernick, *J. Chromatogr.*, 252 (1982) 241.
6 J. Heukeshoven and R. Dernick, *J. Chromatogr.*, 326 (1985) 91.
7 G. W. Welling, G. Groen, K. Slopsema and S. Welling-Wester, *J. Chromatogr.*, 326 (1985) 176.
8 R. van der Zee, S. Welling-Wester and G. W. Welling, *J. Chromatogr.*, 266 (1983) 577.
9 S. D. Power, M. A. Locherie and R. O. Poyton, *J. Chromatogr.*, 266 (1983) 585.
10 N. E. Tandy, R. A. Dilley and F. E. Regnier, *J. Chromatogr.*, 266 (1983) 599.
11 G. Winkler, F. X. Heinz, F. Guirakhoo and C. Kunz, *J. Chromatogr.*, 326 (1985) 113.
12 L. E. Henderson, R. Sowder, T. D. Copeland, G. Smythers and S. Oroszlan, *J. Virol.*, 52 (1984) 492.
13 G. E. Tarr and J. W. Crabb, *Anal. Biochem.*, 131 (1983) 99.
14 J. P. Chang, W. R. Melander and Cs. Horváth, *J. Chromatogr.*, 318 (1985) 11.
15 B. G. Sharifi, C. C. Bascom, V. K. Khurana and T. C. Johnson, *J. Chromatogr.*, 324 (1985) 173.
16 H. D. Kratzin, T. Kruse, F. Maywald, F. P. Thinnes, H. Götz, G. Egert, E. Pauly, J. Friedrich, C. Y. Yang, P. Wernet and N. Hilschmann, *J. Chromatogr.*, 297 (1984) 1.
17 Y. Kato, T. Kitamura, K. Nakamura, A. Mitsui, Y. Yamasaki and T. Hashimoto, *J. Chromatogr.*, 391 (1987) 395.
18 K. R. Brunden, C. T. Berg and J. F. Poduslo, *Anal. Biochem.*, 164 (1987) 474.
19 K. Kalghatgi and Cs. Horváth, *J. Chromatogr.*, 398 (1987) 335.
20 T. Nozawa, J. T. Trost, T. Fukada, M. Hatano, J. D. McManus and R. E. Blankenship, *Biochim. Biophys. Acta*, 894 (1987) 468.
21 H. Michel, K. A. Weyer, H. Gruenberg and F. Lottspeich, *EMBO J.*, 4 (1985) 1667.
22 H. Michel, K. A. Weyer, H. Gruenberg, I. Dunger, D. Oesterhelt and F. Lottspeich, *EMBO J.*, 5 (1986) 1149.
23 K. A. Weyer, W. Schäfer, F. Lottspeich and H. Michel, *Biochemistry*, 26 (1987) 1909.
24 U. K. Laemmli, *Nature (London)*, 227 (1970) 680.
25 B. Grego and M. T. W. Hearn, *Chromatographia*, 14 (1981) 498.
26 M. J. O'Hare, M. W. Capp, E. C. Nice, N. H. C. Cooke and B. G. Archer, *Anal. Biochem.*, 126 (1982) 17.

Journal of Chromatography, 477 (1989) 139–145
Elsevier Science Publishers B.V., Amsterdam — Printed in The Netherlands

CHROM. 21 598

DETERMINATION OF THE ENHANCEMENT OF THE ENANTIOMERIC PURITY DURING RECRYSTALLIZATION OF AMINO ACIDS

B. KOPPENHOEFER, V. MUSCHALEK, M. HUMMEL and E. BAYER*
Institut für Organische Chemie der Universität, Auf der Morgenstelle 18, D-7400 Tübingen (F.R.G.)

SUMMARY

The enantiomeric purity of commercially available amino acids has been determined down to 0.01% before and after recrystallization. The amino acids have been transformed smoothly into the volatile N-trifluoroacetyl amino acid methyl esters, and were investigated by gas chromatography on the chiral stationary phase Chirasil-Val.

INTRODUCTION

The determination of the stereochemical integrity of chiral compounds is a major analytical task for both synthetic organic chemistry and life science. Among different spectroscopic and chromatographic techniques[1,2], gas chromatography (GC) on chiral stationary phases[3–7] such as L or D-Chirasil-Val[8,9] is the most promising approach for the determination of exceedingly high enantiomeric purities[9,10].

In order to calculate the degree of inversion in diazotization reactions of amino acids, the enantiomeric purity of both the starting material and the final product has been determined[11–13]. In peptide synthesis, the degree of racemization has been estimated after hydrolysis[14,15]. However, the enantiomeric purity of the starting amino acids, a well as of any derivatives prepared thereof, is still a matter of debate. In the present study, we report on the enantiomeric purity of several batches of amino acids from commercial sources, and on the further enrichment of the major enantiomer by a simple recrystallization procedure.

EXPERIMENTAL

Materials

L-Amino acids were kindly provided by Merck (Darmstadt, F.R.G.), Fährhaus Pharma (Hamburg, F.R.G.) and Ajinomoto (Tokyo, Japan), D-amino acids by Degussa (Hanau, F.R.G.). L-Serine was obtained from Medac (Hamburg, F.R.G.).

Recrystallization of the amino acids

Typically, a sample of 100 g of the amino acid was dissolved partially in water and then stirred under reflux. Within 5 h, water was added until the amino acid was

0021-9673/89/$03.50

completely dissolved. The solution was allowed to cool to ambient temperature and was then kept at 4°C for several hours. The crystals of the amino acid were filtered off, rinsed with small portions of water and dried carefully.

Alternatively, procedure[16], using water–ethanol (9:1, v/v) as the solvent was employed. Thus, the amino acid was dissolved in water at 50°C, the necessary volume of ethanol was added, the solution was allowed to cool to ambient temperature and was then kept at 4°C for several hours. The crystals were rinsed carefully with water and dried.

Standard procedure for the derivatization of amino acids

A sample of the recrystallized amino acid was dissolved in a solution of hydrogen chloride in methanol, prepared by mixing acetyl chloride and methanol, 1:10 (v/v). A 0.5-ml volume of the reagent was used per derivatization reaction, carried out in a 1-ml Reactivial (Macherey-Nagel, Düren, F.R.G.) and heated for 10 min at 110°C. The solvent was removed completely in a stream of dry nitrogen. The residue was allowed to react with trifluoroacetic anhydride (100 μl) in dichloromethane (500 μl) for 10 min at 110°C. The reagent was carefully evaporated in a stream of dry nitrogen, in order completely to remove the by-product trifluoroacetic acid. The derivative should cover the surface of the Reactivial as a thin film. Eventually, the residue was dissolved in 0.1–0.5 ml dichloromethane.

Gas chromatography

GC was performed with a Carlo Erba Fractovap 2102 or 2150, equipped with a laboratory computer Trivector Trilab II. Fused-silica capillary columns (25 m × 0.3 mm) were coated with Chirasil-Val, as described[17].

RESULTS AND DISCUSSION

While many racemic compounds form a conglomerate, *i.e.*, a mixture of crystals containing either one of the enantiomers, mixed crystals are often encountered[18]. In preparative organic chemistry the enhancement of the enantiomeric excess (e.e.) of enantiomerically enriched mixtures by the formation and recrystallization of a suitable derivative is a technique often applied, and occasionally well documented, *e.g.*, via the calorimetrically determined melting curve or by NMR spectroscopy after diastereomer formation[19].

When we started to monitor by GC the enantiomeric enrichment of amino acids during recrystallization our attention was primarily focused on alanine, for various reasons. First, the trifluoroacetyl derivative N-TFA-Ala-OCH_3 is formed in a smooth and rapid reaction sequence. Secondly, the chromatographic properties on Chirasil-Val are particularly well suited. The capacity factors k', are small, and the resolution factor, α, is fairly high, thus enabling rapid and accurate analysis of the enantiomeric composition. Last not least, some physical properties of particular interest are documented in the literature. While the solubilities of one antipode and the racemate in water differ only slightly, dependent on the temperature[20], as shown in Fig. 1, there are pronounced differences in the crystalline state[21,22]. In the L-form, a particular molecule, depicted by solid lines in Fig. 2a, is obviously surrounded by molecules with L-configuration, only. In the DL-form, the environment of a particular molecule with

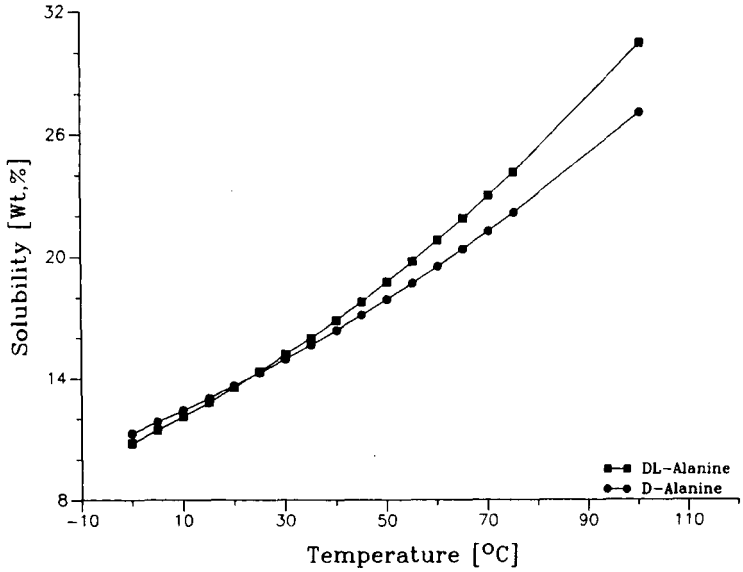

Fig. 1. Solubility of D-alanine and DL-alanine in water as a function of temperature. Values taken from ref. 20.

L-configuration, depicted by solid lines in Fig. 2b, is composed of L- (shaded) and D-stereoisomers. The intermolecular interactions differ accordingly, which is also seen in the hydrogen bonding network. With respect to the recrystallization of L-alanine containing only traces of the D-antipode, Fig. 2a is more relevant. The question is to what extent a molecule with L-configuration can be erroneously replaced by one with D-configuration, apart from the possibility of non-stereospecific growth on a particular face of the crystal[23].

Therefore, the alanine crystals were washed thoroughly with water. The derivatization to N-TFA-Ala-OCH_3 was performed under standard conditions, *i.e.*, esterification with HCl in methanol at 110°C for 10 min, and amide formation with trifluoroacetic anhydride in dichloromethane at 110°C for 10 min. It has been shown that racemization is only significant at higher temperatures[24].

Samples containing the L-antipode in excess were measured on capillaries coated with L-Chirasil-Val, and samples with D in excess on D-Chirasil-Val, in order to make sure that the minor peak is eluted in front of the major one[9]. The data obtained for L- and D-alanine are compiled in Table I. The relative standard deviation was less than 10% of the percentage of the minor enantiomer. The data for D-alanine deserve a comment. In order to circumvent the variability in the enantiomeric purities of different crystals, an average value was determined. Thus, the original crystals were dissolved completely, an aliquot of the solution was taken and dried in a stream of nitrogen, prior to derivatization. The same procedure was followed for crystal fractions 1 and 2. The enhancement in e.e. during recrystallization is evident. The values are found to vary slightly from one crystal to another, and even a lowering in e.e. was observed in the third recrystallization step when looking at one of the crystals. Hence

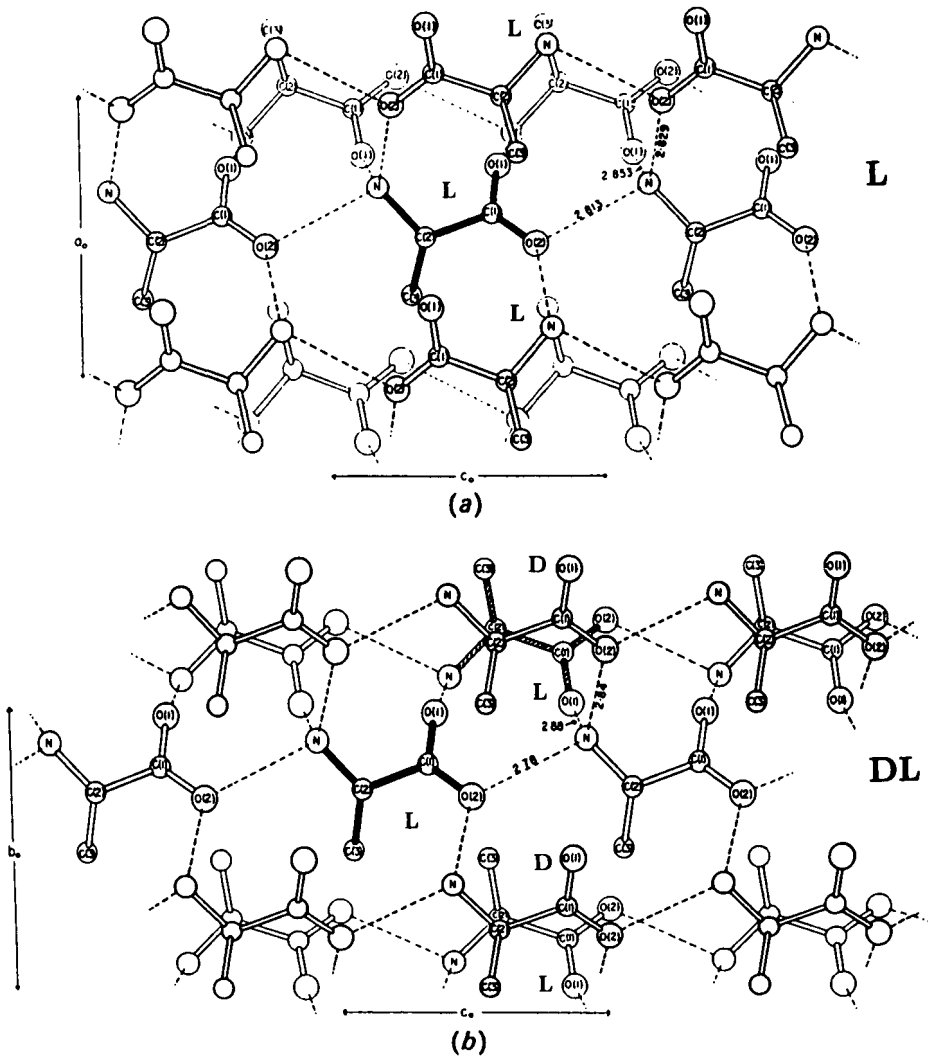

Fig. 2. (a) The crystal structure of L-alanine[21] viewed down the *b* axis. (b) The structure of DL-alanine[22] viewed down the *a* axis.

it is highly recommended that any studies on the enantiomeric purity of solid compounds be performed on an aliquot of the completely dissolved material. The chromatograms for D-alanine are shown in Fig. 3.

Rechromatography of the sampled rough data, followed by checking the y-expanded chromatograms on the screen of the laboratory computer Trilab II, proved to be a useful technique to get reliable data. Where the integrating program could not cope satisfactorily with the rough data, the chromatograms were plotted twice, using different y-factors, and xeroxed three-fold. The peaks were cut and weighed.

Typical average values for some amino acids are listed in Table II, before and

TABLE I

ENANTIOMERIC PURITIES (e.e.) OF ALANINE BEFORE AND AFTER RECRYSTALLIZATION FROM WATER, AS DETERMINED BY GC OF N-TFA-ALA-OCH_3 ON CAPILLARY COLUMNS COATED WITH L- AND D-CHIRASIL-VAL, RESPECTIVELY

Sample	*% of minor antipode before and after recrystallization*	*% e.e.*
L-Ala	0.23	99.54
L-Ala 1st crystals	0.022	99.956
L-Ala 2nd crystals	0.019	99.962
D-Ala	1.75	96.50
D-Ala 1st crystals	0.098	99.804
D-Ala 2nd crystals	0.039	99.922
D-Ala 3rd crystals	0.066	99.868

after recrystallization. The relative standard deviation was less than 10% of the percentage of the minor enantiomer. In all cases investigated, a significant enhancement in e.e. was observed. A chromatogram for one of the recrystallized samples of methionine is shown in Fig. 4.

It is interesting that a commercial sample of L-serine contained an unacceptable high percentage of the D-antipode, *i.e.*, more than 1.2. One should be aware of the fact that all commercial compounds are crystalline samples, in other words, they had already undergone at least one recrystallization step. The surprisingly low e.e. value

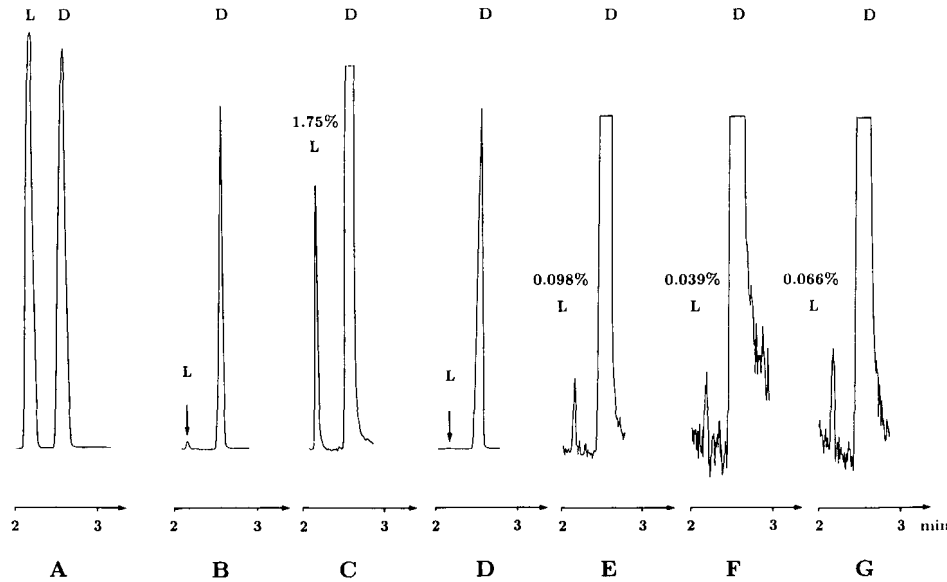

Fig. 3. Enantiomeric purity of alanine, determined N-TFA-Ala-OCH_3 on D-Chirasil-Val (H41, fused-silica capillary column, 25 m × 0.3 mm) at 70°C, 0.4 bar H_2, flame ionization detection (FID). (A) racemic alanine; (B) commercial sample of D-alanine, in scale; (C) expanded; (D) crystals from recrystallization 1; (E) expanded; (F) crystals from recrystallization 2; (G) one crystal from recrystallization 3.

TABLE II

ENANTIOMERIC PURITIES (e.e.) OF L-AMINO ACIDS BEFORE AND AFTER RECRYSTALLIZATION FROM ETHANOL–WATER (1:9), AS DETERMINED BY GC ON A CAPILLARY COLUMN COATED WITH L-CHIRASIL-VAL

Amino acid	*%D before and after recrystallization*		*% e.e. after recrystallization*
L-Val	0.05	0.017	99.966
L-Leu	0.07	0.040	99.920
L-Phe	0.15	0.018	99.964
L-Met	0.17	0.094	99.812
L-Thr	0.25	0.009	99.982
L-Asp	0.42	0.032	99.936
L-Ser	1.26	0.675	98.650

of L-serine, as compared to the rather similar amino acid L-threonine, can be at least partly explained by the low efficiency of the recrystallization step. The crystals thus formed contained still more than 0.67% D.

However, even for alanine which usually shows good enhancement characteristics, an unacceptable high D content of up to 2.5% was occasionally found in commercial samples. We therefore strongly recommend that the enantiomeric purity of commercial batches be checked carefully, prior to any synthesis.

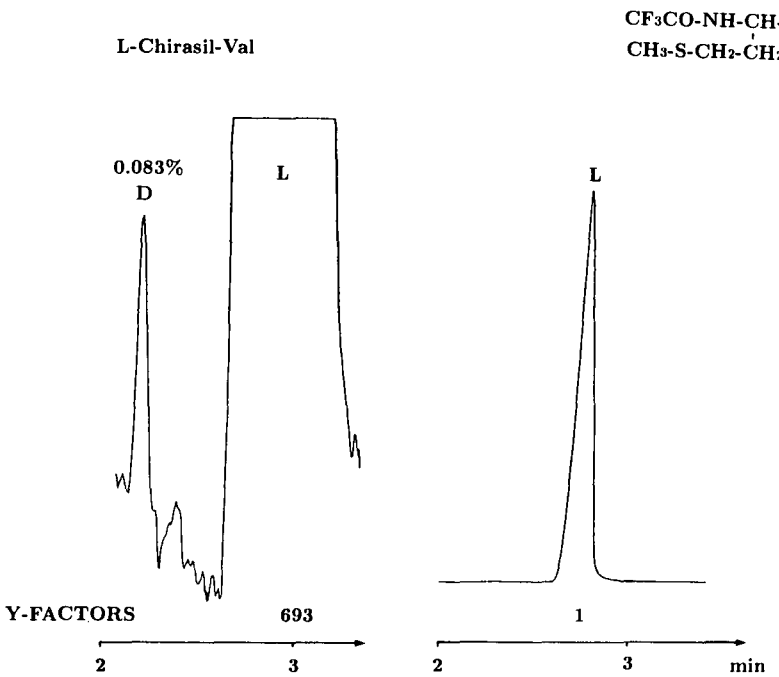

Fig. 4. Enantiomeric purity of one of the recrystallized samples of L-methionine, determined as N-TFA-Met-OCH_3 on L-Chirasil-Val (duran glass capillary column, 20 m × 0.25 mm) at 120°C, 0.4 bar H_2, FID. Right hand: in scale; left hand; expanded in *y*-direction.

CONCLUSIONS

Due to their exceedingly high enantiomeric excess (e.e.), recrystallized amino acids are a useful tool to pinpoint the possible degree of racemization during derivatization under standard conditions. Besides this, they are both a challenge and a measure for the sensitivity and reliability of the state of the art of quantitative GC on capillary columns. In view of the increasing demand for biologically active compounds of high e.e., the enhancement of the enantiomeric purity by recrystallization of solid starting materials should be seriously considered.

ACKNOWLEDGEMENTS

We are indebted to Degussa (Hanau, F.R.G.), for a gift of D-alanine, and to Merck (Darmstadt, F.R.G.), Fährhaus Pharma (Hamburg, F.R.G.) and Ajinomoto (Tokyo, Japan), for kindly providing several batches of L-amino acids.

REFERENCES

1 J. D. Morrison (Editor), *Asymmetric Synthesis*, Vol. 1, Academic Press, New York, 1983.
2 M. Zief and L. J. Crane (Editors), *Chromatographic Chiral Separations*, Marcel Dekker, New York, 1988.
3 E. Gil-Av, *J. Mol. Evol.*, 6 (1975) 131.
4 V. Schurig, *Kontakte (Merck, Darmstadt)*, 1 (1985) 54 (and subsequent articles).
5 W. A. König, *The Practice of Enantiomer Separation by Capillary Gas Chromatography*, Hüthig, Heidelberg, Basel, New York, 1987.
6 E. Bayer, *Z. Naturforsch., Teil B*, 38 (1983) 1281.
7 B. Koppenhoefer and E. Bayer, in F. Bruner (Editor), *The Science of Chromatography*, Elsevier, Amsterdam, 1985, p. 1.
8 H. Frank, G. J. Nicholson and E. Bayer, *J. Chromatogr. Sci.*, 15 (1977) 174.
9 E. Bayer, H. Allmendinger, G. Enderle and B. Koppenhoefer, *Fresenius' Z. Anal. Chem.*, 321 (1985) 321.
10 B. Koppenhoefer, H. Allmendinger and G. J. Nicholson, *Angew. Chem.*, 97 (1985) 46; *Angew. Chem. Int. Ed. Engl.*, 24 (1985) 48.
11 B. Koppenhoefer, R. Weber and V. Schurig, *Synthesis*, (1982) 316.
12 B. Koppenhoefer and V. Schurig, *Org. Synth.*, 66 (1988) 151.
13 B. Koppenhoefer and V. Schurig, *Org. Synth.*, 66 (1988) 160.
14 W. Woiwode, H. Frank, G. J. Nicholson and E. Bayer, *Chem. Ber.*, 111 (1978) 3711.
15 H. Frank, W. Woiwode, G. J. Nicholson and E. Bayer, *Liebigs Ann. Chem.*, (1981) 354.
16 V. Muschalek, *Diploma Thesis*, University of Tübingen, 1983.
17 B. Koppenhoefer, H. Allmendinger, G. J. Nicholson and E. Bayer, *J. Chromatogr.*, 260 (1983) 63.
18 A. Collet, M. J. Brienne and J. Jacques, *Chem. Rev.*, 80 (1980) 215.
19 D. Seebach, P. Renaud, W. B. Schweizer, M. F. Züger and M.-J. Brienne, *Helv. Chim. Acta*, 67 (1984) 1843.
20 H. Stephen and T. Stephen (Editors), *Solubilities of Inorganic and Organic Compounds*, Vol. I, Pergamon, Oxford, 1963.
21 H. J. Simpson, Jr. and R. E. Marsh, *Acta Crystallogr.*, 20 (1966) 550.
22 H. A. Levy and R. B. Corey, *J. Am. Chem. Soc.*, 63 (1941) 2095.
23 L. Addadi, Z. Berkovitch-Yellin, I. Weissbuch, J. van Mil, L. J. W. Shimon, M. Lahav and L. Leiserowitz, *Angew. Chem.*, 97 (1985) 476; *Angew. Chem., Int. Ed. Engl.*, 24 (1985) 466.
24 V. Muschalek, *Thesis*, University of Tübingen, 1987.

Journal of Chromatography, 477 (1989) 147–150
Elsevier Science Publishers B.V., Amsterdam — Printed in The Netherlands

CHROM. 21 656

Note

Indirect photometric detection of cyclodextrins via inclusion complexation in micro high-performance liquid chromatography

TOYOHIDE TAKEUCHI, MASAHIRO MURAYAMA and DAIDO ISHII*
Department of Applied Chemistry, Faculty of Engineering, Nagoya University, Chikusa-ku, Nagoya 464 (Japan)

The unique features of cyclodextrins in various pharmaceutical areas have been widely acknowledged in recent years. An improvement in the stability or solubility of drugs using cyclodextrins has been reported, which is due to the inclusion complexation properties of cyclodextrins. For example, cyclodextrins form inclusion complexes with barbiturates, which improves their solubility and results in increase in gastrointest inal absorption[1–7]. A soluble powder for injections of prostaglandin-El stabilized with α-cyclodextrin is commercially available.

Although many papers have reported the parenteral application of cyclodextrins[9,10], few have discussed the bioanalysis of cyclodextrins[11,12]. The development of methods for the microdetermination of cyclodextrins in plasma is necessary for pharmacokinetic studies. Cyclodextrins show almost no UV absorption. Only refractive index detection can be used, but this method is generally not sensitive. Indirect detection is a good alternative.

Various detection principles have been reported for the visualization of transparent analytes in high-performance liquid chromatography (HPLC), among which indirect photometric detection has most successfully been applied in ion chromatography[13]. In indirect detection, analytes are visualized via interaction with the mobile phase component or postcolumn interaction. In the former case the analyte is visualized by variation of a background due to the mobile phase component, while in the latter case the mobile phase component is transparent to the detector and the secondary species produced by the postcolumn interaction corresponding to the analytes are detected. Indirect detection usually refers to the former case, and postcolumn ion replacement[14–16] and postcolumn enzyme reaction can be included in the latter case[17].

Frijlink *et al.*[12] reported a new method for indirect photometric detection of cyclodextrins via postcolumn complexation with phenolphthalein. The detection principle was based on the finding that the colour intensity of phenolphthalein decreased on formation of the inclusion complex with cyclodextrins[18–20]. The detection limit for β-cyclodextrin was 1.0 μg/ml (ref. 12) and it was suggested that this would be improved by decreasing the noise level due to incomplete postcolumn mixing.

An advantage of micro HPLC lies in the ability to improve the mass detection limit. This is especially important when the amount of sample available is limited. This paper will describe the indirect detection of cyclodextrins via inclusion complexation

0021-9673/89/$03.50

with phenolphthalein in micro HPLC, and the improvement of the mass detection limits of cyclodextrins will be demonstrated.

EXPERIMENTAL

Apparatus

The liquid chromatograph comprised an MF-2 Micro Feeder pump (Azumadenki Kokyo, Tokyo, Japan) equipped with an MS-GAN 050 gas-tight syringe (0.5 ml; Ito, Fuji, Japan), an ML-425 micro valve injector (20 nl; JASCO, Tokyo, Japan), a micropacked separation column dipped in a laboratory-made water-bath, an UVIDEC-100 III spectrophotometer (JASCO) and a RC-128 chart recorder (JASCO).

The separation column comprised fused-silica tubing (100 mm × 0.35 mm I.D.) packed with commercially available alkyl-modified silica, Develosil ODS-3K (3 μm; Nomura Chemical, Seto, Japan) or Capcell Pak C_{18} (5 μm; Shiseido, Tokyo, Japan). The latter material is resistant to alkaline solutions up to pH 10. The detector was set at 550 nm and operated with an offset of 0.12–0.18 a.u.

Reagents

α- and β-cyclodextrin were obtained from Tokyo Chemical Industry (Tokyo, Japan), γ-cyclodextrin from Wako Pure Chemical Industries (Osaka, Japan). Other reagents were supplied by Wako Pure Chemical Industries. All the reagents except for HPLC-grade distilled water were of reagent grade, and were employed without any treatment.

RESULTS AND DISCUSSION

A chromatogram of β- and γ-cyclodextrin is shown in Fig. 1. The Develosil ODS-3K column gave an higher efficiency than the Capcell Pak C_{18} column. The

Fig. 1. Indirect photometric detection of cyclodextrins. Column: Develosil ODS-3K, 100 mm × 0.35 mm I.D. Mobile phase: 0.3 m*M* phenolphthalein dissolved in 3% methanol solution, pH 12.2. Flow-rate: 2.8 μl/min. Samples: $\beta = \beta$-cyclodextrin; $\gamma = \gamma$-cyclodextrin; 2.0 m*M* of each was injected. Sample volume: 20 nl. Wavelength of detection: 550 nm.

sample concentration was 2.0 m*M*, corresponding to an injected amount of 40 pmol each. The peak area of β-cyclodextrin was 1.6 times larger than that of γ-cyclodextrin, and the value was smaller than that observed by the flow injection method, *viz.*, 3.9. If the cyclodextrins are visualized only by inclusion complexation, the peak area ratio should coincide with that observed by the flow injection method. This inconsistency may be explained by the fact that the cyclodextrins perturb the partitioning of phenolphthalein during the chromatographic process, which also contributed to the visualization of the cyclodextrins based on the common indirect detection principle of uncharged species[21,22]. The positive peak, denoted as "S" in Fig. 1, was eluted in 13 min, and may be produced by perturbation of the partitioning of phenolphthalein due to the cyclodextrins.

In addition, α-cyclodextrin was not detected under the operating conditions in Fig. 1. The background of the mobile phase was kept at around 0.18 a.u. by considering the linearity of the signal[23].

The concentration of methanol in the mobile phase affected the mass detection limit, because it can influence the stability of the inclusion complex and the retention times of the analytes as well as of phenolphthalein. A concentration of 3% was selected because the system peak and the cyclodextrins were separated in a reasonable time.

The mass detection limits under the operating conditions in Fig. 1 were 0.58 pmol (or 0.66 ng) for β-cyclodextrin and 0.86 pmol (or 1.1 ng) for γ-cyclodextrin at a signal-to-noise ratio of 2. These values represent a marked improvement compared with those achieved by Frijlink *et al.*[12], *e.g.*, 1.0 μg for β-cyclodextrin. This is due mainly to miniaturization of the separation column and to the use of the single-pump system. The mass detection limit becomes important when the amount of sample available is limited.

On the other hand the concentration sensitivity of this system, *e.g.*, 33 μg/ml β-cyclodextrin, is much worse than the reported[12] value, *e.g.*, 1.0 μg/ml. However, the concentration sensitivity can be improved by a factor of ten because the injection volume can be increased up to 0.2 μl without significant loss of column efficiency. Moreover, the concentration sensitivity of micro HPLC can be improved by the use of the precolumn enrichment method[24], in which the sample volume is not generally limited if the enrichment conditions are carefully selected.

In order to take advantage of this system, two problems must be overcome in the future. First, the alkyl-modified silica employed in this work was not resistant to alkaline solution. The precision of the retention time and the peak area were poor under the conditions in Fig. 1, due to the short life of the separation column and instability of phenolphthalein. This is because a mobile phase with an high pH was used. The relative standard deviations of the retention time and peak area for four successive measurements under the conditions in Fig. 1 were 3.0 and 8.1% for γ-cyclodextrin and 4.9 and 4.8% for β-cyclodextrin, respectively. The efficiency of the separation column deteriorated during operation for 1 week. When the pH of the mobile phase was decreased to around 11, the colour intensity of the effluent from the column decreased in comparison with the original one, probably because the silica material consumed the alkali in the mobile phase, leading to a decrease in the pH value and to a decrease in the colour intensity. Therefore, a packing material which is resistant to alkaline solution must be selected. Fortunately, research on the improvement of the stability of alkyl-modified silica packings in alkaline solution is being

carried out in this field and materials suitable for this purpose will be available in the near future.

In addition, another strategy for this problem is to use the postcolumn mixing method as reported in a previous work on micro HPLC of bile acids[25]. In this case we compromise with a slight deterioration in the mass detection limits, but the precision and accuracy will be substantially improved.

Secondly, the background was gradually decreased and could not be stabilized. This drift of the baseline was due to the instability of the phenolphthalein solution. Cyclodextrins can form inclusion complexes with various compounds. Other reagents which are more stable than phenolphthalein should be found.

The indirect photometric detection based on perturbation of the partitioning of the visualization agent is another strategy to overcome these problems which is being investigated in this laboratory.

REFERENCES

1 K. Koizumi and K. Fujimura, *Yakugaku Zasshi,* 92 (1972) 32.
2 A. L. Thakkar, P. B. Kuehn, J. H. Perrin and W. L. Wilham, *J. Pharm. Sci.*, 61 (1972) 1841.
3 K. Koizumi, K. Mitsui and K. Higuchi, *Yakugaku Zasshi,* 94 (1974) 1515.
4 M. Otagili, T. Miyaji, K. Uekama and K. Ikeda, *Chem. Pharm. Bull.*, 24 (1976) 1146.
5 T. Miyaji, Y. Kurono, K. Uekama and K. Ikeda, *Chem. Pharm. Bull.*, 24 (1976) 1155.
6 K. Koizumi and Y. Kidera, *Yakugaku Zasshi,* 97 (1977) 705.
7 K. Koizumi, H. Miki and Y. Kubota, *Chem. Pharm. Bull.*, 28 (1980) 319.
8 W. Saenger, *Angew. Chem.*, 92 (1980) 343.
9 S. P. Jones, D. J. W. Grant, J. Hadgraft and G. D. Parr, *Acta Pharm. Technol.*, 30 (1984) 213.
10 S. P. Jones, D. J. W. Grant, J. Hadgraft and G. D. Parr, *Acta Pharm. Technol.*, 30 (1984) 263.
11 K. Koizumi, Y. Kubota, Y. Okada and T. Utamura, *J. Chromatogr.*, 341 (1985) 31.
12 H. W. Frijlink, J. Visser and B. F. H. Drenth, *J. Chromatogr.*, 415 (1987) 325.
13 H. Small and T. E. Miller, Jr., *Anal. Chem.*, 54 (1982) 462.
14 S. W. Downey and G. M. Hieftje, *Anal. Chim. Acta*, 153 (1983) 1.
15 T. Takeuchi, E. Suzuki and D. Ishii, *Chromatographia*, 25 (1988) 582.
16 L. J. Galante and G. M. Hieftje, *Anal. Chem.*, 60 (1988) 995.
17 D. Ishii and T. Takeuchi, *J. Liq. Chromatogr.*, 11 (1988) 1865.
18 M. Vikmon, in J. Szetli (Editor), *Proc. First Int. Symp. on Cyclodextrins, Budapest, September 30–October 2, 1981,* Reidel, Dordrecht, 1982, pp. 69–74.
19 M. Mäkelä, T. Korpela and S. Laakso, *J. Biochem. Biophys. Methods*, 14 (1987) 85.
20 Á. Buvári, L. Barcza and M. Kajtár, *J. Chem. Soc. Perkin Trans. II*, (1988) 1687.
21 T. Takeuchi, S. Watanabe, K. Murase and D. Ishii, *Chromatographia*, 25 (1988) 107.
22 J. Crommen, G. Schill and P. Hernè, *J. Chromatogr.*, 25 (1988) 397.
23 T. Takeuchi and D. Ishii, *J. Chromatogr.*, 393 (1987) 419.
24 T. Takeuchi, Y. Jin and D. Ishii, *J. Chromatogr.*, 321 (1985) 159.
25 T. Takeuchi, S. Saito, and D. Ishii, *J. Chromatogr.*, 258 (1983) 125.

Journal of Chromatography, 477 (1989) 151–159
Elsevier Science Publishers B.V., Amsterdam — Printed in The Netherlands

CHROM. 21 496

SUPERCRITICAL-FLUID EXTRACTION OF AQUEOUS SAMPLES AND ON-LINE COUPLING TO SUPERCRITICAL-FLUID CHROMATOGRAPHY

D. THIEBAUT, J.-P. CHERVET, R. W. VANNOORT[a], G. J. DE JONG*, U. A. Th. BRINKMAN and R. W. FREI[b]

Department of Analytical Chemistry, Free University, De Boelelaan 1083, 1081 HV Amsterdam (The Netherlands)

SUMMARY

The potential of segmented-flow systems for on-line liquid/supercritical-fluid extraction was explored. The use of a phase separator (PS), its design and performance were investigated, utilizing phenol and 4-chlorophenol as the test compounds, water as the liquid phase and supercritical carbon dioxide as the extractant. On-line coupling of such a liquid/fluid extraction (SFE) system to supercritical fluid chromatography (SFC) was demonstrated, as was the feasibility of extracting phenol from an urine sample. The extraction efficiency for the test compounds was over 85%. The repeatability was about 8% relative standard deviation (R.S.D.) (n = 8) for the total SFE-PS–SFC system and 4% R.S.D. for both the SFE-PS and the SFC operation. The potential of coupling SFE to other chromatographic and detection principles is discussed.

INTRODUCTION

Supercritical fluids (SFs) possess physical properties intermediate between those of liquids and gases[1]. Their relatively high solvent strength, low viscosity and high solute diffusivity make them attractive for extraction because mass transfer is facilitated. Moreover, the extraction temperature can be low so that the risk of labile analyte degradation is reduced. As solvent strength is related to fluid density[2], selective extraction can be performed by varying the pressure and/or temperature of the fluid[3–5]. In addition, the recovery of the extracted analyte is simplified because many SFs are gases at room temperature and can be removed by decompression. Supercritical fluid extraction (SFE) has repeatedly been performed with solid matrices[6–20]. It has been coupled on-line with conventional packed column liquid chromatography (LC) for SFE–LC of *Radix valerianae*[15], with gas chromatography (GC) after cryofocusing for SFE–GC of flavours and fragrances[16] or polycyclic aromatic hydrocar-

[a] On leave from: Chemistry Division, Department of Scientific and Industrial Research, PO Box 29181, Christchurch 4, New Zealand.
[b] Author deceased.

0021-9673/89/$03.50

bons (PAHs)[3,5] or with supercritical fluid chromatography (SFC) for SFE–SFC[4,10,12,13,17–20].

In contrast, on-line SFE–SFC of aqueous samples has never been reported. These samples are not suitable for direct injection into SFC because of the low solubility of water in supercritical CO_2[21,22]. Moreover, water, like other polar modifiers is known strongly to affect solute retention, even with chemically bonded silica stationary phases[23,24]. Thus, the bulk of the water must be separated from the extraction fluid prior to SFC.

This paper describes a preliminary study of liquid/supercritical fluid extraction and its coupling with SFC by means of a phase separator (PS)[25] in order to remove the aqueous phase from the supercritical CO_2. Thus, after the extraction step the analytes are recovered in the supercritical CO_2 and can be directly switched into the SFC. Such a SFE-PS–SFC system is described for the determination of phenolic compounds in urine samples.

EXPERIMENTAL

Apparatus

Fig. 1 shows the SFE-PS–SFC apparatus. A single carbon dioxide cylinder with eductor tubing was connected to both the syringe pump used for extraction (Model Phoenix 20; Carlo-Erba, Milan, Italy) and the laboratory-made syringe pump used for SFC. The SFE was performed in a constant-pressure mode, and the SFC in a constant-flow mode, both at 40°C using a water-bath.

The reservoir of the extraction pump, maintained at 12°C by a water cooling jacket, was connected to the 1.3 m × 0.5 mm I.D. stainless-steel extraction coil after preheating of the CO_2. Initially, experiments were carried out with a water stream added to the CO_2 before the extraction coil via a T-piece (Fig. 1). The water was delivered by a reciprocating pump (Model 302; Gilson, Villiers-le-Bel, France). In the dual-pump set-up, the sample (5 μl) was directly introduced into the water stream via injection valve 1. In subsequent experiments, the water pump and the T-piece were removed. The samples were then injected as water plugs directly into the supercritical CO_2 using injection valve 2. The phase separator was connected to the extraction coil as depicted in Fig. 1; the upper outlet was connected either to the UV detector or to the SFC injection valve 3 and back-pressure maintained by means of restrictor 1. The lower outlet (waste) was connected to restrictor 2. For monitoring the liquid/supercritical fluid extraction, a single-wavelength UV detector (Knauer, Berlin, F.R.G.) was used. It was equipped with laboratory made 320 μm I.D. fused-silica capillary cell (*i.e.*, optical pathlength 320 μm). The restrictors were made of fused-silica capillaries (6 cm × 320 μm) packed with 5-μm Hypersil ODS particles (Shandon Southern, Runcorn, U.K.).

The SFC system was similar to that described elsewhere[23]. The laboratory-made syringe pump delivered the supercritical CO_2 with a flow-rate of 1.1 ml/min (20°C) and was connected via a preheating coil to injection valve 3, which was fitted with a 200-μl loop. For SFE-PS–SFC measurements, the 320-μm pathlength UV cell was used. A back-pressure regulator (Model 26-1721-24082; Tescom, Minneapolis, MN, U.S.A.) was used to ensure accurate and stable pressure control throughout the SFC system.

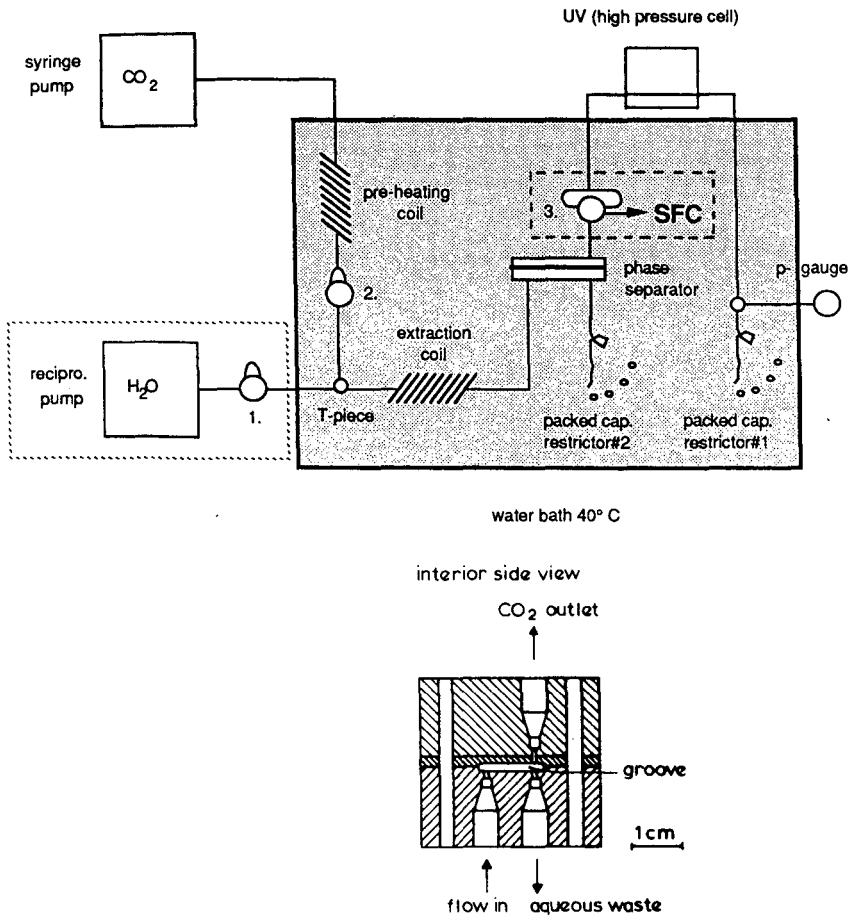

Fig. 1. Schematics of the SFE-PS–SFC apparatus. The single-pump (only CO_2) and dual-pump systems (CO_2 and water) are shown. Insert: expanded interior side view of phase separator.

The flow-rate of liquid CO_2 was regulated by the pumps. Supercritical fluid recovery, defined as the detector carbon dioxide flow-rate/total carbon dioxide flow-rate out of the phase separator, was determined by measuring the flow-rates of CO_2 after decompression using calibrated vessels filled with water, and placed above the outlets of the restrictors in the water-bath.

Chemicals

The 15 cm × 3.1 mm columns were laboratory-made using 5-μm LiChrosorb RP-18 (Merck, Darmstadt, F.R.G.) or 5-μm RSIL-CN (Alltech, Eke, Belgium) as the stationary phases. The CO_2 was technical grade (Hoekloos, Amsterdam, The Netherlands). Analytical grade phenol and 4-chlorophenol were chosen as the medium-polar test compounds to investigate the suitability of the system.

RESULTS AND DISCUSSION

Dual-pump system

Phase separator. Phase separators with a sandwich design as described for liquid–liquid extraction[25] have been used in various areas in the past. The mechanism of separation is based mainly on the wettability of the stainless-steel and PTFE parts by an aqueous and water-immiscible extractant phase, respectively. In addition, density differences are considered. Hence, contrary to the situation normally encountered with liquid–liquid, *e.g.*, water–chlorinated hydrocarbon, mixtures for the system water–supercritical CO_2 ($d < 0.8$ g/ml) the phase separator had to be mounted upside down to function effectively (see Fig. 1). The dimensions and the groove volume (43 μl) were the same as previously reported[25].

The disc material functioning as the hydrophobic surface in the separation process had to be selected carefully to withstand the more rigorous pressure conditions of the supercritical system. The various materials tested for water–supercritical CO_2 separations are shown in Table I. PTFE cannot be used because it deforms at higher pressure and starts to leak. Kel-F changed its colour and shape as a result of the strong tightening which was necessary to withstand the SFE operating pressure. Good stability was obtained with Delrin and PVDF, which did not show any visible change after prolonged use (several months).

SFE system. The dual-pump system was the initial arrangement for study of the liquid/supercritical extraction system and can be seen in Fig. 1. Sample plugs were injected through injection valve 1 and the supercritical carbon dioxide stream was monitored by the UV detector.

As a first step, the existence of a water–supercritical CO_2 segmented system was tested by inserting the UV detector prior to the sandwich phase separator. As expected, this resulted in a very noise signal typical of the coexistence of two immiscible phases. This observation is in agreement with the binary phase diagram for water–supercritical CO_2[21]. Placing the UV detector after the phase separator yielded a low noise background with rather symmetrical signal peaks for the analyte, phenol. The sharp contrast between the system without and with the phase separator is nicely illustrated in Fig. 2. Even with the phase separator inserted, sharp random spikes occurred occasionally. They were caused by water being carried along by the supercritical fluid. The water spikes were never eliminated completely, but they posed no major problem since they were easily distinguished from the analyte signal. The influ-

TABLE I

EVALUATION OF DISC MATERIAL FOR THE PHASE SEPARATOR

Disc material	*PTFE*	*Kel-F*	*PVDF*	*Delrin*
Structure	$(CF_2)n$	$(-CFCl-CF_2)n$	$(CH_2-CF_2)n$	$(-CH_2-O)n$
Pressure stability (150 bar)	Leaks	Good	Good	Good
Lifetime	–	<2 weeks	>4 weeks	>4 weeks
Suitability for SFE-PS	–	±	+	+

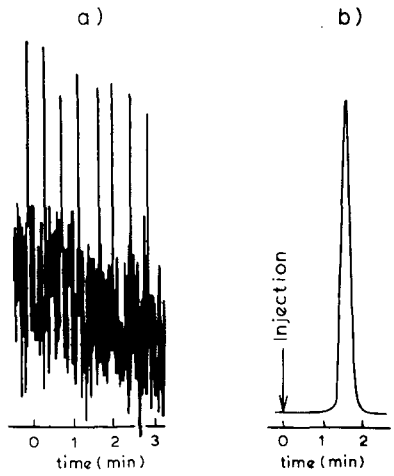

Fig. 2. Dual pump system (a) without and (b) with the phase separator inserted. Conditions: CO_2 at 120 bar, flow-rate 300 μl/min; water at 150 μl/min; temperature 40°C; UV detection at 254 nm (320-μm pathlength) at (a) 0.08 a.u.f.s. and (b) 0.01 a.u.f.s., respectively. Sample: 5 μl water containing 5 μg phenol. Note the difference in attenuation; phenol peak of b will not be visible in a.

ence of the supercritical fluid recovery on the size of the analyte signal and the background noise has not been studied in detail, because variable micro restrictors were not available. Obviously, for sensitivity reasons it is desirable to recover as much of the supercritical CO_2 as is possible. In practice, however, only 10–20% was recovered before spiking became problematical. The extraction efficiency was determined only in the SFE-PS–SFC system as described in that section. The extraction coil of 1.3 m × 0.5 mm I.D. was long enough to obtain distribution equilibrium.

Single-pump system

Although the feasibility studies described above were done with a dual-pump system, injecting an aqueous sample into a water stream, with the subsequent creation of a two-phase system, it should be realized that the injection of an aqueous sample, a biological fluid or an aqueous environmental sample, directly into the supercritical carbon dioxide stream would be of real interest because of its simplicity and, probably, higher sensitivity. The system proposed is shown in Fig. 1, leaving out the reciprocating pump and injection valve 1, *i.e.*, injecting the sample via valve 2. The recovery of the supercritical CO_2 is now increased to *ca.* 50%. For identical analyte concentrations, the peak areas were some three-fold higher with the single-pump approach. This factor cannot easily be explained because not only is the supercritical fluid recovery different for the two systems, but also the ratio of the volumes of the two phases during the extraction and the flow-rate through the detector. Consequently, all further experiments were carried out using direct aqueous plug injections into the supercritical fluid stream, at a flow-rate of *ca.* 150 μl/min. The repeatability of the single-pump SFE-PS procedure was 4% R.S.D. (n = 5) with phenol as the analyte.

On-line coupling of SFE-PS with SFC

In the next stage, the single-pump extraction system was coupled via valve 3

(see Fig. 1) to a conventional SFC apparatus with a packed column, to study the on-line SFE-PS–SFC system. Having previously determined the experimentally observed peak volume after SFE-PS to be *ca.* 100 μl, valve 3 was fitted with a 200-μl loop to ensure total trapping of the compounds before switching to SFC. A plot of the peak height of the analyte *versus* the time of switching valve 3 after sample injection in valve 2 (Fig. 3) confirmed that the time of switching valve 3 was not critical with this size loop. Three runs were performed, each corresponding to a series of analyses performed during 1 h, without refilling of the 20-ml reservoir. The repeatability calculated for the mean peak height of the three runs was quite satisfactory (3% R.S.D.; $n = 3$).

For the on-line SFE-PS–SFC system, both a C_{18}- and a CN-bonded silica stationary phase were used for SFC of the phenolic compounds. On the more polar stationary phase, the capacity factors of the phenolic compounds are higher (see Table II). As a result, the pressure required to elute the analytes is also higher. Therefore, the C_{18} column was preferred for further work. It should briefly be remarked that, by employing a higher supercritical carbon dioxide density for SFC (130 bar) than SFE (118 bar), a volume compression will occur when the extracted compounds are switched into the SFC system via the large sample loop. For the present system, the calculated volume compression was only 8%.

Extraction yields were calculated by comparing the peak areas of the test compounds obtained by SFE-PS–SFC after aqueous or heptane injections, with 100% recovery being assumed for heptane. For 5-μl injections the SFE-PS–SFC system worked smoothly, with extraction yields of at least 85% for both compounds. Obviously, because only 50% of the supercritical CO_2 will go to valve 3 following SFE-PS, the actual quantity injected into the SFC is two times lower (42.5%). The peak height repeatability for the total system was 8% R.S.D. ($n = 8$). This value is quite satisfactory considering that the repeatability of both SFE-PS and SFC was about 4% R.S.D. ($n = 7$). In order to improve the detection limit of the system expressed as the

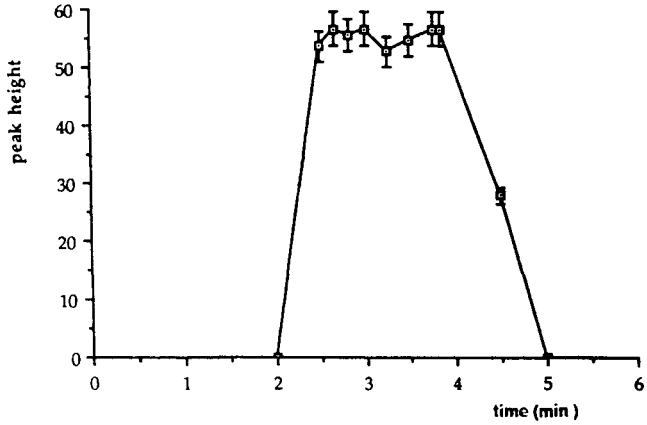

Fig. 3. Recovery of phenol *versus* the time valve 3 is switched after sample injection (in valve 2). SFE conditions: CO_2 at 40°C, pump pressure 118 bar, 150 μl/min. SFC conditions: CO_2 at 40°C and 150 bar (column inlet pressure); flow-rate 1.1 ml/min (20°C); 15 cm × 0.31 cm I.D. LiChrosorb RP-18, 5 μm; UV detection at 254 nm, 0.02 a.u.f.s. with 320-μm pathlength capillary cell. The bars indicate the maximum deviations for three 1-h series of analyses.

TABLE II

DATA FOR SFC OF THE TEST COMPOUNDS ON COLUMNS WITH A C_{18}- OR A CN-CHEMICALLY BONDED PHASE

15 cm × 0.31 cm I.D. columns with 5-μm LiChrosorb RP-18 or 5-μm RSIL-CN; CO_2 at 40°C and indicated inlet pressure.

Compound	*Capacity factor on*	
	C_{18}	*CN*
Phenol	0.2	6.7
4-Chlorphenol	0.8	8.9
Pressure (bar)	130	270

injected concentration, preliminary experiments were done with 50-μl instead of 5-μl injections. Although the expected increase of sensitivity was indeed observed with the larger sample volume, water spikes in the detector signal increased dramatically. Optimization of the phase separator design may well help to eliminate this problem.

Urine sample- Liquid/supercritical-fluid extraction in combination with phase separation can be regarded as a clean-up procedure, and should serve a useful purpose with complex matrices such as urine. Fig. 4a shows a chromatogram obtained upon direct injection into the SFC system of a 5-μl urine sample spiked with 4-chlorophenol as a model compound. Fig. 4b was obtained when injecting the same sample into the SFE-PS–SFC system, and Fig. 4c after the injection of a blank urine sample into this system. These chromatograms show the potential of the SFE system for the analysis of aqueous samples. The sensitivity can, of course, be considerably increased by using a longer-pathlength high-pressure flow-cell.

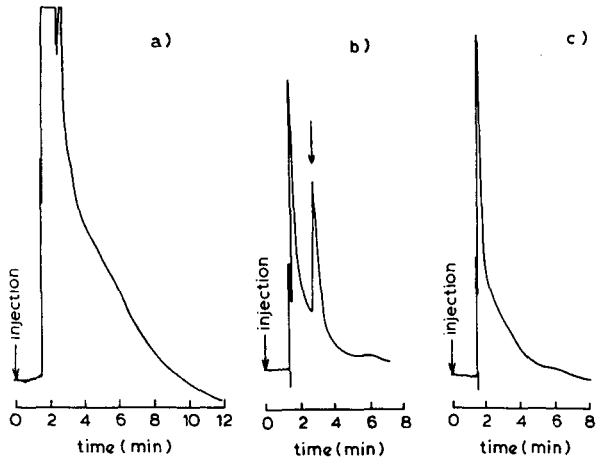

Fig. 4. Comparison of SFC and SFE-PS–SFC of an urine sample spiked with 4-chlorophenol. (a) Direct injection of a spiked (120 μg/ml) urine sample into the SFC. (b) SFE-PS–SFC of the same spiked urine. (c) SFE-PS–SFC of an urine blank. SFE conditions as in Fig. 3. SFC conditions as in Fig. 3 except 130 bar and 0.005 a.u.f.s.

It should be remarked that problems started to occur after some ten injections of urine samples. The restrictors became plugged and, consequently, the extraction flow-rate decreased. In addition, the background noise level increased. A series of methanol injections served to solve these problems.

CONCLUSIONS

The on-line coupling of a continuous liquid/supercritical carbon dioxide extraction system with SFC is reported for the first time. Preliminary results demonstrate the feasibility of the procedure by using phase separation between SFE and SFC. This seems to be a promising on-line sample pretreatment technique for either SFC or other separation techniques.

In the future, attention should be devoted to the optimization of the extraction process (pressure, temperature, flow-rates, phase separator), and to improving the detection limit of the set-up by increasing the injection volume. In addition, other model solutes will have to be chosen in order to investigate the efficiency and selectivity of SFE and to determine the limits of SFE with regard to solute polarity. This should include the use of modifiers.

As for the potential of SFE, besides the possibility of directly analysing aqueous samples by means of on-line coupling to SFC or for that matter, GC or LC, there is also the possibility of an on-line post-column phase switch. In the latter case, a reversed-phase LC separation can be followed by on-line liquid/supercritical fluid extraction and coupling to a mass spectrometer, GC-type detectors, a Fourier-transform IR spectrometer or other detectors that are not easily compatible with current LC mobile phases. As an alternative, after the LC separation, the analytes of interest can be trapped on a suitably selected trapping column, desorbed by means of a supercritical fluid and monitored by the same types of detectors.

REFERENCES

1 P. J. Schoenmakers and F. C. C. J. G. Verhoeven, *Trends Anal. Chem.*, 6 (1987) 10.
2 J. C. Giddings, M. N. Myers, L. McLaren and R. A. Keller, *Science (Washington, D.C.)*, 162 (1968) 67.
3 S. B. Hawthorne and D. J. Miller, *J. Chromatogr. Sci.*, 24 (1986) 258.
4 A. Shishikura, K. Fujimoto, T. Kaneda, K. Arai and S. Saito, *Agric. Biol. Chem.*, 50 (1986) 1209.
5 B. W. Wright, S. R. Frye, D. G. McMinn and R. D. Smith, *Anal. Chem.*, 59 (1987) 640.
6 G. Brunner, *Process Technol. Proc.*, 3 (1985) 245.
7 M. Perrut, *Informations Chimie*, 4 (1986) 129.
8 G. Nicolaon, *Revue Energ.* 375 (1985) 283.
9 C. A. Eckert, J. G. van Alsten and T. Stoicos, *Environ. Sci. Technol.*, 4 (1986) 319.
10 E. Stahl, K. W. Quirin and D. Gerard, *Verdichte gaze zur Extraktion und Raffination*, Springer, Berlin, Heidelberg, 1987.
11 P. J. Göttsch, U. Lenz, W. O. Eisenbach, W. Dolkemeyer and F. Gajewski, *Process Technol. Proc.*, 3 (1985) 345.
12 W. Gmür, J. O. Bosset and E. Plattner, *Mitteil. Gebiete Lebensm. Hyg.*, 78 (1987) 21.
13 W. Gmür, J. O. Bosset and E. Plattner, *J. Chromatogr.*, 388 (1987) 143.
14 M. A. Schneiderman, A. K. Sharma and D. C. Locke, *J. Chromatogr.*, 409 (1987) 343.
15 K. K. Unger and R. Roumeliotis, *J. Chromatogr.*, 282 (1983) 519.
16 S. B. Hawthorne, M. S. Krieger and D. J. Miller, *Anal. Chem.*, 60 (1988) 472.
17 M. E. P. McNally and J. R. Wheeler, *J. Chromatogr.*, 435 (1988) 63.
18 H. Engelhardt and A. Gross, *J. High Resolut. Chromatogr. Chromatogr. Commun.*, 11 (1988) 38.

19 K. Sugiyama, M. Saito, T. Hondo and M. Senda, *J. Chromatogr.*, 332 (1985) 107.
20 R. J. Skelton, Jr., C. C. Johnson and L. T. Taylor, *Chromatographia*, 21 (1986) 3.
21 E. A. Brignole, S. Skjold-Jorgenson and A. Fredenslund, *Process Technol. Proc.*, 3 (1985) 87.
22 S. Tackenouchi and G. C. Kennedy, *Am. J. Sci.*, 262 (1964) 1055.
23 P. Mourier, P. Sassiat, M. Caude and R. Rosset, *J. Chromatogr.*, 353 (1986) 61.
24 C. H. Lochmüller and L. P. Mink, *J. Chromatogr.*, 409 (1987) 55.
25 C. de Ruiter, J. H. Wolf, U. A. Th. Brinkman and R. W. Frei, *Anal. Chim. Acta*, 192 (1987) 267.

Journal of Chromatography, 477 (1989) 161–168
Elsevier Science Publishers B.V., Amsterdam — Printed in The Netherlands

CHROM. 21 541

MULTIDIMENSIONAL PACKED CAPILLARY COLUMN SUPERCRITICAL-FLUID CHROMATOGRAPHY USING A FLOW-SWITCHING INTERFACE

K. M. PAYNE and I. L. DAVIES[a]
Department of Chemistry, 226 Eyring Science Centre, Brigham Young University, Provo, UT 84602 (U.S.A.)
K. D. BARTLE
School of Chemistry, The University of Leeds, Leeds, LS2 9JT (U.K.)
and
K. E. MARKIDES and M. L. LEE*
Department of Chemistry, 226 Eyring Science Centre, Brigham Young University, Provo, UT 84602 (U.S.A.)

SUMMARY

A two-dimensional supercritical-fluid chromatographic (SFC–SFC) system with a flow-switching interface was used with 250 μm I.D. packed capillary columns to separate polycyclic aromatic hydrocarbons (PAHs) in a standard coal tar extract. A solvent-venting injection technique was also used which allowed the injection of several microliters of sample. Compared to open-tubular columns, packed capillary columns provided shorter analysis times and higher sample capacities; compared to conventional size packed columns, they provided higher efficiencies and lower volumetric flow-rates, allowing the total effluent to be introduced into a flame-based detector without the need for splitting.

The performance of packed capillary SFC–SFC was compared to that of open-tubular capillary SFC–SFC. In the first dimension, separation according to the number of aromatic rings was achieved as desired within 30 min, two times faster than previously reported for an open tubular column using the same sample. However, the selectivity and efficiency obtained in the second dimension, using a packed capillary, was not sufficient to fully separate all of the PAH isomers.

INTRODUCTION

In supercritical-fluid chromatography (SFC) as well as gas chromatography (GC), open tubular capillaries are associated with high efficiency. Because of their openness, columns which are longer than several meters can be used to provide a

[a] On leave from the School of Chemistry, The University of Leeds, Leeds, LS2 9JT, U.K.

0021-9673/89/$03.50

large number of theoretical plates. Capillary SFC, however, does not match the speed of analysis offered by packed-column SFC. Mass transfer effects, as a function of linear velocity, are more favorable for packed columns. The Van Deemter curve above the optimum linear velocity for a packed column has less slope than that for an open-tubular column, resulting in a wider range of useable linear velocities with minimal loss of efficiency. It is this fact that allows packed columns to provide faster analysis times while still preserving resolution.

Commonly used packed columns in SFC vary between 250 μm and 4.6 mm I.D. Columns of 1 mm I.D. (microbore) and larger require much greater volumetric flow-rates than packed capillary columns. When operated near optimum conditions, up to several l min^{-1} of gas can flow from the end of a microbore column. An advantage of SFC is the compatibility of the mobile phase used (generally CO_2) with flame-based, highly sensitive detectors, such as the flame ionization detector. In order not to extinguish the flame when using these larger packed columns with mobile phase flow-rates near their optimum, some of the effluent must be split. Splitting of the effluent, to the detector, not only can create discrimination problems, but the increased sample capacity obtained by using packed columns is diminished before the sample reaches the detector.

Packed capillaries with 100–250 μm I.D. provide a convenient compromise between open-tubular capillaries and conventional packed columns. The low volumetric flow-rates of packed capillary columns are comparable to open-tubular capillary flow-rates, yet at the same time, packed capillaries possess much greater sample capacities than open-tubular capillary columns. In comparison to conventional packed columns, packed capillaries provide higher permeability, allowing longer columns to be packed for greater total efficiency. The lower volumetric flow-rates of packed capillaries permit the total effluent to be introduced to mass-flow-sensitive detectors. The small elution volume provides more sensitive detection in concentration-dependent detectors and allows sampling of narrow bands during heart cutting in multidimensional systems[1].

The selectivity and resolving power of a single column is often inadequate for the chromatographic analysis of complex samples. By coupling two chromatographic columns of different selectivities in tandem, and with the use of heart-cutting to selectively transfer fractions of the column effluent from the primary column into the secondary column, dramatic improvements in peak capacity and resolution can be realized[2–4].

In this study, a multidimensional packed capillary SFC–SFC system based on a simple flow-switching interface was evaluated. This system was applied to the separation of polycyclic aromatic hydrocarbon (PAH) components in a standard coal tar extract, a sample which was recently separated using open-tubular SFC–SFC[5].

EXPERIMENTAL

The SFC–SFC system, used in this study, was similar in design to an open-tubular SFC–SFC system previously described[5], with minor modifications for packed capillary use. A schematic diagram of the modified system is shown in Fig. 1.

A ten-port valve (Valco, Houston, TX, U.S.A.) was used to direct the CO_2 mobile phase through both columns in series or only to the second column (Col_2).

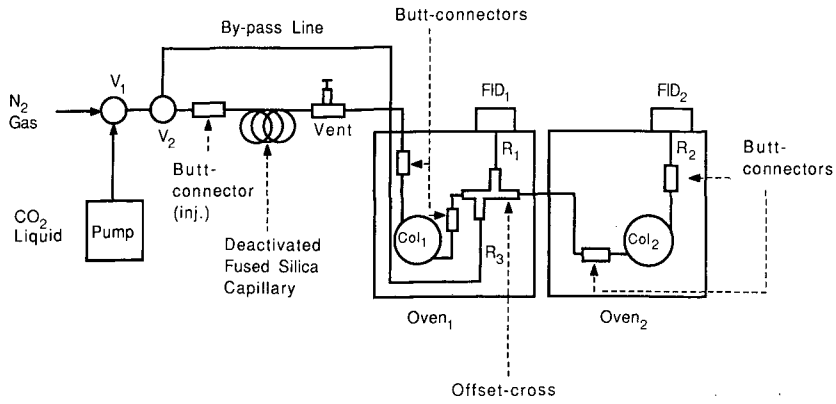

Fig. 1. Schematic diagram of the multidimensional microcolumn SFC–SFC system using a flow-switching interface for packed capillary columns.

The bypass line connecting the bypass valve (V_2) with the offset-cross flow-switching interface was a 20 cm × 25 μm I.D. untreated fused-silica capillary (Polymicro Technologies, Phoenix, AZ, U.S.A.). The end of the bypass line was butt-connected within the first oven to a frit restrictor in order to control the flow-rate to Col_2 and to avoid rapid detector signal changes during heart-cutting. The end of the restrictor was inserted into the offset-cross interface[5].

A solvent-venting technique was employed which allowed the introduction of variable amounts of sample onto the column[6]. The injections were made by inserting an on-column syringe directly into a deactivated fused-silica capillary (1.5 m × 100 μm I.D.) that was purged with nitrogen gas to remove solvent, and then with mobile phase to initiate the chromatographic separation.

Vespel ferrules (Alltech, Deerfield, IL, U.S.A.) were used to secure the 250 μm

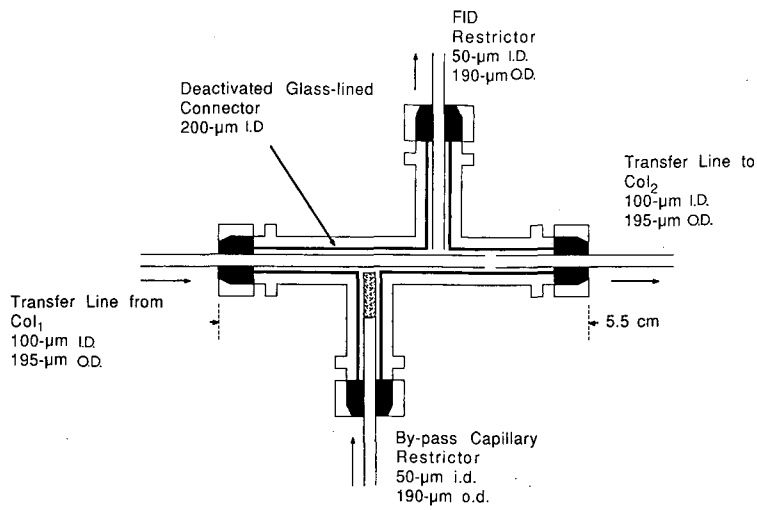

Fig. 2. Details of the offset-cross interface between the primary and secondary columns of the SFC–SFC system of Fig. 1.

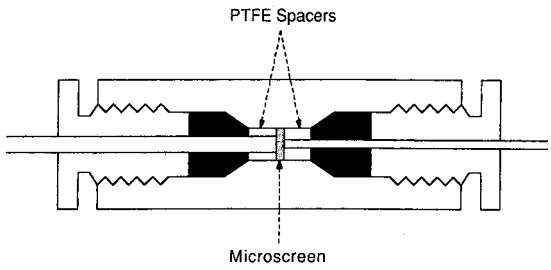

Fig. 3. Schematic diagram of the zero-dead-volume union used for packed capillary connections.

I.D. analytical column within Valco zero-dead-volume unions to either 100 μm I.D. cyanopropyl-deactivated[7] fused-silica transfer lines [appropriate lengths of 100 μm I.D. deactivated transfer lines carried effluent from the vent T-piece to the head of the primary column (Col_1), from Col_1 to the offset-cross (Fig. 2), and from the offset-cross to Col_2 through the copper tube which connected the two ovens] or to 50 μm I.D. frit restrictors. Small segments of 200 μm I.D. PTFE tubing (Chrompack, Middelburg, The Netherlands) were used to eliminate potential dead volumes in the zero-dead-volume unions (Fig. 3). Stainless steel microscreens (Mectron, City of Industry, CA, U.S.A.) were used to support the capillary column packed beds.

Two 250 μm I.D. slurry-packed fused-silica capillary columns were used in this study. Col_1 was 25 cm in length and packed with 7 μm diameter, 300 Å pore, aminosilane-bonded silica (NH_2-silica, Nucleosil, Machery-Nagel, Düren, F.R.G.). Col_2 was 55 cm in length and packed with 5 μm diameter, 300 Å pore, silica packing material which had been modified with a polyoctylhydrosiloxane via a dehydrocondensation reaction procedure developed in our laboratory[8].

$Oven_1$ and $Oven_2$ were held isothermal at 100 and 120°C, respectively. The density programs for both columns began at 0.35 g ml^{-1} and, after 2 min, were ramped at 0.008 g ml^{-1} min^{-1} to a density of 0.75 g ml^{-1}. The linear velocities were 0.9 cm s^{-1} for Col_1 and 0.6 cm s^{-1} for Col_2. A Van Deemter curve was generated to determine the optimum linear velocity for the packed capillary columns (Fig. 4). Column dead times were determined by injecting *n*-hexane and venting for only 15 s

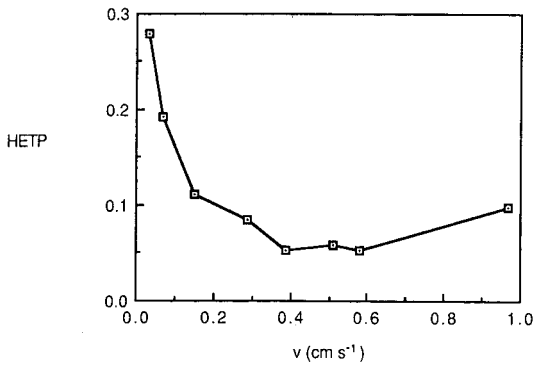

Fig. 4. Plot of a Van Deemter curve generated from a 42 cm × 250 μm I.D. capillary column (packed with 5 μm diameter, 300 Å pore silica particles) under isobaric conditions: 100°C, 150 atm, CO_2 mobile phase.

in order to introduce a small detectable amount of solvent onto the column. The results verified that Col_1 and Col_2 were operated at about 2.0 and 1.5 times their optimum linear velocities, respectively.

The sample analyzed was a National Institute of Standards and Technology standard reference material (SRM) 1597[9], which is a natural, complex, combustion-related mixture of PAHs isolated from a crude coke oven tar[10]. A volume of 1.2 μl was injected without dilution, providing 4 times the mass of solutes that were injected by using the open-tubular system[5]. This quantity of sample was too large to be injected directly onto an open-tubular capillary column.

RESULTS AND DISCUSSION

The flow-switching interface employed in this work was found to be inadequate for the combination of packed capillary/open-tubular capillary column SFC–SFC[5]. This is because the optimum volumetric flow-rates required for each column type differ greatly, and they could not be independently controlled with this type of interface. It was suggested from previous work[5] that two packed capillary columns could be used in series, thereby avoiding these volumetric flow difficulties.

When initially making fractionation cuts, a rapid signal change was noticed as a result of dramatic pressure and flow changes. A restrictor was therefore placed at the end of the by-pass line as it entered the offset-cross to dampen these changes. This modification was unnecessary in previous open-tubular SFC–SFC work[5] due to the steady back pressures maintained by the long 50 μm I.D. capillary columns.

Using two open-tubular columns in SFC–SFC, the total time required to elute the SRM 1597 sample from both columns without fractionation, was about 4 h. To fractionate the sample into individual groups required approximately 11 h. The use of

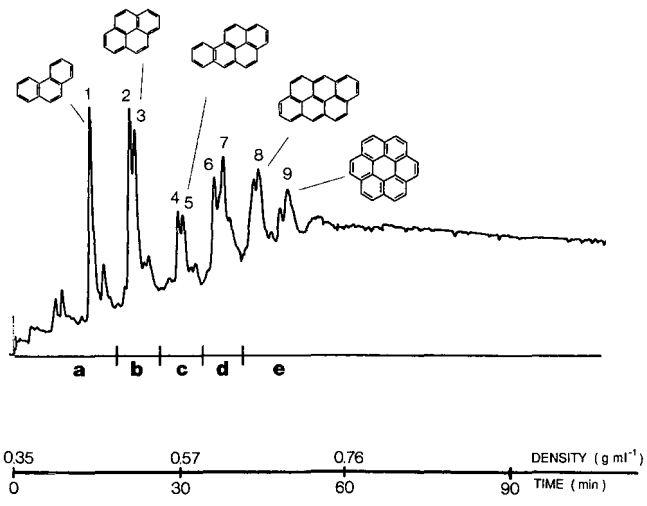

Fig. 5. Packed capillary column chromatogram (first dimension) of a standard coal tar extract (SRM 1597), using the system of Fig. 1. Conditions: see text. Peak identifications: 1 = phenanthrene; 2 = fluoranthene; 3 = pyrene; 4 = benz[*a*]anthracene; 5 = chrysene; 6 = benzofluoranthene isomers; 7 = benzopyrene isomers; 8 = anthanthrene; 9 = coronene.

an open-tubular liquid crystal column in the second dimension to provide shape selectivity, allowed the separation of various isomers including chrysene, triphenylene, benz[*a*]anthracene, and the benzofluoranthenes. Considerable time was needed to elute the sample from the first column, and over 1 h passed before the first peak was detected at the second flame ionization detector. The first column provided more efficiency than was really needed; only a crude PAH ring-number separation was necessary. A short primary column that could provide adequate but fast group type separation would be preferable.

Using packed columns in SFC–SFC, the SRM sample was separated into ring-number fractions in the first dimension in less than 1 h (Fig. 5). The fractionation of

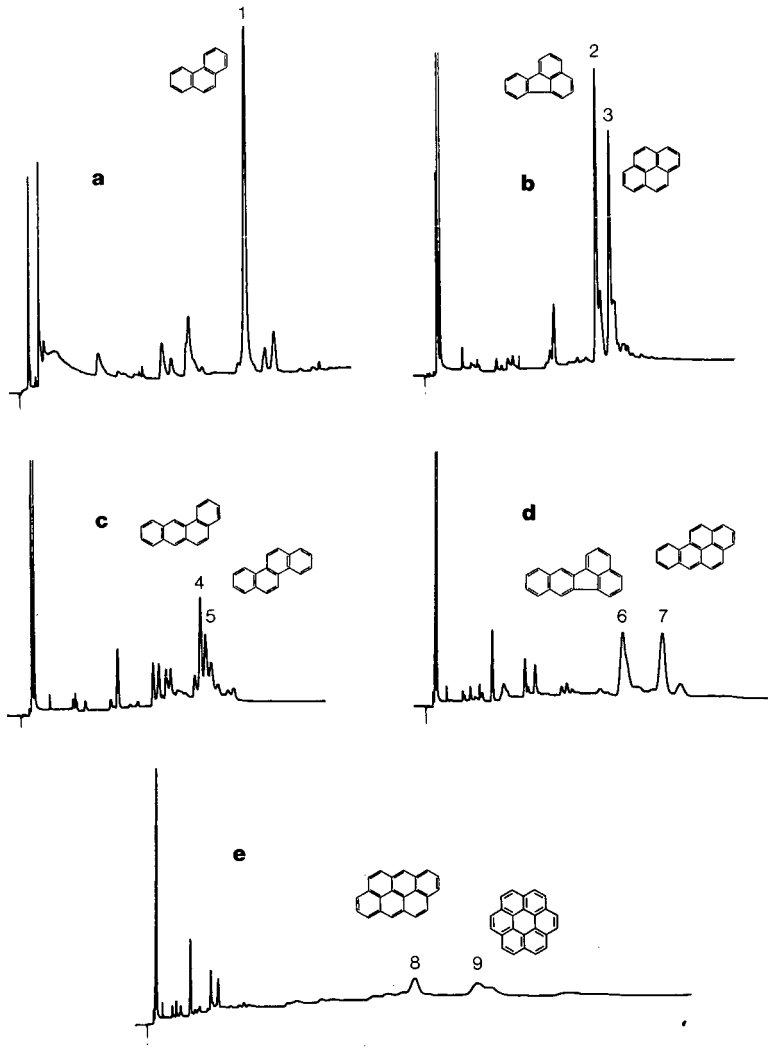

Fig. 6. Packed capillary column SFC–SFC chromatograms from the second dimension (fractions a–e indicated in Fig. 5) of a standard coal tar extract (SRM 1597) by using the system of Fig. 1. Conditions and peak identifications as in Fig. 5.

TABLE I

RELATIVE RETENTION TIMES FOR SELECTED PAHs IN SRM 1597

Detection with flame ionization detector (FID).

Peak No.	*PAH*	*MW*	*Relative retention time*[a]	
			FID_1	*FID_2*
1	Phenanthrene	178	1.00	1.00
2	Fluoranthene	202	1.52	1.24
3	Pyrene	202	1.56	1.30
4	Benz[*a*]anthracene	228	2.14	1.45
5	Chrysene	228	2.20	1.47
6	Benzofluoranthenes	252	2.61	1.65
7	Benzopyrenes	252	2.73	1.83
8	Anthanthrene	276	3.20	2.26
9	Coronene	300	3.57	2.40

[a] Retention relative to phenanthrene.

the sample into five groups, followed by further resolution in the second dimension, was completed within 5 h (Fig. 6). In all, the analysis was completed in less than half the time required for the coupled open-tubular column system. Relative retention data are given in Table I. Good group separation, according to ring number, was quickly achieved by using the NH_2-silica phase in Col_1. Isomers such as chrysene and benz[*a*]anthracene were resolved by using Col_2. However, the benzofluoranthene and benzopyrene isomers were far from being satisfactorily resolved. The fractionation system itself worked well, but greater resolution in the second dimension would be required to achieve the desired separation of isomers. The elution of coronene from Col_2 did not occur until 30 min after the end of the density program (0.76 g ml^{-1}). This is in contrast to the results from the coupled open-tubular system where over 1 h passed before coronene eluted from the second dimension. The limiting factor controlling efficiency in both cases was the compromise chosen between high temperature in order to achieve better efficiency and the pressure limit of the syringe pump (400 atm).

CONCLUSIONS

In the first dimension of multidimensional chromatography, a fast, group-type separation is often the primary goal. In addition, large sample capacity is important for analyses in which the measurement of minor constituents of a sample is desired. These are two broad application areas in which a packed capillary column would be better suited for use in the first dimension than an open-tubular capillary column.

The second dimension must provide sufficient selectivity and efficiency to fully resolve the components of interest. For this particular sample, the liquid crystal stationary phase probably would be the best choice, whether an open-tubular capillary column or a longer packed capillary column were used. As was previously mentioned, the option of using a packed capillary column in tandem with an open-tubular

capillary column was not possible in this study due to the limitations imposed by the offset-cross interface; a rotary valve interface would allow independent control of each dimension, thereby facilitating such a combination[11].

ACKNOWLEDGEMENTS

This work was supported by the Gas Research Institute (Contract No. 5084-260-1129) and by the State of Utah Centers of Excellence Program (Contract No. 872279).

REFERENCES

1 F. J. Yang, in F. J. Yang (Editor), *Microbore Column Chromatography: A Unified Approach to Chromatography*, Marcel Dekker, New York, 1989, p. 1.
2 J. C. Giddings, *Anal. Chem.*, 56 (1984) 1258A.
3 J. C. Giddings, *J. High Resolut. Chromatogr. Chromatogr. Commun.*, 10 (1987) 319.
4 G. Schomburg, H. Husmann, E. Hubinger and W. A. Konig, *J. High Resolut. Chromatogr. Chromatogr. Commun.*, 7 (1984) 404.
5 I. L. Davies, B. Xu, K. E. Markides, K. D. Bartle and M. L. Lee, *J. Microcolumn Sep.*, 1 (1989) 71.
6 M. L. Lee, B. Xu, E. C. Huang, N. M. Djordjevic, H.-C. K. Chang and K. E. Markides, *J. Microcolumn Sep.*, 1 (1989) 7.
7 K. E. Markides, B. J. Tarbet, C. M. Schregenberger, J. S. Bradshaw, K. D. Bartle and M. L. Lee, *J. High Resolut. Chromatogr. Chromatogr. Commun.*, 8 (1985) 741.
8 K. M. Payne, B. J. Tarbet, J. S. Bradshaw, K. E. Markides and M. L. Lee, in preparation.
9 *Certificate of Analysis for Standard Reference Material 1597, Complex Mixture of Polycyclic Aromatic Hydrocarbons from Coal Tar*, National Institute of Standards and Technology, Gaithersburg, MD, 1987.
10 S. A. Wise, B. A. Brenner, G. D. Byrd, S. N. Chesler, R. E. Rebbert and M. M. Schantz, *Anal. Chem.*, 60 (1988) 887.
11 I. L. Davies, Z. Juvancz, K. M. Payne, K. E. Markides, M. L. Lee and K. D. Bartle, *Symposium/Workshop on Supercritical Fluid Chromatography, Snowbird, UT, June 13–15, 1989.*

Journal of Chromatography, 477 (1989) 169–183
Elsevier Science Publishers B.V., Amsterdam — Printed in The Netherlands

CHROM. 21 596

HIGH-PERFORMANCE LIQUID CHROMATOGRAPHIC COLUMNS AND STATIONARY PHASES IN SUPERCRITICAL-FLUID CHROMATOGRAPHY

H. ENGELHARDT*, A. GROSS, R. MERTENS and M. PETERSEN
Angewandte Physikalische Chemie, Universität des Saarlandes, 6600 Saarbrücken (F.R.G.)

SUMMARY

Packed columns show identical efficiencies when used in high-performance liquid chromatography (HPLC) or with fluid carbon dioxide in supercritical-fluid chromatography (SFC). Maximum plate numbers, however, are achieved at linear velocities 5–10 times higher in SFC than in HPLC. The advantage of SFC is the possibility of high speeds of analysis.

Problems with HPLC stationary phases arise from the ever present unshielded surface silanols. The use of columns specially prepared for HPLC separations of basic solutes is advantageous. Polymer-encapsulated stationary phases with aliphatic groups seem to have advantages over polystyrene resins. On the other hand, modifiers can be used to reduce silanophilic interactions. Water as a modifier is compatible with flame ionization detection. Equilibrium in modified systems is achieved very rapidly. In combination with fluid density (pressure and/or temperature) variations, system optimization in SFC seems to be less time consuming than in HPLC.

INTRODUCTION

Supercritical-fluid chromatography (SFC) with open-tubular (capillary) columns has increasingly been reconsidered in recent years[1–3]. The high efficiency and speed of analysis that these columns allow in gas chromatography (GC) can only be achieved in SFC when working with fluids at low densities. The diffusion coefficients are then closer to those achieved in gases. For the elution of solutes a higher solvation power of the fluid is required and this may be achieved by increasing the density of the fluid to values around 0.5 g/cm^3 or even higher. The diffusion coefficients of the solutes in the fluids are increasing and approaching values close to those in liquids[4]. This causes, of course, a decrease in efficiency because the radial diffusion is decreasing. To circumvent these problems, the introduction of secondary mass transfer by tight coiling of the column has been recommended[5]. These problems can be avoided either by using narrow-bore capillary columns with inner diameters less than 50 μm or packed columns with particle sizes around 5–10 μm. Another problem with capillary columns stems from the equipment. It is extremely difficult to keep the flow-rate constant during density and pressure programming. Consequently, an (undesirable)

0021-9673/89/$03.50

flow programme is superimposed on the (desired) density programme, leading to additional peak broadening due to the increasing mass-transfer term. With the high flow-rates applicable with packed columns, pressure and density modifications while keeping the volume flow-rate constant are less problematic[6,7].

Another advantage of the use of packed columns in SFC is the variety of stationary phases available and the knowledge of the influence of surface properties and modifications on solute retention accumulated in high-performance liquid chromatography (HPLC).

In this paper, the application of packed columns in SFC and their advantages and problems are discussed.

EXPERIMENTAL

Equipment

The equipment used was a modified version of that described recently[7], consisting of a reciprocating HPLC pump displacing liquid carbon dioxide and flame ionization detection. After passing into the fluid state, the flow-rate was measured via the pressure drop over a packed column. This was used to regulate the flow-rate of the pump resulting, under isothermal and isobaric conditions, in a constant volume flow-rate and hence constant linear velocity. The pressure at the column outlet was kept constant by an adjustable valve. The decoupling of pressure and flow control permitted the measurements of the H *vs.* u curve at different adjustable densities.

An additional regulating circuit was introduced to keep the linear velocity constant during density programming. When the volume flow-rate of the pump is kept constant while the density of the fluid is increased (increasing the pressure at constant temperature), the linear velocity of the fluid decreases. This can easily be measured by the increase in the dead time with increasing system pressure, as shown in Fig. 1, where the volume flow-rate delivered by the pump was kept constant at 3 cm^3/min. To compensate for increasing density and viscosity during pressure and density programming, the volume flow-rate of liquid carbon dioxide has to be increased to keep the dead time constant. The dependence of dead time is independent of the stationary phase and is only a function of the column dimensions and porosity. For each density a volume flow-rate exists where the dead time with the chromatographic column is constant. The experimentally measured values are stored in a computer and fed to the

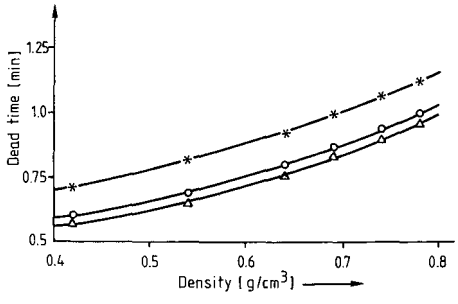

Fig. 1. Dead time as a function of fluid density. Columns, 250 mm × 4.1 mm I.D., packed with silica (LiChrosorb Si 100) and RP-8 and RP-18 derived from it. Inert solute, methane; fluid, carbon dioxide. (✳) Silica; (○) RP-8; (△) RP-18.

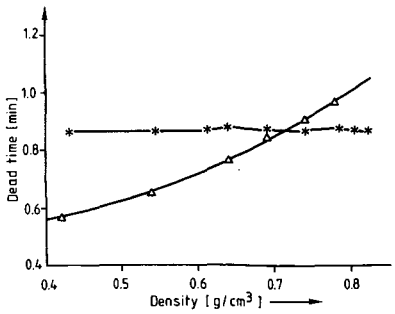

Fig. 2. Dead time as a function of density. Conditions as in Fig. 1. (△) Without flow compensation; (∗) flow compensation for increasing density. For details, see Experimental.

flow-regulating system, increasing the volume flow-rate corresponding to the density programme. As can be seen in Fig. 2, by this means the dead time of the system and hence the linear velocity in the column can be kept constant, and is independent of fluid density.

In pressure- and density-programmed SFC, the reproducibility of the retention time depends strongly on the constancy of the system pressure and the linear velocity. The advantage of the system described here can be seen in Fig. 3, where the same pressure programme was applied without (lower chromatogram) and with (upper chromatogram) flow compensation and hence a constant linear velocity. The relative standard deviation of retention times with this system in the density-programmed mode is 0.25%.

The mobile phase is expanded in the equipment used via a 5-μm orifice directly into the flame[7]. During density programming the volume flow-rate in the gaseous state increases. To keep the flow-rate through the orifice constant, which is necessary for constant response of the detector, a Tescom flow regulator was inserted parallel to the detector, which kept the flow-rate through the orifice constant.

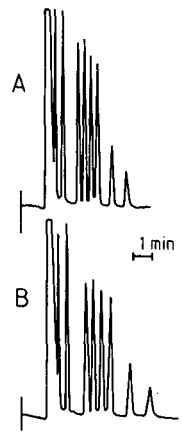

Fig. 3. Demonstration of flow compensation. Separation of C_{10}–C_{22} *n*-alkanes. Column, 250 mm × 4.1 mm I.D., packed with RP-18, 10 μm. Pressure programme, 92–184 bar, linear in 2.5 min. Temperature, 40°C. A, With flow compensation; B, without flow compensation.

Columns and stationary phases

Standard HPLC columns were used. The liquid was first displaced slowly with nitrogen at room temperature. In addition to the commercially available columns PLRP-S (a polystyrene–divinylbenzene resin from Alltech, Belgium, d_p 10 μm) and MH-1 (a polysiloxane-coated silica according to Schomburg *et al.*[8], based on Nucleosil 100, d_p 5 μm, purchased from Gynkothek, Munich, F.R.G.), various columns packed with silica (*e.g.*, LiChrosorb Si 100, d_p 5 and 10 μm, Merck) and chemically modified phases (based on silicas from Merck, Macherey, Nagel & Co. and Grace derivatized in our laboratory by silanization with octadecyl, octyl[9], triamine (γ-diethylenediaminopropyldimethoxy)[10] silanes or encapsulated with polyacrylates[11]) were used. The column length varied between 10 and 25 cm.

Test solutes were purchased from various distributors.

RESULTS AND DISCUSSION

Efficiency with packed columns

In all discussions on SFC, it has been stated that it combines the advantages of GC with respect of high efficiency and speed of analysis with the advantages of LC with respect to high selectivity and ease of optimization by varying the properties of mobile phase. The latter can be easily achieved by varying the density of the mobile phase and/or the temperature. The density increases with increasing pressure, a very large increase in density being obtained close to the critical conditions[12]. Simultaneously with the increase in density, the diffusion coefficients decrease[4]. In fluid carbon dioxide, the diffusion coefficients are in the 10^{-4} cm^2/s range[13]. A value of $7 \cdot 10^{-4}$ cm^2/s was measured for *n*-nonane at a carbon dioxide density of 0.69 g/cm^3, decreasing to $4.5 \cdot 10^{-4}$ cm^2/s at 0.45 g/cm^3 density.

With diffusion coefficients of *ca.* 10^{-5} cm^2/s for low-molecular-weight solutes in liquids, SFC conditions resemble more closely those in liquids than in gases, with diffusion coefficients of *ca.* 10^{-1} cm^2/s. This is obvious when one compares the *H vs. u* curves obtained for non-retarded solutes on packed columns in LC, SFC and GC, as shown in Fig. 4. The efficiency at the minimum of the *H vs. u* curve in LC is comparable to that in SFC. The most important difference, however, is that the minimum in SFC is achieved at linear velocities 5–10 times larger than in LC, thus permitting higher speeds of analysis. The smaller mass-transfer term (*C* term) in SFC (*ca.* 3 ms

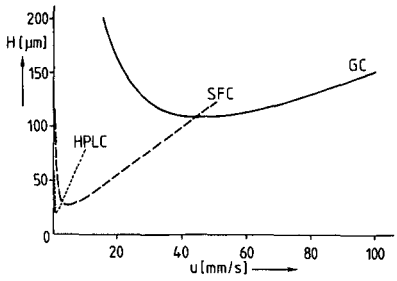

Fig. 4. Efficiency of packed columns in LC, SFC and GC. Column, 250 mm × 4.1 mm I.D., packed with RP-18, 10 μm. HPLC: mobile phase, methanol; solute, benzene. SFC: mobile phase, carbon dioxide; solute, methane. GC: mobile phase, nitrogen; solute, methane.

for 10-μm particles) allows a further increase in the speed of analysis without a significant decrease in efficiency. For comparison, the data obtained with a packed small-particle column in GC[14] have also been included in this plot. The H values in GC are due to the B term in the Van Deemter plot being a factor of 3 higher than in SFC and the maximum plate number (minimum of the H *vs.* u curve) is achieved at linear velocities a factor of 40 larger than in LC and a factor of 10 larger than in SFC. This demonstrates the advantage in GC of the high speed of analysis that is achievable.

In Fig. 5, the H *vs.* u curves in LC and SFC for a 5-μm packed column are compared. The H values under optimum conditions are identical. Reduced H values of *ca.* 3 are obtained. In the LC mode, the minimum of the H *vs.* u curve is *ca.* 0.5–1 mm/s linear velocity. In SFC at low pressure (density 0.64 g/cm^3), the minimum of the H *vs.* u curve is *ca.* 5 mm/s. At higher pressure (density 0.79 g/cm^3), the minimum is shifted to lower linear velocities, because the increasing viscosity causes a decrease in the diffusion coefficient. As can also be seen, the C term is also affected by the density, as expected from theory.

In liquids, the diffusion coefficient decreases with increasing temperature, resulting in higher efficiencies at higher temperatures. Fluids also behave like liquids in this respect. In Fig. 6 the H *vs.* u curves for two different columns measured in each instance at two different temperatures but at an identical density of 0.4 g/cm^3 are shown. The plate heights are reduced at higher temperatures, as expected from theory. Consequently, the efficiency can be increased by increasing the temperature as in LC.

Pressure drop and k'

The most important parameter for adjusting retention in SFC is the fluid density. Increasing the density (at constant temperature) always leads to a decrease in

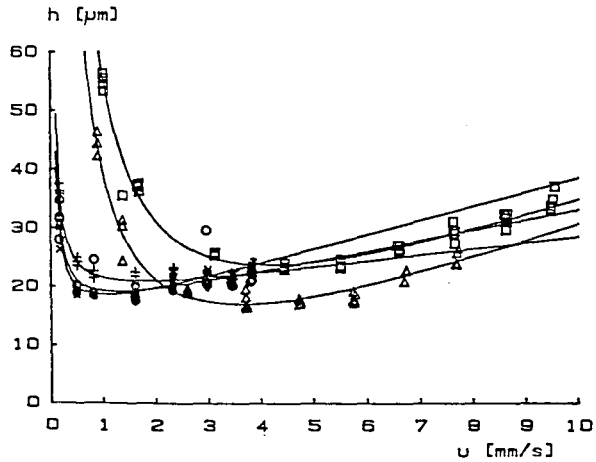

Fig. 5. Efficiency of packed columns in HPLC and SFC. Column, 250 mm × 4.1 mm I.D., packed with RP-18, 5 μm. HPLC: mobile phase, methanol; solutes, (+) nitromethane, (○) anthracene (k' = 0.7) and (×) pyrene (k' = 1.0). SFC: mobile phase, carbon dioxide; solute, methane; temperature, 40°C; pressure, (□) 109 and (△) 140 bar.

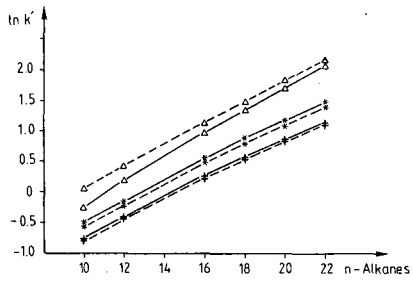

Fig. 6. Influence of column pressure drop on capacity factors. Column, 250 mm × 4.1 mm I.D., packed with RP-18, 10 μm; broken lines, single column; solid lines, two identical columns coupled in series. Temperature, 40°C; pressure, (△) 90, (*) 105, (+) 120 bar.

retention. Pressure and density programming in SFC corresponds to temperature programming in GC and eluent programming, *i.e.*, gradient elution, in LC. The strong dependence of retention time (capacity ratio, k') on density leads to the argument that in packed columns, owing to the lower permeability by a factor of at least 30 compared with open-tubular columns, the velocity of retarded peaks decreases within the column, leading to reduced res olution and additional peak broadening. Also, the permeability of packed columns is a function of the packing procedure. Consequently, another argument against the use of packed columns in SFC is the difficulty involved in transfering a separation from one column to the other with different permeabilities and hence a different pressure drop.

The influence of pressure drop on k' can be seen in Fig. 6. The k' values were measured at three different end pressures (90, 105 and 120 bar) on one column and with two identical columns coupled in series. As can be seen, at low system pressure (90 bar) the k' values are lower with the two-column system compared with the single column. The pressure drop (at 90 bar end pressure) for the single column is 3 bar and that for the two-column system 6.9 bar. The difference in k' values is in the range of 5–8% between the single- and double-column systems. At an end pressure above 100 bar the differences in k' values are less significant and at pressures above 120 bar they are below 2%, despite the higher pressure drop of 5 bar compared with 10 bar.

The pressure dependence of k' values on doubling the pressure drop has only to be considered for systems with low density, where the fluid compressibility is high and the density shows a strong dependence on pressure. However, it is not advisable to work with systems too close to the critical conditions. At low density the solvation power of the fluids is weak, causing peak distortion and asymmetry (fronting).

The pressure drop with packed columns (d_p = 10 μm) with a length of 25 cm in SFC is in the range 2–5 bar. Consequently, it is possible to work reproducibly with packed columns in SFC when the system pressure is at least 20% above the critical pressure. It should be mentioned that with 10-m long open tubes of 50 μm diameter the pressure drop is also in the range 1–2 bar.

Selectivity with packed columns

Fluid carbon dioxide is a non-polar liquid that can be used to dissolve and extract non-polar and slightly polar solutes[15] such as low-molecular-weight hydrocarbons, alcohols and fatty acid esters. The solubility in carbon dioxide decreases

with increasing molecular weight and polarity, *e.g.*, number of hydroxyl groups in a molecule. The dielectric constant of fluid carbon dioxide increases with increasing density and approaches values in the liquid phase similar to that of *n*-pentane[4]. Consequently, in a first approach the retention behaviour of non-polar solutes was studied with HPLC stationary phases.

It has been shown[7] that hydrocarbons can be separated with both silica and reversed-phase columns. With the latter column type, higher retentions have been observed. Much more surprising is the fact that the influence of fluid density on retention is similar with both types of stationary phases. In Fig. 7, the dependence of retention on fluid density is shown for decylbenzene and fluoranthene with silica and RP-8 and RP-18 columns. Density is usually chosen, because linear plots are obtained only if ln k' is plotted against density. However, the equation of state used for the calculation of fluid density has to be valid in the range used. It has been recommended[15] that pressure and temperature be reported instead of densities, because these are the directly measured values. In this paper densities are used, but when necessary the column end pressure and temperatures are also given. As can be seen, with all stationary phases the influence of density on solute retention is identical (at constant temperature). The less polar the stationary phase, the higher is the retention at constant density (isopycnic conditions). Here carbon dioxide exhibits typical polar eluent properties like methanol in RP chromatography. With silica alkanes are eluted almost inert and the aromatic hydrocarbon fluoranthene is much more strongly retarded than decylbenzene. Here additional polar interactions certainly contribute to retention and carbon dioxide acts like a non-polar eluent, *e.g.*, hexane in normal-phase chromatography. Alkanes inert with silica columns are (with identical carbon number) much more strongly retarded than the phenylalkanes with RP columns. Here, hydrophobic interactions contribute to retention in RP and again carbon dioxide can be considered as a reversed-phase eluent. Depending on the properties of the stationary phase, either polar (silanophilic) or non-polar interactions govern solute retention in SFC. The silanophilic interactions are clearly recognizable with more polar solutes as will be discussed later, and have to be minimized in order to be able to separate solutes other than hydrocarbons in SFC. Most of the problems with packed columns stem from the silanophilic interactions with residual silanol groups on the chemically modified silica. As in LC, the silanophilic interactions can be masked by

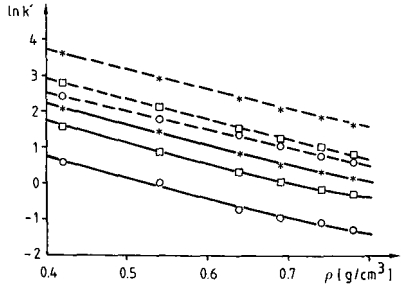

Fig. 7. Retention and fluid density. Columns, 250 mm × 4.1 mm I.D., packed with (○) SiO_2, (□) RP-8 and (∗) RP-18. Mobile phase, carbon dioxide; temperature, 40°C. Solutes: decylbenzene (solid lines) and fluoranthene (dashed lines).

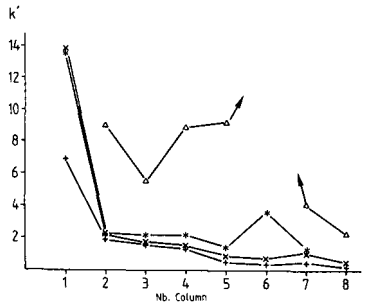

Fig. 8. Selectivity of packed columns. Columns: 1, PLRP-S, 10 μm, 150 mm × 4.6 mm I.D. (Alltech); 2, MH-1, 5 μm, 250 mm × 4.6 mm I.D. (Gynkotech); 3, Si 100 RP-18, 10 μm, 100 mm × 4.1 mm I.D.; 4, Si 80 RP-18, 10 μm; 5, poly(butyl acrylate) on Si 60, 5 μm; 6, polyacrylamide on Si 100, 10 μm; 7, triamine on Si 100, 10 μm; 8, LiChrosorb Si 100, 10 μm. Columns 3–8 were experimental products of our laboratory; dimensions of columns 4–8, 250 mm × 4.1 mm I.D. Mobile phase, carbon dioxide; temperature, 313 K; pressure, 120 bar. Solutes: (+) hexadecane; (×) decylbenzene; (∗) ethyl palmitate; (△) fluoranthene.

coverage with strong bases. In SFC this has been done by several injections of triethylamine before analysis of polar solutes[7]. Another possibility of circumvent these problems is to use polymer-coated stationary phases[8,11], which exhibit excellent properties in LC separations of strongly basic solutes, or polymeric stationary phases such as cross-linked polystyrenes[16].

In Fig. 8 the retentions of test solutes (16 carbon atoms) are plotted for eight different stationary phases. The highest retention was obtained with the polystyrene resin. Fluoranthene could not be eluted with this column, probably owing to strong aromatic–aromatic interactions. The smallest retentions were measured with the silica column. Symmetric peaks were obtained especially with polymer-coated columns (2, 5, 6) and with the triamine-modified stationary phases. These stationary phases are used with advantage in LC for the separation of basic solutes, where symmetric peak shapes are obtained and retention is independent of sample size up to 10^{-4} g of sample per gram of stationary phase. With these stationary phases the surface silanols are totally shielded. For use in SFC, consequently, stationary phases in which the surface silanols are completely covered and do not contribute to retention are recommended. With the totally polymeric stationary phases, the strong solute–surface interactions lead to too high retentions. The same has been found in LC with these columns. Comparing the selectivity of the polymer-coated stationary phases with that of a standard reversed-phase, it can be seen in Fig. 9 much more clearly that the selectivity is independent of pressure or density. It is striking that the polysiloxane-coated phase (where C_{18} groups are in the polysiloxane chains) shows similar selectivity to a standard reversed-phase (RP-18), whereas the selectivity is much higher with a polymeric phase based on butyl acrylate.

The ester functionality shows similar selectivity to the medium-polarity ester phases in GC. In Fig. 10 the separations of the test mixture with RP-18 and the acrylic phase are compared. Those solutes containing an aromatic ring are retarded more strongly with the acrylic ester phase, whereas the aliphatic solutes are eluted earlier compared with RP-18. This shows that (as in GC) it seems possible to adjust the selectivity of a polymer-coated stationary phase by varying the functional groups in the polymeric film.

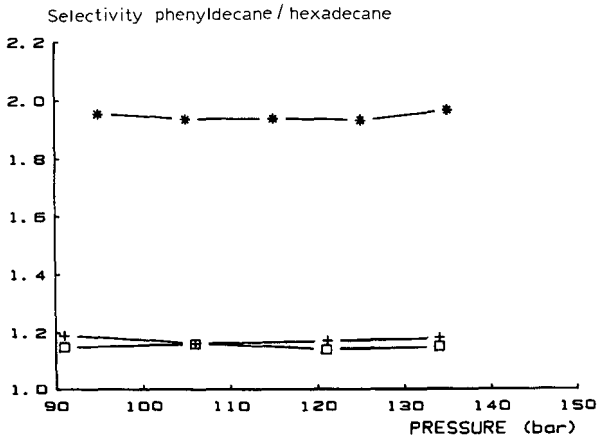

Fig. 9. Selectivity and pressure. Columns, temperature and solutes as in Fig. 8; pressure varied between 90 and 135 bar.

Adjustment of retention

Pressure programming. As discussed above, the retention decreases with increasing density or pressure at constant temperature. The selectivity is not influenced by the density, the slopes of the curves in Fig. 7 being almost parallel. It is therefore possible to reduce analysis time by pressure and density programming. Working at low temperatures, in the range 90–180 bar the density increases from 0.5 to 0.8 g/cm^3. Even in this range the retention decreases only by a factor of 3–5 compared with a factor up to 10 000 in RP chromatography with a gradient from water to methanol. At higher temperatures the change in density with pressure is less pronounced, and consequently pressure programming is less effective. The advantage of pressure programming is, however, that after returning to the initial pressure the column is immediately in its initial conditions and no additional regeneration time is required. It should be mentioned that in this instance the flow-rate has been increased during pressure programming, as discussed above, to keep the linear velocity constant.

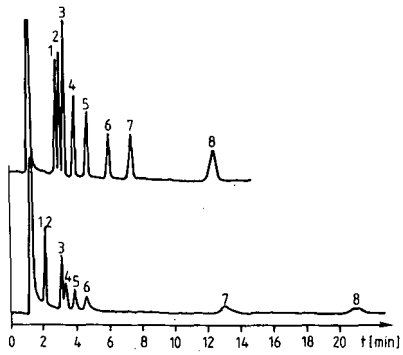

Fig. 10. Separation of test mixture on alkyl and ester phases. Upper chromatogram, RP-18 (column 4 in Fig. 8); lower chromatogram, acrylic ester (column 5 in Fig. 8). Mobile phase, carbon dioxide; linear velocity, 5 mm/s; density, 0.54 g/cm^3; temperature, 40°C. Samples: 1 = 1-hexadecene; 2 = hexadecane; 3 = decylbenzene; 4 = 1-chlorohexadecane; 5 = 1-bromohexadecane; 6 = 1-iodohexadecane; 7 = 2-phenylnaphthalene; 8 = fluoranthene.

Influence of temperature. Increasing the temperature at constant pressure decreases the density, resulting in an increase in retention time. Consequently, to enlarge the scope of density programming, a negative temperature programme (reduction of column temperature) is required. On the other hand, for volatile components it can be shown that increasing temperature can also reduce the retention time. It is questionable whether this group of solutes are not better separated by GC. In Fig. 11 the influence of density and temperature on the separation of polar volatile components is demonstrated. At a constant density (0.57 g/cm^3) the analysis time is reduced and the peak shape improved when the temperature is increased from 40 to 60°C. To keep the density constant, the pressure at column outlet has to be increased from 95 to 140 bar. The influence of density on separation at the lower temperature is also demonstrated in Fig. 11. An increase in density from 0.57 to 0.75 g/cm^3 also improves the peak shape, but the decrease in retention time reduces the resolution. With less volatile solutes, where the vapour pressure is negligible, an increase in temperature always leads to an increase in retention.

Addition of modifier. In LC, where silanophilic interactions also play an important role, these interactions can be minimized in RP chromatography by the addition of modifiers, such as triethylamine and other strong organic bases. In normal-phase chromatography with non-polar eluents, the strong interactions of solutes with the stationary phase are often modified by the addition of small amounts (less than 1%) of polar components such as methanol or water. The problems with water, always present in the eluents, and the extremely long time required to achieve equilibrium, have hindered the application of normal-phase chromatography. The use of modifiers has also been advocated in SFC. However, with organic modifiers, flame ionization detection (FID) cannot be used. Water is only partially soluble in fluid carbon dioxide (less than 0.3%)[17], but is fully compatible with FID when used as a modifier. The

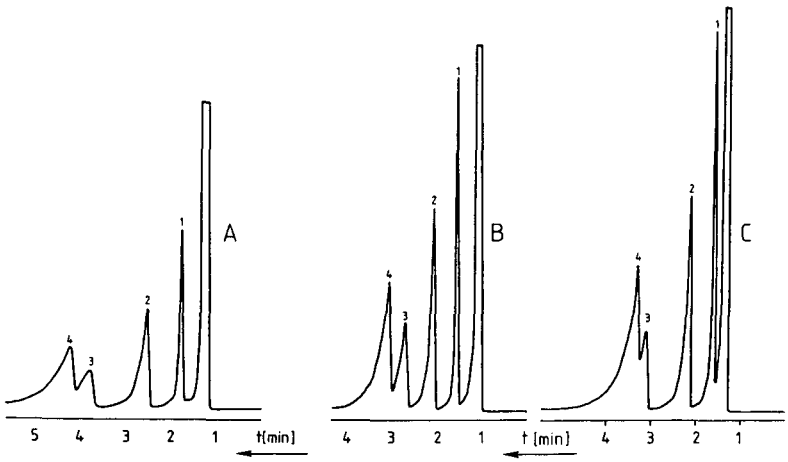

Fig. 11. Influence of density and temperature: isopycnic and isobaric conditions. Column, 250 mm × 4.6 mm I.D., packed with MH-1, 5 μm. Mobile phase, carbon dioxide; linear velocity, 8 mm/s. (A) Density 0.57 g/cm^3, pressure 95 bar, temperature 313 K; (B) density 0.57 g/cm^3, pressure 140 bar, temperature 333 K; (C) density 0.75 g/cm^3, pressure 140 bar, temperature 313 K. Solutes: 1 = phenyl acetate; 2 = acetophenone; 3 = phenol; 4 = 2,6-dimethylaniline.

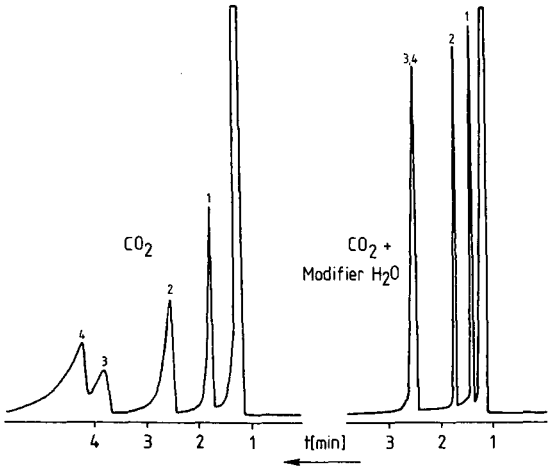

Fig. 12. Water as modifier. Column and solutes as in Fig. 11. Conditions: pressure, 95 bar; temperature, 313 K. Dry and water-saturated carbon dioxide used as mobile phase.

striking influence of water (added via a saturator[18] to the fluid carbon dioxide) can be seen in Fig. 12. The retention decreases, as expected, but much more striking is the improvement in peak shape. This indicates that most of the silanophilic interaction is blocked by water[19].

The influence of water on solute retention can be seen much more clearly in Fig. 13, where the dependence of retention on density is compared for dry and water-saturated carbon dioxide. With the unmodified eluent the k' values decrease by a factor of 11 when the fluid density is increased from 0.5 to 0.8 g/cm^3. Because the vapour pressure of the solutes is negligible in the temperature range used here, the k'

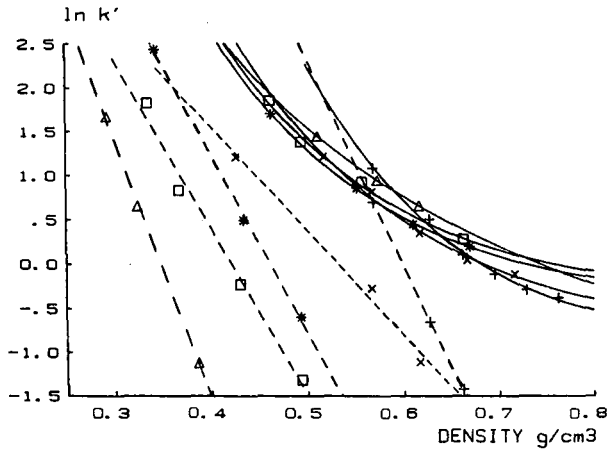

Fig. 13. Influence of temperature and density on retention with water-modified carbon dioxide. Column, 250 mm × 4.1 mm I.D. Solid lines, dry carbon dioxide; dashed lines, water-saturated carbon dioxide. Temperature: (+) 313 K; (×) 318 K; (✳) 323 K; (□) 328 K; (△) 333 K. Solute: C_{22} *n*-alkane.

values are hardly affected by temperature variations. The opposite is true when water-saturated carbon dioxide is used. The k' values depend very strongly on density. With a density variation of only 0.1 g/cm^3 the k' values vary by a factor of 11. Much more striking here is the influence of temperature. On increasing the temperature by 20°C the same k' values are obtained at densities of 0.6 and 0.33 g/cm^3 with water-saturated carbon dioxide. This, of course, is a function of the solubility of water in carbon dioxide, which increases in the fluid range with increasing temperature.

The modifier water is prefentially adsorbed within the pores of the stationary phase. A similar behaviour has been found in normal-phase chromatography when *in situ* partitioning systems have been generated by using non-polar eluents saturated with water or other polar modifiers[20]. The loading of the stationary phase with polar modifier, *e.g.*, the decrease in pore volume, can be determined experimentally by measuring the variation of dead time with a marker that does not interact with the water layer within the pores. As can be seen in Fig. 14, the pore volume of the silica-based stationary phase decreases with increasing water content of the mobile phase, which is a function of pressure/density and temperature. It should be noted that the increase in water solubility[17] in fluid carbon dioxide is most noticeable in the pressure range 90–120 bar at temperatures around 50°C. It is worth mentioning that with the same stationary phase in the system acetonitrile–water (95:5, v/v) the same part of the pore volume is filled with water[10].

One great disadvantage in the use of water-modified systems in normal-phase liquid chromatography is the extremely long time required to achieve constant retention times and to obtain phase equilibrium[21]. Usually it takes 12–20 h to achieve equilibrium in the hexane–water–silica system. The advantage of modified fluid chromatography is that equilibrium conditions are approached much faster. In Fig. 15 the loading of the stationary phase with water (decrease in pore volume) is shown as a function of time. In the first 5–10 min most of the water is already deposited in the pores and equilibrium conditions are approached in about 20 min. The optimization of the separation conditions by variation of temperature and pressure and hence modifier loading of the stationary phase is therefore much faster than in LC.

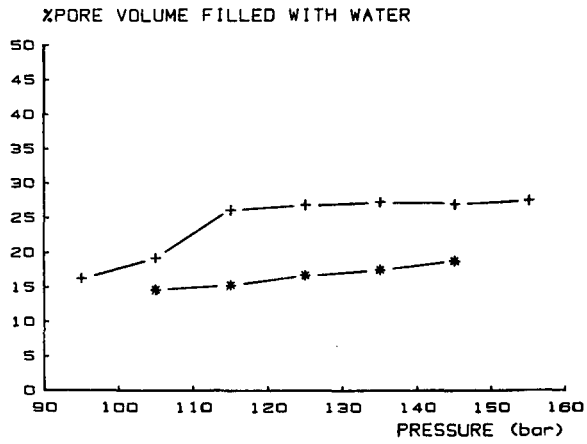

Fig. 14. Coating of stationary phase with water. Column, 250 mm × 4.1 mm I.D., packed with triamine on Si 100. Water-saturated carbon dioxide. Solute, methane; temperature, (*) 318 K; (+) 328 K.

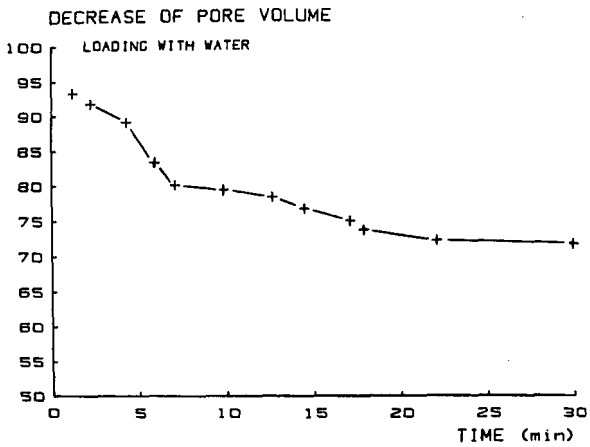

Fig. 15. Kinetics of water coating. Conditions as in Fig. 14 with temperature 328 K.

Sub- versus supercritical chromatography

As density is the main parameter affecting retention and analysis time in SFC, the question arises of whether the densest form of carbon dioxide, the liquid phase, can be used as mobile phase. Of course, to be able to work with liquid carbon dioxide, SFC equipment has to be used also. It seems that the selectivities with the same

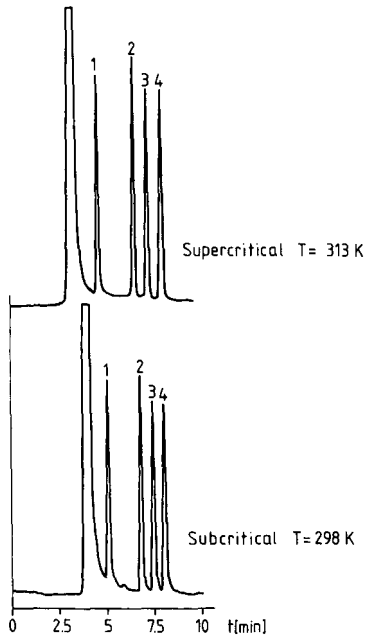

Fig. 16. Selectivity with liquid and fluid carbon dioxide. Column, 250 mm × 4.1 mm I.D., packed with PLRP-S, 10 μm. Pressure, 120 bar; temperature, 298 K (liquid carbon dioxide) and 313 K (fluid carbon dioxide). Solutes: 1 = ethyl benzoate; 2 = ethyl myristate; 3 = methyl pentadecanoate; 4 = ethyl palmitate.

stationary phase are almost identical whether fluid or liquid carbon dioxide is used. In Fig. 16, the separations of fatty acid esters with sub- and supercritical carbon dioxide are compared. The pressure was 120 bar in both instances. As liquids are almost incompressible, the retention is not affected by pressure. The liquid chromatogram was taken at 25°C and the supercritical fluid chromatogram at 40°C. As vapour pressure does not play a role with these solutes, the influence of temperature is not noticeable. The use of liquid carbon dioxide as the mobile phase in chromatography is worthwhile for future consideration, because it seems that some separations, where extremely specific solute–stationary phase interactions play a role, as in enantiomeric separations, can be achieved with improved selectivity when working with liquid (subcritical) carbon dioxide compared with supercritical conditions[22].

CONCLUSIONS

The use of packed columns in SFC results in highly efficient separations with plate heights comparable to those in LC when identical stationary phases are used. The maximum plate number (minimum of the Van Deemter plot) is approached at linear velocities that are a factor of 5–10 higher than with the same column under LC conditions. Consequently, a higher speed of analysis is achievable in SFC.

The use of packed columns increases the potential of SFC, because a variety of stationary phases with distinct and often well understood selectivities are available. This enlarges the scope of the potential applications of SFC, because the selectivity and number of potential fluids are very limited, if not restricted to carbon dioxide alone. The polarity of carbon dioxide corresponds to that of hydrocarbons and consequently the silanophilic interactions can exhibit a disturbing influence, especially if polar solutes are to be separated. The use of modified systems, with water as modifier, can minimize this influence and FID can still be used. The achievement of equilibrium conditions even in modified systems is much faster than in LC, facilitating system optimization where many changes of the operating conditions are necessary[23].

The only stationary phase that can be used in SFC for the separation of more polar phases are those in which the surface silanols of the base material are totally shielded. Preferably stationary phases developed for the LC of basic solutes should be used. New types of stationary phases, either with tentacle-type bonded groups[24] or where the surface is coated with a homogeneous polymer film, have been used in SFC. Polymer-encapsulated silica, where functional groups in the polymer film can be varied, appears promising for future developments in SFC.

ACKNOWLEDGEMENTS

We gratefully acknowledge a Landesgraduierten Stipendium granted to A.G. This work was presented in part at the *8th International Symposium on Capillary Chromatography, Riva del Garda, May 19–21, 1987*, by H.E. and at the *12th International Symposium on Column Liquid Chromatography, Washington, DC, June 19–24, 1988*, by M.P.

REFERENCES

1 W. D. Later, E. B. Richter and R. M. Andersen, *LC/GC Mag.*, 4 (1986) 993.
2 R. M. Smith (Editor), *Supercritical Fluid Chromatography*, Royal Society of Chemistry, London, 1988.
3 C. M. White (Editor), *Modern Supercritical Fluid Chromatography*, Hüthig, Heidelberg, 1988.
4 G. M. Schneider, in G. M. Schneider, E. Stahl and G. Wilke (Editors), *Extraction with Supercritical Gases*, Verlag Chemie, Weinheim, 1978.
5 S. R. Springston and M. Novotny, *Anal. Chem.*, 58 (1986) 2699.
6 K. R. Jahn and B. W. Wenclawiak, *Anal. Chem.*, 59 (1987) 382.
7 H. Engelhardt and A. Gross, *J. High Resolut. Chromatogr. Chromatogr. Commun.*, 11 (1988) 38.
8 G. Schomburg, A. Deege, J. Köhler and V. Bien-Vogelsang, *J. Chromatogr.*, 282 (1983) 27.
9 H. Engelhardt, B. Dreyer and H. Schmidt, *Chromatographia*, 16 (1982) 11.
10 H. Engelhardt and P. Orth, *Chromatographia*, 15 (1982) 91.
11 H. Engelhardt and H. Löw, *Fresenius Z. Anal. Chem.*, 330 (1988) 396.
12 B. Armstrong and K. M. de Reuck, *IUPAC Volume 3 Data on CO_2*, IUPAC Project Centre, Imperial College, London, 1976.
13 H. Stass, *Ph.D. Thesis*, Saarbrücken, 1986.
14 H. Roidl, *Ph.D. Thesis*, Saarbrücken, 1985.
15 P. Sandra and P. Schoenmakers, paper presented at *Erba Days on SFC, Madonna di Campiglio, December 1988.*
16 F. Nevejans and M. Verzele, *J. Chromatogr.*, 406 (1987) 325.
17 E. Stahl, K. W. Quiring and D. Gerard, *Verdichtete Gase zur Extraktion und Raffination*, Springer, Heidelberg, 1987.
18 B. L. Karger, R. C. Castells, P. A. Sewell and A. Hartkopf, *J. Phys. Chem.*, 75 (1971) 3870.
19 F. O. Geiser, S. G. Yocklovich, S. M. Lurcott, J. W. Guthrie and E. J. Levy, *J. Chromatogr.*, 459 (1988) 173.
20 H. Engelhardt and N. Weigand, *Anal. Chem.*, 45 (1973) 1149.
21 H. Engelhardt and W. Böhme, *J. Chromatogr.*, 133 (1977) 67.
22 F. Gasparrini, paper presented at *Erba Days on SFC, Madonna di Campiglio, December 1988.*
23 W. Steuer, M. Schindler and F. Erni, *J. Chromatogr.*, 454 (1988) 253.
24 M. Ashraf-Khorassani, L. T. Taylor and R. A. Henry, *Anal. Chem.*, 60 (1988) 1529.

END OF HONOUR ISSUE

Analytical Artifacts

GC, MS, HPLC, TLC and PC

by **B.S. MIDDLEDITCH,** *Dept. of Biochemical and Biophysical Sciences, University of Houston, Houston, TX, USA*

(Journal of Chromatography Library, 44)

This encyclopaedic catalogue of the pitfalls and problems that all analysts encounter in their work is destined to spend more time on the analyst's workbench than on a library shelf. The author has dedicated the book to "the innumerable scientists who made mistakes, used impure chemicals and solvents, suffered the consequences of unanticipated side-reactions, and were otherwise exposed to mayhem yet were too embarrassed to publish their findings".

Traditionally, the mass spectroscopist or gas chromatographer learnt his trade by participating in a 4-6 year apprenticeship as graduate student and post-doctoral researcher. Generally, no formal training was provided on the things that go wrong, but this information was accumulated by sharing in the experiences of colleagues. Nowadays, many novice scientists simply purchase a computerized instrument, plug it in, and use it. Much time can be wasted in studying and resolving problems due to artifacts and there is also a strong possibility that artifacts will not be recognized as such. For example, most analysts realize that they should use glass rather than plastic containers; but few of them would anticipate the possibility of plasticizer residues on glassware washed using detergent from a plastic bottle.

This book is an easy-to-use compendium of problems encountered when using various commonly used analytical techniques. Emphasis is on impurities, by-products, contaminants and other artifacts. A separate entry is provided for each artifact. For specific chemicals, this entry provides the common name, mass spectrum, gas chromatographic data, CAS name and registry number, synonyms and a narrative discussion. More than 1100 entries are included. Mass spectral data are indexed in a 6-peak index (molecular ion, base peak, second peak, third peak) and there are also formula, author and subject indexes. An extensive bibliography contains complete literature citations.

The book is designed to be *used*. It will not only allow experienced analysts to profit from the mistakes of others, but it will also be invaluable to other scientists who use analytical instruments in their work.

1989 xxiv + 1028 pages
US$ 241.50 / Dfl. 495.00
ISBN 0-444-87158-6

ELSEVIER SCIENCE PUBLISHERS

P.O. Box 211, 1000 AE Amsterdam, The Netherlands
P.O. Box 882, Madison Square Station, New York, NY 10159, USA

Determination of Beta-Blockers in Biological Material

edited by **V. Marko**, *Institute of Experimental Pharmacology, Centre of Physiological Sciences, Slovak Academy of Sciences, Bratislava, Czechoslovakia*

(Techniques and Instrumentation in Analytical Chemistry, 4C)

This is the third volume of a sub-series entitled *Evaluation of Analytical Methods in Biological Systems*. (The first two were *Analysis of Biogenic Amines* edited by G.B. Baker and R.T. Coutts and *Hazardous Metals in Human Toxicology* edited by A. Vercruysse). This new volume addresses beta-blockers - an area of research for which a Nobel Prize in Medicine was awarded in 1988. It provides an up-to-date and comprehensive coverage of the theory and practice of the determination of beta-blockers in biological material. Two main fields of research are dealt with in this book: analytical chemistry and pharmacology, and, as it deals with drugs used in clinical practice, it is also related to a third area: therapy. Thus, it offers relevant information to workers in all three fields.

Some 50 beta-blockers and nine methods of analysis are discussed. The methods are divided into three groups: optical, chromatographic, and saturation methods. In addition to the analytical methods themselves, sample handling problems are also covered in detail, as is the information content of the analytical results obtained. Special chapters are directed to those working in pharmacology and pharmacokinetics. Finally, as recent evidence points to the increased importance of distinguishing optical isomers of drugs, a chapter on the determination of optical isomers of beta-blockers in biological material is also included. An extensive subject index and two supplements giving retention indices and structures of beta-blockers complete the book.

This is the first book to treat beta-blockers from the point of view of their determination and to discuss in detail the use of analytical methods for beta-blockers. It will thus appeal to a wide-ranging readership.

1989 xiv + 334 pages
US$ 152.75 / Dfl. 290.00
ISBN 0-444-87305-8

ELSEVIER SCIENCE PUBLISHERS

P.O. Box 211, 1000 AE Amsterdam, The Netherlands
P.O. Box 882, Madison Square Station, New York, NY 10159, USA

PUBLICATION SCHEDULE FOR 1989

Journal of Chromatography and Journal of Chromatography, Biomedical Applications

MONTH	J	F	M	A	M	J	J	A	S	O	N	D
Journal of Chromatography	461 462 463/1	463/2 464/1	464/2 465/1 465/2	466 467/1 467/2	468 469 470/1 470/2	471 472/1 472/2 473/1	473/2 474/1 474/2 475	476 477/1 477/2	The publication schedule for further issues will be published later			
Bibliography Section		486/1		486/2		486/3		486/4				
Biomedical Applications	487/1	487/2	488/1 488/2	489/1 489/2	490/1 490/2	491/1	491/2	492 493/1	493/2			

INFORMATION FOR AUTHORS

(Detailed *Instructions to Authors* were published in Vol. 445, pp. 453–456. A free reprint can be obtained by application to the publisher, Elsevier Science Publishers B.V., P.O. Box 330, 1000 AH Amsterdam, The Netherlands.)

Types of Contributions. The following types of papers are published in the *Journal of Chromatography* and the section on *Biomedical Applications:* Regular research papers (Full-length papers), Notes, Review articles and Letters to the Editor. Notes are usually descriptions of short investigations and reflect the same quality of research as Full-length papers, but should preferably not exceed six printed pages. Letters to the Editor can comment on (parts of) previously published articles, or they can report minor technical improvements of previously published procedures; they should preferably not exceed two printed pages. For review articles, see inside front cover under Submission of Papers.

Submission. Every paper must be accompanied by a letter from the senior author, stating that he is submitting the paper for publication in the *Journal of Chromatography*. Please do not send a letter signed by the director of the institute or the professor unless he is one of the authors.

Manuscripts. Manuscripts should be typed in double spacing on consecutively numbered pages of uniform size. The manuscript should be preceded by a sheet of manuscript paper carrying the title of the paper and the name and full postal address of the person to whom the proofs are to be sent. Authors of papers in French or German are requested to supply an English translation of the title of the paper. As a rule, papers should be divided into sections, headed by a caption (*e.g.*, Summary, Introduction, Experimental, Results, Discussion, etc.). All illustrations, photographs, tables, etc., should be on separate sheets.

Introduction. Every paper must have a concise introduction mentioning what has been done before on the topic described, and stating clearly what is new in the paper now submitted.

Summary. Full-length papers and Review articles should have a summary of 50–100 words which clearly and briefly indicates what is new, different and significant. In the case of French or German articles an additional summary in English, headed by an English translation of the title, should also be provided. (Notes and Letters to the Editor are published without a summary.)

Illustrations. The figures should be submitted in a form suitable for reproduction, drawn in Indian ink on drawing or tracing paper. Each illustration should have a legend, all the *legends* being typed (with double spacing) together on a *separate sheet*. If structures are given in the text, the original drawings should be supplied. Coloured illustrations are reproduced at the author's expense, the cost being determined by the number of pages and by the number of colours needed. The written permission of the author and publisher must be obtained for the use of any figure already published. Its source must be indicated in the legend.

References. References should be numbered in the order in which they are cited in the text, and listed in numerical sequence on a separate sheet at the end of the article. Please check a recent issue for the layout of the reference list. Abbreviations for the titles of journals should follow the system used by *Chemical Abstracts*. Articles not yet published should be given as "in press" (journal should be specified), "submitted for publication" (journal should be specified), "in preparation" or "personal communication".

Dispatch. Before sending the manuscript to the Editor please check that the envelope contains three copies of the paper complete with references, legends and figures. One of the sets of figures must be the originals suitable for direct reproduction. Please also ensure that permission to publish has been obtained from your institute.

Proofs. One set of proofs will be sent to the author to be carefully checked for printer's errors. Corrections must be restricted to instances in which the proof is at variance with the manuscript. "Extra corrections" will be inserted at the author's expense.

Reprints. Fifty reprints of Full-length papers, Notes and Letters to the Editor will be supplied free of charge. Additional reprints can be ordered by the authors. An order form containing price quotations will be sent to the authors together with the proofs of their article.

Advertisements. Advertisement rates are available from the publisher on request. The Editors of the journal accept no responsibility for the contents of the advertisements.